1-1-2013

Development Of Kinase Catalyzed Biotinylation To Study Phosphoproteomics

Kona Arachchilage Chamara Indunil Bandara Senevirathne
Wayne State University,

DEVELOPMENT OF KINASE CATALYZED BIOTINYLATION TO STUDY PHOSPHOPROTEOMICS

by

KONA ARACHCHILAGE CHAMARA SENEVIRATHNE

DISSERTATION

Submitted to the Graduate School

of Wayne State University,

Detroit, Michigan

in partial fulfillment of the requirements

for the degree of

DOCTOR OF PHILOSOPHY

2013

MAJOR: CHEMISTRY (Organic)

Approved by:

_____
Advisor   Date

_____

_____

_____

DEDICATION

To my mother, father, wife and son, the most important people in my life.

ACKNOWLEDGMENTS

I am happt to express my heartfelt thanks to all the people who helped me to complete my Ph.D. Their advice and help have come in various situations. My special words of thanks goes to these people here.

First I wish to offer my sincere gratitude to my supervisor Prof. Mary Kay Pflum, for her valuable guidance given to me throughout the period of this project. She is an outstanding mentor and an excellent teacher. She always gave me the instruction to improve my professional writing and presentation skills.

I would like to thanks the lab members with whom I've worked together over the past few years in the Pflum lab, Sujith Suwal, Sujith Weerasinghe, Emily Aubie, Sun Choi, Musthfa Aboutaleb, Joe Duran, Todd Faner, Anita Chalasani, Satish Garre, Geetha Padige, Magdalene Wambua, Tony Young, Thilani Anthony, Maheeka Embogama, Pavithra Dehigama, Ahmed Fauda, and Danusha Nalawansha. I had a wonderful and an unforgettable time in the Pflum lab with you all.

I would also like to express my thanks to Dr. Joseph Caruso, Institute of Environmental Health Sciences, who did the mass spectrometry analysis.

Finally, I would like to thank my family members and friends for their help and encouragements during my graduate studies.

TABLE OF CONTENTS

LIST OF TABLES

LIST OF FIGURES

LIST OF SCHEMES

LIST OF ABBREVIATIONS

Amino Acids

A or Ala – alanine

C or Cys – cycteine

D or Asp – aspatate

E or Glu – glutamate

F or Phe – phenylalanine

G or Gly – gllycine

H or His – histidine

I or Ile – isoleucine

K or Lys – lysine

L or Leu – leucine

M or Met – Methionin

N or Asn - asparagine

P or Pro - proline

Q or Gin - glutamine

R or Arg - arganine

S or Ser - serine

T or Thr - threonine

V or Val - valine

W or Trp - tryptophan

X- any amino acid

Y or Try - thyrosine

Z – hydrophobic residue

Nucleic Acids

AMP – adenosine 5'-monophosphate

ATP - adenosine 5'-trihosphate

CoA – coenzyme A

DNA – deoxyribonucleic acid

NADH – nicotinamide adenine dinucleotide

ADP - adenosine 5'-diphosphate

ATP-γS– adenosine 5'-[γ-thio]triphosphate

cAMP – cyclic 3',5'-monophosphate

GTP - guanine 5'-triphosphate

RNA – ribonucleic acid

Proteins

Abl – Abelson kinase

AKT1- v-akt murine thymoma viral oncogene homolog 1

ASK1 (MAP3K5) - mitogen-activated protein kinase kinase kinase 5

BCR – breakpoint cluster region

CAMK4- calcium/calmodulin-dependent protein kinase IV

CBP – CREB binding protein

CDK1- cyclin-dependent kinase 1

CHK1- checkpoint kinase 1

CIP – calf intestinal phosphatase / alkaline phosphatase

CK1 – casein kinase

CK2 – casein kinase 2

CREB – cAMP responsive element binding protein

Csk – C-terminal Src kinase

DAPK1- death-associated protein kinase

EGFR – endothelial growth factor receptor

ELK1 – E 26 like protein

ErbB2 – eryhtrovlastic leukemia viral oncogene homolog 2

ERK1 – extracellular signal-regulated kinase 1

FLT1 - fms-related tyrosine kinase 1

FOS – c-fos protein

Grb2 – growth receptor bound protein 2

GRK5- G - protein-coupled receptor kinase 5

GSK3β- glycogen synthase kinase 3 beta

HIPK1- homeodomain interacting protein kinase 1

JAK3 – janus kinase 3

MAPK – mitogen activated protein kinase

BMP- myelin basic protein

MEK – mitogen activated or extracellular-regulated protein kinase

MLK1 (MAP3K9)- mitogen-activated protein kinase kinase kinase 9

MST1 (STK4) - serine/threonine kinase 4

mTOR – mammalian target of rapamycin

NEK2- NIMA-related kinase 2

NGF – neuronal growth factor

PAK1- p21 protein (Cdc42/Rac)-activated kinase 1

Pl3K – phosphoionositide 3 kinase

PKA – protein kinase A or cAMP regulated protein kinase

PP1 – protein phosphatase 1

PPTase – 4'-phosphopantehinyltransferase

Raf – protein kinase produced by the raf gene

Ras – protein kinase produced by the ras gene

RhoA – aplysia ras-related homolog A

RSK1- ribosomal protein S6 kinase 1

SA-Cy5 – streptavidin –Cy5

Sos 1 – son of sevenless

SPK – serine/threonine protein kinase

SRC- v-src sarcoma (Schmidt-Ruppin A-2) viral oncogene homolog (avian)

TC PTP- T-Cell Protein Tyrosine Phosphatase

TGase – transglutaminase

TGFβR2- transforming growth factor, beta receptor II

TPK – tyrosine protein kinase

TrkA – Trk proto-oncogene A

TRKA (NTRK1)- neurotrophic tyrosine kinase, receptor, type 1

Reagents

BME – β-mercaptoethanol

CDI – carbonyl diimidazole

DMF – dimethyl formamide

DTT – dithiothreitol

EDC – 1-ethyl-3-(3-dimethyl aminopropyl) carbodiimide hydrochloride

EDTA – ethylenediamine tetraacetic acid

FBS – fetal bovine serum

HOBt – N-hydroxy benzotriazole

NHS – N-hydroxy succinimide

TEA – triethylamine

TEAB – triethylammonium bicarbonate

TFA – trifluoroacetic acid

Tris– 2-amino-2-hydroxymethyl-propane-1,3-diol

Techniques

HPLC – high pressure liquid chromatography

IMAC – immobilized metal affinity chromatography

MALDI-TOF – matrix assisted laser desorption/ionization time-of-flight

MS – mass spectrometry

SDS-PAGE – sodiumdodecyl sulfate polyacrylamide gel electrophores

Chapter 1

Introduction: Protein Posttranslational Modification

(Portions of the text in this chapter were reprinted or adapted from: Senevirathne, C., Green, K. D., and Pflum, M. K. H. (2009) Kinase-Catalyzed Biotinylation of Peptides, Proteins, and Lysates, In *Current Protocols in Chemical Biology*, John Wiley & Sons, Inc. and Suwal, S., Senevirathne, C., Garre, S., and Pflum, M. K. (2012) Structural analysis of ATP analogues compatible with kinase-catalyzed labeling, *Bioconjugate chemistry 23*, 2386-2391)

Proteins undergo diverse modifications to regulate their functions and stability.[1] Protein modifications can occur after translation, and are commonly called posttranslational modifications (PTMs). PTMs enhance the cellular diversity of roughly 30,000 human genes. More than 100 PTMs have been recognized to date. Fifteen out of 20 amino acid residues have been identified with various PTMs, which include acetylation, acylation, adenylation, ADP-ribosylation, glycosylation, methylation, phosphopantetheinylation, phosphorylation, prenylation, sulfation, transglutamination, etc.[2] These PTMs influence various cellular processes, functions and disease formation. With a major role in biological systems, characterizing PTMs is important to understanding cell biology and disease formation.

1.1 Protein Phosphorylation

Protein phosphorylation was identified more than 100 years ago;[3] enzyme-mediated reversible phosphorylation was reported in 1954.[4] Kinase-catalyzed protein phosphorylation is an important PTM occurring in cells.[5] Phosphorylation is involved in a variety of biological processes including cell signaling, diseases, cancer, and immunosuppression.[6] Proteins kinases are the enzymes that are responsible for protein phosphorylation, and protein phosphatases are the enzymes that are involved in dephosphorylation.[5, 7] In phosphorylation, adenosine 5'-triphosphate (ATP) acts as a universal phosphate donor and the protein kinase assists in the transfer of a phosphate group from the γ position of ATP.[8] In eukaryote, phosphorylation

occurs on the hydroxyl group of serine, threonine, and tyrosine (Scheme 1.1).[9] In addition, histidine, arginine, and lysine phosphorylation (N-phosphorylation)[10] is possible in procaryote. When the neutral hydroxyl group is replaced with a negatively charged phosphate group, the activity of the protein may change, which influences cell biology.[1] At any given time, 30% of proteins are phosphorylated at serine, threonine, and tyrosine.[5]

Scheme 1.1: Reversible Protein Phosphorylation of Amino Acids Containing Hydroxyl Side Chains
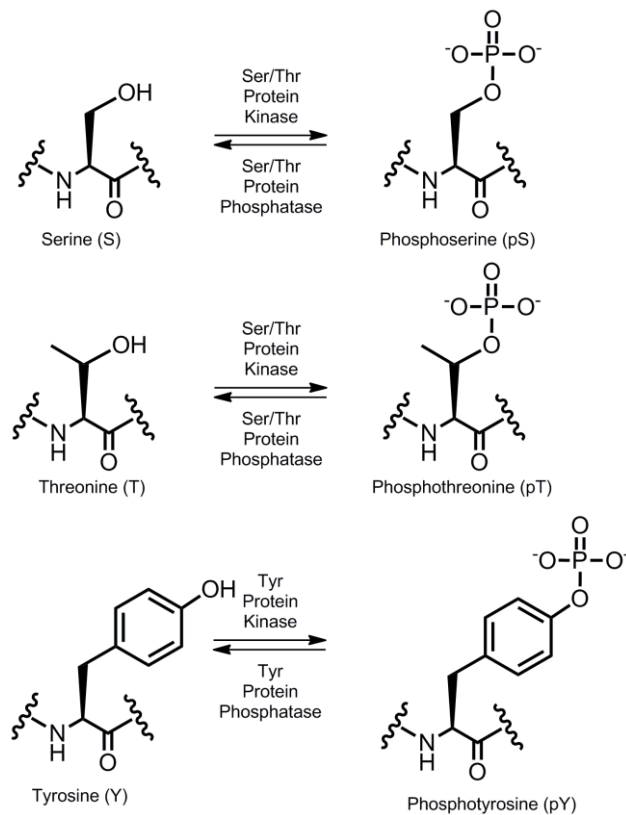
1.2 Phosphorylation and Protein Functions

Phosphorylation influences protein activity through a variety of mechanisms. Protein binding is enhanced upon phosphorylation. For example, p53 is a tumor suppressor transcriptional activator, which is stabilized after phosphorylation (Figure 1.1).[11] There are 22 phosphorylation sites identified on p53, which influence its stability.[11, 12] Stress signals such as UV radiation, DNA damage, etc, activate various kinases to phosphorylate p53.[13] This phosphorylation occurs sequentially, as phosphorylation of serine-15 leads to phosphorylation of additional sites.[14, 15] Upon phosphorylation, p53 is stabilized and dissociated from its inhibitor MDM2,[13] and binds to transcriptional activator p300.[16] p53 binding to DNA enhances gene transcription to protect the cell from stress condition.[17]
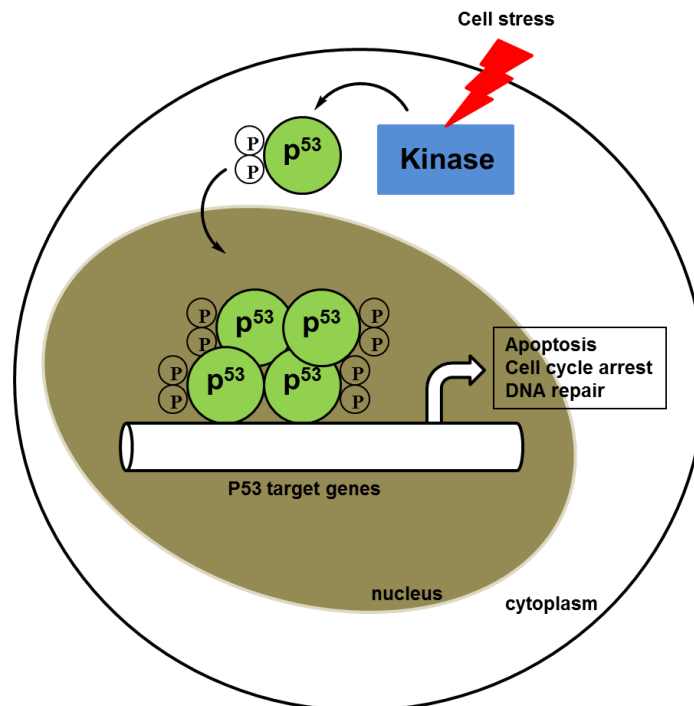
Figure 1.1: Stabilization of p53 with Phosphorylation. Stress signals stimulate several kinases to phosphorylate p53. Upon phosphorylation, p53 is stabilized, translocated to the nucleus, and bound to DNA, which activates transcription of different genes.

Another example of protein-protein interactions that are dependent on phosphorylation involves CREB (cyclic adenosine 3', 5'-monophosphate responsive element binding) protein and CBP (CREB binding protein) (Figure 1.2).[18, 19] Upon phosphorylation, the neutral serine-133 on CREB becomes a negatively charged phosphoserine, which alters its hydrogen bond donor ability into a hydrogen bond acceptor. Once phosphorylated at serine-133, a hydrogen bond can form between CREB S-133 and Y-658 on CBP. Phosphorylation at S-133 is critical for interaction of two proteins, CREB and CBP.[18] The transcriptional activity of CREB is greatly enhanced upon CBP binding.
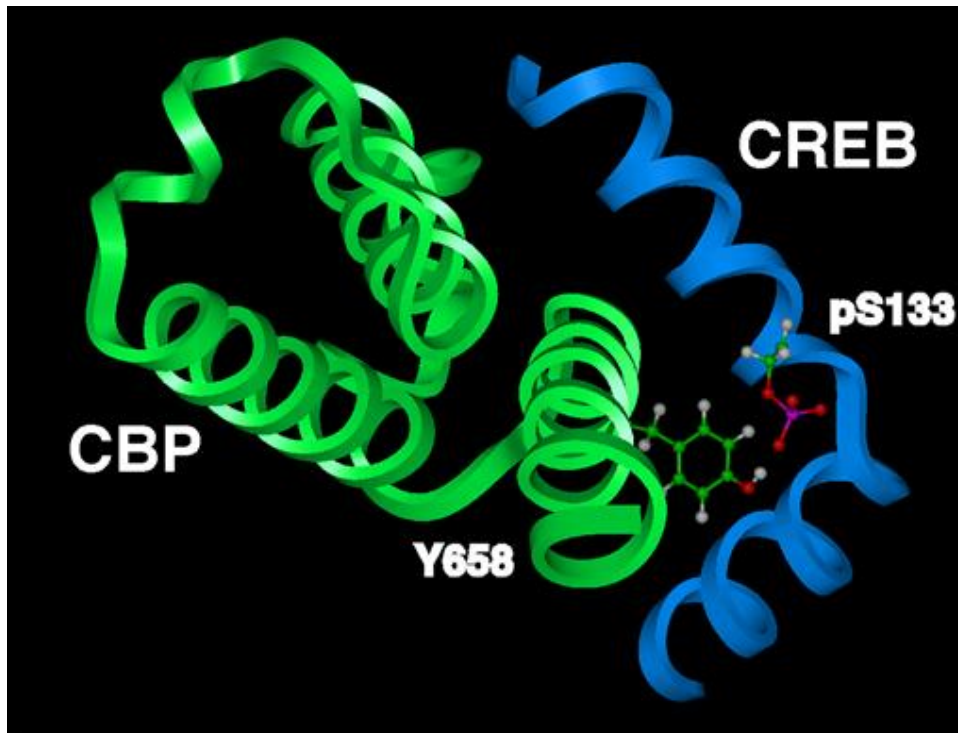
Figure 1.2: Phosphorylation of CREB Facilitates Interactions with CBP. Structure of CREB bound to CBP highlighting phosphoserine 133 (pS133) in red interacting with tyrosine 658 (Y658) in green.

Kinase-catalyzed phosphorylation also influences cell growth, arrest and apoptosis, by mediating cell signaling cascades.[20] For example, signaling pathways depend on phosphorylation to begin neuronal cell growth (Figure 1.3).[21] Binding of neuronal growth factor (NGF) to TrkA leads to autophosphorylation of tyrosine on TrkA (Neurotrophic tyrosine kinase receptor type 1).[21] The phosphotyrosine of TrkA then binds to Grb (Growth factor receptor-bound protein), which binds to Sos (Son of sevenless). The Ras (protein kinase produced by the ras gene)/Raf (protein kinase produced by the raf gene)/MEK (Mitogen activated or extracellular signal regulated protein kinase) pathway is activated by Sos. Activation of the Ras/Raf/MEK pathway promotes phosphorylation of MAPK (Mitogen activated protein kinase).[22] Phosphorylated MARK leads to phosphorylation of ELK-1 (E-26 like protein 1) which then activates the transcriptional machinery for cell growth. MARK can also stimulate p21^{CIP}, which is responsible for growth arrest. Additionally, the activity of RhoA (Ras homolog gene family, member A) can increase via activated Ras. Activated RhoA can stop growth arrest by inhibiting MARK activity toward p21^{CIP}.[21] Although only one example, this kinase signaling pathway demonstrates the fundamental role of phosphorylation in cell biology. The next section focuses on the involvement of phosphorylation in disease formation.
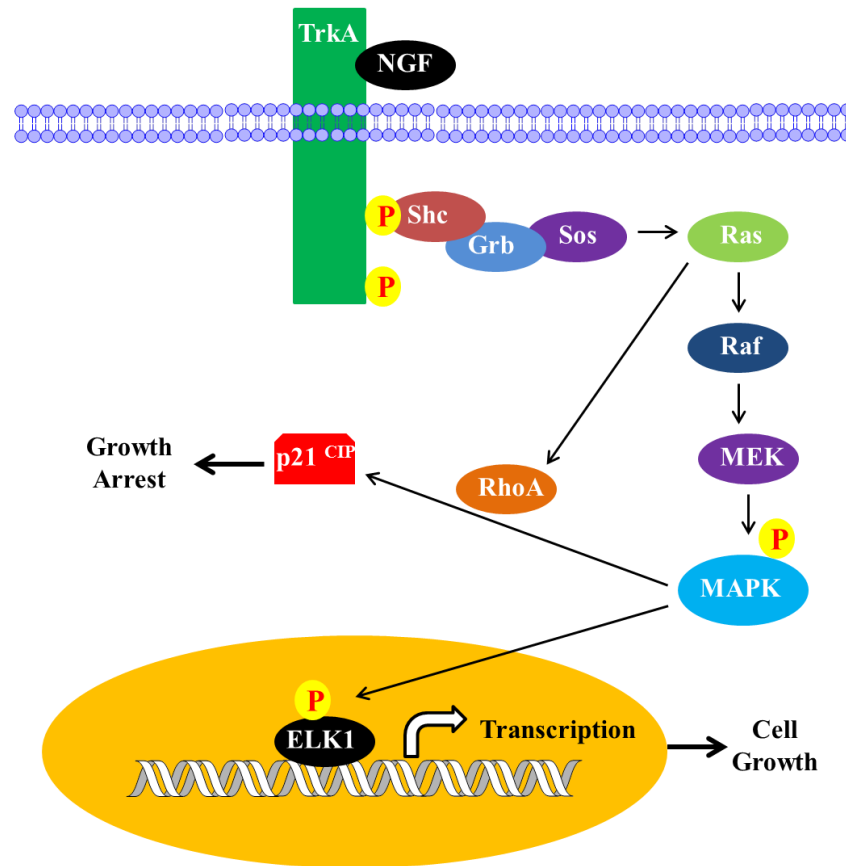
Figure 1.3: Signaling Cascade of Phosphorylation Dependent Cell Growth. NGF binding to TrkA leads to TrkA autophosphorylation. This phosphorylation results in interaction of the receptor with various kinases and activation of the Ras/Raf/Mek pathway. Phosphorylated MAPK initiates phosphorylation of ELK-1, which results in cell growth.

1.3 Protein Phosphorylation in Disease

A number of kinases and phosphorylation pathways are associated with diseases. Aberrant phosphorylation levels and elevated kinase activities are responsible for disease formation, and are highlighted here. As one example, translocation of chromosome 9 and 22 leads to fusion of the Abelson kinase (Abl) gene with the BCR (break point cluster) gene to produce the Bcr-Abl gene fusion.[23] The Bcr-Abl protein product of this gene fusion has higher kinase activity than regular Abl kinase, which leads to formation of chronic myelogenous leukemia (CML).[23-27] Gleevec, an Abl kinase inhibitor and an FDA approved drug, is used to treat CML.[28]

Additionally, several other kinases are linked with cancer formation, such as casein kinase 2 (CK2),[29] phosphoinositide 3-OH kinase (PI3K),[30] cellular Src (c-Src),[31] protein kinase B (PKB),[32] and epithelial growth factor receptor (EGFR).[33] Various other signaling pathways influenced by kinases are also linked to cancer, including PI3K/PKB, Ras-Raf-ERK, JAK-signal transducer and activator of transcription (STAT) pathways.[34, 35]

1.4 Kinase inhibitors

Protein phosphorylation and kinase enzymes play critical roles in disease formation. Hence many pharmaceutical drugs have developed to target kinases (Table 1.1 and Figure 1.4). A number of FDA approved kinase inhibitors are used to treat a wide range of diseases, including diabetes, rheumatoid arthritis, cancer, and immunosupression.[6] However cancer is the most targeted disease. Rapamycin and Everolimus are two natural products that have the same core structure, and are used to treatment of immunosupression by targeting mTOR. Staurosporine is a natural product, used as a general kinase inhibitor used in laboratory research only. Fasudil inhibits ROCK and is used for the treatment of cerebral vasospasms. However, this

sulphonamide is approved only in Japan. Iressa and tarceva both target EGFR kinase for treatment of cancer. Nexavar targets Raf-1 for cancer treatment. Axitinib and Sunitinib target multiple kinases such as VEGFR-1, 2, 3 and PDGFR. Some approved drugs bind to more than one kinase, which may lead to unnecessary side effects.[6]

The main drawback of kinase inhibitors is their non-specific binding to many kinases. Because of the highly conserved active sites of kinases, drugs do not generally differentiate between members of the kinase family. Hence, it is extremely difficult to synthesize molecules that selectively inhibit a single kinase. Gleevec (Imatinib) which selectively inhibited tyrosine kinase Bcr-Abl was the first selective kinase inhibitor. Other examples of selective kinase inhibitors are DRB (5,6-Dichloro-1-β-D-ribofuranosyl benzimidazole) and H8 (N-[2-(methylamino) ethyl]-5-isoquinolonesulfonamide), which selectively inhibit CK2 and PKA, respectively.

Kinase inhibitors show diverse structural features, including riboses, glucoses, polyketides, sulfonamide, piperazines, and heterocyclic derivatives. With the interest of kinases as drug targets, understanding their function and structure has been useful.

Table 1.1: List of FDA Approved Kinase Inhibitors Found in Market [6, 36]

Inhibitor	Kinase Targeted	Disease	Company	Status
Rapamycin	m-TOR	Immunosuppression	Wyeth-Ayerst	FDA approved (1999)
Gleevec	Bcr-Abl	Cancer	Novartis	FDA approved (2001)
Iressa	EGFR	Cancer	Astra-Zeneca	FDA approved (2003)
Tarceva	EGFR	Cancer	OSI Pharm.	FDA approved (2004)
Nexavar	Raf-1	Cancer	Bayer	FDA approved (2005)
Sunitinib	VEGFR, PDGFR	Cancer	Pfizer	FDA approved (2006)
Crizotinib	ALK, ROS-1	Cancer	Pfizer	FDA approved (2011)
Vemurafenib	BRAF	Cancer	Roche	FDA approved (2011)
Axitinib	VEGFR, PDGFR	Cancer	Pfizer	FDA approved (2012)
Bosutinib	Bcr-Abl, Src	Cancer	Pfizer	FDA approved (2012)
Fasudil	ROCK	Cerebral vasospasm	Asahi Chem. Ind	Japan approved (1995)
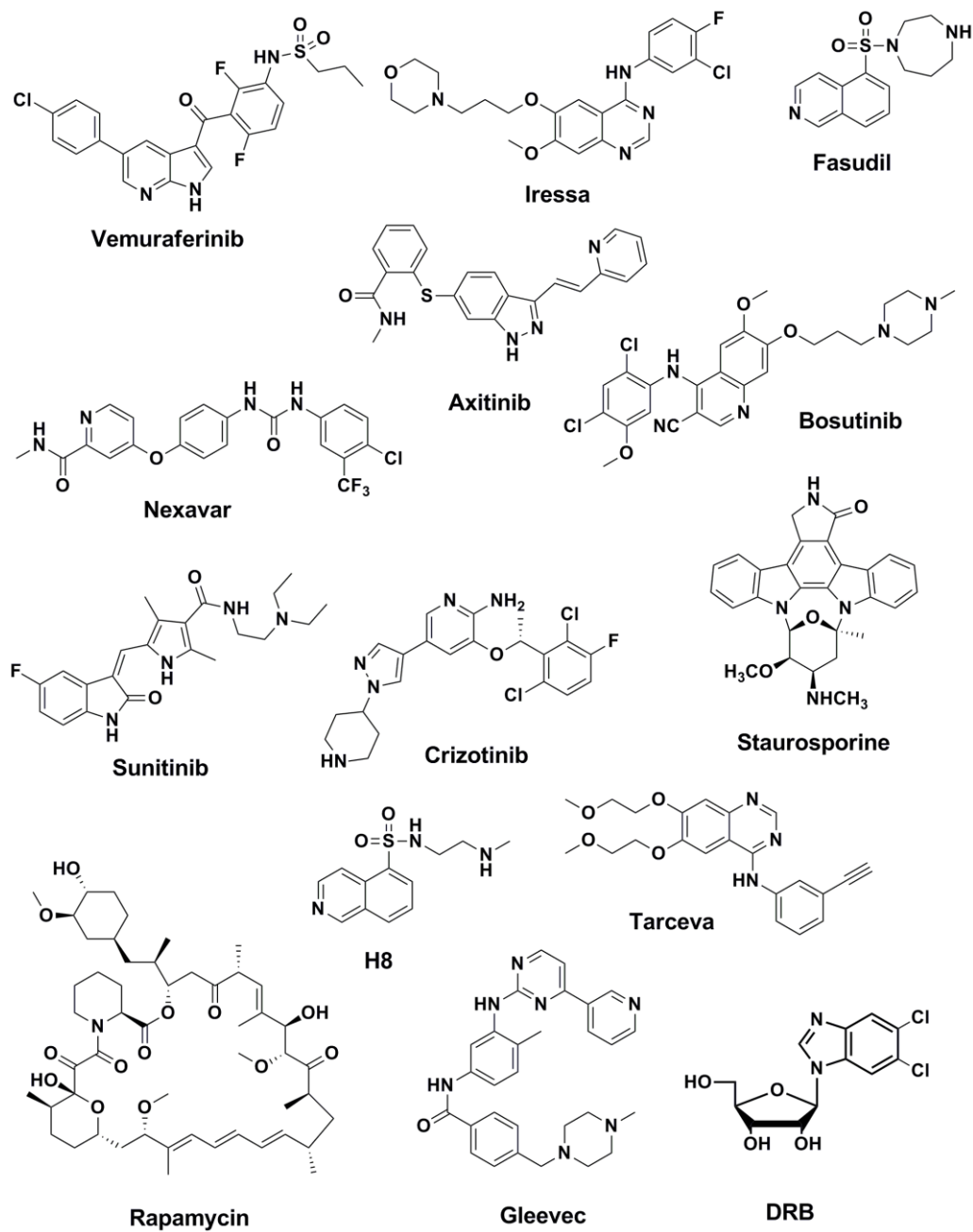
Figure 1.4: Structural Diversity of Kinase Inhibitors. Structure of some kinase inhibitors are shown here. Sturosporine, H8, and DRB are used only in laboratory research. All others are used in treatment of various diseases (see Table 1.1).

1.5 Protein Kinases: Family, Structure, and Enzymatic Mechanism

Kinase enzymes catalyze protein phosphorylation. There are over 500 human kinases known.[37] Protein kinases are classified into two different groups-the serine/threonine protein kinases (SPK) and tyrosine protein kinases (TPK).[38] These classifications are based on each enzymes preferred amino acid substrate. There is a third class of kinases that phosphorylate both serine/threonine and tyrosine side chains, but they not well characterized. One kinase enzyme can act upon multiple protein substrates.[39] Human kinases are divided into 7 major groups according to sequence similarities in their catalytic sites (Figure1.5).[37]
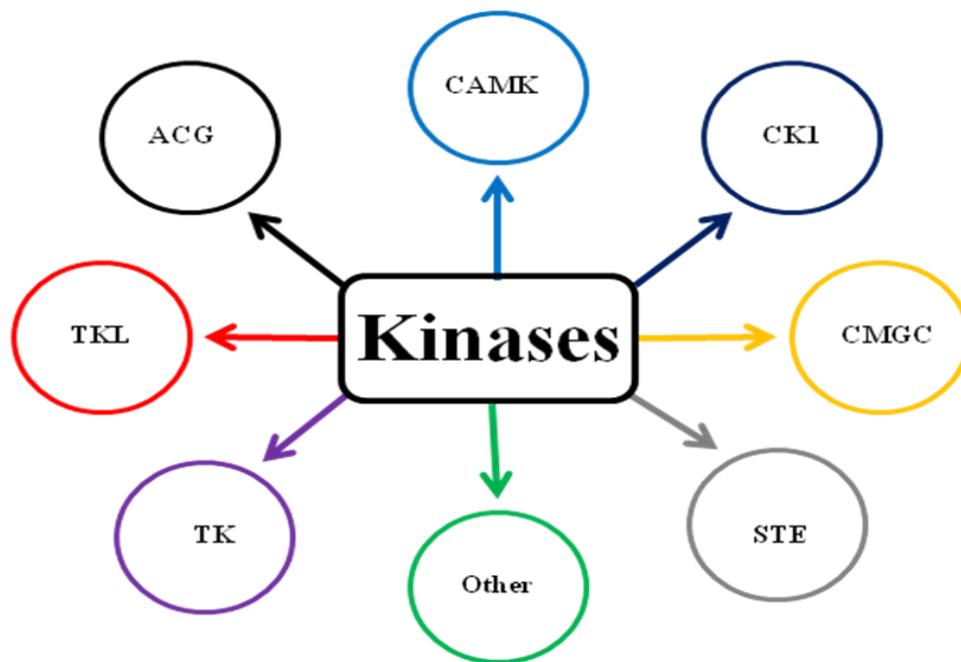
Figure 1.5: Main Groups of Human Kinases. Human kinases are mainly divided into 7 major groups including; **ᵃAGC:** Containing PKA, PKG, PKC families; **CAMK:** Calcium/calmodulin-dependent protein kinase; **CK1:** Casein kinase 1; **CMGC:** Containing CDK, MAPK, GSK3, CLK families; **STE:** Homologs of yeast Sterile 7, Sterile 11, Sterile 20 kinases; **TK:** Tyrosine kinase; **TKL:** Tyrosine kinase-like. **Other:** other kinases not belong to above groups.

Scheme 1.2: Mechanism of Protein Phosphorylation Illustrated with a Serine Residue
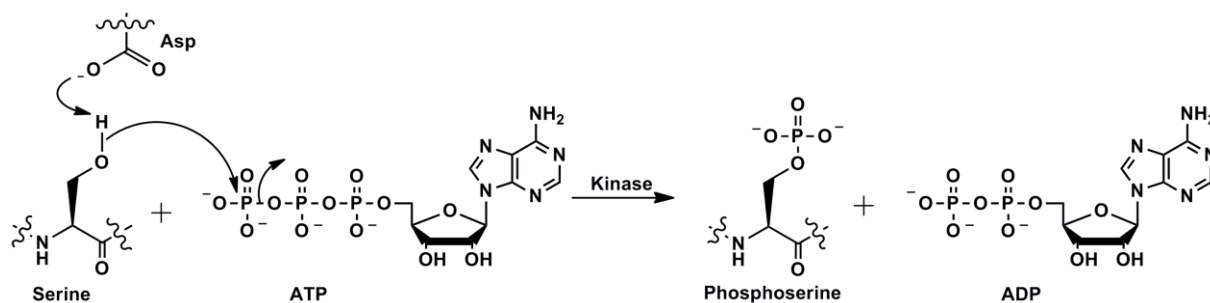
As mentioned in section 1.1, ATP acts as a phosphate donor and binds to the active site of kinases.[8] The catalytic sites of protein kinases display very similar primary structures.[40] Generally there are nine conserved amino acids found in kinase catalytic sites,[41] including G52, K72, Q91, D166, N171, D184, G186, Q208, and R280. Six of these residues stabilize the triphosphate and three of them interact with the adenine base portion. Within the kinase family, this core active site structure is conserved.[38] The kinases consist of two domains, which contain α-helical and β-sheets. The linker portion between the α-helical and β-sheet domains generates the binding region for the ATP molecule.[42] The α-helical domain contains the substrate binding site. The substrate binds to the active site of the kinase through interactions with specific amino acids in the substrate binding site (Figure 1.6).[38] ATP binding to the active site occurs in such a way that adenine portion points inside the conserved site and its phosphates point away from the pocket. ATP binding brings the α-helical and β-sheet domains in close proximity to facilitate tight binding of ATP as well as binding of the protein substrate to the kinase.[43] Hence, the protein kinase forms a ternary complex with its protein substrate and ATP cosubstrate in close proximity to achieve enzymatic phosphorylation.[8] ATP cosubstrate binding is stabilized by two divalent metal ions, either Mg^{2+} or Mn^{2+}, which chelate with charged amino acid residues within

the catalytic site (Figure 1.6).[38] D166 acts as a base during the kinase reaction by removing hydrogen from the hydroxyl group on the protein substrate, to making it nucleophilic.[38] The interactions between the metal ion and oxygen atoms in the phosphoryl group hold the ATP appropriately for nucleophilic attack of the γ-phosphate by the substrate hydroxyl. This produces a phosphorylated substrate and ADP as a byproduct (Scheme 1.2).

The enzymatic phosphorylation mechanism has two possibilities (Figure 1.7).[44, 45] First, an associative mechanism was proposed,[46] which is similar to an S_N2 (bimolecular nucleophilic substitution) type mechanism. In the associative transition state, bonds between the nucleophilic oxygen of the substrate and the γ-phosphate of ATP are formed simultaneously with the ADP leaving group still connected (Figure 1.7 A). Interestingly, recent experimental evidence has been more consistent with a dissociative type transition state for phosphorylation,[44,45,47] similar to S_N1(unimolecular nucleophilic substitution) type reaction. In the dissociative transition state, the ADP leaving group departs in advance of nucleophilic oxygen attack on the electrophilic γ-phosphate of ATP (Figure 1.7 B). Currently, the dissociative mechanism is considered the most appropriate for many kinases.[44, 45, 47]
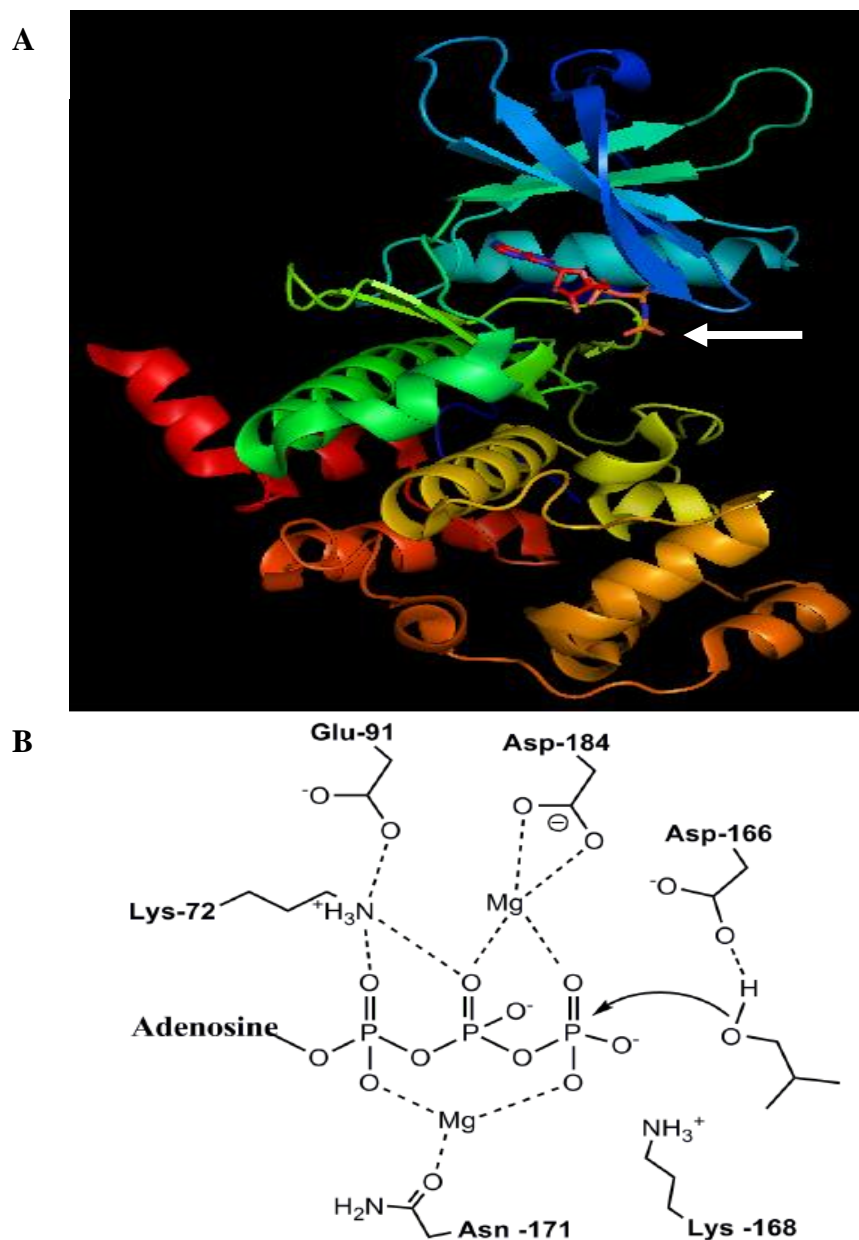
Figure 1.6: Crystal Structure of PKA with Amino Acid Residues. (A) Crystal structure of PKA with peptide substrate inhibitor and Solvent expose ATP. (B) Kinase-catalyzed phosphorylation mechanism showing the major interaction of PKA enzyme with protein substrate, ATP and metal ions with side chains (GenBank ID 6755076, PDB 1ATP).
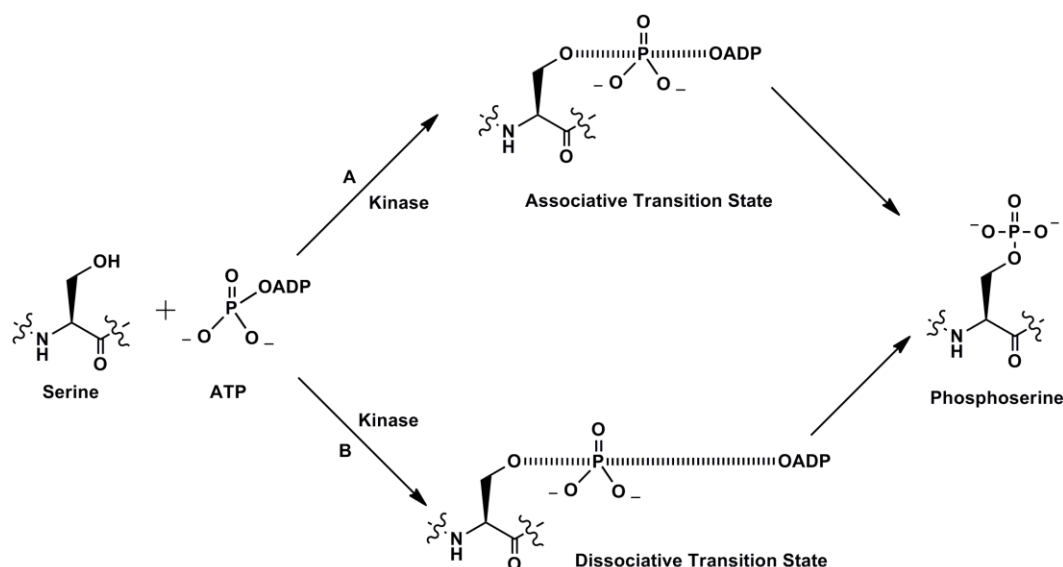
Figure 1.7: Proposed Associative vs Dissociative Phosphorylation Mechanism. (A) The leaving group and incoming nucleophile remain attached to the reactive center in an associative mechanism. (B) The leaving group departs in advance of nucleophile attack at the reactive center in a dissociative mechanism.

The peptide or protein substrate must contain a consensus sequence that can be recognized by a specific kinase.[38] Phosphorylation occurs when the consensus sequence of the substrate is recognized by the appropriate protein kinase, which directs phosphorylation of the serine, threonine, or tyrosine within the consensus sequence. Generally, the amino acids immediately surrounding the phosphorylated residue are critical for kinase recognition. Consensus sequences for many kinases are known and indicate that specific kinases can recognize basic, acidic, hydrophobic or proline residues to direct phosphorylation (Table 1.2). For example, Abl protein kinase is a tyrosine kinase with a hydrophobic consensus sequence of I/V/L-Y-X-X-P/F (X represents any amino acid).[48] Casein Kinase II (CK2) is a serine/threonine kinase with an acidic consensus sequence of S/T-X-X-D/E.[49] Another serine/threonine kinase,

c-AMP dependent protein kinase (PKA) prefers to phosphorylate peptides having a basic amino

acid consensus site of R-R/K-X-S/T.[50]

Table 1.2: Consensus Sequence of Selected Protein Kinases

Kinase	Consensus sequence[51]
Abl	I/V/L-**Y**-X-X-P/F
AKT1	R-X-R-XX-**S/T**
Aurora-A	R/K/N-R-X-**S/T**-B
CDK 1	**S/T**-P-X-R/K
CHK 1	R-X-X-**S/T**
CK2	**S/T**-X-X-D/E
ERK 1	P-X-**S/T**-P
GRK 5	D/E$_n$-**S/T**-X-X-X
GSK 3	X-**S/T**-X-X-X-Sp
PKA	R-R-X-**S/T**-Y
SRC	E-E-I-**Y**-E/G-X-F

1.6 Kinase cosubstrate promiscuity

1.6.1: ATP-γS

Many PTM enzymes show cosubstrate promiscuity.[52-73] Indeed, kinases also show

cosubstrate promiscuity with different ATP analogs. The first reported kinase cosubstrate analog

was adenosine 5'-[γ-thio]-triphosphate (ATP-γS).[74, 75] ATP-γS is an analog of ATP where O is

replaced by S at the γ-phosphate. ATP-γS acts as a cosubstrate for many kinases, making a

thiophosphorylated product (Figure 1.8). The reactivity of thiol on phosphate is used for identify

and purify of thiophosphorylated products. A similar phosphorylation mechanism to ATP occurs

with ATP-γS, with hydroxyl attack on the γ-phosphate group producing a thiophosphorylated

product and the byproduct ADP. However, kinetic analysis with ATP-γS showed low catalytic

efficiency compared to ATP,[76-79] known as the thio effect. Despite the poorer catalytic

efficiency, ATP-γS is widely used in the proteomic field,[76, 80-83] due to the stability of

thiophosphorylated proteins towards phosphatases,[74, 84-86] which can lead to identification of low abundance proteins.
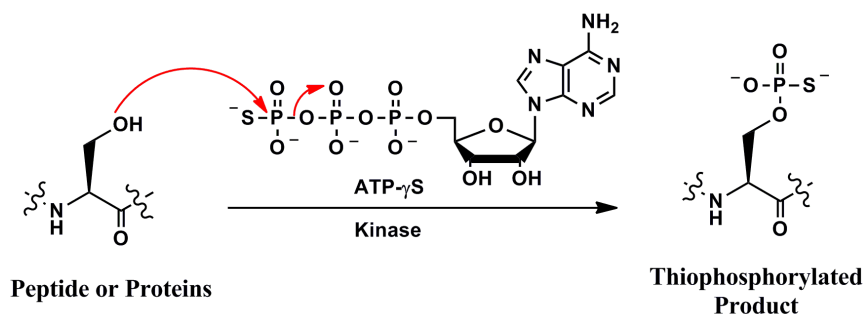
Figure 1.8: Kinase-Catalyzed Phosphorylation with ATP-γS. Serine, threonine, or tyrosine hydroxyl groups on proteins attack the γ-thiophosphate group on ATP-γS to label proteins with a thiophosphoryl group.

In addition to the ATP-γS analog, another class of ATP analogs was synthesized for selective phosphorylation with specific kinases (Figure 1.9).[82, 83] In this case, the ATP analog is modified at both the γ-phosphate group and the adenine base. Kinases were mutated to selectively bind the base modified ATP analogs. This method was used for specific purification of substrates for MS analysis (more details discussed in chapter 4).[87] This method was developed by Shokat and coworkers,[82, 83] and was used to identify substrates for a specific kinases. The method has been applied to various engineered kinases to identify their substrates.

As a significant extension of the ATP-γS analog, the Pflum lab was interested in adding large groups at the γ-phosphate ATP for kinase transfer. The crystal structures of many protein kinases have been reported, such as those for PKA, CK2 and Abl[88-90]. Analyses of crystal structures of protein kinase active sites showed that the γ-phosphate of ATP is solvent-exposed (Figure 1.6). With this analysis, we hypothesized that other γ-phosphate modified ATP analogs should act as kinase cosubstrates. In fact, our group showed that several γ-phosphate modified

ATP analogs act as cosubstrates for kinase-catalyzed phosphorylation,[91-93] as discussed bellow. These analogs can be used to understand and characterize cell signaling pathways leading to disease.
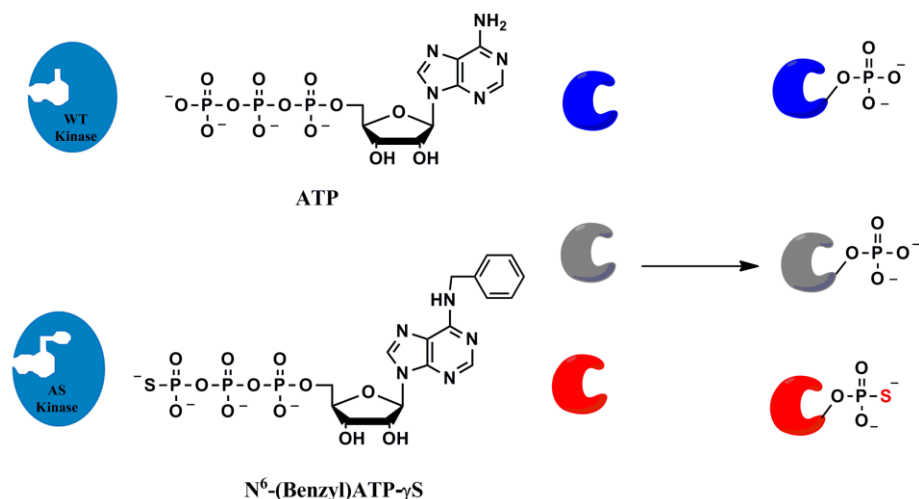
Figure 1.9: Phosphorylation of modified ATP-γS with Mutant Kinase. Cell lysates were incubated with mutant kinases and modified N[6]-Benzyl-ATP-γS. Substrates for the mutant kinase were labeled as thiophosphorylated products. Thiophosphorylated products were purified and identified by MS analysis (more details discussed in chapter 4).

1.6.2: ATP-biotin

To initially validate the cosubstrate tolerance of kinase, we performed kinase-catalyzed biotinylation with an ATP-biotin analog, along with recombinant kinases and peptide substrates (Figure 1.10).[91] Establishing that a kinase of interest is compatible with ATP-biotin was necessary before visualizing phosphoproteins from a complex cellular mixture. Commercially available ATP-biotin was incubated with three synthetic peptides containing either serine (LRRA**S**LG), threonine (RRREEE**T**EEE), or tyrosine (EAI**Y**AAPFAKKK) and the corresponding kinase PKA, CK2, and Abl, respectively. Similar to biotinylation, phosphorylation was performed with ATP as a control reaction. To determine the success of the biotinylation reaction with the peptide substrates, a quantitative mass spectrometric (MS)

analysis method was performed. The relative conversion percentages were calculated, assuming reactions with ATP to be 100% complete (Table 1.3). This initial experiment provided evidence for the cosubstrate promiscuity of kinases.[91, 94]
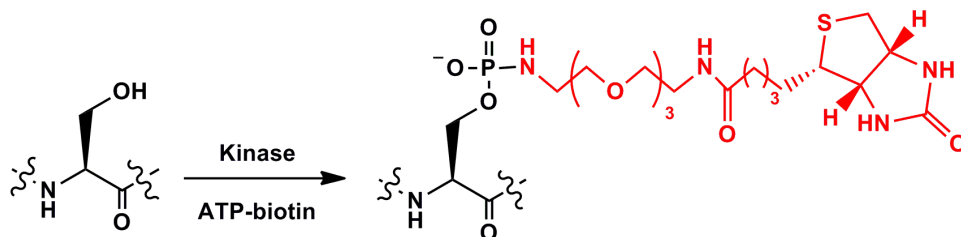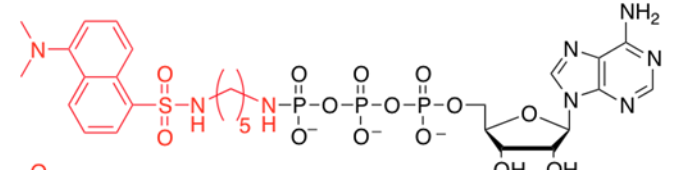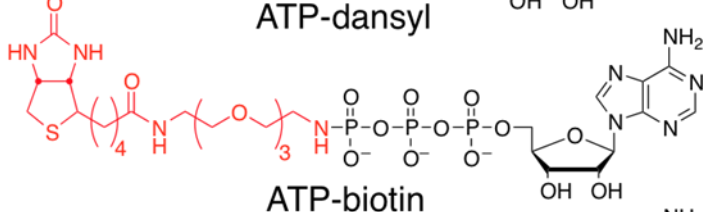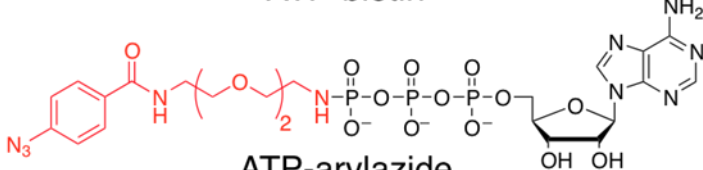
Figure 1.10: Kinase-Catalyzed Biotinylation. Peptides or proteins modified with a phosphorylbiotin group upon biotinylation with ATP-biotin in the presence of kinases. See Table 1.3 for the structure of ATP-biotin.

With the success of peptide labeling using ATP-biotin, the tolerance of kinases to ATP-biotin was further tested with full length protein substrates. Kinase-catalyzed biotinylation was performed with ATP-biotin, CK2 and a full-length protein substrate (β-casein). Biotinylation of full-length protein substrates was analyzed using gel electrophoresis followed by visualizing the biotin tag using an SA-HRP (Streptavidin-horseradish peroxidase) conjugate. The biotinylation reaction was validated by observing biotin on the protein product after gel analysis.[91] In addition to labeling known substrates of a specific kinase *in vitro*, the labeling of substrates in mammalian cell lysates provides a physiologically relevant means of monitoring kinase activity. We found that ATP-biotin collaborates with cellular kinases to biotinylate endogenous substrates in HeLa cell lysates. [91] The results suggest that kinase-catalyzed biotinylation is generally successful using mammalian cell lysates to probe endogenous cellular kinases and substrates.

Table 1.3: Kinase-catalyzed labeling with previously reported ATP analogs [91-93]

ATP analog	PKA	CK2	Abl
ATP-dansyl	91%	81%	87%
ATP-biotin	79%	56%	80%
ATP-arylazide	86%	51%	78%

1.6.3: ATP-dansyl

With the success of kinase-catalyzed biotinylation, we were interested in testing the compatibility of kinases with other γ-phosphate modified ATP analogs. To test additional analog compatibility, commercially available ATP-dansyl was employed (Figure 1.11).[92] Like ATP-biotin, ATP-dansyl was incubated with peptides in the presence of their corresponding kinase PKA, CK2 and Abl, respectively. Quantitative MS analysis was used to analyze the efficiency of dansylation compared to phosphorylation (Table 1.3). These data indicated that ATP-dansyl was also successfully used as a cosubstrate for kinase-catalyzed phosphorylation.[92]
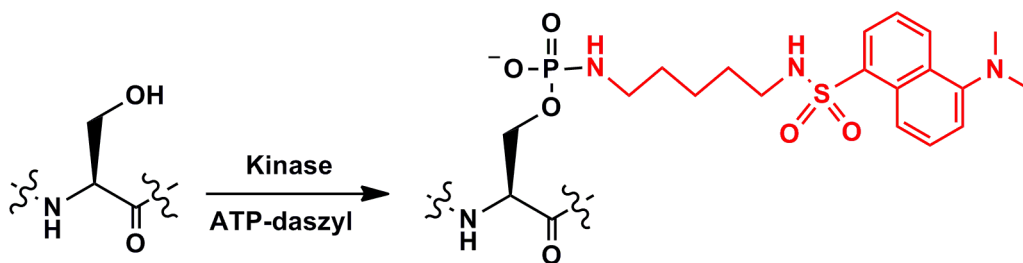
Figure 1.11: Kinase-Catalyzed Dansylation. Peptides modified with a phosphoryldansyl group upon dansylation with ATP-dansyl in the presence of kinases. See Table 1.3 for structure of ATP-dansyl.

With the success of the kinase-catalyzed dansylation of peptides, we further characterized the reaction by conducting kinetics measurements. Using an absorbance assay,[95, 96] measurements with PKA were taken in the presence of ATP vs. ATP-dansyl as cosubstrates. ATP-dansyl maintained a similar K_M value of 23 μM, compared to 24 μM K_M of ATP, indicating γ-phosphate modification did not alter the active site binding. In terms of k_{cat}, ATP-dansyl had a 9-fold reduced value compared to ATP, indicating that dansylation is slower than phosphorylation.[92] These results indicate that kinases permissively accept ATP analogs containing different functional probes, opening the door for the use of multiple γ-phosphate modified ATP analogs in kinase-catalyzed phosphoprotein labeling reactions.

1.6.4: ATP-arylazide

Kinase-catalyzed biotinylation and dansylation demonstrated the promiscuity of kinases towards the γ-phosphate modified ATP analogs. To increase the applicability of γ-phosphate modified ATP analogs as a biological tool, we created an ATP analog containing a photocrosslinking group attached at the phosphate (ATP-ArN$_3$) to covalently link phosphoproteins to kinases in a phosphorylation-dependent manner (Figure 1.12).[93] To understand the compatibility of this photocrosslinker, the kinase reaction was performed with synthetic peptides as describe earlier. As was observed with ATP-biotin and ATP-dansyl, ATP-ArN$_3$ served as a kinase cosubstrate with high conversion percentages (Table 1.3).[93]
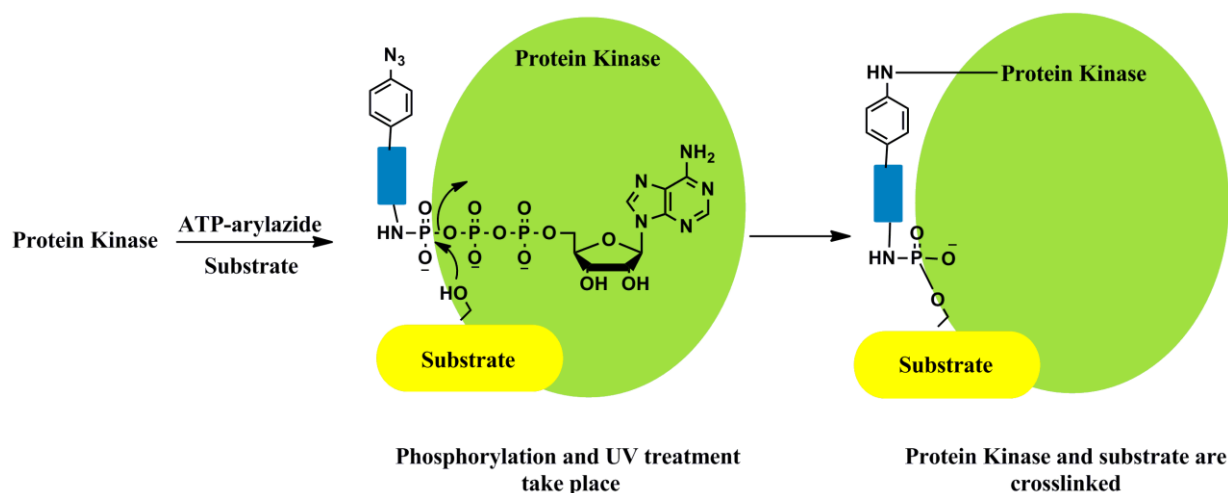
Figure 1.12: Kinase-Substrate Crosslinking with ATP-arylazide. Protein substrates are crosslinked with enzymes upon phosphorylation with ATP-arylazide under UV irradiation. See the Table 1.3 for structure of ATP-arylazide.

To test if the analog would promote crosslinking of the kinase to substrate, we used phosphorylation of casein by CK2 as a model system. SDS-PAGE and western blot analysis were used to identify the kinase-substrate complex. Upon UV irradiation, photocrosslinking with ATP-ArN$_3$ resulted in the appearance of higher molecular weight species consistent with crosslinked complexes of kinase and substrate.[93] In contrast, no higher molecular weight spots were observed with ATP under the same conditions. To assure that the higher molecular weight species was phosphorylation dependent, the phosphoramidate bond connecting the substrate and kinase was cleaved using acid treatment. As expected, the higher molecular weight species was reduced after TFA cleavage.[93] In addition, an antibody specific to the catalytic subunit of CK2 recognized the higher molecular weight species indicated the presence of CK2.[93] All these observations support the formation of kinase substrate crosslinked products via kinase dependent phosphorylation with ATP-ArN$_3$.[93]
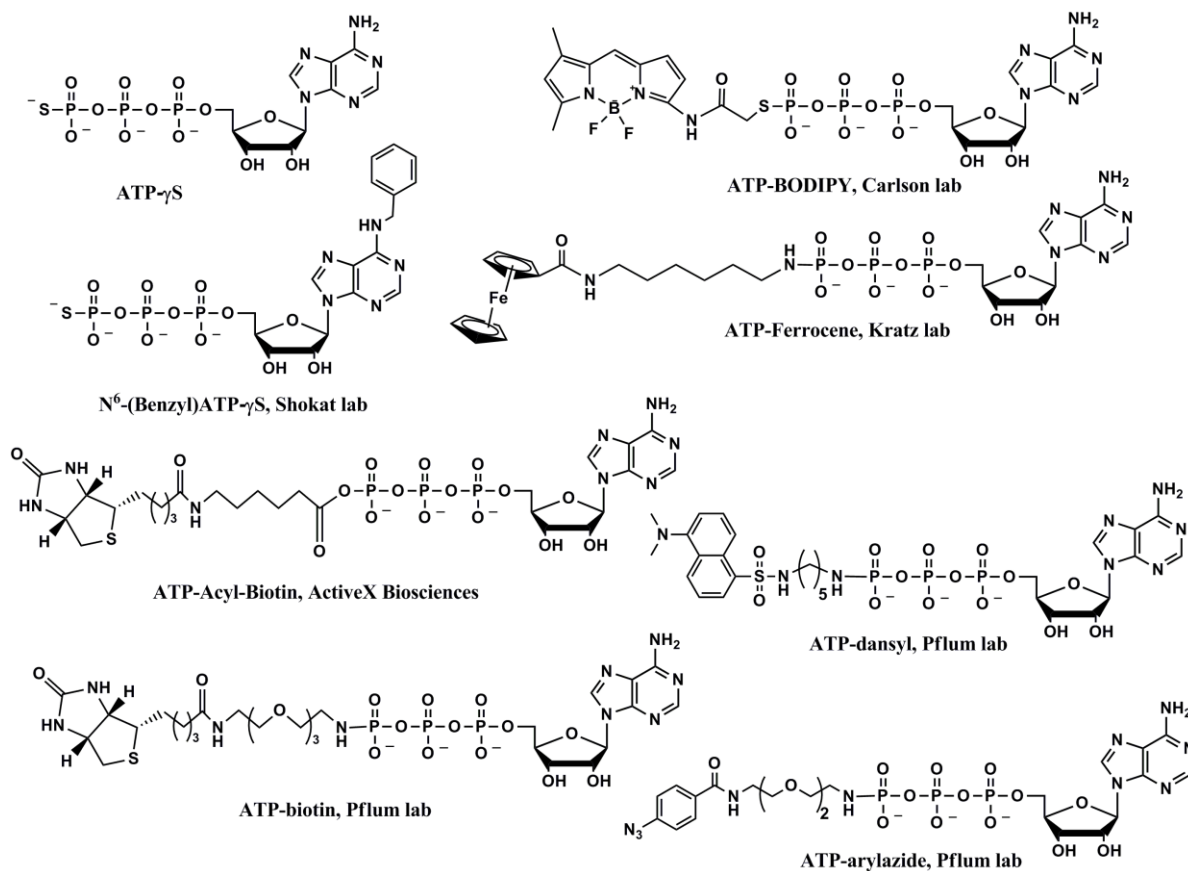
Figure 1.13: Diversity of γ-Phosphate Modified ATP Analogs. Structures of ATP analogs containing various detection tags are shown here. Applications of all these individual compounds were discussed in the text.

1.6.5: ATP-BODIPY

In addition to the ATP analogs studied in the Pflum lab, recently different types of γ-phosphate modified ATP analogs were reported (Figure 1.13). ATP-BODIPY, γ-phosphate modified ATP, was used to label protein in an activity-dependent manner.[97] In this specific case, histidine residues on histidine kinase were autophosporylated with extracellular signal. Then the aspartic acid of response regulator protein attacked phosphate group of histidine kinase. Hence the detection of phosphorylation event is important to understand the activity of histidine kinases. However the phosphoamidate bond on phosphor-histidine is much more labile with very short half-life.[98] Therefore a fluorophore was attached to the ATP using a sulfur atom instead nitrogen (Figure 1.14),[97] which formed a more stable intermediate. This ATP-BODIPY showed competitive binding with ATP, and was applied to measure the activity of histidine kinase catalyzed phosphorylation (Figure 1. 14).[97]
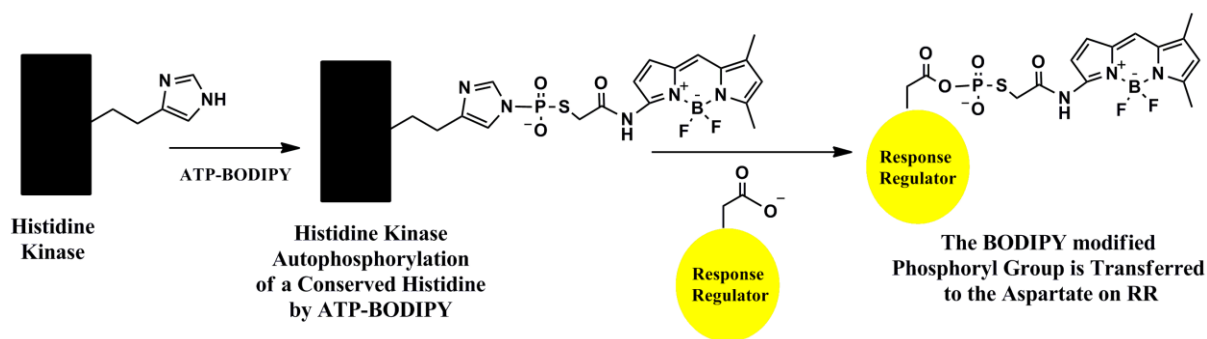
Figure 1.14: Autophosphorylation of Histidine Kinase with ATP-BODIPY. Histidine kinase undergoes autophosphorylation with ATP-BODIPY (See Figure 1.13 for structure) to label the histidine residue with fluorescent modification upon stimulation, with subsequent transfer of the modification to the aspartic acid of response regulator.

1.6.6: ATP-ferrocene

ATP-ferrocene was also successfully used in phosphorylation reactions to transfer the ferrocene-phosphate group to peptide or protein substrates (Figure 1.15).[99] This modification was detected electrochemically and with anti-ferrocene antibodies. Additionally, γ-phosphate modified ATP analogs were shown to compete with ATP for kinase binding.This analog was used to monitor the activity of kinases and identification of kinase inhibitors.[99]
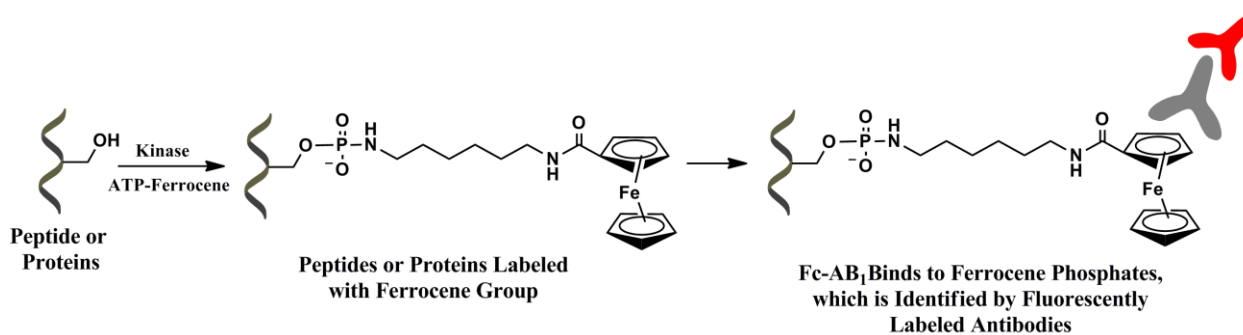
Figure 1.15: Kinase-Catalyzed Phosphorylation by ATP-ferrocene. Peptides or proteins were labeled with ferrocene-phosphate modification upon phosphorylation with kinase and ATP-ferrocene (See Figure 1.13 for structure). The ferrocene-phosphate modification can be identified by antiferrocene antibodies.

1.6.7: ATP-acyl-biotin

Beyond substrate labeling, γ-phosphate modified ATP analogs were also used to label and identify kinases in complex mixtures.[100, 101] This method is based on ATP binding to the active site of kinases. With few exceptions, protein kinases have two conserved lysine residues near the active site.[37, 90, 102] One can be found in the ATP binding region, while the other is found near the C-terminus. In addition, co-crystal structures of kinases indicated that these lysine residues are close to the γ- and β-phosphates of ATP.[90] Hence this method was able to identify most protein kinases. Once ATP-acyl-biotin is bound to the kinase, the acyl-phosphate group is positioned towards a conserved lysine residue in the active site, allowing the amine on lysine to attack the acyl group to release ATP. The reaction forms a covalent bond between kinase and biotin tag through an amide bond (Figure 1.16).[100, 101] Then the proteins were digested, purified with streptavidin beads, and identified by MS/MS analysis. This method was also used to identify kinase inhibitors.[101]
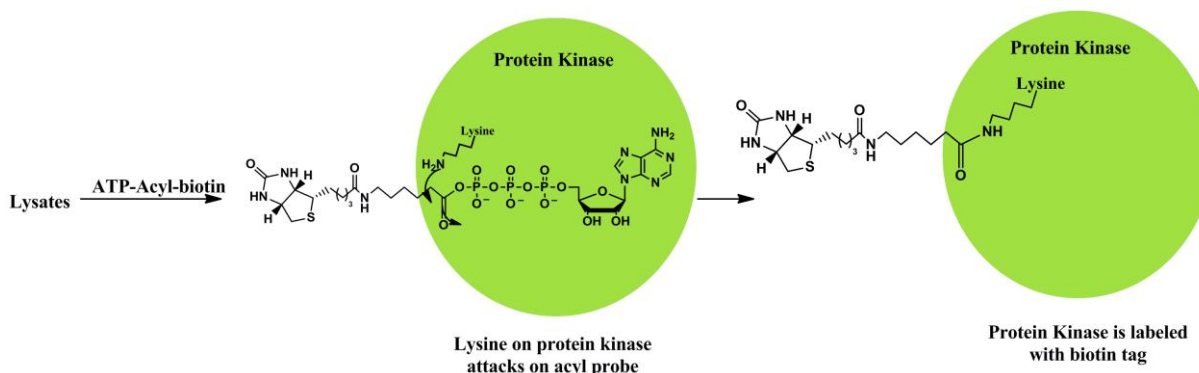
Figure 1.16: Strategy of Kinase Labeling by ATP-Acyl-Biotin. The modified ATP analog binds to the kinase active site and a conserved lysine residue in the kinase attacks the acyl group, leading to labeling the kinase with biotin.

1.7 Significant and Highlight of the Projects

During phosphorylation, the neutral hydroxyl group is replaced by a negatively charged phosphate group, which strongly influences protein activity within cells.[20] Hence characterization of the phosphorylation events and phosphorylated amino acids is useful to study protein function *in vivo*. This posttranslational modification affects various processes in cell biology including, protein shape, function, activity, protein-protein interaction, and cell signaling cascades.[1, 37, 103] With a significant role in biochemical functions, it is important to understand phosphorylation. Techniques to understand and monitor phosphorylation involve radiolabel with ^{32}P,[104] immobilizing metal affinity chromatography,[105] covalent modifications of the phosphate,[106] phosphate staining, such as with Pro-Q diamond stain,[107] and visualization using specific antibodies.[108] Besides these methods, the Pflum lab has developed the use of γ-modified ATP analogues as tools for studying phosphorylation.[91-93] These methods are discussed further in chapters 2 and 4.

Based on kinase cosubstrate promiscuity, several kinase-catalyzed labeling methods have been reported. We aim here to characterize the kinase-catalyzed labeling as a biological tool in proteomic research. First, we explored the generality of kinase cosubstrate promiscuity by testing biotinylation with 26 kinases throughout the kinome phylogenetic tree. Using the ADP-Glo assay with peptide and protein substrates (Promega), all kinases maintained reasonable conversions with ATP-biotin, with most displaying only modestly reduced catalytic efficiencies (k_{cat}/K_M) compared to ATP (Chapter 2). To characterize the scope and limitations of the biotinylation reaction, we probed the sensitivity of biotinylated phosphoproteins to phosphatases. Our goal was to ultimately apply the biotinylation reaction to phosphoproteomics, making an understanding of phosphobiotin stability in lysates critical. We found that the modification is

resistant to both Ser/Thr and Tyr phosphatases (Chapter 3). These results argue that the stable biotin tag will facilitate identification of low abundance phosphoproteins. Given the generality of kinase-catalyzed biotinylation and stability to phosphatases, finally, we applied kinase-catalyzed biotinylation to phosphoprotein identification using MS analysis. We compared avidin purification to the widely used titanium oxide (TiO_2) affinity chromatography. In addition, kinase-catalyzed biotinylation captured full-length phosphoproteins, which is not possible with TiO_2 chromatography. The significant conclusion is that kinase-catalyzed biotinylation is well suited for low abundance phosphoprotein detection and complements existing methods to provide a more complete view of the phosphoproteome (Chapter 4).

The enzymatic reactions with ATP-biotin, ATP-danzyl, ATP-ArN$_3$, and other analogs established that kinases promiscuously accept γ-phosphate modified ATP analogs as cosubstrates. By studying both kinases and phosphatases, kinase-catalyzed labeling experiments will build a more detailed and complete picture of the complex cell signaling pathways governing disease. In total, the chemical tools established with different ATP analogs will provide innovative and unprecedented approaches to monitor the role of phosphorylation in biology.

Chapter 2

The Generality of ATP-biotin as Kinase Cosubstrate

(Portions of the text in this chapter were reprinted or adapted from: Senevirathne, C., Green, K. D., and Pflum, M. K. H. (2009) Kinase-Catalyzed Biotinylation of Peptides, Proteins, and Lysates, In *Current Protocols in Chemical Biology*, John Wiley & Sons, Inc. and Senevirathne, C., and Pflum, M. K. (2013) Biotinylated Phosphoproteins from Kinase-Catalyzed Biotinylation are Stable to Phosphatases: Implications for Phosphoproteomics, *Chembiochem: a European journal of chemical biology 14*, 381-387)

In this chapter we focus on a systematic study of the labeling of substrates with ATP-biotin in a kinase dependent manner. The Pflum lab recently discovered the utility of γ-modified ATP analogues as tools for studying phosphorylation.[91-93] We found that kinases promiscuously accept γ-modified ATP analogs as cosubstrates (Chapter 1). Here we explore the generality of ATP-biotin with a variety of recombinant kinases, showing that 26 kinases accept ATP-biotin as cosubstrate and can be used for protein labeling. The kinetic data indicate that kinase-catalyzed biotinylation occurs with catalytic efficiency appropriate for phosphoproteomics application. A summary of phosphoprotein detection and identification methods is also discussed in this chapter.

2.1 Current Methods Used to Identify Phosphopeptides and Phosphoproteins

Historically, 2-D gel analysis has been used to detect phosphoproteins. In this method, proteins are separated by their isoelectric points (pI), followed by their molecular weight (Figure 2.1). Differences in the pI and size of the proteins are seen between phosphorylated and unphosphorylated proteins. Due to these differences, the shifted proteins can be isolated and characterized.[109, 110] However, 2-D analysis is challenging with proteins that are highly acidic, basic, too large, too small, highly hydrophobic or additionally modified (other posttranslational

modification, e.g. sulfation), which can cause a non-phosphorylation dependent shift in pI and

molecular weight. [111, 112]
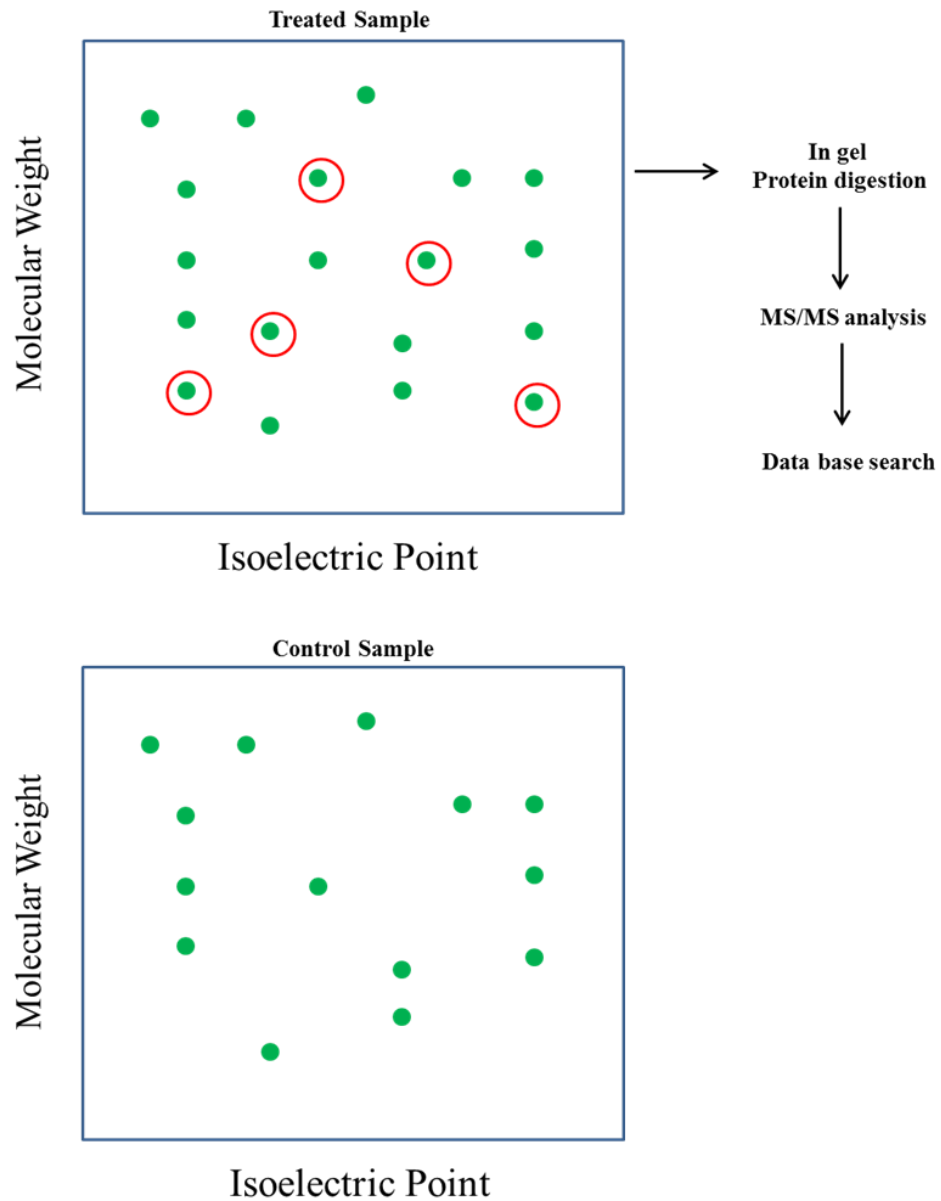
Figure 2.1: Theory of Two-Dimensional Gel Electrophoresis. Proteins are separated by isoelectric point followed by molecular weight. Treated protein sample (top) is compared to untreated sample (bottom). The shifted proteins in the treated sample (red circled) are digested and analyzed by MS/MS analysis.

Another classic method to identify protein phosphorylation involves radioactive labeling with ^{32}P-labeled ATP with subsequent visualizing of the ^{32}P labeled phosphoproteins by autoradiography.[104, 113] With the *in vivo* method, radiolabelled inorganic phosphate (^{32}P$_i$) is used to metabolically incorporate into ATP, which undergoes phosphorylation to label phosphoproteins. ATP-γ^{32}P is directly used with lysates to label phosphoproteins. The method is not efficient since the ^{32}P labeled ATP competes with the natural ATP. In addition, large amounts of radioactive material are required, making the method hazardous. Hence, less hazardous ATP-γ^{35}S has become popular with phosphoproteins labeling.[83]

Phosphoprotein-specific detection using Pro-Q Diamond phosphoprotein stain (Invitrogen)[107] and western blotting [108] are also used widely. Pro-Q is a fluorescent stain which detects phosphate groups at serine, threonine and tyrosine within SDS-polyacrylamide gels. Generally, Pro-Q stain is coupled with total protein detection using SYPRO Ruby stain for better quantification. Pro-Q Diamond phosphoproteins detection does not required any antibody or hazardous radioactive material. In additon, Pro-Q Diamond is compatible with MS analysis, which is an advantage of this phosphoproteins detection.[114] Western blotting requires generation of specific antibody reagents for each phosphoprotein of interest, making it less appropriate for visualizing all phosphoproteins in a complex mixture.[110, 115] For phosphoproteomics applications, antibodies recognizing a single phosphotyrosine amino acid have been used successfully, while the poor binding affinity of antibodies recognizing phosphoserine or phosphothreonine has limited their use.[110, 115]

Mass spectrometric (MS) analysis is also widely used to identify protein phosphorylation.[116-118] In MS analysis, a phosphorylated peptide within 80 Da greater mass would be expected, which facilitates its identification.[119] MS analysis can be coupled with

different separation systems and mass analyzers to increase sensitivity and accuracy.[120, 121] Despite many improvements, MS has limitations. For example, the ion suppression of charged phosphates in MS analysis results in difficulty detecting phosphopeptides in complex mixtures.[122] To minimize the influence of ion suppression, unphosphosphorylated peptides are often removed from the mixtures prior to MS analysis. As a result, multiple phosphopeptide purification methods have been developed to enhance phosphoproteomics analysis (see Chapter 4 for more details).

2.2 Kinase-Catalyzed Biotinylation

While a variety of methods are available to visualize phosphoproteins in complex mixtures, each method has its strengths and weaknesses, making the development of alternate strategies of interest. To provide an alternative, the Pflum lab has reported use of γ-modified ATP analogues as tools for studying phosphorylation. In particular, we demonstrated that an ATP analogue with biotin attached to the γ-phosphate (ATP-biotin) acts as a cosubstrate for kinases and transfers biotin along with the phosphate group onto peptides and proteins (Figure 2.2).[91] The biotinylation reaction was successful with synthetic peptides and full-length protein substrates. Importantly, kinase-catalyzed biotinylation was successfully applied to cell lysates. The availability of a facile means of biotin-labeling phosphoproteins and phosphopeptides in complex mixtures using kinases as the catalyst represents a useful method to detect phosphoproteins. In this chapter, we focus on the systematic study of the generality of ATP-biotin with recombinant kinases.
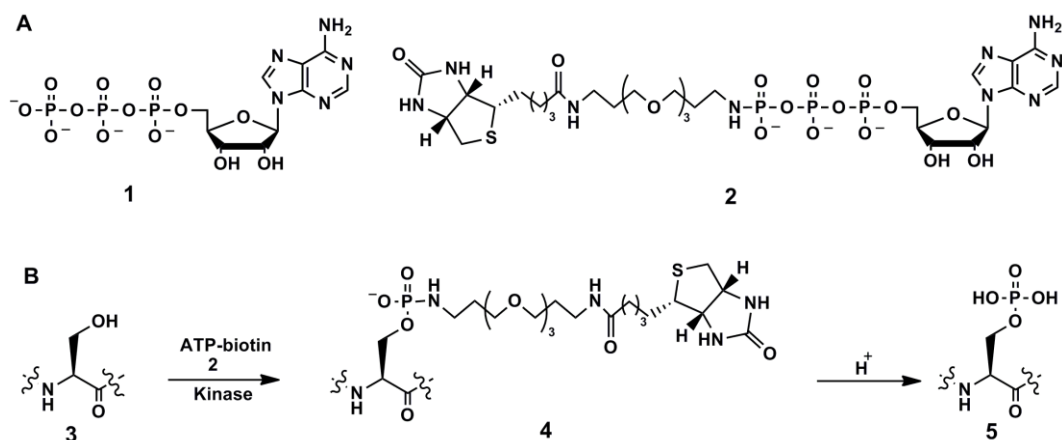
Figure 2.2: Kinase-catalyzed biotinylation. (A) Chemical structure of ATP **1** and γ-modified ATP analogues ATP-biotin **2** are shown. (B) Peptides or proteins (**3**) undergo biotinylation with a kinase and ATP-biotin (**2**) to create biotinylated phosphopeptide (**4**), which can be subjected to avidin purification. The phosphoamidate bond is cleaved with acid to yield phosphopeptides or phosphoproteins (**5**).

To characterize the generality of ATP-biotin for future applications, a diverse set of kinase substrate pairs were selected from the human kinome. There are over 500 human kinases are known up to date. These protein kinases are divided into different groups, families and subfamilies according to the sequence similarity (Figure 1.5).[37, 102] Kinases are mainly categorized into seven groups and oriented as a kinome tree (Figure 2. 3),[37] which represents the catalytic domain sequence similarity between kinases. Deviation of the sequence of two kinases is represented by the distance within the branches. Twenty-six kinases were selected to maximize kinome representation, as it is impossible to test all human kinases. Depending on the availability of kinase substrate pair, at least one kinase from each group was selected (Figure 2.3 and Table 2.1). Twenty-six kinases were selected from different places on kinome tree to increase the diversity and kinase representation (Figure 2.3 and Table 2.1). Different ranges of substrates were selected including, peptides, poly-peptides, and proteins (Table 2.4). Hence

selected kinases and their substrates display the diversity of enzyme-substrate pairs and better human kinase illustration.
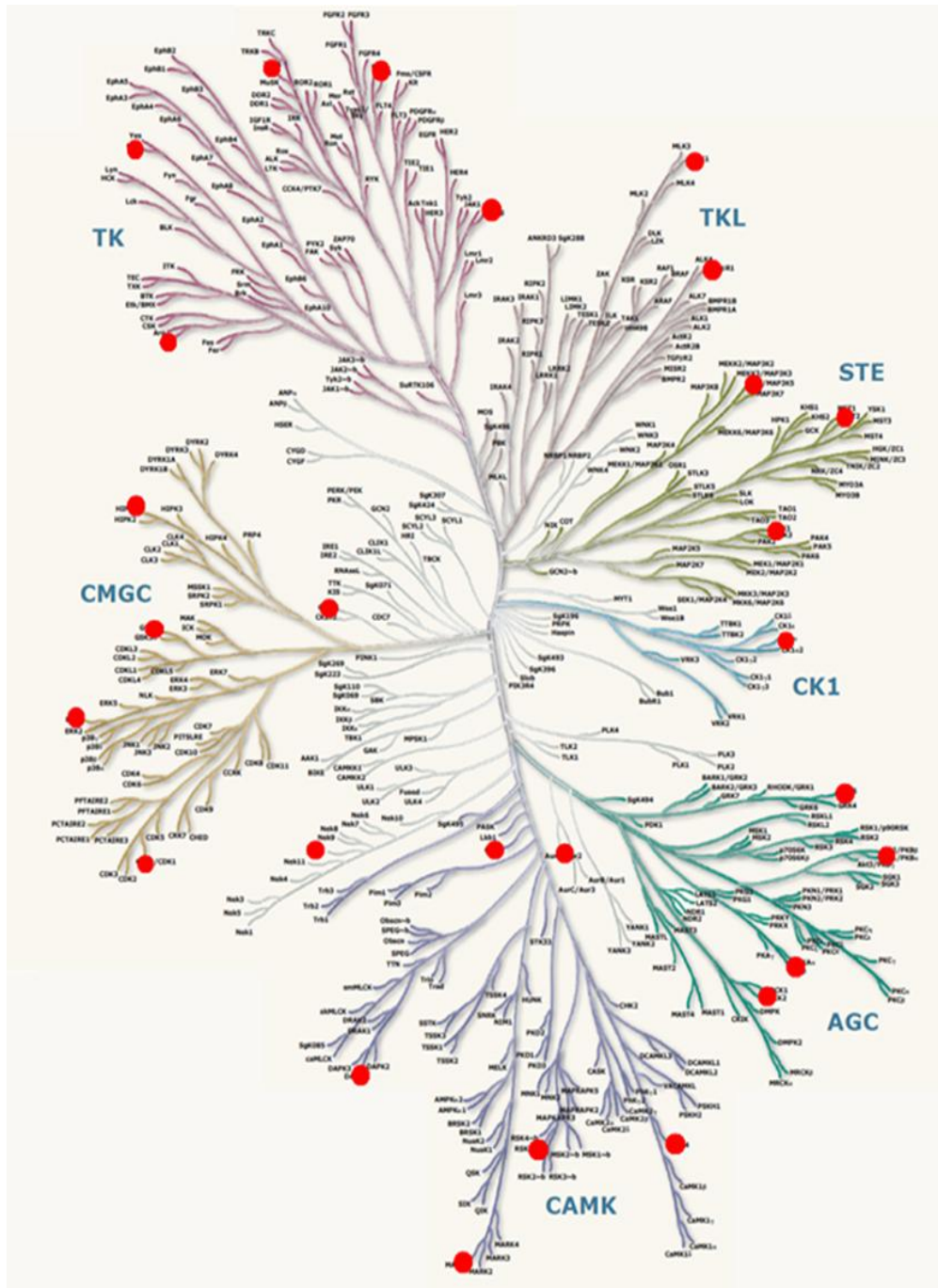
Figure 2.3: Human Kinome Tree. Selected Kinase for labeling and kinetic analysis in the human kinome is highlighted in red. The figure is obtained from Manning et al. 2002, Sci, 298, 5600. Illustration reproduced courtesy of Cell Signaling Technology, Inc. (www.cellsignal.com).

Table 2.1: Selected Protein Kinase from Human Kinome Tree for Study with ATP-biotin

Kinase	Type	Group[a]
Abl	Tyrosine	TK
AKT1	Serine/Threonine	AGC
ASK1	Serine/Threonine	STE
Aurora A	Serine/Threonine	Other
CAMK4	Serine/Threonine	CAMK
CDK1	Serine/Threonine	CMGC
CHK1	Serine/Threonine	CAMK
CK1	Serine/Threonine	CK1
CK2	Serine/Threonine	CMGC
DAPK1	Serine/Threonine	CAMK
ERK1	Serine/Threonine	CMGC
FLT1	Tyrosine	TK
GRK5	Serine/Threonine	AGC
GSK3β	Serine/Threonine	CMGC
HIPK1	Serine/Threonine	CMGC
JAK3	Tyrosine	TK
MARK1	Serine/Threonine	CAMK
MLK1	Serine/Threonine	TKL
MST1	Serine/Threonine	STE
NEK 2	Serine/Threonine	Other
PAK1	Serine/Threonine	STE
PKA	Serine/Threonine	AGC
RSK1	Serine/Threonine	AGC
SRC	Tyrosine	TK
TGFβR2	Serine/Threonine	TKL
TRKA	Tyrosine	TK

[a]**AGC:** Containing PKA, PKG, PKC families; **CAMK:** Calcium/calmodulin-dependent protein kinase; **CK1:** Casein kinase 1; **CMGC:** Containing CDK, MAPK, GSK3, CLK families; **Other:** other kinases; **STE:** Homologs of yeast Sterile 7, Sterile 11, Sterile 20 kinases; **TK:** Tyrosine kinase; **TKL:** Tyrosine kinase-like.

In this chapter, we focus on the general use of ATP-biotin with variety of recombinant kinases. However, a systematic study of ATP-biotin with kinases has not reported yet. Phosphoprotein labeling and monitoring using promiscuous kinase-catalyzed biotinylation will advance the proteomic field.

2.2.1 Synthesis of ATP-biotin

Initially the Pflum lab used commercially available ATP-biotin for biotinylation studies (Chapter 1, section 1.7.2). To study the generality of kinase-catalyzed biotinylation, we synthesized ATP-biotin **2** (Scheme 2.1) using a similar strategy as previously published.[93] Commercially available biotin **6** was activated by TBTU, and then treated with 4, 7, 10-trioxa-1-13-tridecanediamine **7** to yield biotin amine **8**. Biotin amine **8** was then coupled with the disodium salt of ATP using EDCI in water while maintaining the pH between 5.6-5.8 to give ATP-biotin **2**. Intermediate biotin amine **8** and the final ATP-biotin **2** were characterized by HRMS, ^{1}H, ^{13}C and ^{31}P NMR (Figures A 2.1-2.9). The synthesized ATP-biotin analog has two extra methylene in linker compared to the commercially available ATP-biotin analogue used in previous work.[91]

Scheme 2.1: Synthesis of ATP-biotin
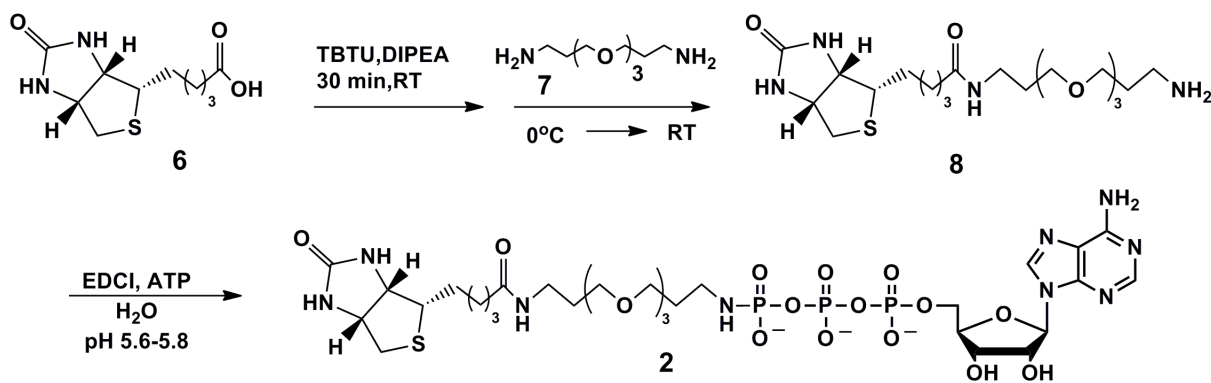
2.2.2 Labeling of Peptides with ATP-biotin

From previous studies, we have shown that three different recombinant kinases (PKA, CK2 and Abl) successfully utilized different γ-modified ATP analogs (ATP-biotin, ATP-danzyl, and ATP-arylazide).[91-93] However no analog has been tested with additional kinases. With the ability to label and purify with avidin, the ATP-biotin analog was selected for systematic analysis with various kinases. Kinase-catalyzed biotinylation was studied with commercially available peptides containing either serine, threonine, or tyrosine along with 10 different recombinant kinases, AKT1, CAMK4, CHK1, FLT1, GSK3β, MARK1, MST1, PAK1, RSK1 and SRC (Table 2.1). Biotinylated phosphopeptides were created by incubating ATP-biotin with AKT1 and AKT(PKB) substrate (CKRPRAASFAE), CAMK4 and Autocamtide (KKALRRQETVDAL-amide), CHK1 and CHKtide (KKKVSRSGLYRSPSMPENLNRPR), FLT1 and IGF1Rtide (KKKSPGEYVNIEFG), GSK3β and GSK3 peptide substrate (YRRAAVPPSPSLSRHSSPHQ(pS)EDEEE), MARK1 and CHKtide (KKKVSRSGLYRSPSMPENLNRPR), MST1 and Axltide (KKSRGDYMTMQIG), PAK1 and PAKtide (RRRLSFAEPG), RSK1 and S6K substrate (KRRRLASLR), or SRC and SRC substrate (KVEKIGEGTYGVVYK-amide) in the manufacturer provide buffer (1X, Promega). As a control, the phosphorylation reaction with ATP was also performed. To unambiguously show that biotinylation is kinase-dependent, at the same time ATP-biotin was also incubated with peptide substrates without kinase. The reaction products were separated with 16% Tris-tricine peptide gels (Biorad) and transferred to PVDF membrane. Peptides were visualized with coomassie stain, which indicated equal loading of peptides in each lane (Figure 2.4, top gels for each kinase). Biotinylated peptides were visualized with SA-Cy5 conjugate (Figure 2.4, bottom gels for each kinase). The results indicate that all ten kinases successfully transferred the phosphorylbiotin group to the peptide substrates (Figure 2.4, bottom gels, lane 3). As expected,

no biotin labeling was observed in the absence of kinases (Figure 2.4, bottom gels, lane 1) indicating that biotinylation occurred through a kinase-catalyzed pathway. These data demonstrate that ATP-biotin is compatible with several kinases and their corresponding peptide substrates.
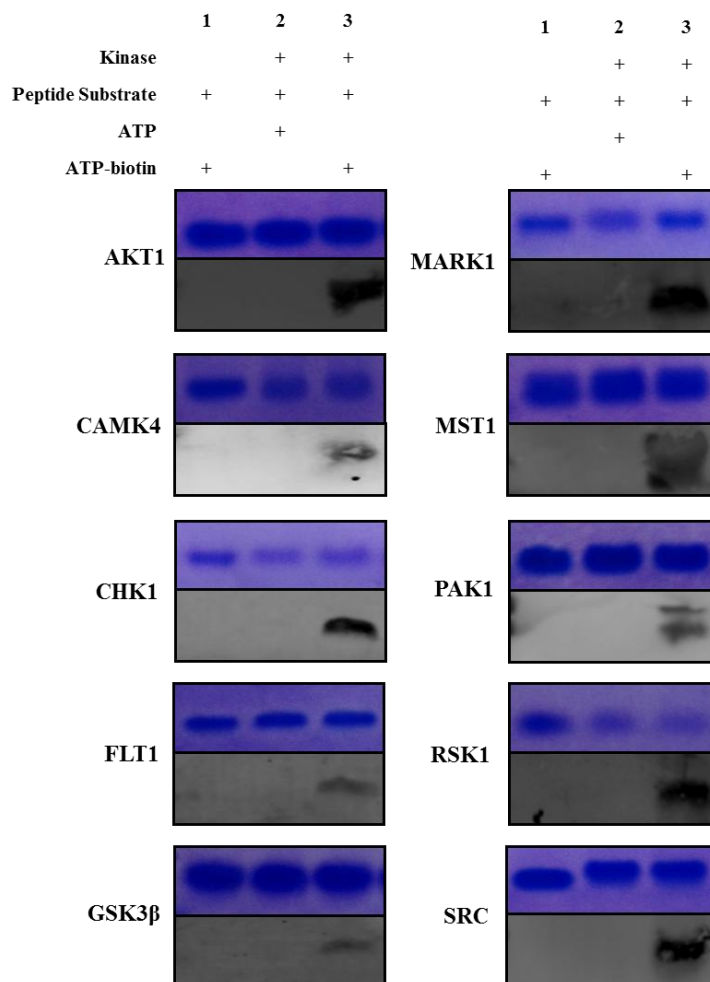
Figure 2.4: Labeling of Peptides using ATP-biotin. Peptides were subjected to kinase-catalyzed biotinylation. The reactions were separated on 16% Tris-tricine gel and visualized by Coomassie Stain (top gel images for each kinase) and SA-Cy5 (bottom gel images for each kinase). Reaction contents are indicated above the lanes. Full gel images can be found in appendix Figure A 2.10.

2.2.3 Labeling of Proteins with ATP-biotin

With successful peptide labeling with ATP-biotin and various kinases, our next goal was to label full-length proteins with additional kinases. Previously, Dr. Green used β-casein and CREB full-length protein substrate with CK2 and PKA enzymes in successful biotinylation reactions. In our systematic study of ATP-biotin with kinases, we used 16 additional kinases and their corresponding protein substrates. Phosphorylated proteins or biotinylated phosphoproteins were created by incubating ATP or ATP-biotin with Abl, ASK1, Aurora A, DAPK1, ERK1, HIPK1, MLK1, or TGFβR2 with Myelin basic protein (MBP), CDK1 with Histone H1 protein, CK1 with dephosphorylated Casein protein, CK2 and GRK5 with β-Casein protein, and JAK3, and TRKA with poly (Glu$_4$, Tyr$_1$) peptide substrate in the manufacturer provide buffer (1X, Promega). To verify that labeling is kinase-catalyzed, ATP-biotin was incubated with protein substrate only. Crude reaction mixtures were separated by 16% SDS-PAGE and transferred to a PVDF membrane. Proteins were visualized with Sypro Ruby Stain (Figure 2.5, top gels for each kinase) and biotinylated proteins with SA-Cy5 conjugate (Figure 2.5, bottom gels for each kinase).

The results are shown in Figure 2.5 and Figure 3.5, and indicate that all the 16 kinases were compatible with ATP-biotin as a cosubstrate. Similar to the peptide labeling, protein labeling with ATP-biotin was observed in the presence of kinase (Figure 2.5, bottom gels, lane 3). Incubating ATP-biotin with full-length proteins in the absence of kinases did not show biotin labeling with SA-Cy5 (Figure 2.5, bottom gels, lane 1), indicating no kinase-independent reaction between ATP-biotin and protein substrates, confirming that the labeling is kinase-mediated. The conclusion of the labeling experiments is that kinases promiscuously accept ATP-biotin as a cosubstrate. This study used peptides, poly-peptides, and proteins as cosubstrates with 26 different kinase enzymes, which represent the human kinome. The data indicated that the all

the 26 kinases tested here were able to accommodate ATP-biotin in kinase-dependent phosphorylation and labeled their corresponding peptide, polypeptide, and protein substrates.
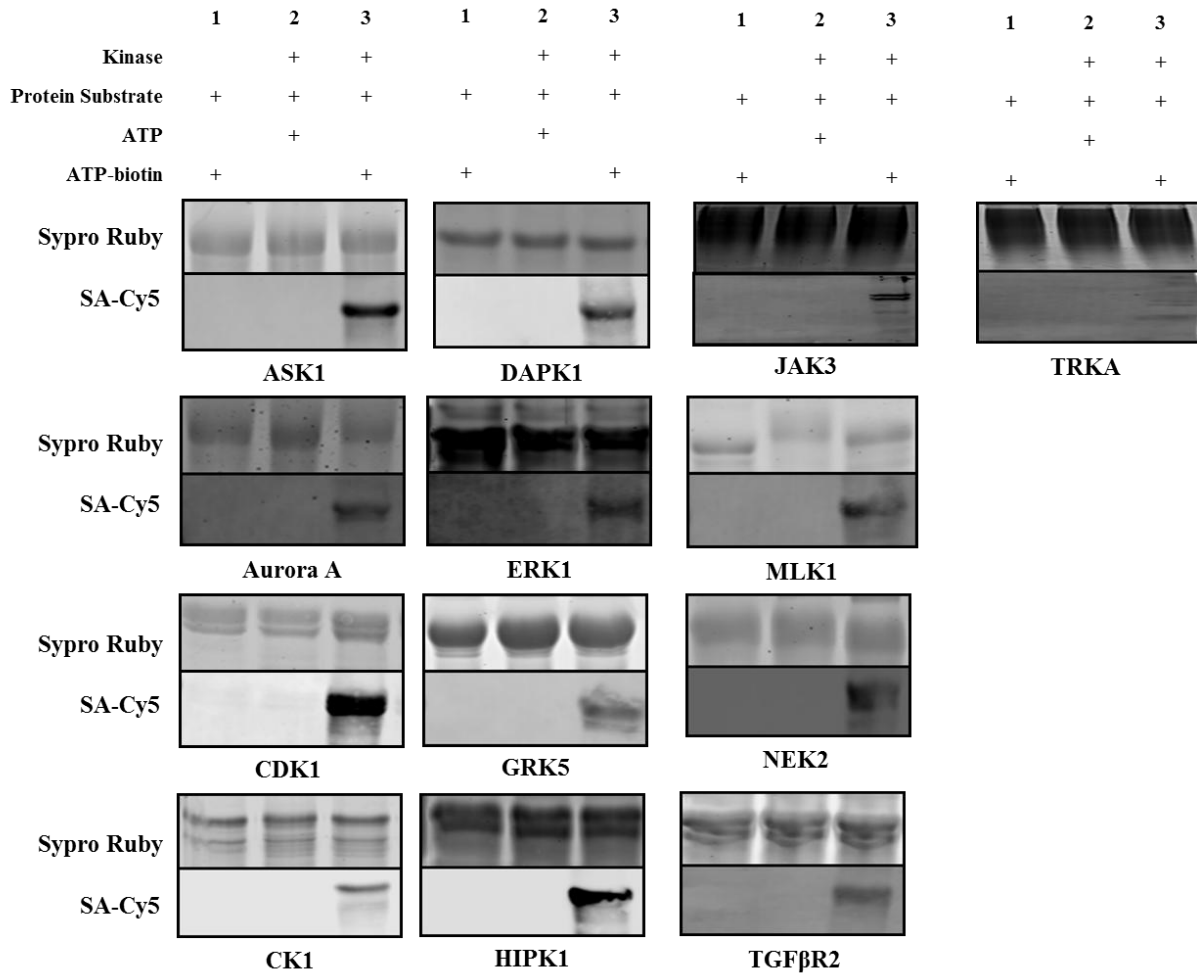
Figure 2.5: Labeling of Proteins using ATP-biotin. Proteins are subjected to kinase-catalyzed biotinylation with ATP-biotin and 16 recombinant kinases. The reactions are separated on 16% SDS-PAGE and visualized by Sypro Ruby Stain (top gels) and SA-Cy5 (bottom gels). Reaction contents are indicated above the lanes. Gel images for Abl, CK2, and PKA can be found in Figure 3.5. Full gel images can be found in appendix Figure A 2.11 and Figures A 3.4, 3.5, 3.6.

2.2.4 Quantification of Biotinylation-HPLC Analysis

The results of the previous sections indicate that many kinases can utilize ATP-biotin and can be used to label peptides, poly-peptides, and proteins. Next we were interested in determining the efficiency of these biotinylation reactions compared to phosphorylation. In prior work, quantitative MS analysis was used to determine the efficiency of biotinylation with peptides and proteins.[91-93] However this time we quantified the reaction using HPLC analysis with peptides and gel analysis with proteins (discussed in section 2.2.5). Phosphorylated peptides or biotinylated phosphopeptides were created by incubating ATP or ATP-biotin with Abl and Abl peptide substrate (EAIYAAPFAKKK), AKT1 and AKT(PKB) substrate (CKRPRAASFAE), CAMK4 and Autocamtide (KKALRRQETVDAL-amide), CK2 and CK2 peptide (RRREEETEEE), FLT1 and IGF1Rtide (KKKSPGEYVNIEFG), GSK3β and GSK3 substrate (YRRAAVPPSPSLSRHSSPHQ(pS)EDEEE), PAK1 and PAKtide (RRRLSFAEPG), PKA and kemptide (LRRASLG), RSK1 and S6K substrate (KRRRLASLR), or SRC and SRC substrate (KVEKIGEGTYGVVYK-amide) in the manufacturer provide buffer (1X, Promega). After each kinase reaction, the crude mixtures were analyzed by HPLC (Figure 2.6 and Appendix A, section 2.4). As the HPLC buffer was acidic (~pH=2), the phosphoamidate bond was broken to yield a phosphopeptide after the biotinylation reaction. This bond cleavage is possible as the reaction mixture was heated to denature the kinase (95 °C, 1 min) and equilibrated with the acidic HPLC buffer prior to injection. However, without heat deactivation or acidic pre-equilibration, unreacted ATP-biotin was seen without loss of the phosphoamidate bond breaking (retention time 10.3 min, Figure A 2.49, top).On the other hand phosphoamidate bond cleavage was still observed with the peptides, yielding a phosphopeptide product (Figure A 2.49, bottom). The biotin-amine, cleaved product was also observed (retention time 12.6 min,

Figure A 2.4 and 2.7). Cleavage of phosphoamide bond on peptides is more facile and can be explained by mechanism through neighboring group participating (Figure A 2.50).

HPLC analysis indicated that peptide substrates were efficiently phosphorylated with ATP (Figure 2.6). In the reaction with Abl, CAMK4, PAK1, and PKA phosphorylation was 100% with all the three trials, indicating all the peptides were converted onto phosphopeptides. With other kinases tested, with peptide substrates showed phosphorylation conversion ranging from 26% to 94%. Specifically, 94($\pm$6)% (AKT1), 91($\pm$6)% (CK2), 35($\pm$1)% (FLT1), 26($\pm$2)% (GSK3β), 94($\pm$6)% (RSK1), and 63($\pm$5)% (SRC) conversion was observed. A similar trend in conversion efficiencies was observed with ATP-biotin. Kinase-mediated biotinylation indicated that the conversion was 85($\pm$6)% with Abl, 49($\pm$2)% with AKT1, 62($\pm$3)% with CAMK4, 46($\pm$2)% with CK2, 30($\pm$6)% with FLT1, 11($\pm$2)% with GSK3β, 67($\pm$1)% with PAK1, 61($\pm$6)% with PKA, 74($\pm$1)% with RSK1, and 59($\pm$1)% with SRC. As some kinases do not show 100% conversion with phosphorylation, overall conversion efficiency of the biotinylation was calculated compared to ATP phosphorylation. This showed overall biotinylation efficiencies were 85($\pm$6)% with Abl, 53($\pm$2)% with AKT1, 62($\pm$3)% with CAMK4, 51($\pm$3)% with CK2, 86($\pm$13)% with FLT1, 42($\pm$5)% with GSK3β, 67($\pm$1)% with PAK1, 61($\pm$6)% with PKA, 79($\pm$5)% with RSK1, and 94($\pm$4)% with SRC. The data indicated that the percent conversion of biotinylation with peptide substrates ranged from 42% to 94% compared to ATP phosphorylation (Table 2.2). Thus, kinase-catalyzed biotinylation is occurring with comparable efficiency to the ATP phosphorylation.
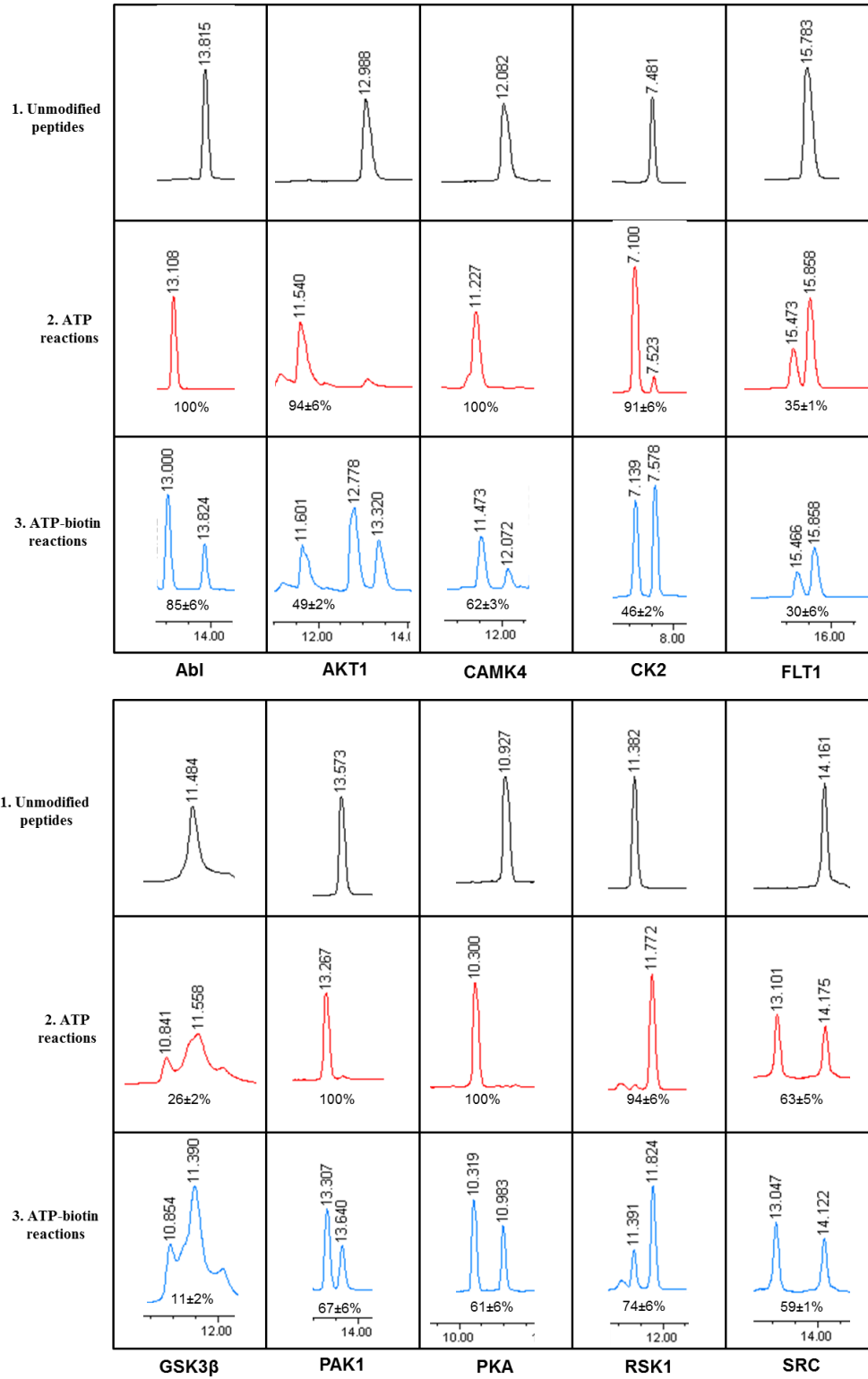
Figure 2.6: Quantification of Biotinylation with Petides. (1) HPLC analysis of unmodified peptides (Abl peptide at ~13.8 min; AKT1 peptide at ~13.0 min; CAMK4 peptide at ~12.1 min; CK2 peptide at ~7.5 min; FLT1 peptide at ~15.8 min; GSK3β peptide at ~11.5 min; PAK1 peptide at ~13.6 min; PKA peptide at ~10.9 min; RSK1 peptide at ~11.4 min; SRC peptide at ~14.2 min). **(2)** HPLC analysis of ATP-phosphorylated peptides (Abl phosphopeptide at ~13.1 min; AKT1 phosphopeptide at ~11.5 min; CAMK4 phosphopeptide at ~11.2 min; CK2 phosphopeptide at ~7.1 min; FLT1 phosphopeptide at ~15.5 min; GSK3β phosphopeptide at ~10.8 min; PAK1 phosphopeptide at ~13.3 min; PKA phosphopeptide at ~10.3 min; RSK1 phosphopeptide at ~11.8 min; SRC phosphopeptide at ~13.1 min). **(3)** HPLC analysis of ATP-biotin phosphopeptides (Abl phosphopeptide at ~13.0 min; AKT1 phosphopeptide at ~11.6 min; CAMK4 phosphopeptide at ~11.5 min; CK2 phosphopeptide at ~7.1 min; FLT1 phosphopeptide at ~15.5 min; GSK3β phosphopeptide at ~10.9 min; PAK1 phosphopeptide at ~13.3 min; PKA phosphopeptide at ~10.3 min; RSK1 phosphopeptide at ~11.8 min; SRC phosphopeptide at ~13.0 min). The peaks at ~12.7 min with AKT1 and GSK3β are from biotin-amine due to phosphoamidate cleavage. The complete HPLC traces are shown in section A 2.4, Figure A 2.12- A 2.21.

2.2.5 Quantification of Biotinylation-Gel Analysis

To determine the efficiency of biotinylation with the remaining 16 kinases, gel analysis was performed. Phosphorylated proteins or biotinylated phosphoproteins were created by incubating ATP or ATP-biotin with ASK1 and MBP, Aurora A and MBP, CHK1 and MBP, CDK1 and Histone H1 protein, CK1 and dephosphorylated casein protein, DAPK1 and MBP, ERK1 and MBP, GRK5 and β-Casein protein, HIPK1 and MBP, JAK3 and poly (Glu$_4$, Tyr$_1$) peptide substrate, MARK1 and MBP, MLK1 and MBP, MST1 and MBP, NEK2 and MBP, TGFβR2 and MBP, or TRKA and poly (Glu$_4$, Tyr$_1$) peptide substrate in the manufacturer provide buffer (1X, Promega). As a control only full-length protein substrate was loaded to assess the initial phosphorylation state of the proteins. As phosphorylation produces phosphoproteins and biotinylation produces phosphorylbiotin products, direct quantification with Pro-Q was not appropriate here. However, the phosphoamidate bond can be easily cleaved under acidic conditions to yield phosphoproteins that are the same product obtained with the ATP reaction. After kinase reaction, ATP and ATP-biotin reaction products were treated with 50%

TFA to obtain phosphoproteins for direct comparison of biotin reactions. Crude reaction mixtures were separated by 16% SDS-PAGE. Total proteins were visualized with Sypro Ruby Stain (Figure 2.7, top gels) and phosphoproteins were observed with Pro-Q Diamond Stain (Figure 2.7, bottom gels). We used Pro-Q Diamond Stain for quantification of kinase conversion with ATP and ATP-biotin reactions. Sypro Ruby Stain provided evidence for equal protein loading for each lane.

Myelin basic protein (MBP) displayed no or minimum phosphorylation before the kinase reaction, depending on the batch used in each particular reaction. The MBP that was used with AST1, Aurora A, DAPK1, ERK1, and HIPK1 was completely dephosphorylated (Figure 2.7, lane 1, bottom gels), whereas MBP used with CHK1, MARK1, MLK1, MST1, NEK2, and TGFβR2 displayed minimal initial phosphorylation on the proteins (Figure 2.7, lane 1, bottom gels). Poly-(Glu$_4$, Tyr$_1$) peptide substrate used with JAK3 and TRKA and β-casein used with GRK5 also showed minimum phosphorylation of purchased material (Figure 2.7, lane 1, bottom gels). Finally, purchased dephosphorylated casein protein used with CK1 does not indicate any phosphorylation before the kinase reaction. For the quantification, Pro-Q signal with untreated substrate was subtracted from the signal after the kinase-dependent phosphorylation or biotinylation.

Pro-Q gel analysis indicated that kinase-catalyzed phosphorylation gave an intense signal on the gel (Figure 2.7, lane 2) compared to the untreated protein substrate only (Figure 2.7, lane 1). Similarly, biotinylated proteins also gave high signal (Figure 2.7, lane 3) compared to the unreacted substrates (Figure 2.7, lane 1). For the quantification, ATP phosphorylation was assumed to be 100% conversion and biotinylation efficiency was calculated relative to ATP reaction. Reactions with Aurora A, ERK1, JAK3, NEK2, and TGFβR2 showed over 90%

conversion with biotinylation compared to phosphorylation. Other kinases also indicated good conversions with ATP-biotin, from 44% to 82%. The data from the quantitative analyses indicated that the biotinylation occurred to a reasonable extent compared to phosphorylation.

To compare the HPLC and gel analysis methods, CAMK4 was tested with both peptide substrate and protein substrate. The percent conversion of biotinylation with CAMK4 was 62% with peptide (HPLC analysis, Figure 2.6) and 41% with protein (gel analysis, Figure A 2.22 gel C).
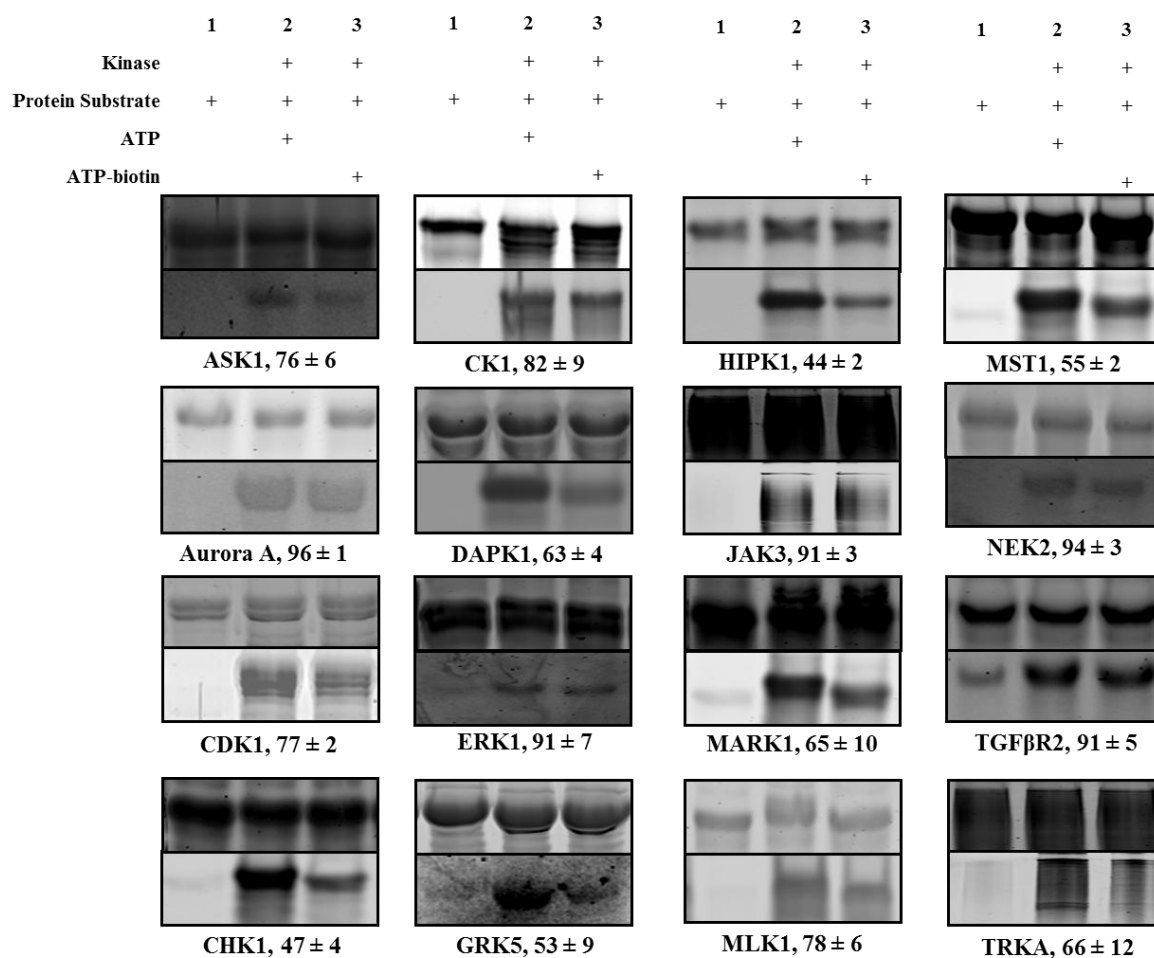
Figure 2.7: Quantification of Biotinylation with Proteins. Proteins were subjected to kinase-catalyzed phosphorylation or biotinylation. Both phosphorylated and biotinylated samples were incubated with 50% TFA for 15 minutes. The reactions were separated by 16% SDS-PAGE and visualized by Sypro Ruby Stain (top) and Pro-Q Diamond Stain (bottom). Reaction contents are indicated above the lanes. Full gel images can be found in appendix Figure A 2.22.

Table 2.2: Efficiency of Kinase-Catalyzed Biotinylation with 26 Kinases

Kinase	Method	% Conversion
ABL	HPLC	85 ± 6
AKT1	HPLC	53 ± 2
ASK1	Gel	76 ± 6
Aurora A	Gel	96 ± 1
CAMK4	HPLC (Gel)	$62 \pm 3 \ (41 \pm 2)$
CDK1	Gel	77 ± 2
CHK1	Gel	47 ± 4
CK1	Gel	82 ± 9
CK2	HPLC	51 ± 2
DAPK1	Gel	63 ± 4
ERK1	Gel	91 ± 6
FLT1	HPLC	86 ± 13
GRK5	Gel	53 ± 9
GSK3β	HPLC	42 ± 5
HIPK1	Gel	44 ± 5
JAK3	Gel	91 ± 3
MARK1	Gel	65 ± 10
MLK1	Gel	78 ± 6
MST1	Gel	55 ± 2
NEK2	Gel	94 ± 3
PAK1	HPLC	67 ± 1
PKA	HPLC	61 ± 6
RSK1	HPLC	79 ± 5
SRC	HPLC	94 ± 4
TGFβR2	Gel	91 ± 5
TRKA	Gel	66 ± 12

2.3 ADP-Glo Assay-Theory and Control Reactions

The efficiency of the biotinylation reaction was further characterized by a kinetic analysis using the ADP-Glo assay (Promega). The assay was performed as follows (Figure 2.8). The kinase reactions were performed at 30 °C for 30 minutes. Then an equal amount of ADP-Glo reagent was added to the mixture and incubated for 40 minutes at room temperature in the dark, which terminated the kinase reaction and degraded the unreacted ATP. Then an equal amount of kinase detection reagent (KDR) was added to the reaction mixture and allowed to react 60 minutes at room temperature, which converted ADP into ATP. At the same time, the luciferase/luciferin reaction took place with the newly formed ATP. This luciferase/luciferin reaction produced a luminescence signal to measure the amount of formed ATP. Hence the signal corresponded to the amount of ADP produced in kinase reaction and the activity of the kinase reaction. Signal was determined with a micro plate luminescence reader (Tecan).

Because the ATP-Glo assay was developed for ATP reactions, several control reactions were performed to characterize the ADP-Glo assay with ATP-biotin (Figure 2.9). First, experiments were done without performing a kinase reaction (Figure 2.9 A). Blank reactions not containing any ATP or ATP-biotin gave only background signal (Figure 2.9 A, lane 1). No significant signal was observed with ATP alone (Figure 2.9 A, lane 2) or ATP-biotin alone (Figure 2.9 A, lane 3), indicating that both were degraded by the ADP-Glo reagent. Luminescence signal was observed when ADP was treated with ADP-Glo reagent and kinase detection reagent itself (Figure 2.9 A, lane 4) or in the presence of ATP (Figure 2.9 A, lane 5) or ATP-biotin (Figure 2.9 A, lane 6). These ADP reactions indicate luminescence was produced with newly formed ATP from ADP.
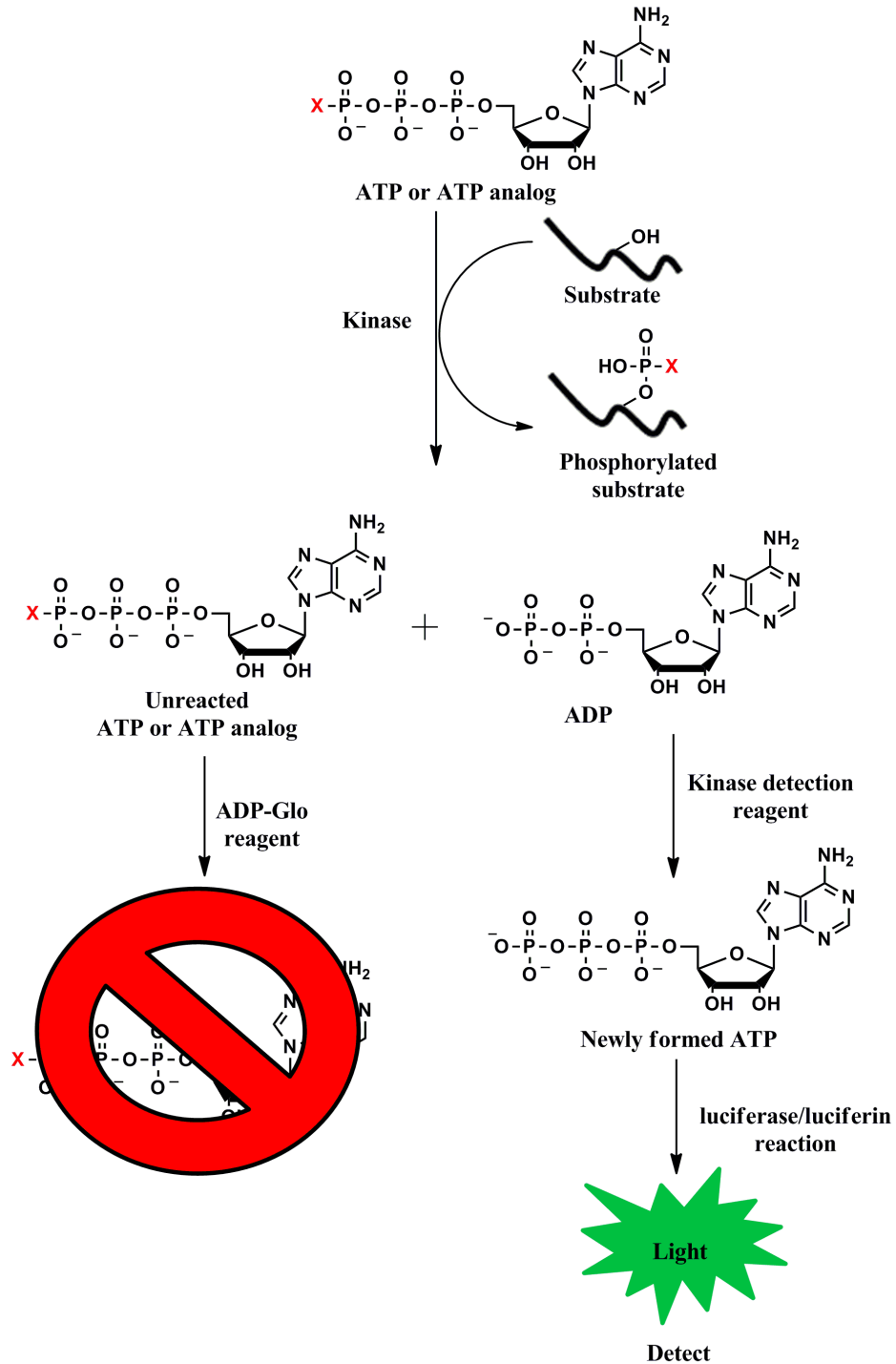
Figure 2.8: Theory of ADP-Glo the Assay. Kinase reactions with ATP or ATP analog produced ADP as a byproduct. Addition of ADP-Glo reagent inhibited the kinase reaction and degraded remaining ATP or ATP analog. Kinase detection reagent converted ADP into ATP and this newly formed ATP was used in a luciferase reaction to produce light.

Next, the same components were tested with kinase detection reagent only. When ATP (Figure 2.9 A, lane 7) or ADP (Figure 2.9 A, lane 8) was treated with only the kinase detection reagent, the signal intensity was the same as when ADP was treated with ADP-Glo reagent and KDR (Figure 2.9 A, compare lane 4 and 8). In contrast, the ATP-biotin reaction produced only back ground signal (Figure 2.9 A, lane 9). Also, addition of ATP-biotin to ATP or ADP did not significantly affect the luminescence signal (Figure 2.9 A, lane 10 and 11). As expected, a combination of the ATP and ADP almost doubled the signal compared to itself (Figure 2.9 A, compare lane 12 with lane 7 and 8). These reactions indicate that the ATP-biotin does not produced signal with KDR.

Then we performed controls including the kinase reaction (Figure 2.9 B). After the kinase reaction, luminescence signal was observed in reactions containing ATP (Figure 2.9 B, lane 8) or ATP-biotin (Figure 2.9 B lane 9) as cosubstrates. However in the absence of kinase, ATP (Figure 2.9 B, lane 6) or ATP-biotin (Figure 2.9 B, lane 7) did not show any significant signal with peptide substrate. Additionally, incubation of kinase with ATP (Figure 2.9 B, lane 4) or ATP-biotin (Figure 2.9 B, lane 5) without peptide substrate did not give any luminescence. Similarly, kinase alone (Figure 2.9 B, lane 2) or peptide alone (Figure 2.9 B, lane 3) gave only background signal (Figure 2.9 B, lane 1). These results indicated that ADP-Glo assay works with ATP-biotin similar to ATP, and ATP-biotin does not interfere with assay reagent and can be used for further analysis.
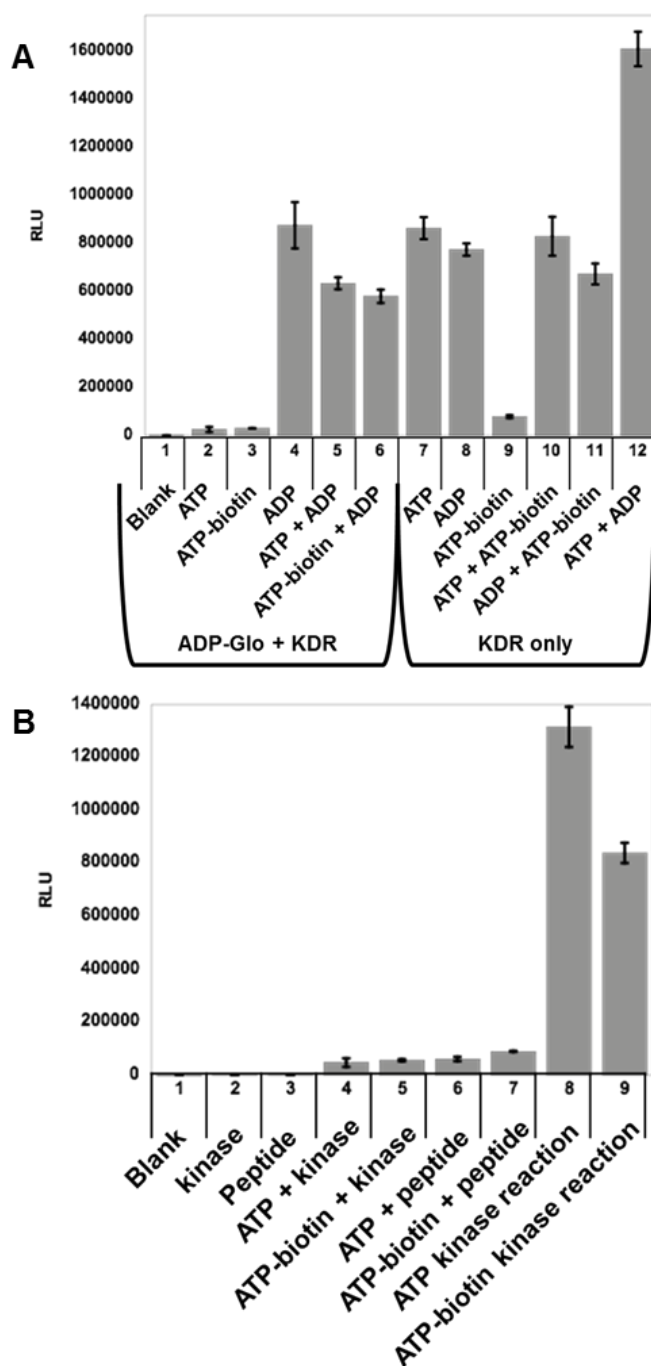
Figure 2.9: Control Experiments with ADP-Glo Assay. Several control experiments were carried out to validate the ADP-Glo assay with ATP-biotin. (**A**) ADP-Glo assay performed without a kinase reaction. Lanes 1-6 included both ADP-Glo reagent and kinase detection reagent. Lanes 7-12 used kinase detection reagent only. (**B**) ATP and ATP-biotin controls with kinase reaction. Lanes 1-9 included both ADP-Glo reagent and kinase detection reagent. Lane 8 and 9 represent the kinase reaction with peptide substrate and, ATP and ATP-biotin respectively.

Next we were interested in finding the degraded product of ATP or ATP-biotin with the ADP-Glo reagent. Graduate student Maheeka Embogama performed the following control experiment. If ATP-biotin was not degraded by the ADP-Glo reagent, would it could be used by luciferase to produce signal. However, the above luminescence data indicated that ATP-biotin is either degraded or not used by ADP-Glo reagent (Figure 2.9 A, lane 3) and not used by luciferase/luciferin reaction to enhance the luminescence signal (Figure 2.9 A, lane 5,6, 9, 10 and 11). To determine the fate of ATP-biotin in the ADP-Glo assay, HPLC analysis was performed with ATP vs.-7- ATP-biotin with the ADP-Glo reagent (Figure 2.10) and kinase detection reagent (Figure 2.11). The data indicate that ADP-Glo reagent converts ATP (Figure 2.10, t_R=42.2 min) to an unidentified substance (Figure 2.10, t_R=12.5 min), this reagent has no effect on ADP (Figure A 2.51, t_R=38.2 min), AMP (Figure A 2.51, t_R=32.6 min), adenosine (Figure A 2.51, t_R=7.3 min), or adenine (Figure A 2.51, t_R=6.9 min). Interestingly, ATP-biotin (Figure 2.10, t_R=27.9 min) does not convert to any of these products indicating that the ATP-biotin is not a substrate for ADP-Glo reagent. As expected, reaction of ATP with kinase detection reagent produced AMP (Figure 2.11, t_R=32.8 min), which is a byproduct in luciferase/luciferin reaction. Similarly, ATP-biotin also produced AMP (Figure 2.11, t_R=32.8 min) with kinase detection reagent, indicating that the ATP-biotin is a substrate for luciferase. However, this conversion was around 60% compared to 100% with ATP, and luminescence produced by this hydrolysis did not show significant luminescence signal, from previous analysis (Figure 2.9 A, lane 9). To further clarify, ATP or ATP-biotin was incubated with kinase detection reagent and luminescence signal was measured every 2.5 minutes (Figure A 2.52) for a one hour period time. The data indicated that the amount of signal produced by ATP-biotin is 10-fold less compared to the signal

produced by ATP. These control reaction data indicate that ATP-biotin is compatible with the ADP-Glo assay for the kinetic analysis.
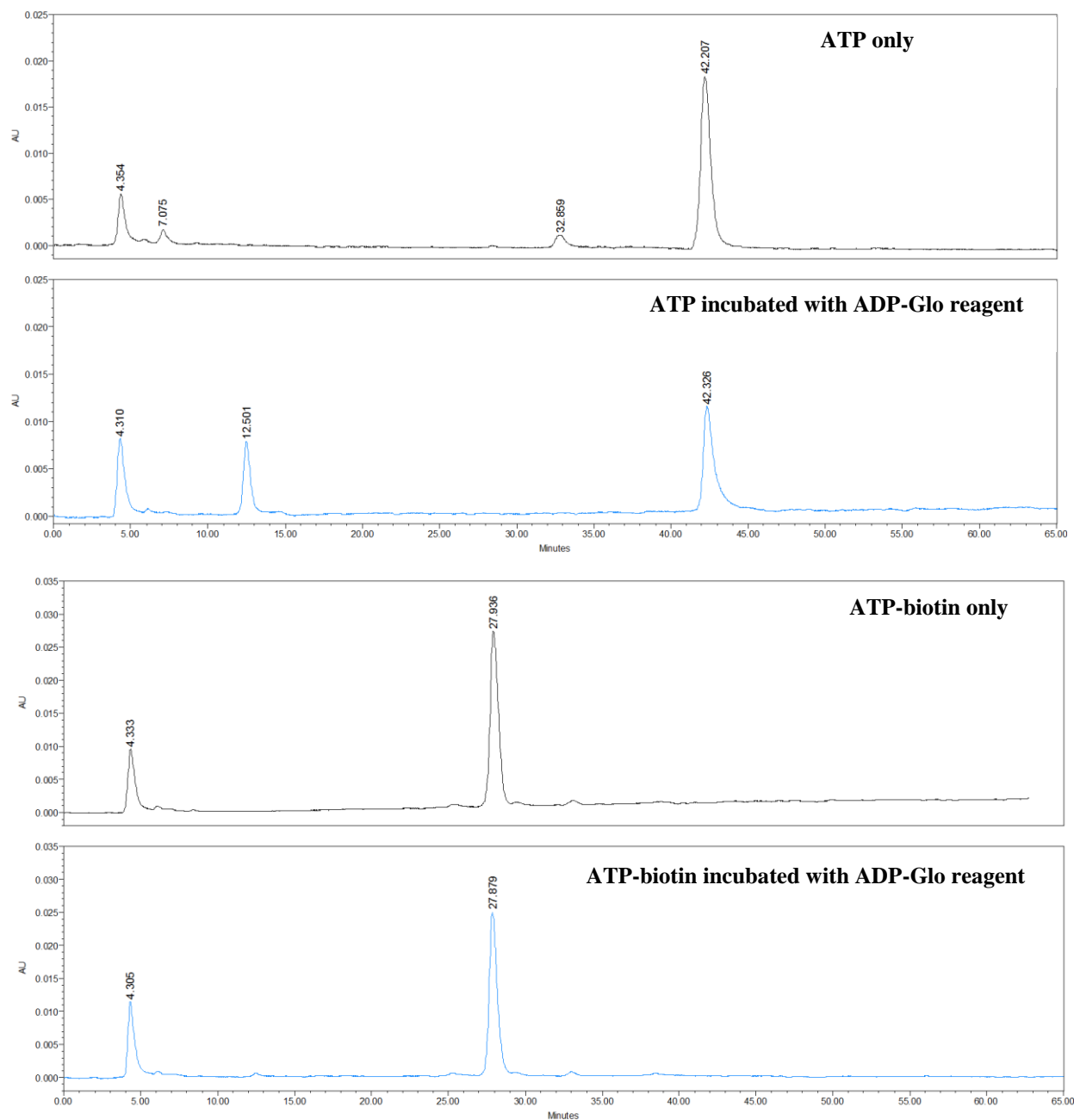
Figure 2.10: Control Experiments with ADP-Glo Assay using HPLC. ATP (t_R=42.2) min or ATP-biotin (t_R=27.9 min) incubated with ADP-Glo reagent and separated with HPLC. ATP (t_R=42.3 min) is degraded to an unidentified substance (t_R=12.5 min) whereas ATP-biotin (t_R=27.9 min) remained intact.
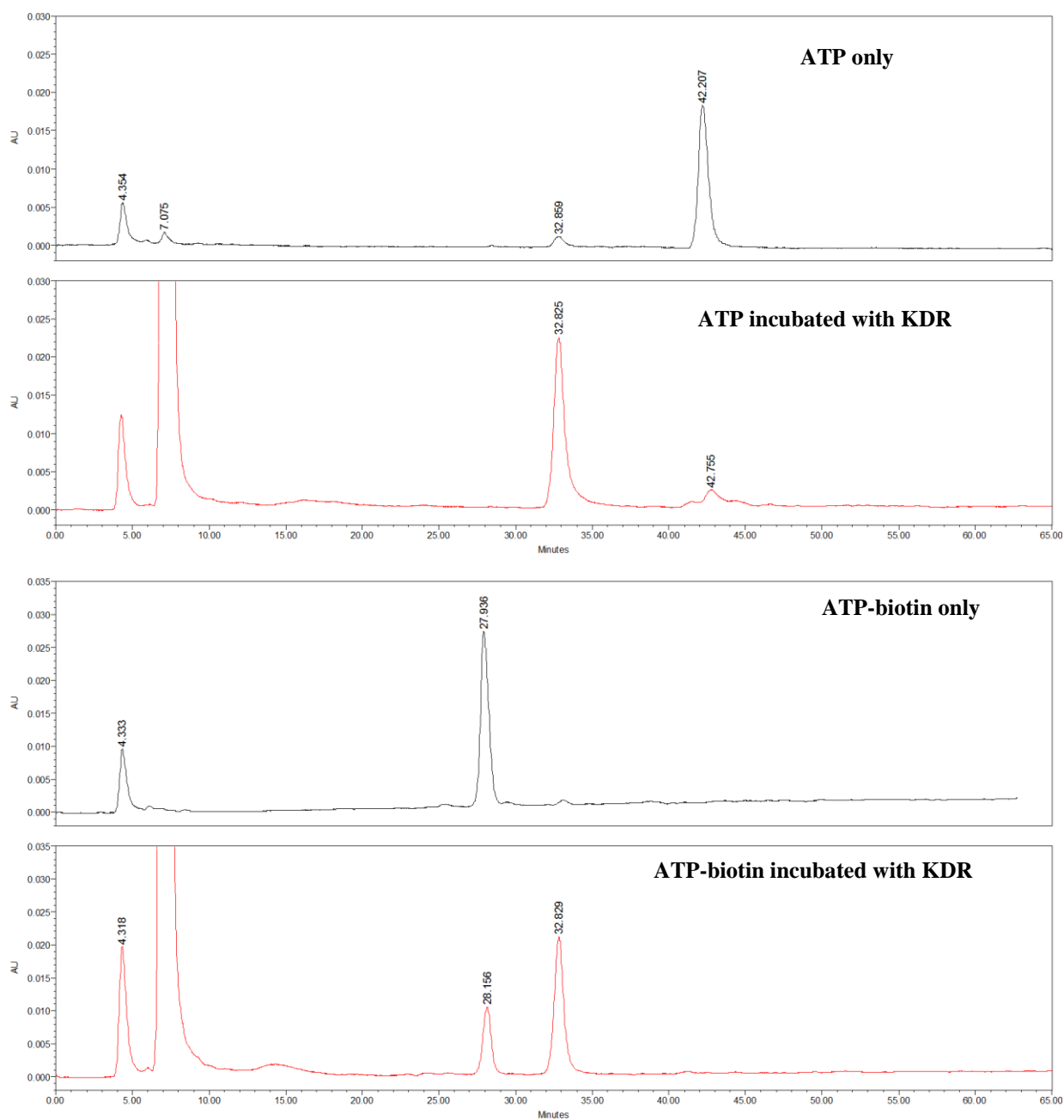
Figure 2.11: Control Experiments with ADP-Glo Assay using HPLC. ATP (t_R=42.2) min or ATP-biotin (t_R=27.9 min) incubated with kinase detection reagent and separated with HPLC. ATP (t_R=42.3 min) was fully degraded to AMP (t_R=32.8 min), whereas ATP-biotin (t_R=28.1 min) was only partially degraded to AMP (t_R=32.8 min).

2.4 ADP-Glo Assay- Kinetic Analysis

The efficiency of the biotinylation reaction was further characterized using the ADP-Glo assay. Unlike the widely used enzyme-coupled assay, [95, 96] the ADP-Glo assay is an end point assay. Thus kinetic measurements were obtained by performing the reaction with different substrate concentrations (1, 3, 10, 30, and 100 µM) and time points (5, 10, 20, 30, and 40 min). We screened all 26 kinases and determined kinetic parameters such as K_M, k_{cat} and k_{cat}/K_M.

With the kinetic analysis, ATP-biotin displayed similar K_M values compared to ATP for tested kinases, ranging from 0.6-fold to 2.9-fold increased values (Table 2.3). ATP-biotin showed a higher K_M for 22 kinases and lower K_M for 4 kinases (GRK5, NEK2, PAK and PKA), when compared to ATP. In addition, ATP-biotin showed only 2-fold higher K_M for 4 enzymes (DAPK, GSK3β, HIPK and TGFβR2). This data suggested that the γ-phosphate modification does not affect significantly ATP analog kinase binding efficiency.

To assess the efficiency of phosphoamidate transfer using ATP-biotin, k_{cat} values were compared to those of phosphate transfer. ATP-biotin showed similar k_{cat} (1-1.5 fold reduced values) compared to ATP for 8 kinases. In contrast, the analog displayed reduced k_{cat} relative to ATP (ranging from 2 to 53-fold) for the remaining 16 kinases. Significantly, ATP-biotin showed 19-fold and 53-fold reduced k_{cat} compared to ATP with ASK1 and GSK3β, respectively. Altogether, the reduced k_{cat} demonstrated that unnatural phosphorylbiotin transfer with ATP-biotin is slower than natural phosphate transfer with ATP. We also assessed the catalytic efficiencies (k_{cat}/K_M) for biotinylation and phosphorylation reactions. As expected, ATP-biotin showed lower catalytic efficiencies compared to ATP ranging from 1.1 to 135-fold reduced. These data indicated that ATP-biotin is an efficient substrate for some kinases and less efficient substrate for other kinases, compared to the natural ATP substrate.

There is no direct correlation between catalytic efficiencies and the earlier percent conversion data. For example, kinases demonstrating low catalytic efficiencies, such as ASK1 and GSK3β (Table 2.3) have reasonable ATP-biotin conversion under equilibrium condition (76% ASK1 and 42% GSK3β, Table 2.2). In addition, ATP-biotin showed similar catalytic efficiencies as ATP with NEK2 and PAK1 (Table 2.3), but 94% and 67% conversions, respectively. However, the remaining 22 kinases showed 2to7 fold reduced catalytic efficiencies for biotinylation compared to phosphorylation. These numbers are comparable to the catalytic efficiencies of ATP-γS, which is widely used compound for protein labeling.[81-83, 87] One report indicated that ATP-γS shows an 8-fold reduced k_{cat}/K_M compared to ATP. The data suggested that most kinases utilize ATP-biotin with good catalytic efficiencies and can be used for phosphoproteomics analysis.

Table 2.3: Kinetic constant for Enzymes

Kinase	K_M (µM)		Ratio	k_{cat} (s^{-1})		Ratio	k_{cat}/K_M (mM S)$^{-1}$		Ratio
	ATP	ATP-biotin		ATP	ATP-biotin		ATP	ATP-biotin	
ABL	8.8 ± 1.6	12.0 ± 1.1	1.4	1.27 ± 0.06	0.27 ± 0.008	4.7	143.8	22.3	7
AKT1	20.5 ± 2.1	23.7 ± 2.8	1.2	1.99 ± 0.01	0.39 ± 0.02	5	96.8	16.3	6
ASK1	12.4 ± 2.3	16.0 ± 2.6	1.3	0.95 ± 0.05	0.05 ± 0.003	19	76.5	3.2	24
Aurora	23.8 ± 1.3	36.4 ± 2.5	1.5	2.49 ± 0.05	1.53 ± 0.04	1.6	104.8	41.9	2.5
CAMK4	13.1 ± 0.6	14.0 ± 2.5	1.1	0.37 ± 0.006	0.12 ± 0.006	3.1	28.5	8.6	3.3
CDK1	19.5 ± 1.2	27.8 ± 3.0	1.4	6.90 ± 0.14	3.88 ± 0.16	1.8	354.7	139.6	2.5
CHK1	15.0 ± 1.9	19.2 ± 2.8	1.3	1.60 ± 0.06	0.96 ± 0.05	1.7	104.8	49.7	2.1
CK1	4.3 ± 0.9	7.3 ± 0.5	1.7	0.12 ± 0.006	0.10 ± 0.002	1.2	27.3	13.6	2.0
CK2	5.8 ± 1.8	8.9 ± 1.9	1.5	1.36 ± 0.11	0.63 ± 0.04	2.1	233.8	71.2	3.3
DAPK1	3.9 ± 0.9	11.5 ± 1.4	2.9	0.18 ± 0.01	0.17 ± 0.01	1.0	45.6	15.1	3.0
ERK1	41.8 ± 3.0	47.1 ± 3.9	1.1	0.65 ± 0.02	0.22 ± 0.01	2.9	115.5	4.8	3.3
FLT1	33.3 ± 2.5	36.6 ± 3.8	1.1	0.14 ± 0.004	0.06 ± 0.002	2.4	4.2	1.6	2.7
GRK5	9.2 ± 1.6	9.1 ± 1.0	1.0	0.02 ± 0.001	0.01 ± 0.0002	2.6	1.9	0.8	2.4
GSK3β	4.7 ± 0.6	11.4 ± 1.8	2.4	0.53 ± 0.02	0.01 ± 0.0004	53	113.6	0.8	135
HIPK1	5.2 ± 0.4	14.6 ± 2.5	2.8	1.30 ± 0.03	1.06 ± 0.06	1.2	251.8	73.1	3.4
JAK3	10.4 ± 1.3	15.4 ± 1.6	1.5	0.99 ± 0.04	0.89 ± 0.03	1.1	95.1	58.1	1.6
MARK1	10.2 ± 0.7	12.7 ± 1.3	1.2	2.21 ± 0.04	1.32 ± 0.04	1.7	217.1	104.0	2.1
MLK1	24.3 ± 3.0	27.7 ± 2.7	1.1	1.12 ± 0.05	0.28 ± 0.01	4.0	46.2	10.2	4.5
MST1	17.2 ± 2.9	24.9 ± 3.7	1.4	0.37 ± 0.02	0.22 ± 0.01	1.7	21.6	8.7	2.5
NEK2	25.0 ± 4.0	20.9 ± 2.9	0.8	0.58 ± 0.03	0.42 ± 0.02	1.4	23.3	20.0	1.2
PAK1	23.3 ± 3.0	20.7 ± 2.3	0.9	0.04 ± 0.002	0.03 ± 0.001	1.3	1.8	1.6	1.1
PKA	24.4 ± 1.5	15.0 ± 2.3	0.6	3.03 ± 0.07	0.41 ± 0.02	7	124.0	28.0	4.4
RSK1	25.3 ± 1.9	35.8 ± 4.0	1.4	3.40 ± 0.10	1.90 ± 0.09	1.8	132.7	52.4	2.5
SRC	15.3 ± 2.5	16.2 ± 1.8	1.1	0.83 ± 0.04	0.55 ± 0.02	1.5	54.4	33.8	1.6
TGFβR2	1.4 ± 0.3	4.1 ± 0.9	2.9	0.03 ± 0.001	0.02 ± 0.001	1.2	20.0	5.9	3.4
TRKA	28.6 ± 2.1	28.2 ± 2.0	1.0	1.12 ± 0.03	0.56 ± 0.02	2.0	41.9	19.8	2.1

2.5 Conclusion and Future Direction

Analysis of ATP-biotin with 26 selected kinases indicated that peptide, poly-peptide, or protein substrates were labeled in a kinase-dependent manner (section 2.2.2 and 2.2.3). Previous work done by our group[91-93] and others with different ATP analogs such as, ATP-γS,[81] ATP-ferrocene[99] and ATP-BODIPY[97] also successfully labeled the corresponding substrates in invitro assay. Specially, ATP-γS is used for substrate labeling.[81-83, 87] Interestingly, commercially available ATP-biotin, which is two carbons shorter in the linker, was also used to label peptides and lysates with gel analysis.[123] Additionally, the ATP-acyl-biotin derivative was used to identify over 200 kinases in ATP binding manner.[100, 101] These data indicate the ability of ATP analogs to bind to a variety of kinases in complex mixture.

In addition, the efficiency of biotinylation was measured with an end point assay (section 2.2.4 and 2.2.5) and kinetic analyses (section 2.4). The end point analysis was performed using HPLC (for peptides) or gel electrophoresis (for poly-peptides and proteins), and indicated that conversion efficiencies ranged from 41% to 96%. This data suggest that under equilibrium conditions (higher concentration and longer reaction time) the kinases utilize ATP-biotin more efficiently to transfer the phosphorylbiotin group. The percent conversion of CAMK4 was tested with both HPLC (peptide, 62%) and gel (protein, 42%) methods, indicating that the efficiency of biotinylation with substrate and the method of analysis.

As mentioned earlier ATP-γS is widely used for protein labeling and shows higher K_M (10-fold) compared to ATP.[76] Interestingly, opposite results were observed with k_{cat}, indicating 1.5-fold higher value and 18 to 137-fold lower numbers.[76-79, 124] This variation can be due to the quality of enzymes, which depends on source and purification.[95, 125] The kinetic constants of ATP-γS indicate that modification on γ-phosphate with electronically different and large atoms effects binding and catalytic mechanism.[76-78, 124] The biotinylation reaction was characterized

using the ADP-Glo assay. ATP-biotin showed similar K_M and decreased k_{cat} compared to ATP. However the biotinylation displayed similar catalytic efficiency (k_{cat}/K_M) as thiophosphorylation. Biotinylation demonstrated a catalytic efficiency (k_{cat}/K_M) ranging from 1.1- to 135-fold reduced compared to natural phosphorylation, indicating that some kinases can utilize ATP-biotin nearly as well as ATP. Altogether, kinases accept ATP-biotin as a cosubstrate at a level useful for phosphoproteomic research.

In the future, we will use ATP-biotin to test its generality with other kinase such as lipid kinase, sugar kinase, nucleotide kinase etc. We would also like to discover the labeling with kinase and to find correlation between kinase active site properties and binding of ATP analogs. Cell permeable version of ATP-biotin analog will help to understand the phosphorylation event within the cellular content. We also hope to use biotinylation to study kinase inhibitors and kinase substrate pairs. In addition, we will test other ATP analogs containing different functionalities.

2.6 Experimental

2.6.1 Materials

Biotin, triethylamine, 1-(3-dimethylaminopropyl)-3-ethylcarbodiimide hydrochloride (EDCI), 4, 7, 10-trioxa-1, 13-tridecanediamine, diisopropylethylamine (DIPEA), N, N-dimethylformamide (DMF), and pyrrolidine were purchased from Acros. Adenosine 5'-triphosphate (ATP), glycerol, sodium hydroxide (NaOH), potassium chloride (KCl), magnesium chloride ($MgCl_2$), sodium chloride (NaCl), sodium dodecyl sulfate (SDS), glacial acetic acid, acetonitrile, and SA-Cy5 conjugate were purchased from Fisher. HPLC grade trifluoroacetic acid (TFA) and acetonitrile were obtained from VWR and EM Millipore, respectively. D_2O and CD_3OD were obtained from Cambridge Isotope Labs. Ammonium bicarbonate, β-casein was bought from Sigma. PKA, CK2, Abl, enzymes, sodium fluoride, sodium orthovanadate and Abl peptide were purchased from New England Biolabs. All other kinases (AKT1, ASK1, Aurora A, CAMK4, CDK1, CHK1,CK1, DAPK1, ERK1, FLT1, GRK5, GSK3β, HIPK1, JAK3, MARK1, MLK1, MST1, NEK2, PAK1, RSK1, SRC, TGFβR2, and TRKA), AKT(PKB) substrate, Autocamtide, CHKtide, IGF1Rtide, GSK3, Axltide, PAKtide, S6K substrate, SRC peptide substrate, Kemptide, CK2 peptide peptide, poly (Glu_4, Tyr1) peptide substrate, Myelin Basic Protein (MBP), dephosphorylated Casein protein, Histone H1 protein and ADP-Glo assay were obtained from Promega. Triton X-100 was purchased from Fluka. Coomassie Briliant Blue was obtained from NuSep. Immobilion P and P^{sq} PVDF membrane were purchased from Millipore. Sypro Ruby and Pro-Q diamond stain was obtained from Invitrogen. Ready Gel 16% Tris-tricine was purchased from Bio-Rad.

2.6.2 Instrumentation

^{1}H NMR, ^{13}C NMR and ^{31}P NMR were recorded on a Varian Mercury (400 MHz) spectrometer. The peaks appearing at δ 4.78 and δ 5.12 in ^{1}H NMR are due to D_2O. The signals appearing at δ 1.58 and δ 3.52 in the ^{1}H NMR and δ 8.2 and δ 46.4 in the ^{13}C NMR are due to the triethylamine counter ion. IR spectra were carried out in $CHCl_3$ on FT/IR-460 plus (JASCO Co. Ltd.) spectrometer. High resolution mass spectra (HRMS) were obtained on LCT Premier XT (Waters). HP 8452A Diode array UV-Vis spectrophotometer was used to measure absorbance of ATP-biotin. The purified final product was lyophilized using VirTis BT 3.3 EL Benchtop lyophilizer. A SPD131 DDA ThermoSavant speed vac was used to evaporate solvents *in vacuo*. The luminescence values for the ADP-Glo assay were measured with a fluorimeter (GENios Plus Tecan). The SDS-PAGE apparatus was purchased from BioRad (Protean III) and a mini-gel setup was used. Western blotting was carried out using the Mini-Transblot Electrophoretic Transfer Cell apparatus from Bio-Rad. Peptides were analyzed using a Waters 1525 binary HPLC pump and Waters 2998 photodiode array detector. A reverse phase C-18 column (YMC America, INC 250×4.6 mm, 4μm, 8 nm) was used to separate peptide mixtures. After SOS – Page separation proteins were visualized using a Typhoon 9210 scanner (Amersham Biosciences).

2.6.3 Synthesis of biotin-PEG amine (8)

Biotin **6** (977.24 mg, 4 mmol) was dissolved in DMF (5 mL). TBTU (1.5412 g, 4.8 mmol) and DIPEA (0.836 mL, 4.8 mmol) were added and the mixture was stirred at room temperature for 30 min. The mixture was added dropwise to a solution of 4, 7, 10-trioxa-1-13-tridecanediamine **7** (2.2 mL, 10 mmol) in DCM (250 mL) at 4 ℃. After addition was complete, the reaction mixture was stirred overnight at room temperature. The reaction progress was

monitored by TLC (3:1:0.5 EtOH: DCM: NH_4OH, R_f =0.60). The solvent was removed *in vacuo*. The product was purified by flash chromatography on silica gel with EtOH/DCM (1:1→3:1 v/v) to yield 82% of biotin-PEG-amine **8** as dark brown solid (1.463 g, 3.28 mmol). Figures A 2.1-2.4; IR (CHCl$_3$, cm^{-1}): 724, 798, 847, 1129, 1184, 1434, 1658, 2939, 3052, 3206, 3457. ^{1}H NMR (400 MHz, D$_2$O): δ 1.19-1.27 (m, 2H), 1.36-1.65 (m, 8H), 2.08 (t, J=7.2 Hz, 2H), 2.56 (t, J=6.8 Hz, 2H), 2.82 (dd, J=12.8 and 4.8 Hz, 2H), 3.09 (t, J=6.4 Hz, 2H), 3.12-3.18 (m, 1H), 3.40 (t, J=6.0 Hz, 2H), 3.43 (t, J=6.4 Hz, 2H), 3.51 (s, 8H), 4.25 (dd, J=8 and 4.4 Hz, 1H), 4.43 (dd, J=8.0 and 4.8 Hz, 1H). ^{13}C NMR (100 MHz, D$_2$O): δ 25.1, 27.6, 27.9 28.2, 30.7, 35.4, 36.2, 37.6, 39.6, 55.3, 60.1, 61.9, 68.3, 68.8, 69.2, 69.3 69.5, 165.1, 176.5. HRMS (ESI): m/z calculated for C$_{20}$H$_{39}$N$_4$O$_5$S [M+H]$^+$ 447.2641, observed 447.2633.

2.6.4 Synthesis of ATP-biotin (2)

Adenosine 5'- triphosphate disodium salt (27.5 mg, 0.05 mmol) was dissolved in water (5 mL) and the pH of the solution was raised to 7.0 by adding 1M sodium hydroxide. 1-(3-Dimethylaminpropyl)-3-ethylcarbodiimide hydrochloride (EDCI, 383.42 mg, 2 mmol) dissolved in water (1 mL) was added to the reaction mixture. The pH of the solution was adjusted to 5.6 with 1 M hydrochloric acid and a pH range between 5.6-5.8 was maintained throughout the reaction. Biotin-PEG-amine **8** (894.44 mg, 2 mmol) was added to the ATP solution and progress of the reaction was monitored by TLC (6:3:1 *i*PrOH: NH_4OH: H_2O R_f =0.69). The reaction was stirred for 4 hours and then treated with triethylamine (TEA) to reach pH 8.0. The product was purified on DEAE Sephadex-A25 anion exchange column. The column was run with flow rate of 4 mL/min. A stepwise elution using 5%, 10%, 25%, 37.5%, 50%, 75% and 100% triethylammonium bicarbonate buffer (TEAB) was applied. The product eluted between 37.5-50% TEAB. Purified product was lyophilized to yield 20% of ATP-biotin **2** as a white TEA salt

(10.2 mg, 0.01 mmol). Figures A 2.5-2.9; UV (MeOH): λ 259 nm. ^{1}H NMR (400 MHz, D$_2$O): δ 1.68-2,16 (m, 8H), 2.57 (t, J=7.2 Hz, 2H), 3.24-3.46 (m, 6H), 3.58-3.64 (m, 4H), 3,84-4.01 (m, 12H), 4.57-4.59 (m, 2H), 4.72-4.74 (m, 2H), 4.89-4.92 (m, 2H), 6.48 (t, J=6.0 Hz, 1H), 8.63 (s, 1H), 8.92 (s, 1H). ^{13}C NMR (100 MHz, D$_2$O): δ 25.1, 26.4, 27.8, 28.0, 36.2, 37.5, 38.5, 39.6, 42.1, 55.2, 60.1, 61.9, 65.1, 66.6, 68.2, 68.7, 69.2, 69.3, 69.4, 70.3, 74.2, 84.0, 86.6, 110.8, 118.5, 140.0, 149.1, 152.3, 164.1, 176.6. ^{31}P NMR (400 MHz, D$_2$O): δ -0.06 (d, γ-P), -10.35 (d, α-P), -21.78 (t, β-P). HRMS (ESI): m/z calculated for C$_{30}$H$_{51}$N$_9$O$_{17}$P$_3$S [M-H]$^-$ 934.2337, observed 934.2329.

2.6.5 Storage of ATP-biotin (2)

The quality of the ATP-biotin is very important for biotinylation reaction. Like any triphosphate, ATP-biotin is prone to hydrolyze to ATP or ADP. Degraded ATP will compete with ATP-biotin in the kinase reaction. Therefore, lyophilized product (section 2.6.4) of ATP-biotin was dissolved in the storage buffer (Tris-base, 25 mM, pH 7.5) and stored at -80 °C as single use aliquots. In addition, it is critical that freeze thaw cycles be avoided with ATP-biotin. However, ATP-biotin will degrade over time and should be used within 3 months.

2.6.6 Kinase-Catalyzed Phosphorylation and Biotinylation

Phosphorylated or biotinylated peptides were created by incubating ATP or ATP-biotin (2 mM) with a kinase enzyme (Table 2.4) and its corresponding peptide substrate (0.25 mM) in the manufacturer provide buffer (1X). As a control, reactions were performed without kinases. The final volume of the reactions was 25 µL. The reaction mixtures were incubated at 30 ºC for 2 hours without shaking. After reaction, the mixtures were heated at 95 ºC for 1 minute to denature the kinase activity. Crude sample was separated on a 16% Tris-tricine gel (section

2.6.7) and transferred to Immobilion P^{SQ} PVDF membrane, and visualized with Coomassie stain and SA-Cy5 conjugate as described in sections 2.6.11 and 2.6.10. For HPLC quantification, crude samples were pre-equilibrate in 50 µL HPLC buffer A (99.9% water with 0.1% trifluoroacetic acid) for 10-15 minutes and used directly for HPLC analysis, as described in section 2.6.9.

Phosphorylated proteins or biotinylated phosphoproteins were generated as described above. In this case, after heat denaturation, the crude sample was separated by 16% SDS-PAGE and transferred to Immobilion P PVDF membrane, and visualized with Sypro Ruby Stain and SA-Cy5 conjugate as described in sections 2.6.10 and 2.6.12. For quantification experiments, 25 µL of TFA (50% TFA final concentration) was added to both phosphorylated and biotinylated samples and incubated for 15 minutes to cleave the biotin tag. Then the samples were evaporated to dryness using a speed vac and subsequently neutralized with 1.5 M Tris-base (pH 12). Then crude samples were used in SDS-PAGE separation, and gel imaging with Sypro Ruby Stain (section 2.6.12) and Pro-Q Diamond Stain (section 2.6.13).

Table 2.4: Enzymes and substrates used for labeling and quantification

Kinase	Kinase Concentration (nM)	Substrate
ABL	125	MBP, (EAIYAAPFAKKK)[a]
AKT1	94	CKRPRAASFAE
ASK1	133	Myelin Basic Protein
Aurora A	112	Myelin Basic Protein
CAMK4	101	KKALRRQETVDAL-amide
CDK1	102	Histone-H1
CHK1	98	KKKVSRSGLYRSPSMPENLNRPR, (MBP)[a]
CK1	129	Casein Protein (dephospho)
CK2	165	Casein Protein, (RRREEETEEE)[a]
DAPK1	113	Myelin Basic Protein
ERK1	182	Myelin Basic Protein
FLT1	85	KKKSPGEYVNIEFG
GRK5	70	Casein Protein
GSK3β	110	YRRAAVPPSPSLSRHSSPHQ(pS)EDEEE
HIPK1	113	Myelin Basic Protein
JAK3	125	Poly (4:1 Glu, Tyr) Peptides
MARK1	64	KKKVSRSGLYRSPSMPENLNRPR, (MBP)[a]
MLK1	104	Myelin Basic Protein
MST1	96	KKSRGDYMTMQIG, (MBP)[a]
NEK2	105	Myelin Basic Protein
PAK1	88	RRRLSFAEPG
PKA	150	MBP, (LRRASLG)[a]
RSK1	74	KRRRLASLR
SRC	96	KVEKIGEGTYGVVYK-amide
TGFβR2	0.118	Myelin Basic Protein
TRKA	0.121	Poly (4:1 Glu, Tyr) Peptides

a= In some case different substrates were used in biotinylation and quantification experiments. Substrates in paranthesis were used for quantification experiments. Abl, CK2, PKA, and Abl substrates were purchased from New England Biolab. All other enzymes and substrates were purchased from Promega.

2.6.7 Tris-Tricine Gel Electrophoresis

The tris-tricine gels were either purchased from Bio-Rad (cat no: 4563063) or prepared as follows. The tris-tricine gel was prepared in two layers, an upper "stacking" layer and a lower "separating" layer, as described in Nature Protocols.[126] A 16% separating layer was prepared consisting of a 10 mL of 3X Gel buffer (0.3% w/v SDS, 3 M Tris, brought to pH 8.45 with HCl), 10 mL of 40% v/v 29:1 acrylamide:bisacrylamide, and 3 mL of glycerol, which was diluted to 30 mL with distilled water. Polymerization was initiated by the addition of 100 µL of 10% ammonium persulfate, followed by 10µL of TEMED. After addition to the gel setup, distilled water was added on top of the separating layer to ensure a smooth edge and removed before adding the stacking layer. The upper stacking layer was composed of 4 mL of 3X gel buffer (0.3% w/v SDS, 3 M Tris, brought to pH 8.45 with HCl), and 1 mL of 40% v/v 29:1 acrylamide:bisacrylamide, which was diluted to 12 mL by addion of distilled water. Polymerization was initiated by the addition of 90 µL of 10% ammonium persulfate followed by 9 µL of TEMED, before loading on top of the separating layer. The gel running chamber was filled with a 1X Tris-Tricine-SDS running buffer, which was composed of 0.1% SDS, 100 mM Tris, and 100 mM tricine (at pH 8.3). A protein molecular weight marker (5 µL, Spectra Multicolor Low Range Protein Marker, Thermo Scientific) was used as a standard. The gel was run at a constant 100 V for 2 hours.

2.6.8 Sodium Dodecyl Sulfate Polyacrylamide Gel Electrophoresis (SDS-PAGE)

The polyacrylamide gel was prepared in two layers, an upper "stacking" layer and a lower "separating" layer (as described in *Molecular Cloning*, Appendix 8.40-8.45).[127] The lower layer contained approximately 4 mL of a 16% separating layer consisting of 1 mL of 4X Tris/SDS separating buffer (0.4% w/v SDS, 1.5 M Tris, brought to pH 8.8 with HCl), 1.6 mL of

40% w/v 37:1 acrylamide:bisacrylamide, 1.38 mL of distilled water, and 10% ammonium persulfate. Polymerization was initiated by the addition of 4 µL of TEMED. After addition to the gel setup, methanol was added on top of the separating layer to ensure a smooth edge and removed before adding the stacking layer. The upper stacking layer was composed of 0.5 mL of 4X Tris/SDS stacking buffer (0.4% w/v SDS, 1.5 Tris, brought to pH 6.8 with HCl), 0.25 mL of 40% w/v 37:1 acrylamide: bisacrylamide, 1.24 mL of distilled water, and 10 µL of 10% ammonium persulfate. Polymerization was initiated by the addition of 2 µL of TEMED. The gel running chamber was filled with a 1X SDS running buffer, which was composed of 0.1% SDS, 0.025M Tris, and 0.25 M glycine (at pH 8.3). A protein molecular weight marker (5uL, EZ-RUN Pre-Stained Protein Marker, Fisher) was loaded onto the gel as a standard. The gel was run at a constant 200 V for 1 hour.

2.6.9 HPLC Analysis

For HPLC analysis, peptide reactions (25 µL) were incubated in Buffer A (50 µL; 99.9% water with 0.1% trifluoroacetic acid) for atleast 15 min at room temperature to pre-equilibrate. Reverse phase chromatographic separation of peptides was performed using a C18 column (YMC America INC; 250×4.6 mm, 4µm, 8 nm) and Waters 1525 binary HPLC pump. The elution gradient used started at 95% Buffer A in Buffer B (99.9% acetonitrile with 0.1% trifluoroacetic acid), and decreased to 70% Buffer A over 15 min. The flow rate was 1 mL/min and the peptide absorbance was detected at 214 nm. The percentage of phosphopeptide was calculated by dividing the area under the phosphopeptide peak by the total area under both the phosphopeptide and unmodified peptide peaks.

2.6.10 Biotin Visualization

Proteins separated by gel were transferred to a polyvinyldene fluoride (PVDF) membrane (Immobilon P or P^{SQ}, Millipore). The membrane was pre-wet with methanol and proteins were transferred using the Mini-Transblot Electrophoretic Transfer Cell apparatus from BioRad, with CAPS/methanol buffer (0.01M CAPS [*N*-cyclohexyl-3-aminopropanesulfonic acid] at pH 10.5, and 10% methanol) used to fill the transfer chamber. The transfer was carried out at 90 V for 1 hour. After the transfer was complete, the membrane was incubated overnight in a blocking solution of 5-10% (w/v) non-fat dry milk in PBST (0.1% Tween-20 in 1X PBS buffer: 137mM NaCl, 2.7 mM KCl, 10 mM Na_2HPO_4, 2 mM KH_2PO_4, pH 7.4). The membrane was washed with PBST and then incubated in a 1:500 dilution of SA-Cy5 for one hour (longer time incubation can lead to non-specific labeling). The membrane was rinsed with PBST for 5 minutes, thrice, to remove the excess antibody, and visualized using the Typhoon scanner at an excitation wavelength of 633 nm and an emission at 670 nm.

2.6.11 Coomassie Stain

The tris-tricine gel was fixed in 50 mL of fixing solution (50% methanol and 10% acetic acid in water) and incubated with gentle rocking at room temperature for 30 minutes. The used fix solution was removed and 50 mL of undiluted Coomassie Brilliant Blue stain (NuSep) was added. The gel was incubated in the staining solution at room temperature overnight, with gentle rocking. The gel was then transferred to another clean container containing 100 mL of the destaining solution (6% acetic acid), and incubated at room temperature for 10-12 hours. The coomassie stained gel was imaged using a commercial scanner (HP Scanjet G4010).

2.6.12 Sypro Ruby Stain

The polyacrylamide gel was submerged in 50 mL of fixing solution (50% methanol and 7% acetic acid in water) and incubated with gentle rocking at room temperature for 30 minutes. The used fix solution was removed and the process was repeated. The used fix solution was poured off and 50 mL of undiluted Sypro Ruby gel stain (Invitrogen) was added. In this and subsequent steps, the gel was protected from light by covering the container with aluminum foil. The gel was incubated in the staining solution at room temperature overnight, with gentle rocking. The gel was then transferred to another clean container containing a sufficient volume of the washing solution (10% methanol and 7% acetic acid in water), and incubated at room temperature for 30 minutes. The washing solution was discarded and the gel was rinsed with distilled H_2O for 5 minutes to remove excess acid to prevent corrosive damage to the instrument used for visualization. The Sypro Ruby stained gel was imaged using the Typhoon scanner at an excitation wavelength of 450 nm and an emission of 610 nm.

2.6.13 Pro-Q Staining

The gel (independent gel from same crude reaction) was incubated in 50 mL of fixing solution (50% methanol and 10% acetic acid in water) overnight, and then the solution was discarded. The gel was rinsed with distilled water for 30 minutes, three times. Then 50 mL of undiluted Pro-Q Diamond gel stain (Invitrogen) was added. In this and subsequent steps, the gel was protected from light by covering the container with aluminum foil. The gel was incubated in the staining solution at room temperature for 60-90 minutes, with gentle rocking. The gel was then transferred to another clean container containing 100 mL of the washing solution (20% acetonitrile, 50 mM sodium acetate pH 4), and incubated at room temperature for 90 minutes, three times. The washing solution was discarded and the gel was rinsed with distilled water for 5

minutes to wash off excess acid to prevent corrosive damage to the instrument used for visualization. The Pro-Q stained gel was imaged using the Typhoon scanner at an excitation wavelength of 532 nm and an emission of 555 nm.

2.6.14 Gel Image Quantification

Gel bands were quantified using ImageQuant 5.1 by drawing the same size rectangular shape around comparable bands. The background correction was calculated by substracting the untreated protein signal from kinase reaction signal. The percentage of phosphoproteins or biotinylated phosphoproteins observed after kinase reaction was calculated by dividing the protein signal with ATP-biotin treatment to the protein signal with ATP treatment. The percentages displayed in Figure 2.7 are average percentages and standard error of observed phosphoprotein or biotinylated phosphoprotein from three independent trials.

2.6.15 Kinetics analysis

Kinase kinetic analysis was performed using the ADP-Glo kinase assay (Promega). All kinase assays were performed in white, flat-bottom 96-well half-area micro plates (Corning). For kinase reactions, ATP or ATP-biotin (1, 3, 10, 30, and 100 μM final concentrations) were incubated with corresponding peptide (0.2 μg/μL final concentration) or protein (0.1 μg/μL final concentration) substrates and manufacture's provided buffer (Table 2.5). The kinase reaction was initiated by adding protein kinase (manufacture's recommended amount; see Table 2.5). The final volume of the reactions was 20 μL. The reaction mixtures were incubated at 30 °C for 5, 10, 20, 30, and 40 minutes for each concentration. After the incubation period, an equal amount of ADP-Glo reagent (20 μL) was added to the mixture and incubated for 40 minutes at room temperature. Then, an equal amount of kinase detection reagent (40 μL) was added to the

reaction mixture and allowed to react 60 minutes at room temperature. Finally, luminescence signal was determined with a micro plate luminescence reader (GENios Plus Tecan). The concentration of ADP produced during the reaction was determined using a standard curve. Then the concentration of ADP produced in the reaction was plotted with the time. The initial rates of the reactions were obtained from the slope of the linear portion of the plots. The experimental results (rate vs concentration) were fitted by non-linear regression using Kaleidagraph ("Michaelis-Menten-Kinetic" model was used, $V = V_{max} * [S] / (K_M + [S])$, V=rate of the reaction and [S]= substrate concentration) to obtain the K_M and V_{max}, and V_{max} was divided by the concentration of enzyme (Table 2.5) to obtain the k_{cat} value. The fold change of the relevant kinetic constants were calculated by dividing the the kinetic constants with ATP-biotin reaction by the kinetic constants with the ATP reaction.

Table 2.5: Enzymes and substrates used for ADP-Glo assay

Kinase	Kinase Concentration (nM)	Substrate	Substrate Concentration µg/µL
ABL	15.0	EAIYAAPFAKKK	0.2
AKT1	5.9	CKRPRAASFAE	0.2
ASK1	4.2	Myelin Basic Protein	0.1
Aurora	1.4	Myelin Basic Protein	0.1
CAMK4	1.3	KKALRRQETVDAL-amide	0.2
CDK1	0.7	Histone-H1	0.1
CHK1	3.1	KKKVSRSGLYRSPSMPENLNRPR	0.2
CK1	16.1	Casein Protein (dephospho)	0.1
CK2	10.0	RRREEETEEE	0.2
DAPK	2.1	Myelin Basic Protein	0.1
ERK1	4.6	Myelin Basic Protein	0.1
FLT1	13.3	KKKSPGEYVNIEFG	0.2
GRK5	10.0	Casein Protein	0.1
GSK3	3.4	YRRAAVPPSPSLSRHSSPHQ(pS)EDEEE	0.2
HIPK	1.4	Myelin Basic Protein	0.1
JAK3	1.6	Poly (4:1 Glu, Tyr) Peptides	0.1
MARK1	0.4	KKKVSRSGLYRSPSMPENLNRPR	0.2
MLK1	3.9	Myelin Basic Protein	0.1
MST1	3.0	KKSRGDYMTMQIG	0.2
NEK2	3.3	Myelin Basic Protein	0.1
PAK1	10.5	RRRLSFAEPG	0.2
PKA	12.0	LRRASLG	0.2
RSK1	0.7	KRRRLASLR	0.2
SRC	1.2	KVEKIGEGTYGVVYK-amide	0.2
TGFβR2	18.4	Myelin Basic Protein	0.1
TRKA	0.8	Poly (4:1 Glu, Tyr) Peptides	0.1

Footnote: Figure 2.3 in this chapter were reprinted with permission from Cell Signaling Technology, Inc. (www.cellsignal.com). Request ID 315230.

Chapter 3

Stability of Biotinylated Phosphoproteins from Kinase-Catalyzed Biotinylation

(Portions of the text in this chapter were reprinted or adapted with permission from: Senevirathne, C., and Pflum, M. K. (2013) Biotinylated Phosphoproteins from Kinase-Catalyzed Biotinylation are Stable to Phosphatases: Implications for Phosphoproteomics, *Chembiochem: a European journal of chemical biology 14*, 381-387.)

Previous data indicated that many recombinant kinases and cellular kinases accept ATP-biotin as a cosubstrate. However the dynamics of the modified reaction were not characterized. Given that phosphorylation is a reversible process, we were interesting in testing the dynamics of biotinylation in a cellular contex. If the modification is sensitive to the phosphatases in lysates, biotinylation can be used to monitor dynamic of phosphorylation. Or if the modification is stable to phosphatases, the method would be great tool for identifying low abundance phosphoprotein in complex mixture. This chapter is focused on studying the phosphatase stability of the phosphorylbiotin group towards the use of kinase-catalyzed biotinylation for phosphoproteomics.

3.1 Phosphatase Activity with Phosphoryl Biotin Tag

Recently we reported use of γ-phosphate modified ATP analogs for studying phosphorylation.[91-94] In particular, we demonstrated that an ATP analog with biotin attached to the γ-phosphate (ATP-biotin (**2**), Figure 3.1) acts as a cosubstrate for kinases and transfers a phosphorylbiotin group to peptides and proteins (Figure 3.1).[94] With these successes, kinase-catalyzed biotinylation has application towards characterizing the complete phosphoproteome. However, cellular experiments are complicated by the presence of protein phosphatases, which could alter the biotinylation state of the labeled phosphoproteins (Figure 3.1). To assess the suitability of kinase-catalyzed biotinylation for phosphoproteomics applications, the sensitivity of the phosphorylbiotin tag to phosphatase activity must be characterized.
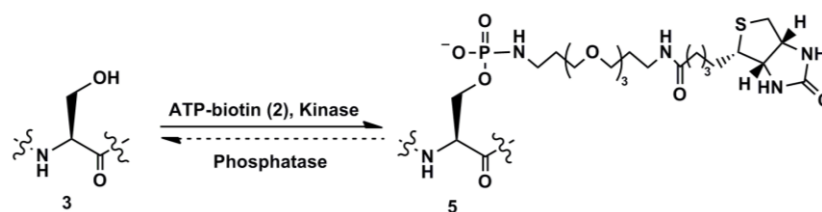
Figure 3.1: Protein Phosphorylation, Biotinylation and Dephosphorylation. Biotinylation with kinases and ATP-biotin gives biotinylated phosphopeptide products (5). The sensitivity of biotinylated phosphopeptides to phosphatases is studied in this chapter.

3.2 Protein Dephosphorylation: Phosphatases, Structure and Enzymatic Mechanism

Many biological processes involve kinases and phosphatases, including cell signaling, and cancer formation, for examples.[6, 128] In contrast to kinases (over 500), a fewer number of phosphatases (over 150) are known. Phosphatases are divided into two major classes-[7] serine/threonine phosphatases[129] and tyrosine phosphatases,[130] which hydrolyze phosphoserine/threonine or phosphotyrosine, respectively. Unlike kinases, phosphatases have differing active sites and mechanisms depending on their substrate.[10, 130-134] Serine/threonine phosphatases have an active site that utilizes catalytic metals (Mn, Fe, Zn) to bind the phosphate[135-137] and activates water for phosphate ester hydrolysis (Figure 3.2 A).[138] In contrast, tyrosine phosphatases hydrolyze the phosphate ester by employing a nucleophillic cysteine (Figure 3.2 B).[130, 139, 140] To characterize the compatibility of the two active sites with phosphoryl biotin degradation, we tested two serine/threonine phosphatases (protein phosphatase 1 (PP1) and calf intestinal phosphatase (CIP)) and one tyrosine phosphatase (T-cell protein tyrosine phosphatase (TCPTP)).
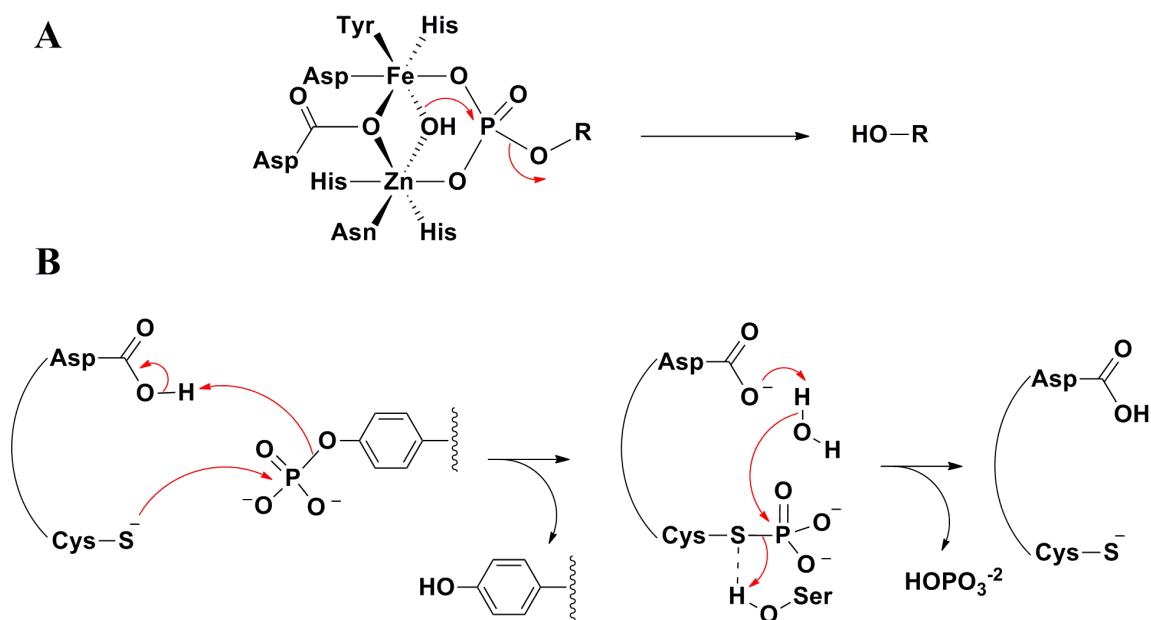
Figure 3.2: Mechanism of the Dephosphorylation by Protein Phosphatases. (A) Protein serine/threonine phosphatases employ two metal ions which activate a water molecule to attack the phosphate group during dephosphorylation. (B) Protein tyrosine phosphatases employ an amino acid cysteine to attack the phosphate group during dephosphorylation.

3.3 Stability of Modifications on Phosphate towards Phosphatases

Kinases utilize γ-thio-ATP (ATP-γS (**6**), Figure 3.3) to generate thiophosphorylated proteins. Prior work revealed that the thiophosphoryl group is insensitive to phosphatases[74, 86, 141] and provided the foundation for use of ATP-γS and thiophosphorylation in phosphoproteomics applications.[80, 81, 87, 124, 142] With this precedent, we examined whether the phosphorylbiotin modification is similarly insensitive to phosphatases. If the biotin tag is stable under cellular conditions, then kinase-catalyzed biotinylation would be an excellent tool to visualize and purify phosphorylated proteins in lysates, with the ability to monitor low abundance phosphoproteins.
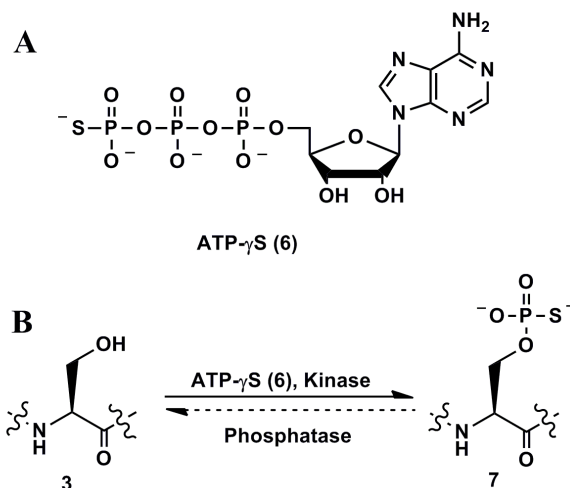
Figure 3.3: Irreversible Kinase-Catalyzed Thiophosphorylation. (A) Chemical structure of ATP-γS (6). (B) Peptides or proteins (3) undergo thiophosphorylation with kinases and ATP-γS to give thiophosphopeptides or thiophosphoproteins products (7), which cannot be removed by phosphatases. The insensitivity of thiophosphopeptides and thiophosphoproteins to phosphatases is well documented.

Here we test the susceptibility of the phosphorylbiotin tag of kinase-catalyzed biotinylation towards protein phosphatases. We found that the phosphorylbiotin group on peptide and protein substrates was relatively insensitive to protein phosphatases. To understand how phosphatase stability would impact phosphoproteomics research applications, kinase-catalyzed biotinylation of cell lysates was performed in the presence of kinase or phosphatase inhibitors. We found that biotinylation with ATP-biotin was sensitive to inhibitors, although with variable effects compared to ATP phosphorylation. The results suggest that kinase-catalyzed biotinylation is well suited for phosphoproteomics studies, with particular utility towards monitoring low abundance phosphoproteins or characterizing the influence of inhibitor drugs on protein phosphorylation.

3.4 Phosphatase Activity with Biotinylated Phosphopeptides

Two steps were employed to assess the phosphatase sensitivity of biotinylated phosphopeptides. First, biotinylphosphopeptides were prepared by incubating ATP-biotin with peptide/kinase pairs: PKA (Protein Kinase A) and serine-containing substrate (LRRASLG), CK2 (Casein Kinase 2) and a threonine-containing substrate (RRREEETEEE), and Abl (Abl Protein Tyrosine Kinase) and a tyrosine-containing substrate (EAIYAAPFAKKK). After generating the biotinylphosphopeptides, the second step involved heat denaturation of the kinase, followed by incubation with PP1, CIP, or TCPTP. As a control, identical experiments were carried out with ATP as a cosubstrate. All reactions were analyzed using high performance liquid chromatography (HPLC). In the presence of acidic HPLC Buffer A (0.1% TFA in water, pH ~2), the phosphoramidate bond of the biotinylphosphopeptide was cleaved to remove the biotin group and yield a phosphopeptide product (see chapter 2, section 2.2.4 for more information).[143] Therefore, ATP and ATP-biotin reactions produced HPLC traces containing identical unmodified (Figure 3.4 A) or phosphorylated peptide products (Figure 3.4 B and C).

Under conditions where ATP control reactions demonstrated 90% to 100% kinase conversion to phosphopeptide products (Figure 3.4 B, top), the ATP-biotin reactions demonstrated 46-85% conversion (Figure 3.4 C, top). The efficiencies of the kinase reactions with ATP-biotin were comparable to the quantitative mass spectrometric analysis reported previously (56-80%),[91] demonstrating the reliability of the HPLC analysis. After phosphatase treatment, ATP phosphorylated peptides were almost completely hydrolyzed; only 0-11% phosphopeptides remained by HPLC (Figure 3.4 B, bottom), indicating that the phosphatase maintains 89-100% activity.
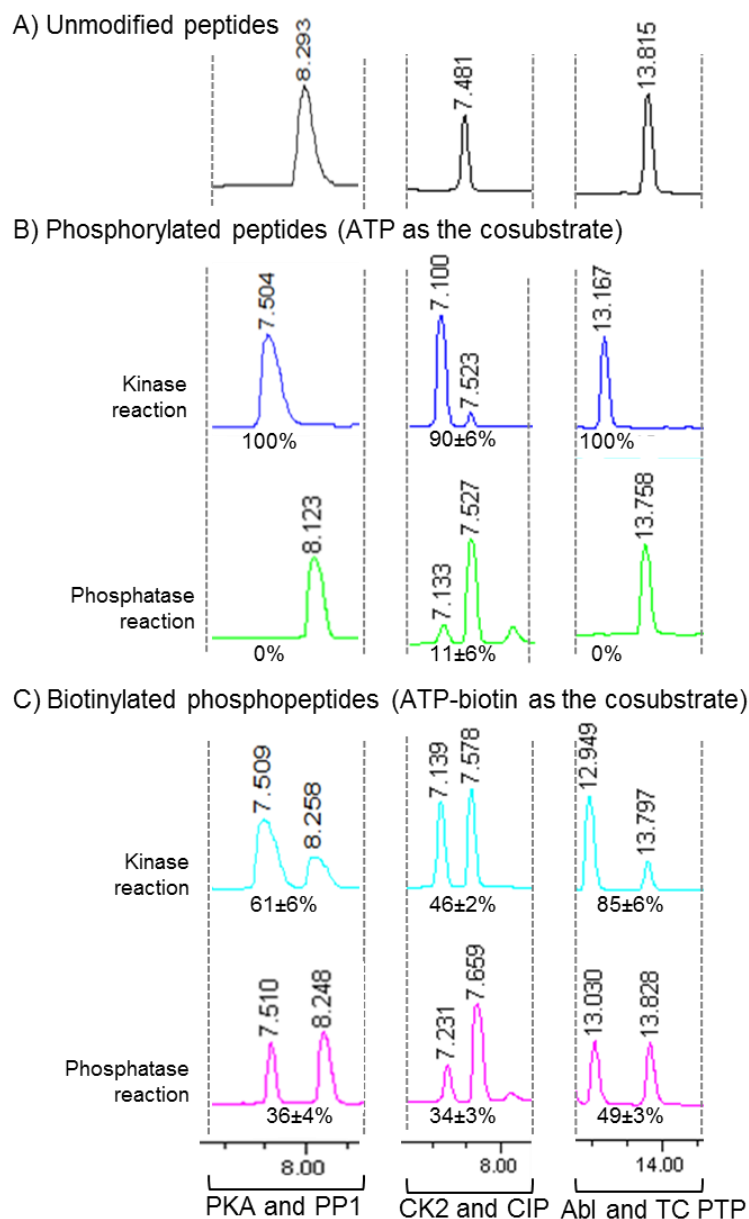
Figure 3.4: HPLC analysis and quantification of phosphorylated and biotinylated peptides before and after phosphatase treatment (A) HPLC analysis of unmodified peptides (PKA peptide at ~8.3 min; CK2 peptide at ~7.5 min; Abl peptide at ~13.8 min). **(B)** HPLC analysis of ATP-phosphorylated peptides (top; PKA phosphopeptide at ~7.5 min; CK2 phosphopeptide at ~7.1 min; Abl peptide at ~13.2 min) after phosphatase treatment (bottom). **(C)** HPLC analysis of ATP-biotin phosphopeptides (top; PKA phosphopeptide at ~7.5 min; CK2 phosphopeptide at ~7.1 min; Abl phosphopeptide at ~12.9 min) after phosphatase treatment (bottom). The percentages in B and C represent the average percentage phosphopeptide observed from 3 independent trials with standard error. The complete HPLC traces are shown in Figure A 3.1, A 3.2, and A 3.3.

In contrast, a significant amount of biotinylated phosphopeptide products were observed after phosphatase treatment; 34-49% phosphopeptides were still observed after phosphatase reaction (Figure 3.4 C, bottom). Comparing the percentage of biotinylated product before and after phosphatase incubation (Figure 3.4 C, bottom versus top) revealed that 59% (PP1), 74% (CIP), and 58% (TCPTP) of the modification remained intact. Therefore, while phosphatases maintained 89-100% activity with phosphopeptide substrates, only 26-42% activity was seen against biotinylated phosphopeptides. Of the three phosphatases tested, CIP was the least active (26%) with PP1 and TCPTP maintaining similar activities (41% and 42%). These studies indicate that the phosphorylbiotin modification is less susceptible to phosphatase hydrolysis than a phosphate modification.

3.5 Phosphatase Activity with Biotinylated Phosphoproteins

Our next goal was to study the sensitivity of full-length biotinylated phosphoproteins to phosphatase activity. While the kinase/phosphatase pairing was the same as with the peptides experiments, the full-length substrates used were myelin basic protein (MBP) with PKA and Abl and β-casein with CK2 (Figure 3.5). Similar to the peptide experiments, a two-step reaction series was employed with kinase reaction first, followed by phosphatase incubation. In this case, the crude products were analyzed by gel methods.

Control reactions with ATP demonstrated the sensitivity of phosphoproteins to degradation by phosphatases; only 6-7% of total phosphoproteins were observed by Pro-Q staining (Figure 3.5, lanes 2, 6, and 10, Pro-Q), indicating that phosphatases maintain 93-94% activity at removing phosphates. In contrast, a significant amount of biotinylated phosphoproteins was still detected after phosphatase treatment; 72-83% of total biotinylated phosphoproteins were observed (Figure 3.5, lanes 4, 8, and 12, SA-Cy5), indicating that the

phosphatases demonstrated only 17-28% activity at removing the biotin tag. Consistent with the stability of the biotin tag to phosphatases, 37-66% biotinylated phosphoproteins were detected after phosphatase incubation using Pro-Q staining (Figure 3.5, lanes 4, 8, and 12, Pro-Q). Comparing the percentage of Pro-Q-visualized biotinylphosphoproteins after and before phosphatase incubation (Figure 3.5, lanes 4 vs 3, 8 vs 7, and 12 vs 11, Pro-Q) revealed that 85% (PP1), 66% (CIP), and 90% (TCPTP) of the modification remained intact. The Pro-Q analysis indicated that phosphatases maintained 10-34% activity against biotinylated phosphopeptides. The differences in activity comparing biotin (17-28%) and phosphate (10-34%) detection (Figure 3.5, SA-Cy5 versus Pro-Q) may be due to the presence of phosphorylation sites on the substrates prior to kinase reaction, which would skew the Pro-Q staining data.
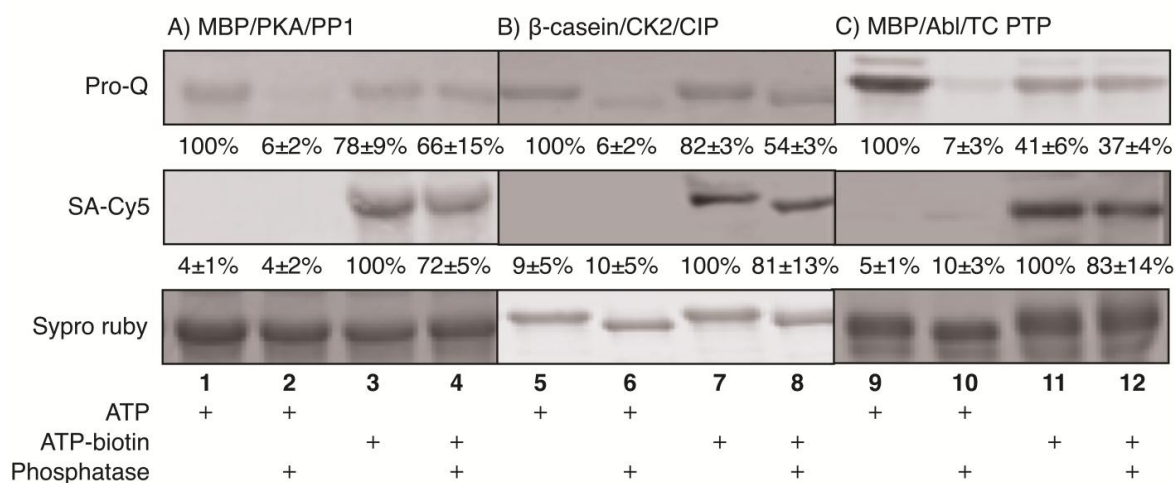
Figure 3.5: Gel analysis and quantification of phosphorylated and biotinylated proteins before and after phosphatase treatment. The contents of each reaction are indicated below each lane. Pro-Q staining visualizes phosphoproteins, SA-Cy5 staining detects biotin-labeled proteins, and Syproruby stains for total protein content. The percentages of phosphorylated (Pro-Q) or biotinylated (SA-Cy5) proteins were calculated relative to lanes 1, 5, or 9 (Pro-Q, 100%) or lanes 3, 7, or 11 (SA-Cy5, 100%). The full gel images, along with additional control reactions, are shown in Figure A 3.4, A 3.5, and A 3.6 of appendix.

A comparison of the activity data suggests that full-length biotinylated proteins are less sensitive to phosphatases than biotinylated peptides (17-28% versus 26-42%). The protein data represents the aggregate reactivities of all phosphorylation sites in the protein to phosphatases. As a result, the data suggest that the majority of phosphorylation sites on full length proteins are less susceptible to phosphatase hydrolysis than in isolated peptides. The steric bulk of full-length proteins may prevent phosphatase binding and catalysis. The significant conclusion from the experiments is that the phosphorylbiotin group, particularly on full length proteins, shows significant stability to phosphatase degradation.

3.6 Inhibitor Studies in Cell Lysates

With an eye towards future phosphoproteomics applications, we were interested in probing how the phosphatase stability of the phosphorylbiotin tag would impact lysate labelling. Because cell lysates naturally contain phosphatases, typical phosphoproteomics experiments include phosphatase inhibitors in the cell lysates to stabilize phosphorylation.[144, 145] With the stability of the phosphorylbiotin tag, we hypothesized that robust kinase-catalyzed labeling will occur in lysates without the need for phosphatase inhibitor treatment. In addition, we wondered how phosphatase inhibitors would impact kinase-catalyzed labeling. Given the interest in kinases and phosphatase inhibitors as drug targets,[146-149] inhibitor experiments would also establish the utility of kinase-catalyzed labelling as a drug characterization tool.

3.6.1 Phosphatase Inhibitors

In contrast to kinase inhibitors (chapter 1.4), there are few inhibitors designed to target protein phosphatases (Figure 3.6). However, a handful of phosphatase inhibitors are used to treatment of diseases, such as diabetes, obesity and cancer.[128, 150, 151] Sodium stibogluconate is the FDA approved phosphatase inhibitor used to treat for cutaneous leishmaniasis.[148, 152] In

addition, suramin, phenylarsine oxide, aplidin, alendronate, vanadate, etidronate, and gallium nitrate are used as drugs.[153] Interestingly, finding new phosphatase inhibitor drugs has become actively investigated recently.[148, 150] However, it is challenging to find selective inhibitors due to similarities in the active sites of protein phosphatases and poor cell permeability of hydrophilic inhibitors.
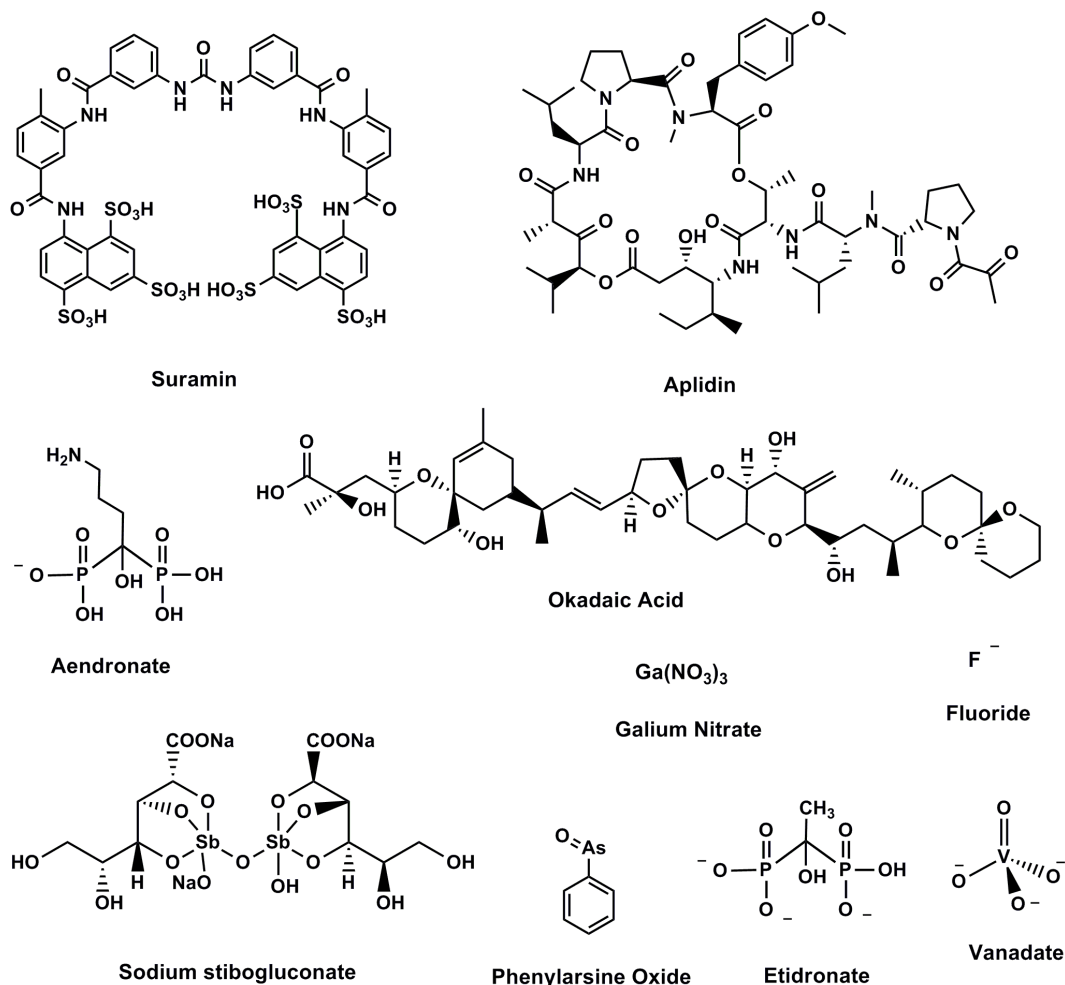
Figure 3.6: Structures of Common Phosphatase Inhibitors. Structures of widely used phosphatase inhibitor molecules are shown here including: Sodium stibogluconate, FDA approved drug; suramin, phenylarsine oxide, aplidin, alendronate, etidronate, and gallium nitrate, used in clinical trials; Vanadate, fluoride and okadaic acid are used in primary laboratory research.

3.6.2 Inhibitor Studies in Cell Lysates: 1-D Gel Analysis

HeLa cell lysates were incubated with ATP-biotin in the presence of a kinase inhibitor (staurosporine) or phosphatase inhibitors (sodium vanadate and sodium fluoride). As a control, inhibitor experiments were also performed with ATP incubation. As expected, reactions performed in the presence of kinase inhibitors showed only trace levels of phosphorylated (Figure 3.7, lane 3, Pro-Q,) and biotinylated (Figure 3.7, lane 6, SA-Cy5) proteins. Quantification and comparison between kinase inhibitor treated and untreated lanes revealed that only 18±2% of phosphorylated (Figure 3.7, lanes 3 versus 2, Pro-Q) and 27±5% of biotinylated (Figure 3.7, lanes 6 versus 5, SA-Cy5) proteins were visible (Figure A 3.8). The slightly elevated level of biotinylation remaining with kinase inhibition may be due to the natural presence of biotinylated proteins in cell lysates. These experiments indicate that kinase inhibitors similarly reduce phosphorylation or biotinylation. Because monitoring changes in phosphorylation after inhibitor treatment has been used as a drug characterization tool,[154-156] a future direction is use of ATP-biotin labeling to characterize kinase inhibitor activities.

In contrast to the kinase inhibitor experiments, phosphatase inhibitors had differing effects on phosphorylation and biotinylation. As expected with ATP phosphorylation, reactions containing phosphatase inhibitors showed robust phosphoprotein signal (Figure 3.7, lane 4, Pro-Q). Comparison of the phosphatase treated and untreated reaction lanes showed that the phosphoprotein signal was elevated to 118±9% (Figure 3.7, lane 4 versus 2, Pro-Q). These results are consistent with the use of phosphatase inhibitors to augment phosphorylation levels in phosphoproteomics applications.[144, 145] In the case of the ATP-biotin reactions, a biotin signal was also observed in phosphatase inhibitor treated reactions (Figure 3.7, lane 7, SA-Cy5). However, comparison of the treated and untreated reaction lanes revealed that the biotin signal

was reduced to 81±6% (Figure 3.7, lanes 7 versus 5, SA-Cy5, Figure A 3.8). The decrease in

biotinylation can be rationalized considering the kinase/phosphatase equilibrium in lysates.

Because phosphorylated amino acids will be unavailable for ATP-biotin labeling, active

phosphatases are needed to remove phosphoryl groups and promote kinase-catalyzed

biotinylation. If phosphatase activity is reduced by inhibitors, ATP-biotin labeling will not occur

on already phosphorylated sites, reducing the level of biotinylation.   Therefore, these

experiments are consistent with the hypothesis that active phosphatases are critical for robust

kinase-catalyzed labeling in lysates.
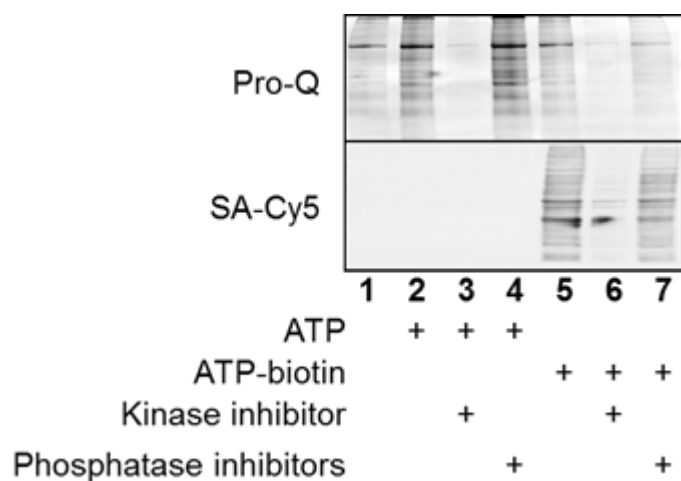
Figure 3.7: Inhibitor Studies with 1-D Gel Analysis: Gel analysis of phosphoproteins (ProQ, top) or biotinylated phosphoproteins (SA-Cy5, bottom) from HeLa cell lysates incubated with ATP or ATP-biotin in the absence or presence of kinase or phosphatase inhibitors. The contents of each reaction are indicated below each lane. Additional trials are shown in Figure A 3.7.

3.6.3 Inhibitor Studies in Cell Lysates: 2-D Gel Analysis

To further test the sensitivity of biotinylation to phosphatase inhibitors, two dimensional (2-D) gel analysis was performed (Figure 3.8). 2-D gel analysis is a classical method that offers visualization of many more proteins in lysates than 1-D methods.[157, 158] In addition, 2-D gel methods have been used widely in phosphoproteomics analysis.[159, 160] HeLa cell lysates were incubated with either ATP or ATP-biotin in the absence or presence of phosphatase inhibitors (sodium vanadate and sodium fluoride). After reaction, proteins were separated by their isoelectric points (pI) in the first dimension, followed by molecular weight in the second dimension. As expected, ATP-labeled lysates treated with phosphatase inhibitors contained more phosphoproteins compared to untreated reactions (Figure 3.8 A, see boxed area). In contrast, ATP-biotin-labeled lysates showed a greater number of biotinylated proteins in the untreated reaction than the phosphatase inhibitor-treated reaction (Figure 3.8 B, see boxed area). The reduction in ATP-biotin labeling upon phosphatase inhibitor treatment is consistent with the 1-D gel analysis (Figure 3.7), which provide further evidence for the hypothesis that active phosphatases are needed for robust kinase-catalyzed biotinylation.

A) ATP labeling

Untreated   Phosphatase inhibitor treated

170

kDa

7

3   pH   10   3   pH   10

B) ATP-biotin labeling

Untreated   Phosphatase inhibitor treated

170

kDa

7

3   pH   10   3   pH   10
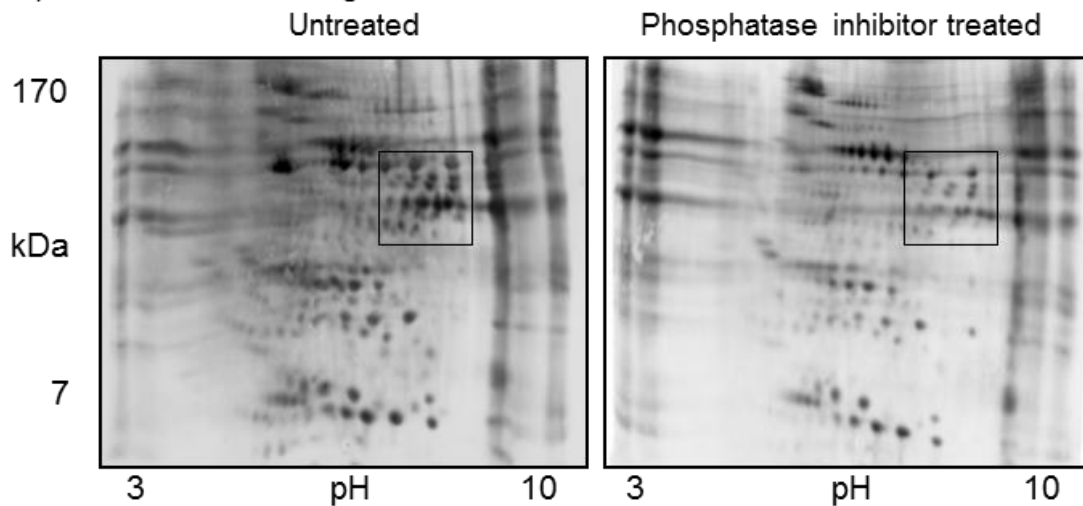
Figure 3.8: Inhibitor Studies with 2-D Gel Analysis (A) Reactions of HeLa cell lysates and ATP without (untreated) or with phosphatase inhibitors (phosphatase inhibitor treated). Proteins were visualized with Pro-Q diamond phosphoprotein stain. (B) Reactions of HeLa cell lysates and ATP-biotin without (untreated) or with phosphatase inhibitors (phosphatase inhibitor treated). Biotinylated proteins were visualized with SA-Cy5. The boxed region of the images highlights changes due to inhibitor treatment.

A comparison of the boxed areas within the 2-D gel images shows that the phosphatase inhibitor-treated ATP labeling (Figure 3.8 A, right) and untreated ATP-biotin labeling (Figure 3.8 B, left) showed similarities.   We note that the differences in charge state of the phosphorylated and biotinylated proteins (see Figure 3.1) likely influence migration in the gels, making direct comparison of ATP and ATP-biotin labeled reactions difficult by 2-D methods. The comparison is further complicated by the use of different visualization methods (Pro-Q versus SA-Cy5). However, the combined data from 1-D and 2-D methods is consistent with the hypothesis that robust kinase-catalyzed biotinylation occurs without the need for phosphatase inhibitor treatment.   Therefore, kinase-catalyzed biotinylation is appropriate for phosphoproteomics application using untreated lysates.

3.7 Conclusion and Future Work

We have shown that the phosphorylbiotin product of kinase-catalyzed biotinylation is stable to phosphatases. In vitro experiments suggest that both Ser/Thr and Tyr phosphatase are similarly ineffective at phosphorylbiotin hydrolysis. These results are consistent with prior work documenting that the product of ATP-γS labeling, a thiophosphorylated protein, is also insensitive to phosphatase degradation.[74, 85, 86, 141]   The combined results suggest that phosphoproteins containing a phosphate modification will generally display phosphatase insensitivity. ATP-γS has been used for phosphoprotein labeling and detection directly in lysates, without the need for phosphatase inhibitors.[80, 81, 87, 124, 142]   The use of untreated lysates combined with the added functionality of the biotin group makes ATP-biotin labeling attractive for phosphoproteomics applications. In particular, the likelihood of detecting low abundance phosphoproteins is enhanced due to the stability of the biotin tag to phosphatases and the ability to purify labeled proteins directly. Use of kinase-catalyzed biotinylation for detection of low

abundance phosphoproteins is currently under investigation. In addition, the sensitivity of ATP-biotin labeling to both kinase and phosphatase inhibitors indicates that kinase-catalyzed labeling has future application to phosphoproteomic-based drug characterization efforts. In conclusion, the stability of the phosphorylbiotin product of ATP-biotin labeling to phosphatases suggests that kinase-catalyzed biotinylation will be an excellent tool for phosphoproteomics research.

In future work, we hope to monitor phosphatase activity using kinase-catalyzed labeling. For that first, phosphatase knock down cell line will be generated. The strategy would involve labeling of untreated versus phosphatase knock down lysates with ATP-biotin. This method is based on the fact that phosphatase activity is required for robust biotinylation, by removing phosphates that generates sites for biotin labeling. After gel purification, those proteins that are substrates to the knocked down phosphatase would be identifiable to due to a reduction of biotin label compared to the untreated sample. This analysis will be coupled with MS-based protein characterization to provide a simple method to identify substrates. Hence, kinase-catalyzed labeling could lead to the identification of phosphatase substrates, which is a key step to characterizing phosphatase biology and cell signaling.

3.8 Experimental

3.8.1 Materials

ATP-biotin was synthesized as explained in Chapter 2, section 2.6.3 and 2.6.4. Adenosine 5'-triphosphate disodium (ATP), glycerol, sodium hydroxide (NaOH), potassium chloride (KCl), magnesium chloride (MgCl$_2$), sodium chloride (NaCl), sodium dodecyl sulfate (SDS), glacial acetic, acetonitrile, staurosporine and SA-Cy5 conjugate were purchased from Fisher. HPLC grade trifluoroacetic acid (TFA) and acetonitrile were obtained from VWR and EM Millipore, respectively. N, N-dimethylformamide (DMF) was purchased from Acros Organics. D$_2$O and CD$_3$OD were obtained from Cambridge Isotope Labs. Ammonium bicarbonate, β-casein and myelin basic protein (MBP) were bought from Sigma. PKA, CK2, Abl, CIP, PP1, TC PTP enzymes, sodium fluoride, sodium orthovanadate and Abl peptide were purchased from New England Biolabs. Kemptide and CK2 peptides were bought from Promega. Triton X-100 was purchased from Fluka. HeLa cells were obtained from the National Cell Culture Center (www.nccc.org). Protease inhibitor cocktail V was purchased from Calbiochem, and Bovine serum albumin (BSA) was obtained from Santa Cruz Biotechnology. Immobilion P PVDF membrane was purchased from Millipore. Sypro Ruby and Pro-Q diamond stain was obtained from Invitrogen. 2-D gel starter kit, rehydration/equilibration trays, ReadyStrip IPG strip (pH 3-10), and Ready Gel Tris-HCl Gel were purchased from Bio-Rad.

3.8.2 Instrumentation

The absorbance values for Bradford assay were measured with a fluorimeter (GENios Plus Tecan). The SDS-PAGE apparatus was purchased from BioRad (Protean III) and a mini-gel setup was used. Western blotting was carried out using the Mini-Transblot Electrophoretic

Transfer Cell apparatus from BioRad. Protein IEF cell (Bio-Rad, used with permission from Honn lab) was used for 2-D gel analysis. The peptides were analyzed using a Waters 1525 binary HPLC pump and Waters 2998 photodiode array detector. Reverse phase C-18 column (YMC America, INC 250*4.6 mm, 4μm, 8 nm) was used to separate peptide mixtures. The separated proteins were visualized using a Typhoon 9210 scanner (Amersham Biosciences).

3.8.3 Kinase-Catalyzed Phosphorylation and Biotinylation

Phosphorylated peptides or biotinylated phosphopeptides were created by incubating ATP or ATP-biotin (2 mM) with PKA (20 units/μL) and Kemptide peptide substrate (400 μM, LRRASLG), CK2 (20 units/μL) and CK2 peptide substrate (400 μM, RRREEETEEE), or Abl (20 units/μL) with Abl peptide substrate (400 μM, EAIYAAPFAKKK). The final volume of the reactions was 20 μL and the manufacturer-supplied buffers were used at a 1X concentration (NEB). The reaction mixtures were incubated at 30 ℃ for 2 hours. After reaction, the mixtures were heated at 95℃ for 1 minute to denature the kinase. The reactions were split into two 10 μL portions. One 10 μL sample was used directly for HPLC analysis, as described below, while the second 10 μL sample was treated with phosphatase, as described below.

Phosphorylated or biotinylated proteins were created by incubating ATP or ATP-biotin (2 mM) with PKA (25 units/μL) and myelin basic protein (MBP, 0.2 mM), CK2 (5 units/μL) and β-casein (0.2 mM), or Abl (5 units/μL) and MBP (0.2 mM) in the manufacturer-provided buffer (1X, NEB). As a control, reactions were performed without kinases. The final volume of the reactions was 10 μL. The reaction mixtures were incubated at 30˚C for 2 hours. After the reaction, the mixture was heated at 95 ℃ for 1 minute to denature the kinase. Only with CK2 reactions, ATP or ATP-biotin was removed using a 10 kDa Centriprep spin column (Millipore); we found that ATP or ATP-biotin interfered with subsequent treatment with CIP. The reactions

were split into two 5 µL portions. One 5 µL sample was diluted up to 20 µL and used for SDS-PAGE analysis, as described below, while the second 5 µL sample was treated with phosphatase, as described below.

3.8.4 Phosphatase-Catalyzed Dephosphorylation

Protein or peptide phosphorylation and biotinylation were performed as described in section 3.8.3. Then phosphatases were added to the appropriate reaction mixtures. For PKA reactions, PP1 (1.0 units/µL, final concentration) in the manufacturer-provided buffer (1X, NEB) was added and the reaction mixture was incubated at 30˚C for 2 hours. For CK2 reactions, CIP (2.5 units/µL, final concentration) in the manufacturer-provided buffer (1X, NEB) was added and the reaction was incubated at 37 ºC for 2 hours. For Abl reactions, TCPTP (2.5 units/µL, final concentration) in the manufacturer-provided buffer (1X, NEB) was added and the reaction was incubated at 30˚C for 2 hours. The final volume of the reaction mixtures was 20 µL. The crude protein products were analyzed by SDS-PAGE with subsequent gel imaging, as described below, while the peptide reactions were analyzed by HPLC analysis, as described below.

3.8.5 HPLC Analysis

For HPLC analysis, peptides were pre-equilibrated in Buffer A (50 µL; 99.9% water with 0.1% trifluoroacetic acid). Reverse phase chromatographic separation of peptides was performed using a C18 column (YMC America INC; 250×4.6 mm, 4µm, 8 nm). The elution gradient started with 95% Buffer A in Buffer B (99.9% acetonitrile with 0.1% trifluoroacetic acid), and decreased to 70% Buffer A over 15 min. Due to overlap of several peaks, the PKA/PP1 reaction used a different gradient starting at 90% Buffer A in Buffer B, and decreasing to 70% Buffer A over 15 min. The flow rate was 1 mL/min and the peptide absorbance was detected at 214 nm.

The percentage of observed phosphopeptide was calculated by dividing the area under the phosphopeptide peak by the total area under both the phosphopeptide and unmodified peptide peaks. Figure 3.4 B and 3.4 C show the average percentage and standard error of observed phosphopeptide from three independent trials (Figures A 3.1-3.3).

3.8.6 Starting a New Cell Culture

The strain of HeLa cells used was HeLa S3 obtained from ATCC (American Type Culture Collection). These cells were stored into aliquots (1.0 mL, 10×10^6 cells) in cryogenic vials and stored in a liquid nitrogen storage tank upon receipt. When starting a new cell culture, an aliquot was removed from the liquid nitrogen tank and thawed quickly in a 37 °C water bath. The solution of cells was then transferred to a 15 mL centrifuge tube and centrifuged at 1000 rpm for approximately 5 minutes. The supernatant was carefully discarded and the pellet of cells was resuspended into 5 mL of Ham's F-12 media (F-12 Nutrient Mixture, Invitrogen) containing 10% v/v fetal bovine serum (FBS, Invitrogen). The cells were grown in a 37°C incubator under a 5% CO_2 environment with 95% relative humidity. The cell concentration during growth was maintained between $0.5-1.0 \times 10^6$ cells per mL.

3.8.7 Long Term Cell Storage

Cells near confluency (approximately 1×10^6 cells per mL) were collected by centrifugation at 1000 rpm for 5 minutes. The cell pellet (approximately 10×10^6 cells) was resuspended in 1.5mL of fresh Ham's F-12 media with 10% v/v FBS containing a final concentration of 10% v/v DMSO. The cells were slowly cooled in a cryogenic vial (Corning) and then stored in a liquid nitrogen storage tank (Thermolyne).

3.8.8 Collection of Cells for Experiment

To HeLa cells at confluency, triple express (5-10 mL) was added to the flask to cover the surface and incubated at 37 °C for 10 minutes. The released cells (make sure cells were lifted and floating) were transferred to a centrifuge tube and centrifuged at 1000 rpm for 5 minutes. The supernatant was discarded and cells were gently washed with 1X PBS (phosphate buffered saline) consisting of 137 mM NaCl, 2.7 mM KCl, 10 mM Na_2HPO_4, 2 mM KH_2PO_4, pH 7.4. The cell pellet was stored at -80 °C until needed, or used immediately.

3.8.9 Large-Scale HeLa Cell Lysis Procedure

Frozen HeLa cells (National Cell Culture Center, 10×10^9 cells) were thawed and kept on ice. HeLa cells were lysed in lysis buffer (10 mL; 50 mM Tris, pH 8.0, 150 mM NaCl, 10% glycerol, 0.5% Triton X-100 and 1X protease inhibitor cocktail V). Cells were incubated with rotation at 4 °C for 10 minutes. The soluble fraction was separated from the cell debris by spinning at 12,000 rpm at 4 °C for 15 minutes. The supernatant was collected and the concentration of total protein in the lysate was determined via a Bradford assay (generally 5-6 mg/mL total protein). The lysate supernatant was stored at -80 °C.

3.8.10 Bradford Assay

The Bradford reagent dye (Bio-Rad Protein Assay, manufactured by Bio-Rad Laboratories) was prepared by diluting 1 part dye reagent concentrate with 4 parts of ddH_2O and filtering through a 0.22μm pore size filter (Millex-GP, Millipore) to remove particles. To create a standard curve, several dilutions of bovine serum albumin (BSA, Fisher Scientific) ranging from 0.5 to 5.0 mg/mL were prepared in H_2O, which were within the linear range of this assay. Several dilutions of the lysate were also prepared, typically around 1/50 of the original

concentration of the unknown to ensure the resulting concentration fell within the linear range of the assay. Each standard solution (10 µL) and each unknown dilution (10 µL) was pipetted into separate wells of a flat-bottom transparent 96-well microtiter plate (Assay Plate, Costar). The diluted Bradford reagent dye (200µL) was added to each well and the plate was incubated at room temperature for at least 5 minutes. The absorbance was measured with a fluorimeter (GENios Plus) at a wavelength of 595 nm. A standard curve was generated from the known concentrations of the BSA standards using Microsoft Excel to plot the known concentrations of the standards against the corresponding measured absorbance values. A best-fit linear equation was generated each time the assay was run in order to minimize any errors that may have resulted from fluctuations in the instrument over time. To determine the concentration of the unknown sample, the observed absorbance value of the unknown dilution was used with the equation of the best-fit line to calculate the concentration of the diluted lysate. The resulting concentration of the diluted sample was then multiplied by the dilution factor to obtain the concentration of the original lysate.

3.8.11 Kinase and Phosphatase Inhibitor Studies

For the lysate reactions, HeLa cell lysates (100 µg of total protein) were incubated with either ATP or ATP-biotin (2 mM) in the presence kinase inhibitor (Staurosporine, 0.10 mM) or phosphatase inhibitors (sodium fluoride and sodium orthovanadate, 0.10 mM each) in the manufacturer-provided buffer for PKA (1X, NEB) for 2 hours at 30 °C. The final volume of the reactions was 25 µL. The products were analyzed by SDS-PAGE (Chapter 2, section 2.6.9) with subsequent gel imaging (Chapter 2, section 2.6.10 and 2.6.13) and quantification of the entire lane (Chapter 2, section 2.6.14). The percentage of phosphoproteins or biotinylated

phosphoproteins observed after inhibitor treatment was calculated by dividing the protein signal after treatment to the protein signal before treatment.

3.8.12 Two-Dimentional Gel Analysis

The reactions with lysates with or without phosphatase inhibitors were performed as described in section 3.8.11. Protein sample after reaction (100 µg) was mixed with 125 µL of manufacturer (Bio-Rad) provided rehydration/sample buffer (2% CHAPS, 8 M urea, 50 mM DTT, 0.2% (w/v) Bio-Lyte 3/10 ampholytes and trace Bromophenol Blue). Then the mixture was loaded into the rehydration/equilibration tray channel, except for 1 cm at each end. The process was repeated for remaining samples, taking care not to introduce any air bubbles. ReadyStrip IPG strip (pH 3-10) was peeled from the coversheet and the strip was gently placed onto the sample (gel side down, taking care not to introduce any air bubbles). The IPG strip was left to rehydrate for one hour. Then 2 mL of mineral oil was overlaid to prevent evaporation. The rehydration/equilibration tray was covered with the plastic lid and left overnight (12-16 hours) to rehydrate the strips and maximize sample absorption. The next day, a paper wick was placed at both ends of the IEF focusing tray channels covering the wire electrode and the paper wick was wetted with 10 µL of nanopure water (Bio-Rad). The cover was removed from rehydration/equilibration tray and the strip was held vertically for 10 seconds to drain the mineral oil. Then the IPG strip was transferred to the focusing tray (gel side down) and the strip was covered with 2 mL of mineral oil. The focusing tray was placed into the PROTEIN IEF cell and focusing was performed (250 V for 20 min, 4000 V for 2 hours and at 4000 V for 10 000 Vhours, 50 µA per strip and temperature maintain at 20 ˚C). After electrophoresis was completed, the IPG strip was removed from the focusing tray and the strip was held vertically for 10 seconds to drain the mineral oil. Then the strip was transferred into a new

rehydration/equilibration tray (gel side up) and equilibrated for 10 minutes in buffer 1 containing 0.375 M Tris-HCl (pH 8.8), 6 M urea, 30% (v/v) glycerol, 2% (w/v) SDS and 2% (w/v) DTT. Next, the strip was incubated with buffer 2 containing 0.375 M Tris-HCl (pH 8.8), 6 M urea, 30% (v/v) glycerol, 2% (w/v) SDS and 2.5% (w/v) iodoacetamide. The IPG strip was removed from the rehydration/equilibration tray and was dipped into the graduated cylinder containing 1X Tris/glysine/SDS running buffer. Then an agarose solution (Bio-Rad) was poured into the top of the SDS-PAGE gel as stacking layer and the IPG strip was placed within the agarose layer (taking care not to introduce any air bubbles). The gel was run at a constant 200 V for 45 minutes.

3.8.13 Biotin Visualization

The biotin visualization was performed as described in Chapter 2, section 2.6.10.

3.8.14 Sypro Ruby Stain

The Sypro Ruby staining was performed as described in Chapter 2, section 2.6.12.

3.8.15 Pro-Q Staining

The Pro-Q staining was performed as described in Chapter 2, section 2.6.13.

3.8.16 Gel Image Quantification

Gel bands were quantified using ImageQuant 5.1 by drawing the same size rectangular shape around comparable bands.   The percentage of phosphoproteins or biotinylated phosphoproteins observed after phosphatase treatment was calculated by dividing the protein signal after treatment to the protein signal before treatment. The percentages displayed in Figure 3.5 are average percentages and standard error of observed phosphoprotein or biotinylated

phosphoprotein from three independent trials. To calculate phosphatase activity, the average percentage of phosphoproteins or biotinylated phosphoproteins observed after phosphatase treatment was subtracted from 100%.

Footnote: Portions of the text in this chapter were reprinted or adapted with permission from

Licensee: chamara senevirathne
License Date: Mar 11, 2013
License Number: 3106010371572
Publication: ChemBioChem
Title: Biotinylated Phosphoproteins from Kinase-Catalyzed Biotinylation are Stable to Phosphatases: Implications for Phosphoproteomics
Type Of Use: Dissertation/Thesis

Chapter 4

Phosphoproteomic Analysis using Kinase-Catalyzed Biotinylation

Protein phosphorylation plays a fundamental role in protein function, and aberrant phosphorylation level and elevated kinase activity are responsible for the disease formation. Here we report development of a new phosphoproteomic enrichment tool combining kinase-catalyzed biotinylation with avidin affinity chromatography. Given the limitations of metal ion affinity chromatography with full-length phosphoprotein enrichment, kinase-catalyzed biotinylation may provide new opportunities for future proteomics research.

4.1 Current Methods Used to purify Phosphopeptides and Phosphoproteins

Since phosphorylation has a significant role in protein function, the detection and isolation of phosphopeptides and phosphoproteins are important goals for proteomic research.[117] Mass spectrometric (MS) analysis has been widely used to identify protein phosphorylation.[116, 118, 161, 162] MS analysis can be coupled with different separation systems and mass analyzers to increase sensitivity and accuracy.[120, 121] Despite many improvements, MS has limitations. For example, the ion suppression of the charged phosphate in MS analysis results in difficulty detecting phosphopeptides in complex mixtures.[122] To minimize the influence of ion suppression, unphosphosphorylated peptides are often removed from the mixtures prior to MS analysis. As a result, multiple phosphopeptide purification methods have been developed to enhance phosphoproteomics analysis. Phosphoprotein and phosphopeptide enrichment techniques can be grouped into four main classes: immunoprecipitation, chemical modification, affinity chromatography, and modified ATP analogs [83, 106] (Figure 4.1).
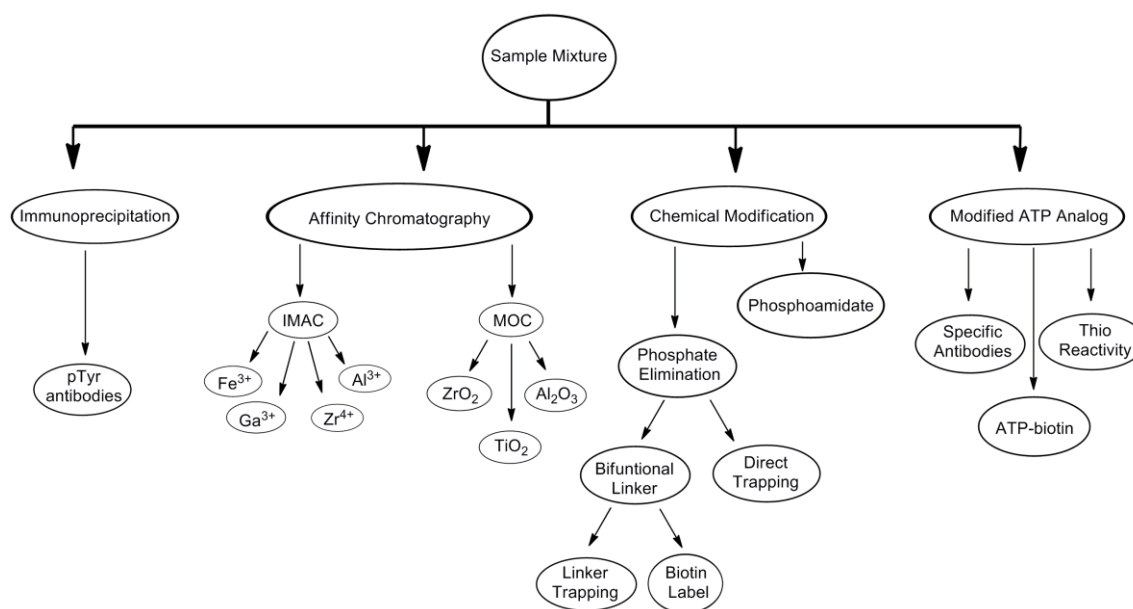
Figure 4.1: Overview of Phosphopeptide and Phosphoprotein Isolation Methods. Schematic representation of current methods of phosphopeptide and phosphoprotein purification is shown here. The purification methods are classified into four major groups; immunoprecipitation, affinity chromatography, chemical modification and modified ATP analogs strategies.

4.1.1: Immunoprecipitation

Phosphoproteins can be immunoprecipitated by antibodies generated specifically against phosphopeptides.[108] For phosphoproteomics applications, antibodies recognizing a single phosphotyrosine amino acid have been used successfully, while the poor binding affinity of antibodies recognizing phosphoserine or phosphothreonine has limited their use.[110, 115] The antibody is immobilized to solid phase resin through covalent bond before immunoprecipitation. A mixture of protein sample is incubated with the immobilized antibody, and proteins containing a phosphotyrosine will bind with the antibody (Figure 4.2). Unbound proteins are removed during washing steps and only the phosphotyrosine containing proteins are retained. Then pure

phosphoproteins are eluted from the resin by applying denaturing conditions. The isolated

phosphoproteins can be analyzed by MS after digestion.
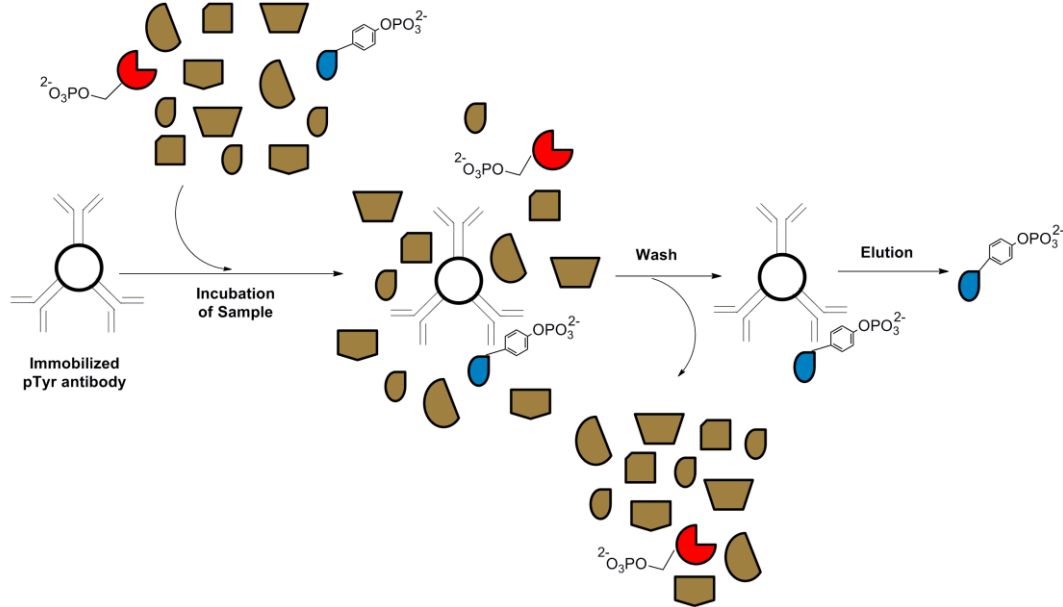
Figure 4.2: Immobilized Antibody Purification of Phosphoproteins. Phosphotyrosine specific antibodies are attached to a solid resin. Incubation of the sample results in the binding of phosphotyrosine proteins only and unbound proteins can be washed away. The isolated proteins are eluted, digested and analyzed with MS.

4.1.2: Affinity Chromatography

Affinity chromatography is the most popular and widely used method in phosphopeptide

isolation. Affinity chromatography can be subdivided in to two strategies; Immobilized Metal

Affinity Chromatography (IMAC) and Metal Oxide Chromatography (MOC). Various metal

ions (Ga^{3+}, Fe^{3+} and Al^{3+}) [105, 163-165] and, metal oxides (TiO_2, ZrO_2 and Al_2O_3) [166-168] facilitate

phosphopeptide enrichment for IMAC and MOC, respectively. In IMAC, the metal ion is usually

bound to the resin using iminodiacetic acid (IDA) or nitrilotriacetic acid (NTA) (Figure 4.3),

whereas MOC uses the metal oxide as the resin (Figure 4.4). Both methods purify

phosphopeptides using a similar type of mechanism. Application of peptide mixtures leads to

binding through electrostatic interactions between the negatively charged phosphates and positively charged metal. Unmodified peptides can be removed from the resin upon washing. Then phosphopeptides can be eluted from the resin and analyzed by MS. However, it is widely reported that metal ion chromatography is biased towards phosphopeptides containing negatively charged aspartic and glutamic acid residues,[169] which enhance binding affinity to the positively charged metal. In addition, full-length phosphoprotein enrichment remains technically challenging with metal ion chromatography.
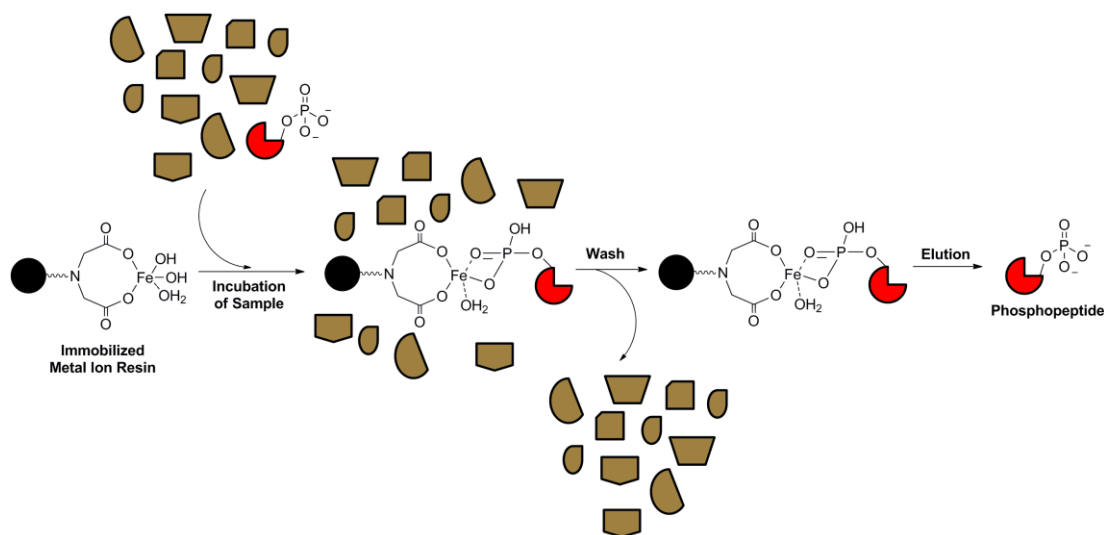
Figure 4.3: Immobilized Metal Affinity Chromatography (IMAC) Purification. Incubation of peptide mixture with IMAC column results in binding of phosphopeptides to the resin. Washing removes unphosphorylated peptides to elute pure phosphopeptides. Purified phosphopeptides can be analyzed by MS.
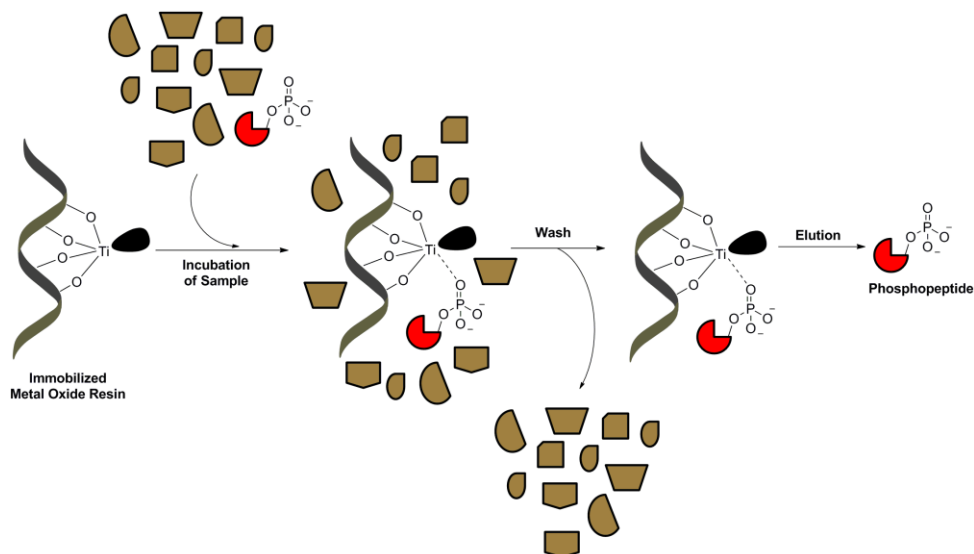
Figure 4.4: Immobilized Metal Oxide Chromatography (MOC) Purification. Incubation of peptide mixture with MOC column results in binding of phosphopeptide to the resin. Washing removes unphosphorylated peptides to elute pure phosphopeptides. Purified phosphopeptides can be analyzed by MS.

4.1.3: Chemical Modification

In terms of chemical modification strategies, two examples include β-elimination of the phosphate groups of phosphoserine and phosphothreonine[170, 171] and covalent phosphate modification methods (via a phosphoamidate).[172-174] For the β-elimination method (Figure 4.5), alkali treatment of phosphorylated serine or threonine **1** formed dehydroalanine **2,** which can be treated with a biotin (path A) or bifunctional tagging groups (path B).[170] Introducing a biotin tag facilitates direct affinity purification (path A, compound **3**).[171] On the other hand, incubation with ethanedithiol attaches a thiol group (path B, compound **4**), which can be cross-linked with NHS activated biotin for subsequent purification (path B, compound **5**) or, the free thiol can be directly attached to solid support resin via a disulfide linker (path A, compound **6**), which will release purified peptides upon reduction. Dehydroalanine intermediate (**2**) formation with O-linked sugars and alkylated cysteine under alkaline conditions is the major drawback of this

method. In addition, because a thiol group is introduced, all the cysteines should be blocked by oxidation initially. Finally, this method is suitable only for phosphoserine and phosphothreonine as phosphotyrosine is resistance to β-elimination.
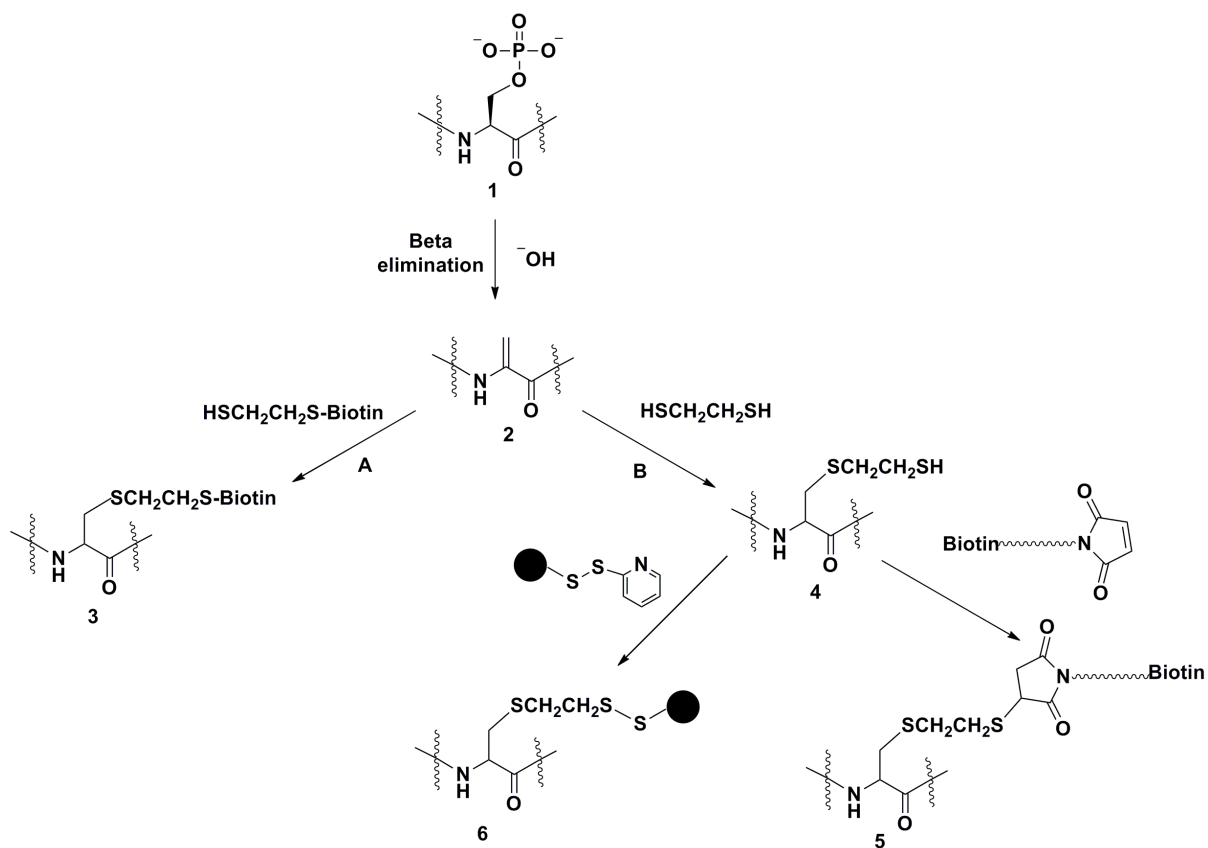
Figure 4.5: Purification of Phosphopeptide using Phosphate Elimination. Treatment of alkali leads to formation of dehydroalanine intermediate (**2**). (A) Nucleophilic addition of a biotin-tag to the intermediate (**3**) facilitates subsequent purification. (B) Addition of ethanedithiol introduces free thiol on the peptide (**4**) which can be trapped by NHS-biotin (**5**) or solid support disulfide (**6**) functionalities. Purified peptides can be analyzed by MS.

Unlike the β-elimination method, the phosphoamidate methods (Figure 4.6) enriches all the three type of phosphorylated peptides.[172] In this method all amino and carboxylic functionality has to be protected (intermediate **8** and **9**) to overcome intramolecular or intermolecular reactions. Then a thiol containing linker is attached to the phosphate group through a phosphoamidate bond (intermediate 11). The modified phosphopeptide can be attached to solid resin upon incubation with immobilized iodoacetyl groups (intermediate **12**) and unmodified peptides are washed away. Finally, pure phosphopeptide (compound **13**) can be cleaved off from the solid resin.
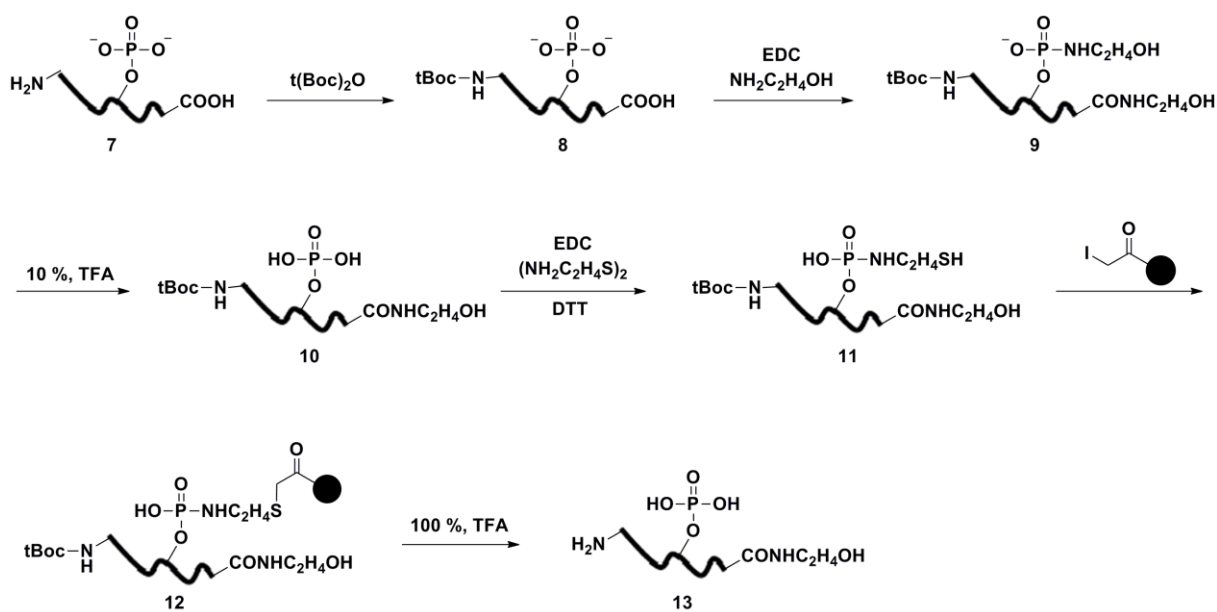
Figure 4.6: Purification of Phosphopeptide using Phosphoamidate Chemistry. Amino and carboxylic groups are first blocked to avoid any side reactions (intermediate **8** and **9**). Then a free thiol group is introduced on the phosphate via a phosphoamidate bond (**11**). The peptide is attached to the solid resin (**12**) to remove unphosphorylated peptides. Phosphopeptides (**13**) can be obtained upon TFA treatment which hydrolyze phosphoamidate bond. Purified phosphopeptides can be analyzed by MS.

4.1.4: Modified ATP Analog

A fourth strategy involves ATP analogs along with lysates containing analog-sensitive kinase mutants to label phosphoproteins for subsequent identification.[83, 87] Here, ATP-γS modified on the base was used with a mutant kinase. Incubation of ATP analog and mutant kinase with cell lysate lead to protein labeled with a thiophosphate. Then the mixture was reacted with PNMB (para-nitrobenzylmethansulfonate, Figure 4.7 A). Both the thiophosphates, cysteines react to form nitrobenzylated proteins. However, only the nitrobenzyl thiophosphorylated proteins can be purified with a specific antibody that recognizes this modification. Enriched proteins were then subjected to digestion and subsequent MS identification. As an alternative to specific antibody purification, thiophosphoproteins are digested and bound on solid support by reacting with immobilized iodoacteamide (Figure 4.7 B).[87] Washing removes all the unbound peptides, whereas thiophosphopeptides and cysteine containing peptide remain on beads. Phosphopeptides are released upon elution with oxidative conditions ($HOOSO_3H$) and cysteine containing peptides remain bound to the beads. This is a powerful method to identify substrates for a particular kinase.
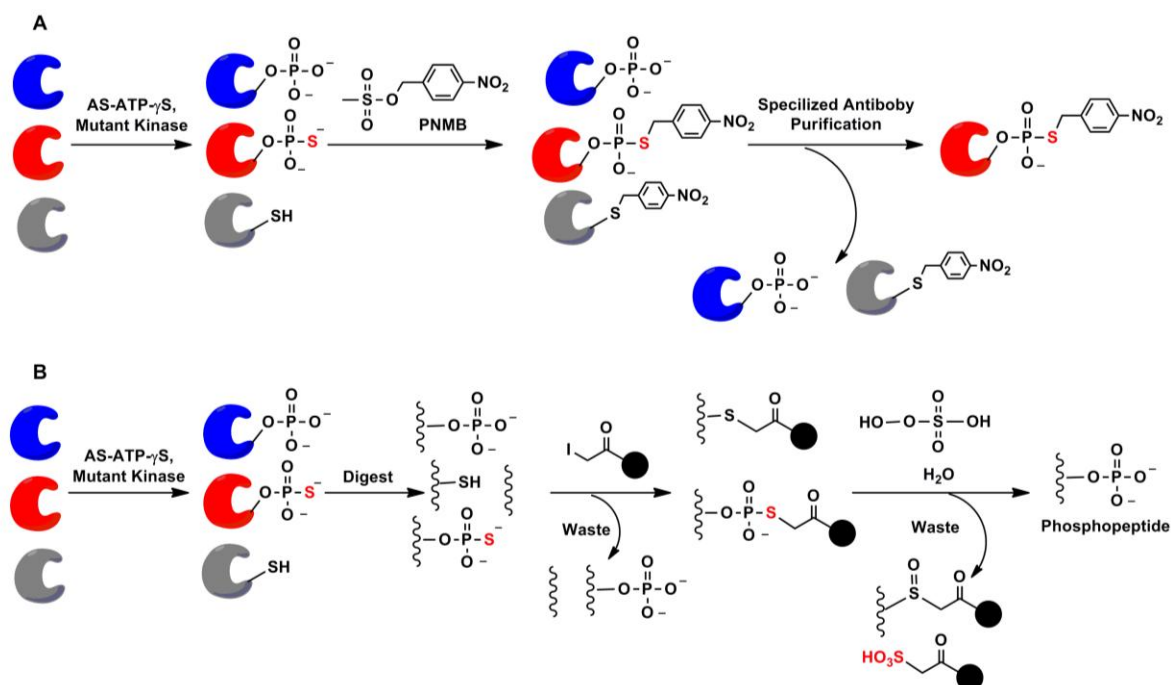
Figure 4.7: Purification of Phosphopeptide using Modified ATP-γS and Mutant Kinases. Incubation of cell lysates with mutant kinases and modified ATP-γS lead to formation of thiophosphorylated proteins. (A) Reaction of thiophosphorylated proteins with PNMB facilitates the purification of phosphproteins with specific antibody against this modification. (B) Thiophosphorylated proteins are digested and bound to solid resin together with cysteine containing peptides. Only the phosphopeptides are released from the resin upon oxidation with HOOSO$_3$H acid. Isolated peptides can be analyzed by MS.

4.1.5: Our Strategy with Modified ATP Analog

Enrichment strategies that complement these phosphopeptide purification strategies would promote a deeper study of the phosphoproteome. As an alternative method for phosphoprotein enrichment, we reported use of γ-modified ATP analogues for labeling kinase substrates.[91-94] We demonstrated that an ATP analogue with biotin attached to the γ-phosphate (ATP-biotin **2**, Figure 2.2) acts as a cosubstrate for kinases and transfers biotin along with the phosphate group (Figure 2.2 B) to substrate peptides and proteins. Specifically, cellular kinases

accept the ATP-biotin as a cosubstrate. Based on these studies, we envisioned applying kinase-catalyzed biotinylation to the enrichment of phosphopeptides and/or phosphoproteins from cell lysates.

4. 2: Purification of Phosphopeptides: β-casein Model Study

4.2.1: Avidin Purification with Regular Elution

We were interested in using kinase-catalyzed biotinylation for enrichment of phosphopeptides from cell lysates to facilitate MS analysis. To develop a purification protocol based on kinase-catalyzed biotinylation, bovine β-casein was modified by ATP-biotin in the presence of CK2 (Figure 4.8). The reaction mixture was reduced and alkylated, and then digested with trypsin to create a mixture of peptides containing biotinylated phosphopeptides. The digested mixture was loaded onto a NeutrAvidin column (Thermo Fisher). The column was washed, and biotinylated peptides were eluted with mild heating (45 °C for 5 minutes) in the presence of 5 mM competitive biotin (Figure 4.8, condition a). Peptides were separated by reverse phase chromatography and introduced into a Thermo Fisher LTQ-XL mass spectrometer. After ionization, abundant species were fragmented with CID or ETD to produce MS2 spectra. MS data analysis was performed using Proteome Discoverer 1.3 (Thermo Fisher) and searches were conducted using Mascot (ver 2.3; Matrix Sciences) to score MS2 spectra simultaneously against a bovine protein database. The presence of a phosphoryl biotin modification (+508 Da) on serine, threonine, or tyrosine was included in the search as a dynamic modification. One modified peptide containing a single phosphorylated amino acid was identified with high confidence (Table 4.1 and 4.2, Table A 4.1 and Figure A 4.1).

4.2.2: TiO$_2$ Purification

At the same time we were interested in comparing our methodology with another phosphopeptide enrichment technique. We selected TiO$_2$ affinity chromatography because it is widely used for phosphopeptide enrichment.[166-168] Full-length β-casein was incubated with ATP and CK2 and the same digest protocol was followed. The peptide mixture was loaded onto a TiO$_2$ tip column, washed, eluted (5% ammonium hydroxide and 5% pyrrolidine, Figure 4.9) and subjected to MS analysis. In this case we searched for the presence of a phosphate modification (+80 Da) on serine, threonine, or tyrosine. A total of 253 MS2 spectra were scored as phosphopeptides, which correspond to 12 different sequences (Table 4.1 and 4.2, Table A 4.2, Figure A 4.2 and Figure A 4.3). Among these peptides, 11 unique sites of phosphorylation were identified, which is similar to previous MS analyses of casein phosphopeptides using TiO$_2$ enrichment.[116, 117, 175]

4.2.3: Avidin Purification with Acidic Elution

Previous work established that biotin can interfere with MS analysis due to ion suppression.[172] As a result, competitive biotin elution with avidin might not be suitable for high efficiency phosphopeptide MS analysis. To avoid the biotin group during the MS analysis step, we sought a different condition that would elute phosphopeptides from the avidin column, instead of biotinylated phosphoproteins. We rationalized that a low pH elution would cleave the acid-labile phosphoramidate bond (Figure 2.2 B and Figure 4.8, condition b) and release phosphopeptides from the avidin bead, which would improve subsequent MS analysis.

To validate the use of acidic elution conditions, we explored whether TFA cleavage would increase the number of observed β-casein phosphopeptides. As described, biotinylated β-casein peptides were loaded onto an avidin column. In this case, phosphopeptides were eluted

after cleavage with 50% TFA (Figure 4.8, condition b). MS was performed and analyzed identically to the TiO_2 sample, where serine, threonine, or tyrosine residues with a phosphate group (+80 Da) were identified. This time, 14 spectral counts were identified corresponding to 3 different sequences and 3 unique sites of phosphorylation (Table 4.1 and 4.2, Table A 4.3, and Figure A 4.4). While the acidic conditions improved enrichment, the number of phosphopeptides identified was not comparable to TiO_2 affinity purification.

One barrier to kinase-catalyzed biotinylation of β-casein may be that potential sites have already been phosphorylated. To further enhance the biotin/avidin purification strategy, we speculated that a greater number of phosphosites would be biotinylated, resulting in more efficient enrichment, if we created conditions where kinases and phosphatases are in equilibrium. To test this hypothesis, calf intestinal alkaline phosphatase (CIP) was added to the reaction mixture during kinase-catalyzed biotinylation of β-casein. Phosphopeptide purification and MS analysis were then performed. In this case, we observed 259 spectral counts corresponding to 10 different phosphopeptides (Table 4.1 and 4.2, Table A 4.4, Figure A 4.5 and Figure A 4.6). From the peptides, 14 unique sites of phosphorylation were identified, which is similar to the results with TiO_2 purification. The data indicated that kinase-catalyzed biotinylation should be performed under equilibrium conditions to expose all phosphorylation sites to biotinylation.
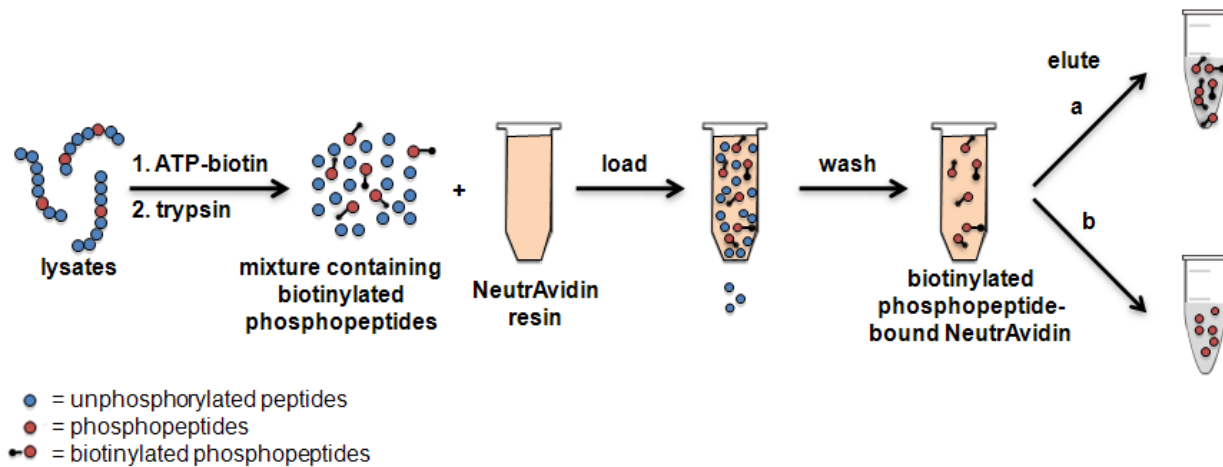
Figure 4.8: Isolation of Phosphopeptide using ATP-biotin and Avidin Affinity Purification.
Kinase-catalyzed biotinylation generates biotinylated proteins, which were digested and loaded onto an avidin affinity column. Biotinylated peptides were bound to the resin and all other peptides were washed away. Phosphopeptides were eluted using two conditions: (a) Biotin elution generated biotinylated peptides/proteins for MS analysis; (b) 50% TFA elution generated phosphopeptides/proteins for MS analysis due to cleavage of the biotin group.
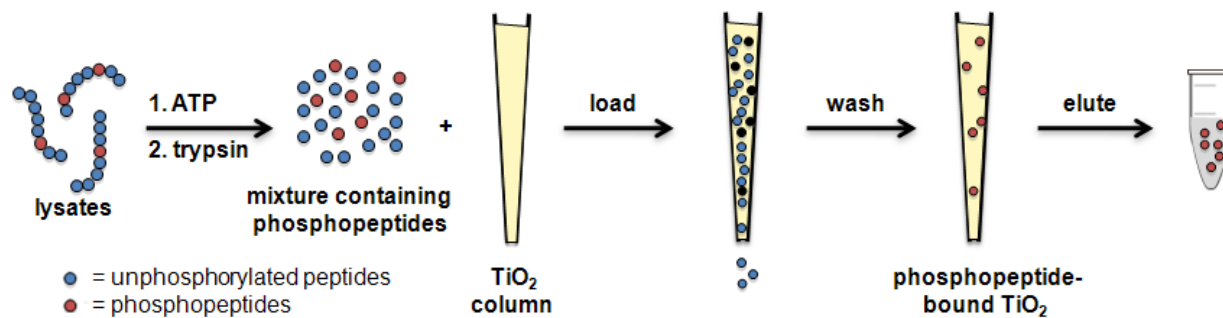
Figure 4.9: TiO$_2$ Affinity Purification. Casein or cell lysates were incubated with ATP and digested with trypsin. The mixture was loaded onto a TiO$_2$ column and unphosphorylated peptides were washed away. Elution with ammonium hydroxide and pyrrolidine resulted in release of the resin bound phosphopeptides for MS analysis.

4.2.4: β-Casein Model Study Analysis

β-casein was used as a model phosphoprotein to establish optimal conditions for the biotinylation and subsequent MS analysis. We found that optimal biotinylation occurred only in the presence of phosphatase activity. Because purified casein is naturally phosphorylated, biotinylation cannot occur on sites already in the phosphorylated state. The presence of phosphatase activity in the reaction ensures that biotinylation can occur on all phosphorylation sites, even those previously phosphorylated. Because cell lysates naturally contain kinases and phosphatases, the presence of phosphatases in the biotinylation reaction mimics the natural environment of the cell,[1] leading to robust biotinylation and optimal enrichment. In chapter 3, we found that the phosphorylbiotin group on peptide and protein substrates was relatively insensitive to active phosphatases, which is critical for robust kinase-catalyzed labeling demonstrated here.[1]

In addition to maintaining equilibrium phosphorylation conditions during the biotinylation reaction, we found that removal of the biotin group prior to MS analysis was essential. The biotin group likely leads to ion suppression in the MS instrument,[172] which would reduce the number of modified peptides observed. Alternatively, the biotin group can be lost during post-enrichment manipulations via hydrolysis of the acid-labile phosphoramidate,[171] which would also reduce the number of observed biotinylated peptides. The optimized strategy takes advantage of the acid-labile phosphoramidate bond where phosphopeptides are eluted from avidin affinity resin after biotin cleavage. With biotin cleavage, phosphopeptides are recovered after enrichment, making the MS analysis identical to that used with other methods, such as TiO_2 chromatography.

Table 4.1: Comparison of Casein phophopeptides identified using Avidin versus TiO$_2$ affinity chromatography.

Protein/Peptide	Avidin biotin elution	Avidin acid elution	Avidin acid elution CIP included	TiO$_2$
α-S1-Casein				
DIGsEsTEDQAMEDIK			13	1
DIGsEStEDQAMEDIK				2
DIGSEsTEDQAMEDIK			2	
VNELsKDIGsEStEDQAMEDIK			1	
VPQLEIVPNsAEER		1	17	16
VPQLEIVPNsAEERLHSMK				4
YKVPQLEIVPNsAEER		9	26	16
YKVPQLEIVPNsAEERLHSMK				1
α-S2-Casein				
NANEEEYsIGsssEEsAEVATEEVK			2	
NAVPITPTLNREQLsTsEENSKK				6
NAVPITPTLNREQLStsEENSKK				1
NAVPITPTLNREQLsTSEENSKK				1
KTVDMEsTEVFTKK				3
TVDMEsTEVFTK			3	6
TVDMEStEVFTK			10	
TVDMEsTEVFTKK			11	7
TVDmEStEVFTKK				4
TVDMEsTEVFTKKTK				2
β-Casein				
FQsEEQQQtEDELQDK			14	7
FQsEEQQQTEDELQDK	4		96	78
FQSEEQQQtEDELQDK				1
IEKFQsEEQQQtEDELQDK		4	16	10
IEKFQsEEQQQTEDELQDK			47	82
IEKFQSEEQQQtEDELQDK				1
KIEKFQsEEQQQTEDELQDK				4
κ-Casein				
sPAQILQWQVLSNTVPAK			1	
Total phosphopeptides	4	14	259	253
Number of different peptides	1	3	10	12
Number of multiply phosphorylated peptides	0	4	44	29
Number of singly phosphorylated peptides	4	10	215	224
Number of each phosphorylated amino acid	4(pS)	14(pS), 4(pT)	268(pS),40(pT)	257(pS)26(pT)
Number of unique phosphorylated sites	1	3	14	11

To more thoroughly compare the biotin versus metal ion purification methods, we searched for similarity between phosphopeptides identified in the two methods (Table 4.1). Eight phosphorylated sites were found in common comparing both methods; these included S50 and T56 of β-casein and S61, S63, T64, S130, S158 and T159 of α-casein (Figures A 4.2 and 4.5). Interestingly, several additional phosphosites where identified in α-casein (S56, S68, S71, S72, S73 and S76) and κ-casein (S90) using avidin purification, which were not observed with the TiO$_2$ method. Three phosphosites (S144, T145 and S146) were identified only with the TiO$_2$ method. The ratio of singly to multiply phosphorylated peptides from TiO$_2$ and avidin enrichment were 8:1 and 4.5:1, respectively, which is similar to prior reports.[176, 177] Of the total phosphorylated peptides recovered from the biotinylation method, 86% were phosphorylated at serine while 14% were modified at threonine. Similarly, the TiO$_2$ method identified 90% and 10% of phosphopeptides modified on serine and threonine, respectively.

To assess how accurately the biotinylation reaction reflects the endogenous phosphorylation profile, we compared the casein phosphorylation sites observed here to those identified in prior reports. Phosphorylated S50, T56 (β-casein), S56, S61, S63, S71, S72, S73, S76, S130 and S158 (α-casein) were also identified in previous studies.[116-118]Biotin-avidin purification identified 14 phosphorylated sites, including S50 and T56 of β-casein, S56, S61, S63, T64, S68, S71, S72, S73, S76, S130, S158 and T159 of α-casein and S90 of κ-casein. The biotinylation method identified eleven sites that were previously reported (S50, T56 (β-casein), S56, S61, S63, S71, S72, S73, S76, S130 and S158 (α-casein)).[116-118, 175] Three series of adjacent sites were absent (S30, S32, S33, S34 (β-casein), 23, 24, 25, 28, and 79, 81, 82, 83 (α-casein)), which may suggest that biotinylation is less effective when a series of consecutive sites exists. We note that TiO$_2$ purification also did not identify these series of sites. In addition, prior

reports observe similarly different profiles, which may reflect variance in experimental conditions or casein samples. Three phosphorylated sites were only observed with avidin purification (T64, S68 (α-casein) and S90 (κ-casein)). The κ- casein isoform is in low abundance in milk, which made prior removal of α- and β-casein necessary for reported profiling.[178] It is notable that a novel, presumably low abundance, serine phosphorylation site in κ-casein is observed with biotin-avidin purification. The data with casein indicate that the biotinylation strategy enriches for similar phosphorylation sites compared to other reports and reasonably reflects the endogenous phosphorylation profile. In addition, the fact that a novel phosphorylation site on the low abundance κ-casein protein is observed suggests the method provides sensitive detection. In total, this study has established kinase-catalyzed biotinylation for phosphopeptide enrichment and subsequent MS analysis.

4.3: Purification of Phosphopeptides: HeLa cell lysates

4.3.1: Avidin Purification

Having established a purification technique for biotin-labeled phosphopeptides, we applied the method to phosphoproteomic analysis of cell lysates. Briefly, HeLa cell lysates were incubated with ATP-biotin to label endogenous substrates with endogenous kinases. The biotinylated phosphoproteins were reduced and alkylated, followed by digestion and purification using avidin beads. After TFA cleavage and elution of phosphopeptides, MS data analysis was performed with dynamic modification of +80 Da on serine, threonine, and tyrosine residues. Overall, spectral counts of 447 located on 147 proteins were identified (Table 4.2 and Table A 4.5). While 153 different phosphopeptides were observed, 304 unique sites of phosphorylation were characterized.

4.3.2: TiO$_2$ Purification

For comparison, the recovery of phosphopeptides from HeLa cell lysates using TiO$_2$ affinity chromatography was also determined. Lysates were incubated with ATP, reduced, alkylated, digested, and enriched using a TiO$_2$ tip column. MS analysis was performed and results indicated that 490 spectral counts were detected on 188 different proteins (Table 4.2 and Table A 4.6). In this case, 220 different phosphopeptides and 309 unique sites of phosphorylation were identified, similar to previous reports.[118] Comparing the avidin and TiO$_2$ methods, both enriched similar number of phosphopeptides and unique phosphorylation sites.

Table 4.2: Summary of the phosphopeptides/proteins identified using avidin purification and TiO$_2$ purification

Sample	Enrichment	Peptide FDR[a]	Total Proteins	Modified Proteins	Spectral count	Unique Peptides	Unique Sites
Peptide enrichment							
Casein							
ATP	TiO$_2$	0.9	3	3	253	12	11
ATP-biotin	Avidin with biotin elution	0.8	4	1	4	1	1
ATP-biotin	Avidin with TFA elution	0.6	3	2	14	3	3
ATP-biotin[b]	Avidin with TFA elution	0.8	4	4	259	10	14
HeLa cell lysate							
ATP	TiO$_2$	1.3	317	188	490	220	309
ATP-biotin	Avidin	1.1	277	147	447	153	304
Protein enrichment							
Casein							
ATP-biotin	Avidin	0.6	4	3	69	6	5
HeLa cell lysate							
ATP-biotin	Avidin	1.2	468	118	341	126	237

[a] FDR = false discovery rate as a percentage
[b] Casein + ATP-biotin = sample was treated in the presence of CIP

4.3.3: HeLa Cell Lysate Study Analysis

The optimized conditions established with β-casein were used to enrich phosphopeptides from HeLa cell lysates. These experiments were performed in duplicate to increase the number of phosphoproteins identified. Comparing the identified peptides, each replicate resulted in the identification of distinct phosphopeptides; 40 (26%) or 51 (23%) phosphoproteins were common for the two trials using avidin or TiO_2 enrichment, respectively (Figure 4.10 A). More importantly, a comparison of the biotinylation and TiO_2 methods indicated that only 2 peptides (1.3 %) were identified in common (Figure 4.10 B). The enrichment of a distinct subset of phosphopeptides is in contrast to a prior report showing 33-35% overlap between TiO_2, Fe(III), and covalent phosphate modification methods.[169] A 19% overlap was observed when comparing TiO_2 to SnO_2 enrichment.[176] The data suggest that kinase-catalyzed biotinylation enriches a distinct subset of phosphopeptides compared to other methods.

To explain the limited overlap between the biotinylation and TiO_2 methods, the phosphorylated amino acid residues on the observed peptides were analyzed. The percentage of singly versus multiply phosphorylated peptides was quite similar, with biotinylation and TiO_2 methods showing preference for singly phosphorylated peptides (85% versus 70% singly phosphorylated peptides from TiO_2 versus avidin purification, respectively, Tables A 4.5 and A 4.6). On the other hand, the percentage of phosphorylation at serine, threonine and tyrosine was different for avidin and TiO_2 enrichment (46, 42, and 12% compared to 86, 12, and 2%, respectively); both methods enrich serine and threonine over tyrosine, although the biotinylation method enriched for serine and threonine equally and was more effective at phosphotyrosine enrichment. The ratio of singly to multiply phosphorylated peptides from TiO_2 and avidin enrichment was 5.8:1 and 2.3:1, respectively. In total, the data show that kinase-catalyzed biotinylation in cell lysates has a

comparable efficiency of phosphopeptide identification compared to the widely used TiO_2 affinity chromatography method.
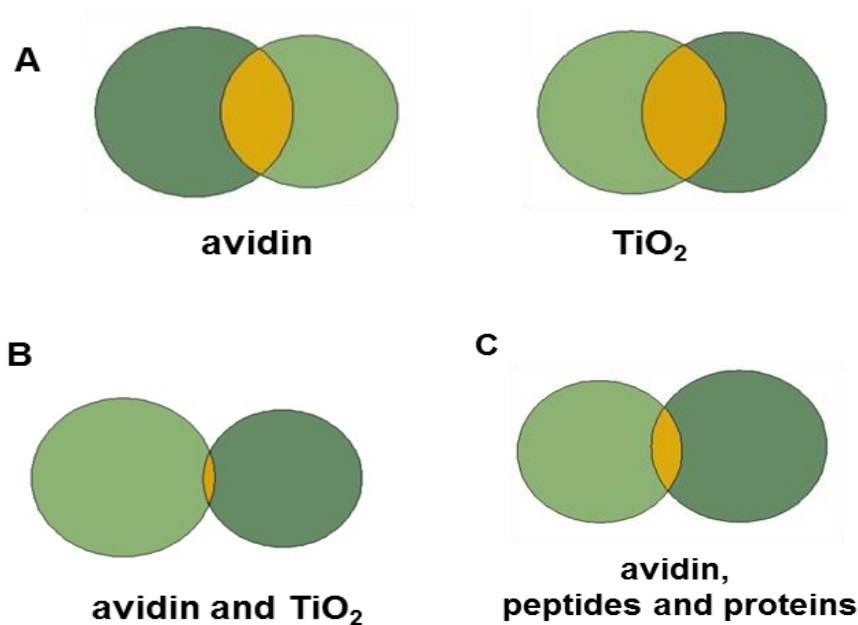
Figure 4.10: Peptide Data Analysis. (A) Venn diagrams showing the overlapping peptides identified in duplicate from avidin purification (left) and TiO_2 enrichment (right). (B) Venn diagram showing the overlapping peptides identified in the avidin and TiO_2 purification strategies. Only 2 individual phosphopeptides are found in common (1.3%). (C) Venn diagram showing the overlapping peptides identified using avidin purification and either peptide and protein isolation. Only 21 individual phosphopeptides are found in common (17%).

We also compared the amino acid composition of the identified phosphopeptides (Figure 4.11). With TiO_2 enrichment, a bias towards phosphopeptides containing the acidic amino acids, Asp and Glu, was observed. The bias of metal ion affinity chromatography in favor of acidic peptides is well documented in prior reports [169] and is likely derived from the nonspecific interaction of the negatively charged acidic side chains with the positively charged metal ion. Unlike the TiO_2 method, avidin enrichment showed no acidic peptide bias. As a comparison, the amino acid composition of all peptides derived from human proteins was analyzed (Figure 4.11,

gray bars) using the UniProtKB database (http://www.uniprot.org). As expected, the TiO$_2$ method enriches peptides with a higher percentage of aspartic and glutamic acid residues compared to the human protein database. In addition, both methods showed an elevated enrichment of alanine-containing peptides. However, the avidin method did not show a significant bias towards any other amino acid, which distinguishes it from metal-based or chemical phosphate modification methods.[169]
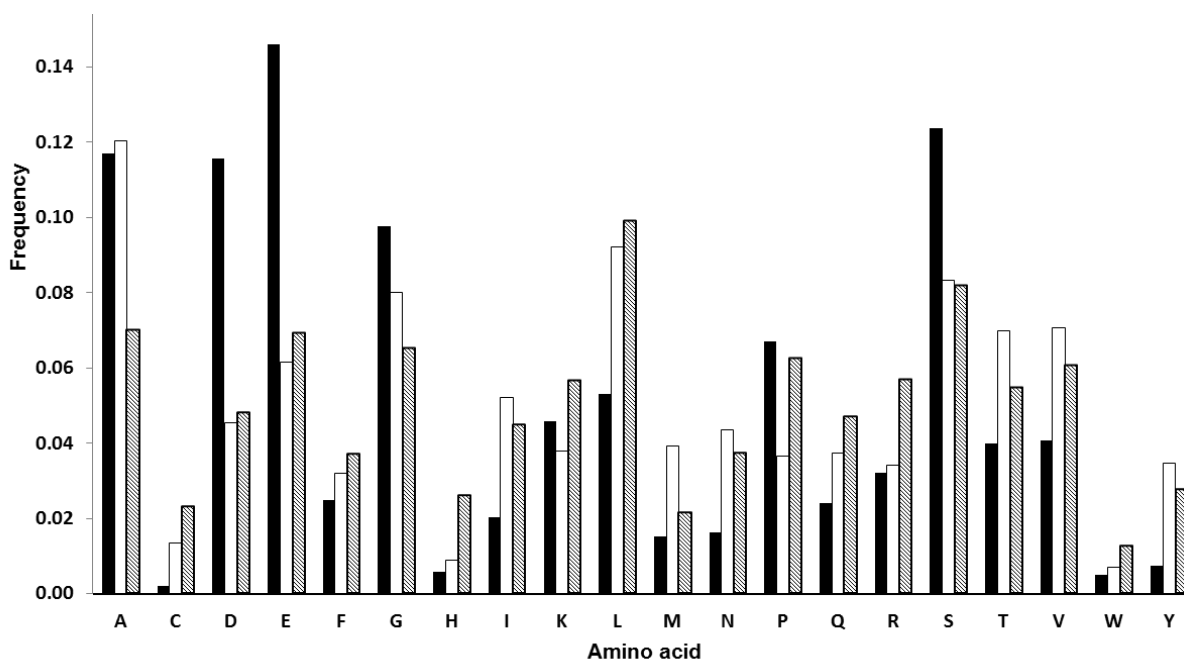
Figure 4.11: Amino Acid Analysis. Amino acid composition of the identified phosphopeptides from HeLa cell lysates with TiO$_2$ (closed bars, black) and avidin (open bars, white) enrichment, respectively. For comparison, the amino acid composition of all human proteins obtained from the UniProtKB database is shown (gray bars).

Based on the amino acid analyses, one reason the two methods enrich distinct proteins may be due to the slight bias of TiO_2 enrichment toward singly modified peptides (85% versus 70%). However, previous reports showed that IMAC had a similar increase in multiply phosphorylated peptides (9%), yet displayed 35% overlap in phosphopeptide population compared to TiO_2 enrichment.[169] Therefore, the limited overlap between the avidin and TiO_2 purification strategies is likely independent of the multiplicity of phosphorylation. In contrast, IMAC, TiO_2, and chemical covalent phosphate modification methods showed a similar bias toward Asp, Glu, Ser but against Tyr,[169] which suggests that amino acid bias is a contributor to their 35% overlap. Therefore, the results suggest that kinase-catalyzed biotinylation enriches a different subset of phosphopeptides from HeLa cell lysates compared to metal ion affinity due to its effective purification of Thr and Tyr phosphorylated peptides and lack of obvious amino acid bias. In addition, the biotinylation method isolates only dynamically phosphorylated proteins, but TiO_2 enriches both dynamically and statically phosphorylated proteins.

A necessary requirement of the avidin purification method is that ATP-biotin must be added to cell lysates to generate biotinylated phosphoproteins. Others have used modified ATP cosubstrates for labeling of lysates and detection of phosphopeptides and phosphoproteins.[81] Most notably, Shokat and colleagues have developed a chemical modification strategy using ATP analog-sensitive kinase mutants to label phosphoproteins.[82, 83, 179] Substrates identified using ATP-analog sensitive kinases were confirmed in secondary cell biology studies, demonstrating their biological relevance.[180, 181] Because kinase-catalyzed biotinylation utilizes a similar lysate-labeling reaction to these prior successful strategies, the avidin purification method described here is expected to isolate biologically relevant substrates.

4.4: Purification of Full-Length Proteins

Having established phosphopeptide enrichment using kinase-catalyzed biotinylation, we were interested in extending our methodology towards purification of full-length phosphoproteins. To enable MS analysis of intact proteins (for example, top-down or medium-down proteomics),[182, 183] a method to purify phosphoproteins from complex mixtures is needed. Metal affinity chromatography has been used exclusively for phosphopeptide enrichment, presumably because full length proteins interact with TiO_2 independent of phosphorylation state.[184] On the other hand, avidin affinity chromatography is established to enrich full-length proteins from cellular mixtures.[171, 185]

4.4.1: Avidin Purification with β-Casein Model Study

To initially test compatibility with full-length phosphoprotein enrichment, ATP-biotin was incubated with full-length β-casein and CK2. The biotinylation reaction mixture was then loaded onto an avidin affinity column, washed, eluted, and separated by SDS-PAGE (Figure 4.12 and Figure A 4.7). Biotinylated casein was visualized using Western blot analysis and an anti-biotin antibody, indicating that β-casein was labeled with biotin (Figure 4.12, lane 2, bottom gel). The flow through (Figure 4.12, lane 3) and final washing steps (Figure 4.12, lanes 4 and 5) did not show the presence of protein, which indicates biotinylated casein bound to the beads. Finally, phosphorylated caseins were obtained after cleavage of the biotin tag with TFA (Figure 4.12, lane 6). The peptides resulting from in-gel digestion of the purified phosphoproteins (Figure 4.12, lane 6, top gel) were analyzed by LC/MS/MS. Sixty-nine spectral counts were observed with 6 different peptides and 5 unique phosphorylation sites (Table 4.2 and Table A 4.7). Of the total phosphorylated peptides recovered, 80% were phosphorylated at serine, and 20% at threonine. The ratio of singly to multiply phosphorylated peptides from protein enrichment was

3:1. Given that these casein experiments were performed without phosphatase incubation, the phosphoprotein enrichment identified a similar number of unique phosphorylated sites (5 unique sites, Table 4.1 and 4.2) compared to phosphopeptide enrichment (3 unique sites, Table 4.1 and 4.2). These results establish a protocol for enzymatic biotinylation as a means to purify intact phosphoproteins from protein mixtures.
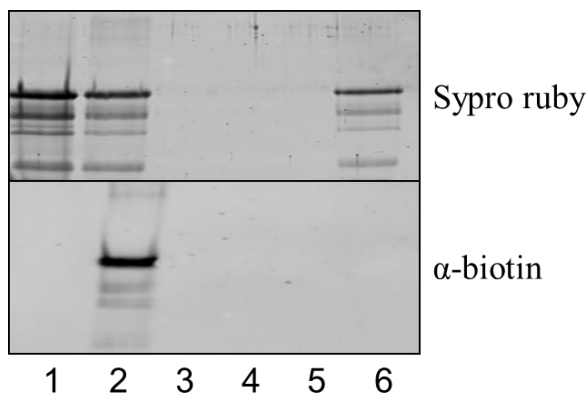
Figure 4.12: Capturing Biotinylated Proteins from β-Casein (A) β-casein (lane 1) was biotinylated with CK2 and ATP-biotin (lane 2), loaded onto an avidin column (flow through, lane 3), washed (lane 4 and 5) and eluted using 50% TFA (lane 6). The proteins were visualized with SYPRO ruby stain (top) and a biotin-specific antibody (α- biotin, bottom). Two trials are shown in Figure A 4.7.

4.4.2: Avidin Purification with HeLa Cell Lysates

The phosphoprotein enrichment method was then applied towards HeLa cell lysates to confirm that the biotinylation reaction is appropriate to a proteomic application. HeLa cell lysates were incubated with ATP-biotin and biotinylated proteins were purified using avidin beads. As a control, lysates incubated with ATP did not show significant enrichment of proteins (Figure A 4.9), indicating that ATP-biotin and kinase-catalyzed biotinylation are required. Biotinylated proteins in the lysates were separated and visualized by SDS-PAGE (Figure 4.13 and Figure A 4.8). While many protein bands were observed by SYPRO Ruby stain (Figure 4.13,

lanes 1 and 2, top), only a subset of proteins were biotinylated (Figure 4.13, lane 2, bottom).

Phosphoproteins obtained after TFA cleavage of the biotin tag (Figure 4.13, lane 6) were

subjected to in-gel digestion and LC/MS/MS analysis. The analysis indicated that 118 proteins

were phosphorylated with 341 spectral counts (Table 4.2 and Table A 4.8). From 126 different

phosphopeptides, 237 unique phosphorylation sites were identified. The protein purification

method identified 43%, 36% and 21% of phosphopeptides modified on serine, threonine and

tyrosine, respectively and the ratio of singly to multiply phosphorylated peptides was 1.4:1.

These results establish that kinase-catalyzed biotinylation followed by avidin purification is able

to enrich full-length phosphoproteins for MS analysis of intact proteins.
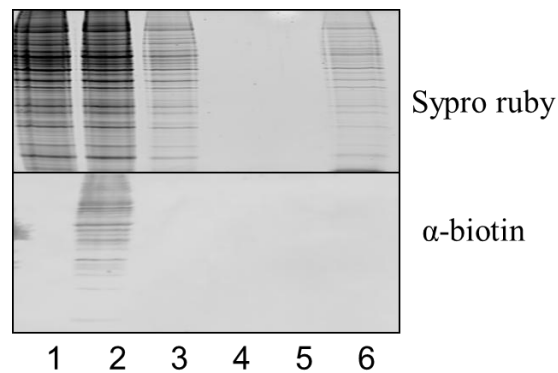
Figure 4.13: Capturing Biotinylated Proteins from HeLa cell Lysates: HeLa cell lysates (lane 1) were biotinylated with ATP-biotin (lane 2), loaded onto an avidin column (flow through, lane 3), washed (lane 4 and 5) and eluted with 50% TFA (lane 6). The proteins were visualized with sypro ruby stain (top) and a biotin-specific antibody (α- biotin, bottom).

4.4.3: Full-Length Proteins Analysis

While enrichment of phosphopeptides from complex mixtures is widely reported,

particularly using metal ion affinity chromatography, the isolation of intact phosphoproteins is

poorly documented. Metal ion chromatography is not compatible with full-length protein

purification. However, intact phosphoproteins have been enriched using a chemical approach

involving β-elimination/Micheal addition to attach biotin to phosphoproteins, followed by avidin purification and gel analysis.[186] Unfortunately, this strategy has not been combined with MS-based phosphoproteomic analysis. To facilitate analysis of full-length phosphoproteins, the kinase-catalyzed biotinylation method was applied to the enrichment of intact casein as well as proteins from HeLa cell lysates. Like with phosphopeptide enrichment, the presence of phosphatases and elution using biotin cleavage provided optimal results. We found that a similar number of phosphoproteins were observed using full-length protein enrichment compared to phosphopeptide enrichment; 118 phosphoproteins were identified with full-length protein enrichment compared to 147 and 188 phosphoproteins identified with avidin and TiO_2 phosphopeptide enrichment, respectively. A comparison of the avidin-based peptide and protein enrichment experiments revealed that 21 peptides (17%, Figure 4.10 C) were in common, which is similar to the overlap of the two peptide purification trials (26 %, Figure 4.10 A). Additionally, the peptide and intact protein enrichment data are very similar in their Ser/Thr/Tyr phosphorylation percentages (46, 42, and 12% versus 43, 36 and 21%) and singly to multiply phosphorylated peptide ratios (2.3:1 versus 1.4:1). These comparisons reveal that the peptide and protein enrichment strategies are performing consistently. With the availability of a phosphoprotein purification strategy, studies relying on intact proteins, such as 2-D gel analysis or top-down proteomics, can be readily applied to analysis of the phosphoproteome.

4.5: Conclusions and Future Direction

In conclusion, we have established kinase-catalyzed biotinylation for phosphoproteomic analysis. This avidin-based purification method provides a useful alternative to metal ion affinity chromatography by maintaining the same efficiency of enrichment. The fact that distinct phosphopeptides were identified using avidin and TiO_2 enrichment strongly suggests that the two

methods can be coupled to more fully characterize the phosphoproteome. We also utilized the biotinylation method to isolate intact phosphoproteins from complex mixtures. The ability to enrich either phosphopeptides or phosphoproteins using kinase-catalyzed biotinylation will expand the studies possible for phosphoproteomics research.

As a future direction of this method, dynamic regulation of the phosphorylation can be study with the purification method. In addition, protein purification coupled to immunoprecipitation can be used to identification of intact protein using top-down MS analysis.

4.6: Experimental

4.6.1 Materials

ATP-biotin was synthesized as explained in Chapter 2, section 2.6.3 and 2.6.4. Adenosine 5'-triphosphate disodium (ATP), glycerol, sodium hydroxide (NaOH), potassium chloride (KCl), magnesium chloride ($MgCl_2$), sodium chloride (NaCl), sodium dodecyl sulfate (SDS), glacial acetic acid, and acetonitrile were purchased from Fisher. Proteomics grade trypsin, monoclonal Anti-Biotin-Peroxidase antibody produce in mouse (A0185), ammonium bicarbonate, β-casein, tris (2-carboxyethyl) phosphine (TCEP), and iodoacetamide (IAM) were bought from Sigma. CK2 and CIP enzymes were purchased from New England Biolabs. Triton X-100 was purchased from Fluka. HeLa cells were obtained from the National Cell Culture Center. Protease inhibitor cocktail was purchased from Calbiochem, and Bovin serum albumin (BSA) was obtained from Santa Cruz Biotechnology. Pierce^R detergent removal spin columns (cat. number 87777) and ICAT-TM catridge-cation exchange column was purchased from Thermo Scientific and Applied Biosystems, respectively. Immobilion P PVDF membrane was purchased from Millipore. SYPRO Ruby stain was obtained from Invitrogen. Biotinylated phosphopeptides/ proteins were enriched using NeutraAvidin Agarose Resin (Thermo Scientific) or Phos-TiO kit (GL Sciences).

4.6.2 Instrumentation

The purified final product was lyophilized using VirTis BT 3.3 EL Benchtop lyophilizer. A SPD131 DDA ThermoSavant speed vac was used to evaporate solvents *in vacuo*. Quantitative mass spectrometric analysis was performed on MALDI-TOF MS (Bruker Ultraflex). The absorbance values for Bradford assay was measured with a fluorimeter (GENios Plus Tecan). Microcentrifuges and mini vortex mixer was purchased from VWR and Eppendorf respectively. The SDS-PAGE apparatus was purchased from BioRad (Protean III) and a mini-gel setup was

used. Western blotting was carried out using the Mini-Transblot Electrophoretic Transfer Cell apparatus from BioRad. Peptides were ionized with the ADVANCE ion source (Michrom) and introduced into an LTQ-XL mass spectrometer (Thermo Fisher Scientific). The separated proteins were visualized using a Typhoon 9210 scanner (Amersham Biosciences).

4.6.3 HeLa Cell Lysis Procedure

The HeLa cell lysis was performed as described in Chapter 3, section 3.7.9.

4.6.4 Bradford Assay

The Bradford assay was performed as described in Chapter 3, section 3.7.10.

4.6.5 Kinase-catalyzed Phosphorylation or Biotinylation

Phosphorylated or biotinylated proteins were prepared as follows. β-casein (0.2 mM) was mixed with CK2 (20 units/μL) and either ATP or ATP-biotin (2 mM) in the manufacturer supplied kinase reaction buffer for 2 hours at 30 °C with or without calf intestinal phosphatase (CIP, 20 units/μL). The total reaction volume was 10 μL. For HeLa cell lysates, 25 μg of total protein was incubated with either ATP or ATP-biotin (2 mM) in the manufacturer supplied 1X CK2 buffer for 2 hours at 30 °C in a total 20 μL volume. To generate a peptide digest for MS analysis, the sample was reduced, alkylated and trypsin digested (see section 4.6.6 for details). The protein or peptide samples were used immediately.

4.6.6 Trypsin Digestion Procedure

SDS (dissolved in H_2O, 0.1% final concentration) was added to the protein sample (section 4.6.5) and the mixture was vortexed and spun down. Then, TCEP (dissolved in 50 mM ammonium bicarbonate) was added to the sample to a final concentration of 5 mM, and the

sample was vortexed, spun down, and incubated at room temperature for 45 minutes. Iodoacetamide (dissolved in 50 mM ammonium bicarbonate) was added to the sample to a final concentration of 15 mM and vortexd, spun down, and incubated in the dark for 30 minutes. Trypsin (dissolved in 1 mM hydrochloric acid, 1:20 w/w ratio trypsin:protein) was then added to the sample and vortexed, spun down, and incubated for 16 hours at 37 °C for optimum enzymatic digestion.

4.6.7 Isolation of Biotinylated Peptides/Proteins

A NeutrAvidin bead slurry (250-300µL) was centrifuged (1000 x g, 1 min, RT) to collect the beads. The beads were then washed five times with 200 µL of wash buffer (0.025 M Tris-HCl, pH 7.4, 0.15 M NaCl, 0.0001 M EDTA, 5% glycerol). Biotinylated peptides or proteins (section 4.8.5) were diluted with wash buffer (0.025 M Tris-HCl, pH 7.4, 0.15 M NaCl, 0.0001 M EDTA, 5% glycerol), up to 200 µL. Then the samples were incubated with the washed NeutrAvidin beads for 2 hours at 4 ºC with rocking. The beads were collected (1000 x g, 1 min, RT) and washed five times with 200 µL of wash buffer prior to elution.

To elute the phosphopeptides/proteins using biotin competition, elution buffer (40 µL, 0.025 M Tris-HCl, pH 7.4, 1% SDS, 0.005 M biotin) was added to the beads and the mixture was heated to 45 ºC for 5 minutes. Eluted biotinylated phosphopeptide samples were passed through an ICAT^{TM} cation exchange column (Applied Biosystems) using the manufacturer protocol prior to MS analysis.

To elute phosphopeptides/proteins using acidic cleavage conditions, 50% TFA in water (40 µL) was added to the beads and the mixture was heated to 45 ºC for 5 minutes. The supernatant containing phosphopeptides/phosphoproteins was collected after centrifugation (1000 x g, 2 min, RT). The TFA was evaporated using a Speedvac and then used for gel analysis

after neutralizing with 1.5 M Tris-base (pH 8.8). Or, the remaining solution was passed through a detergent removal column (Thermo Fisher) using the manufacturer's protocol prior to MS analysis.

4.6.8 TiO$_2$ Isolation of Phospho Peptides

Phosphopeptide isolation was performed using a Phos-TiO kit (GL Sciences) using the manufacturer recommended protocol. Peptides were generated after phosphorylation and trypsin digestion as described in section 4.6.5 and 4.6.6 respectively. The peptide sample (total protein mass for casein and HeLa lysate was 48 µg and 25 µg, respectively, before trypsin digest) was mixed with 100 µL of buffer B (1 mL of 100% lactic acid) and 3 mL of buffer A (1 mL of 2% TFA solution and 4 mL of acetonitrile), and loaded onto the TiO$_2$ Spin Tip. The Spin Tip was centrifuged (1000 x g, 10 min, RT). The sample in the tube was reapplied to the Spin Tip again to assure complete binding. The Spin Tip was rinsed (3000 x g, 2min, RT) with 20 µL of buffer B followed by 20 µL of buffer A. The peptides were eluted (1000 x g, 5min, RT) with 5% ammonium hydroxide solution in water (50 µL), followed by 5% pyrrolidine solution in water (50 µL). The combined, eluted sample was evaporated using a Speedvac prior to MS analysis.

4.6.9 Western Blotting

The biotin visualization was performed as described in Chapter 2, section 2.6.10. Here, the membrane was western blotted with anti-biotin IgG (Sigma) in a 1:500 dilution.

4.6.10 Sypro Ruby Stain

The Sypro Ruby staining was performed as described in Chapter 2, section 2.6.12.

4.6.11 In-Gel Protein Digestion

Gel slices were excised and cut into 1 mm^3 cubes. Gel pieces were washed with a 1:1 mixture of 50 mM ammonium bicarbonate and acetonitrile (250 µL). Proteins were reduced with 10 mM TCEP in 25 mM ammonium bicarbonate buffer (200 µL, to cover gel pieces) for 40 minutes at room temperature, and the solution was discarsted. Then the cysteine residues were subsequently alkylated by adding 50 mM iodoacetamide in 25 mM ammonium bicarbonate buffer (200 µL, to cover gel pieces) for 10 minutes at room temperature in dark, and the solution was removed. In-gel digestion was performed overnight at 37 °C after the addition of sequencing grade trypsin (dissolved in 1 mM hydrochloric acid, 1:20 w/w ratio trypsin: protein, Promega) in 25 mM ammonium bicarbonate and 10% acetonitrile (200 µL, to cover gel pieces). The digestion solution was also collected. Peptides were sequentially extracted from the gel using 0.1% formic acid and acetonitrile (1:1 mixture, 200 µL) for 10 minutes at room temperature, followed by acetonitrile (200 µL) alone for 10 minutes at room temperature. Volatile buffers and salts were removed by desiccation using a Speedvac concentrator.

4.6.12 Mass Spectrometric Analysis
(Analysis was performed by Joseph Caruso at the Institute of Environmental Health)

Digested samples (secion 4.6.7 and 4.6.8) not separated by SDS-PAGE were either purified using a Pierce Detergent Removal Spin column (Thermo Fisher) or manually desalted by reverse phase chromatography using a Michrom peptide cap-trap (Thermo Fisher Scientific), and dried in a Speedvac. For LC/MS/MS, peptides were re-suspended in 5% acetonitrile, 0.1% formic acid and 0.005% trifluoroacetic acid (TFA). Reverse phase chromatographic separation of peptides was performed with a Paradigm MS4 HPLC (Michrom Bioresources) at 500 nL/min over a Magic C18AQ column (Michrom; 0.1x150 mm, 3µm, 200 Å). The gradient started at 95%

Buffer A [2% acetonitrile, 0.1% formic acid] and 5% Buffer B [95% acetonitrile, 0.1% formic acid], and increased to 10% Buffer B over 2 min, and then 35% Buffer B over 45 min. Mass analysis was performed using a LTQ-XL linear ion trap mass spectrometer (Thermo Fisher). Abundant peptides were selected for fragmentation in either collision-induced dissociation (CID) or electron transfer dissociation (ETD) mode. For CID, the seven most abundant ions in the MS1 scan (m/z 400-1800) were selected for fragmentation, and for ETD the top five ions in the MS1 scan (m/z 400-2000) were selected. Settings for CID and ETD included an isolation width of 2 Da, normalized collision energy of 35, activation Q of 0.25 and an activation time of 30 ms (CID) or 100 ms (ETD). Dynamic exclusion was turned on (repeat count = 1; repeat duration = 5 s; list size = 500; exclusion duration = 20 s). When samples were run in CID mode, a MS3 scan was triggered if a neutral loss of a phosphate group was detected within the top 3 fragment ions of the MS2 scan. The neutral loss list consisted of 49.0, 32.7 and 24.5 for doubly-, triply- and quadruply-charged phosphopeptides, respectively. Peak lists were generated from the RAW files using Proteome Discoverer (ver 1.3; Thermo Fisher) and exported into Mascot (ver 2.3; Matrix Science). Search criteria included static modification of cysteine (carbamidomethylation, +57.02), and dynamic modifications of Met (oxidation, +15.99), protein N-terminus (acetylation, +42.01), and Ser, Thr and Tyr (phosphorylation, +79.97). MS2 and MS3 spectra were searched against tryptic peptide sequences (up to 1 missed cleavage) within the latest bovine (NCBI) or human (UniProtKB) databases. Charge states of +2, +3 and +4 were assigned for CID MS2 spectra, and the ETD Spectrum Charger node within Proteome Discoverer was used to determine the charge state of peptides analyzed by ETD. A simultaneous search was performed against a scrambled database to estimate the false discovery rate (FDR). Reported peptides scored above a 1.3% FDR threshold. Mascot search results were exported to Scaffold (ver 3.6; Proteome

Software) and a subset database was researched using the X! Tandem algorithm. Phosphosite localization probabilities were generated using ScaffoldPTM (ver 2.0; Proteome Software).

4.6.13 Data Analysis

Peptide and proteins cutoffs used for Scaffold are listed in each supplementary table. 99% protein and 90% (Table A 4.7), 80% (Table A 4.1, A 4.2 and A 4.3) and 55% (Table A 4.4) peptide probability cutoffs were used with casein samples in Scaffold. For HeLa lysates, 90% protein and 55% peptide probability cutoffs (Table A 4.8) and 50% protein and 80% (Table A 4.5) or 79% (Table A 4.6) peptide probability cutoffs were used for full length and peptide enrichment experiments, respectively.

Frequency of amino acid composition (Figure 4.11) was calculated by dividing the times a particular amino acid was observed by the total number of amino acids.

APPENDIX A

2.1 Compound Characterization
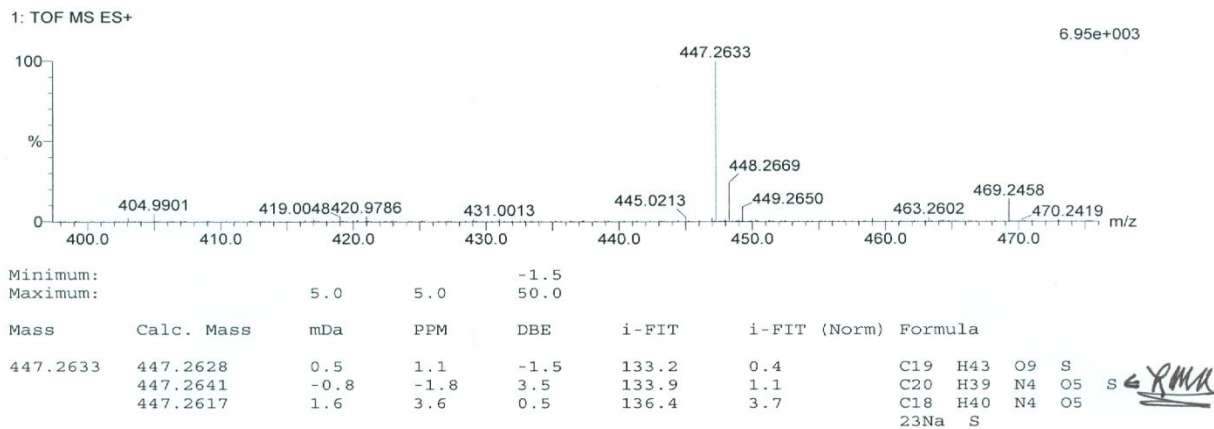
Figure A 2.1: HRMS of biotin-PEG amine **8**
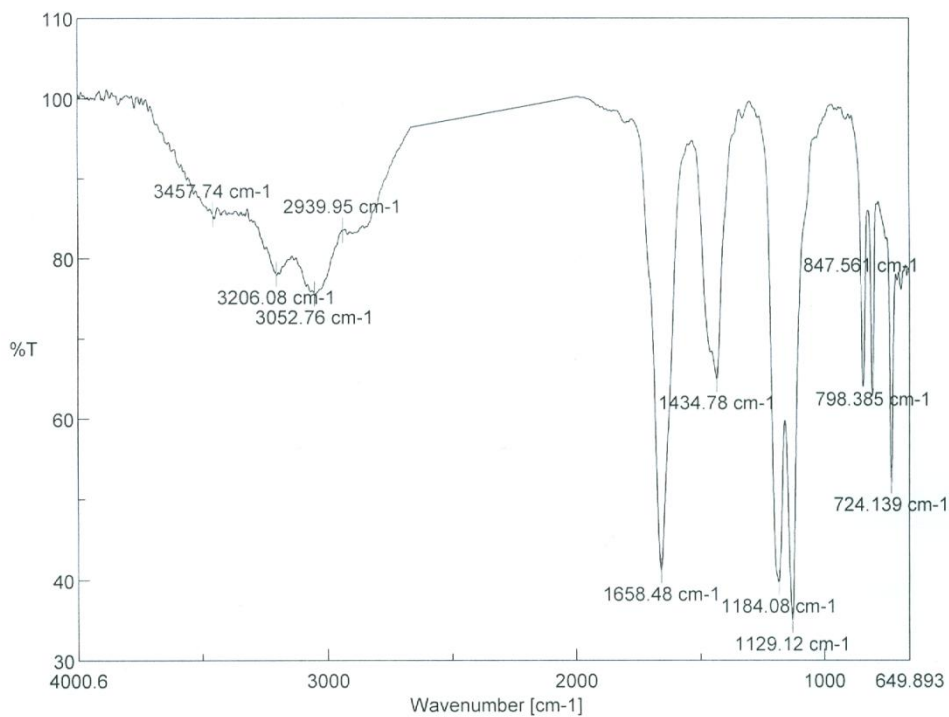
Figure A 2.2: The IR spectrum (4000-650 cm^{-1}) of biotin-PEG amine **8**

File: xp
Pulse Sequence: s2pul
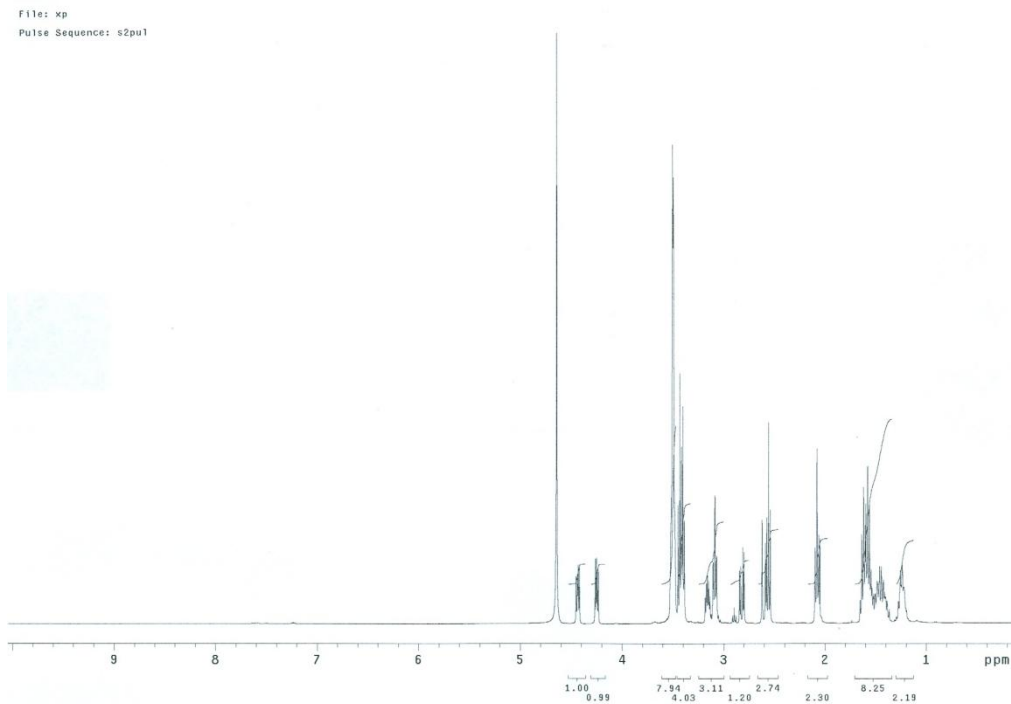
Figure A 2.3: ^{1}H-NMR of biotin-PEG amine **8** recorded in D_2O solvent
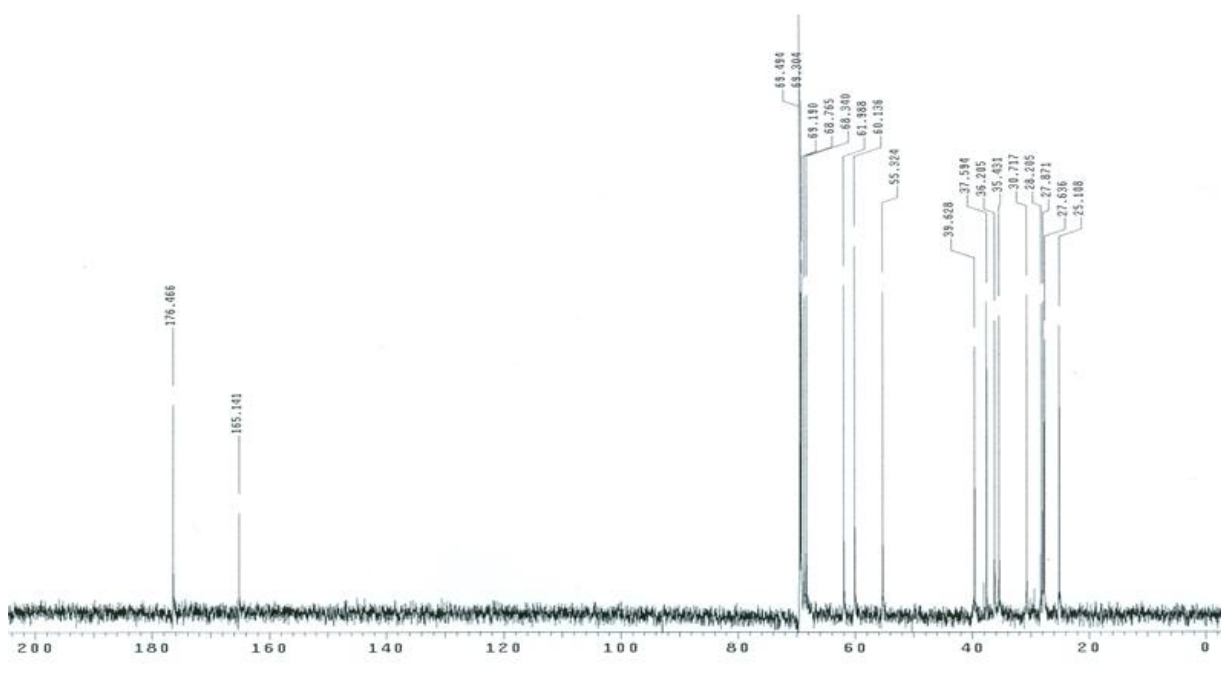
Figure A 2.4: ^{13}C-NMR of biotin-PEG amine **8** recorded in D_2O solvent
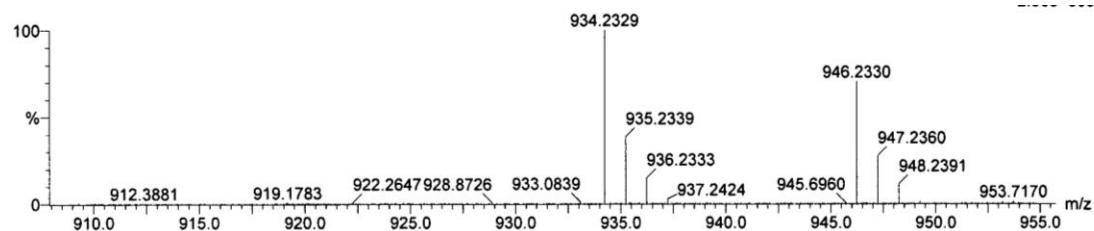
Figure A 2.5: HRMS of ATP-biotin **2**
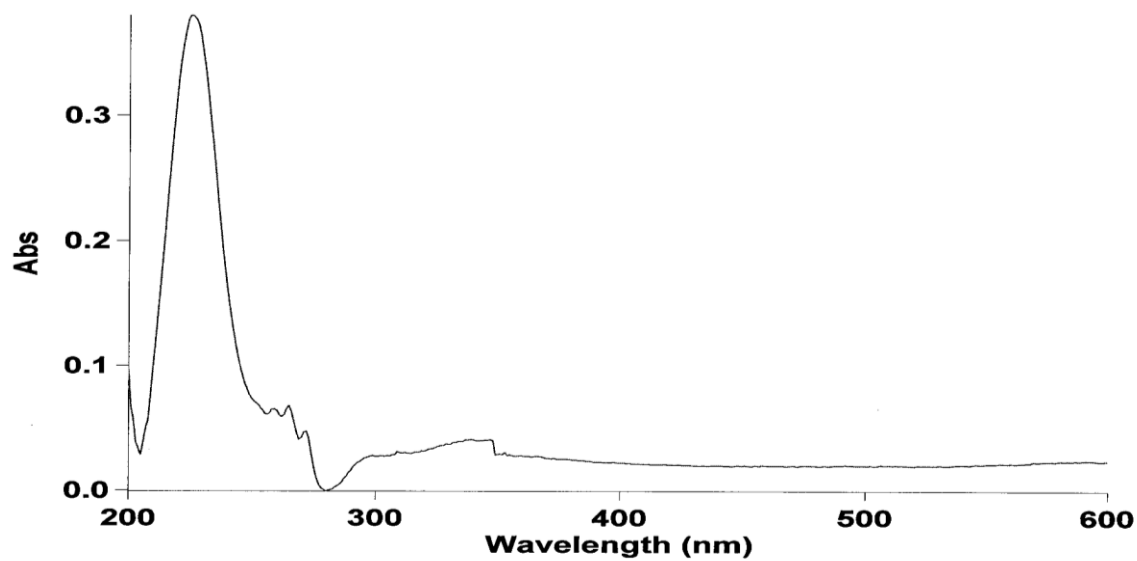
Figure A 2.6: The UV absorbance spectrum (200-600 nm) of ATP-biotin **2**
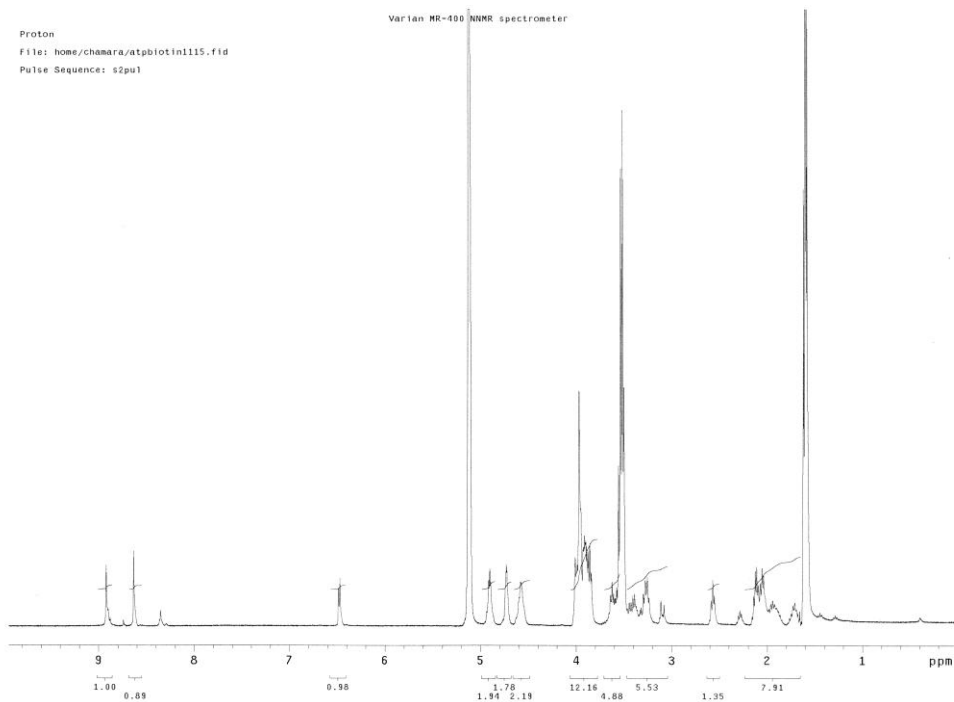
Figure A 2.7: ^{1}H-NMR of ATP-biotin **2** recorded in D$_2$O solvent
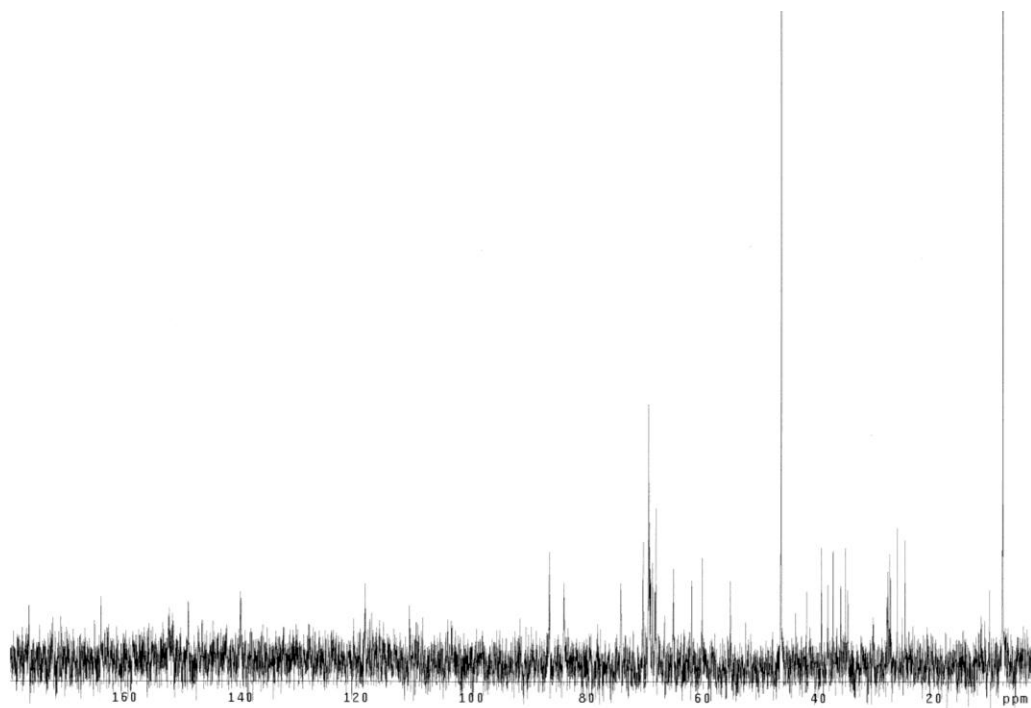
Figure A 2.8: ^{13}C-NMR of ATP-biotin **2** recorded in D$_2$O solvent
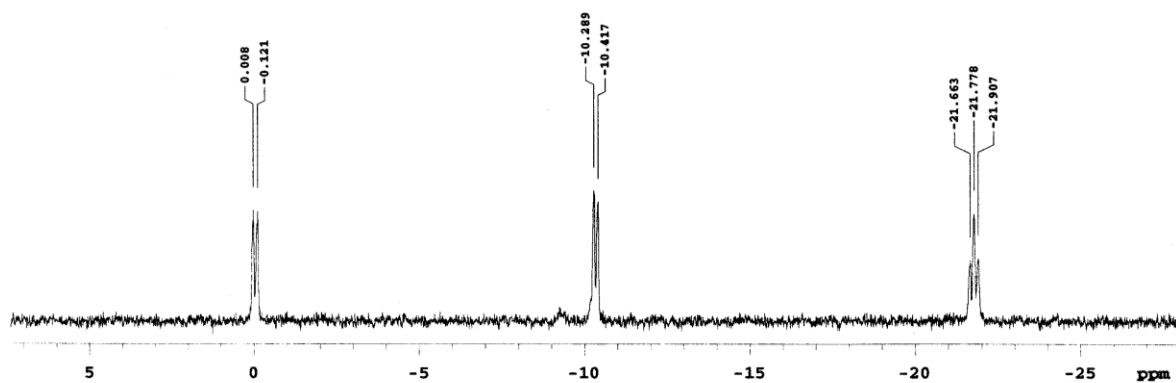
Figure A 2.9: ^{31}P-NMR of ATP-biotin **2** recorded in D$_2$O solvent

2.2 Complete Gel Images for Peptide Labeling

(A) Reaction with AKT
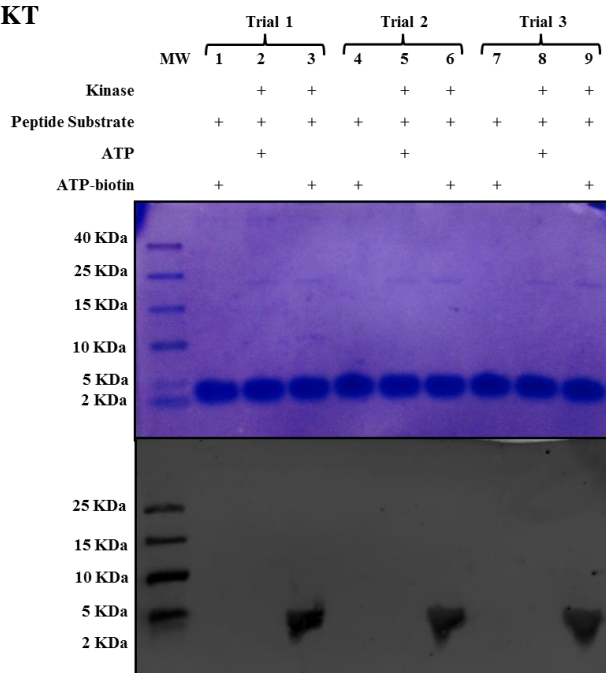
(B) Reaction with CAMK4
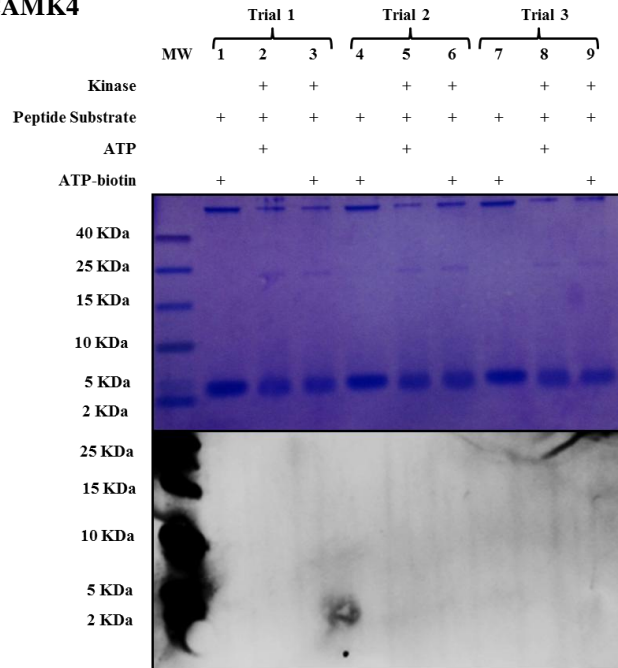
(C) Reaction with CHK1

(D) Reaction with FLT1

	MW	Trial 1			Trial 2			Trial 3		
		1	2	3	4	5	6	7	8	9
Kinase			+	+		+	+		+	+
Peptide Substrate		+	+	+	+	+	+	+	+	+
ATP			+			+			+	
ATP-biotin		+		+	+		+	+		+

(E) Reaction with GSK3β

	MW	Trial 1			Trial 2			Trial 3		
		1	2	3	4	5	6	7	8	9
Kinase			+	+		+	+		+	+
Peptide Substrate		+	+	+	+	+	+	+	+	+
ATP			+			+			+	
ATP-biotin		+		+	+		+	+		+
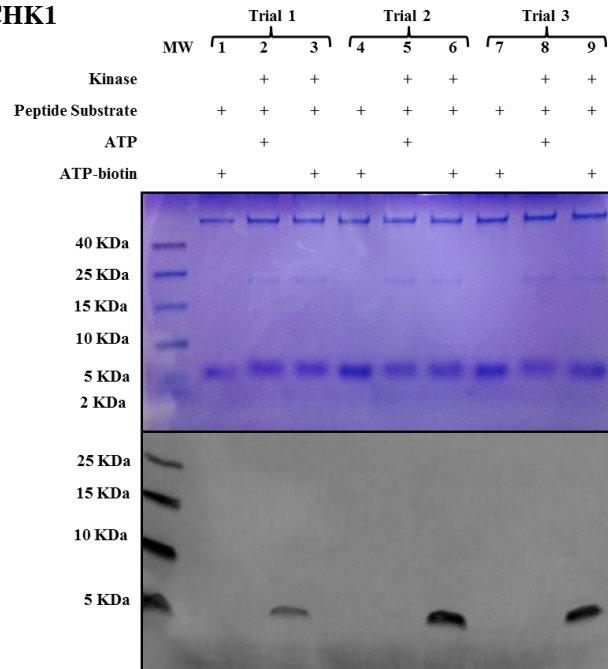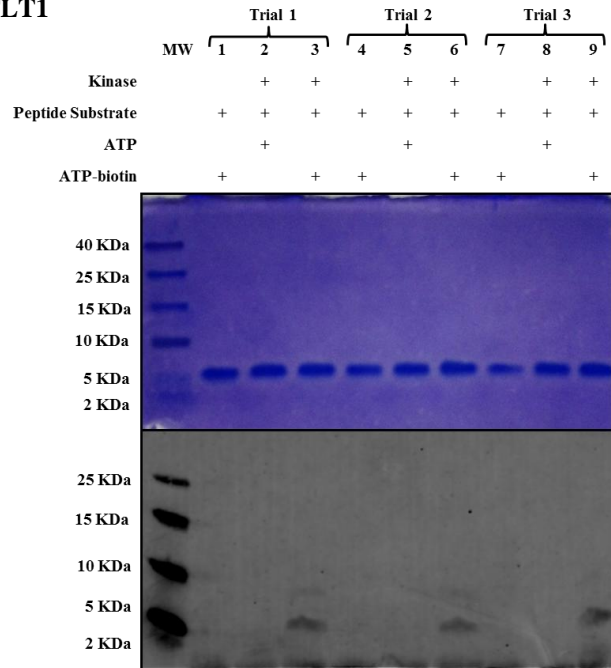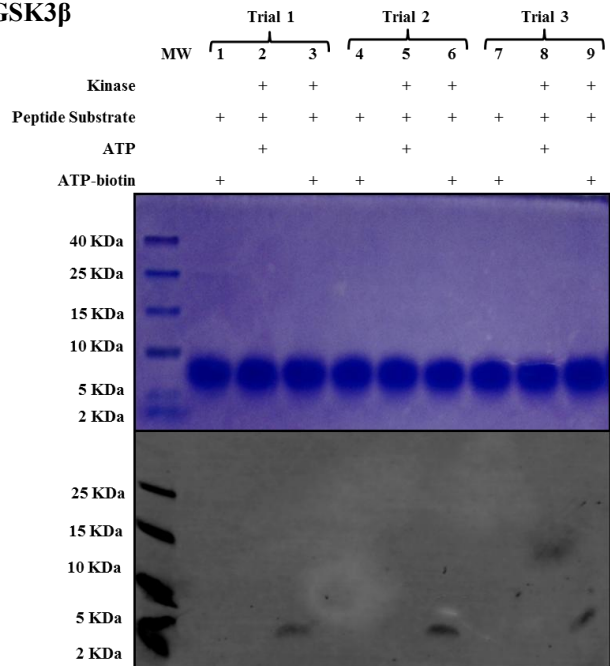
(F) Reaction with MARK1
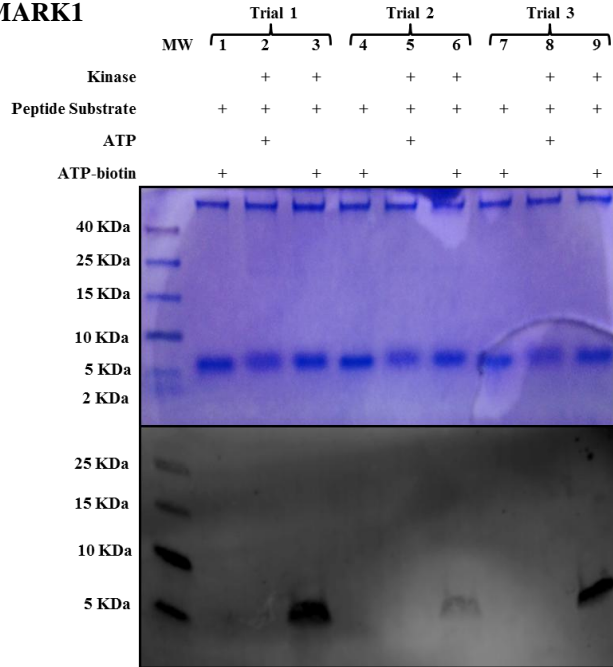
(G) Reaction with MST1
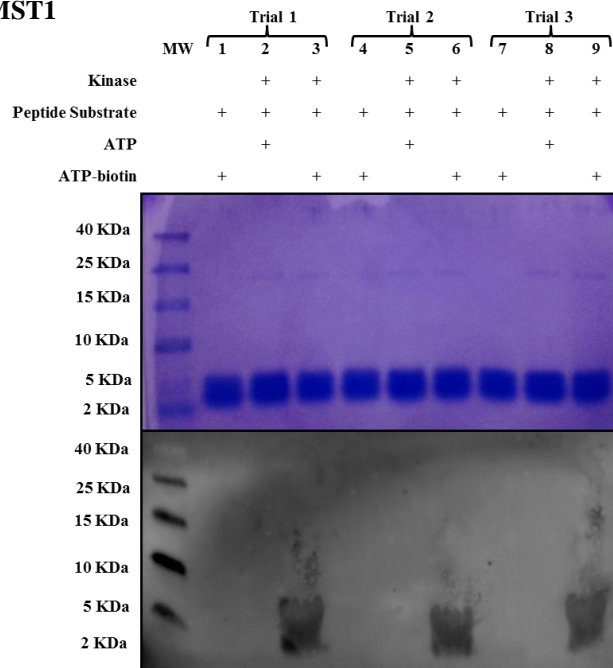
(H) Reaction with PAK1
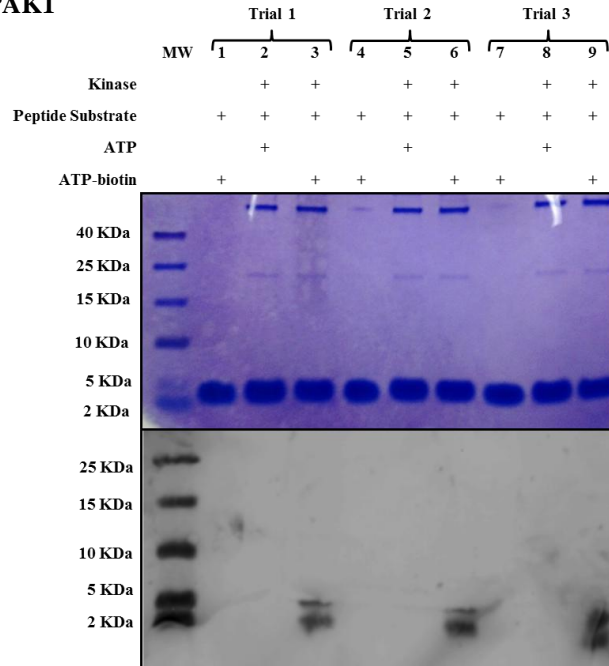
(I) Reaction with RSK1
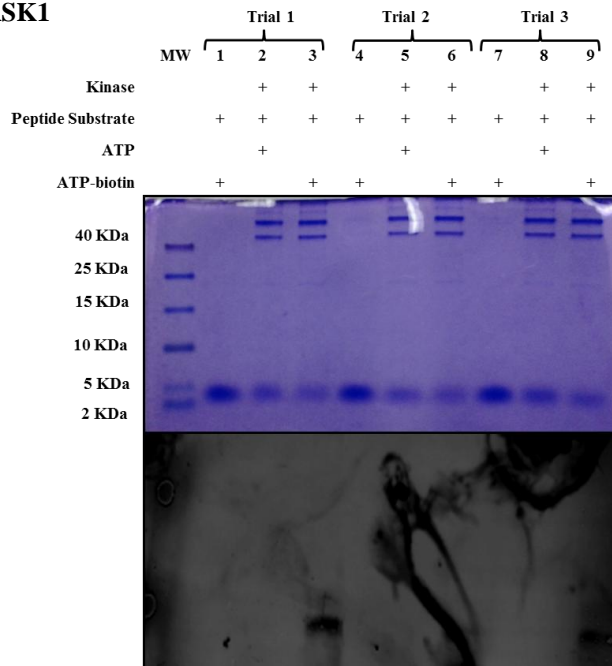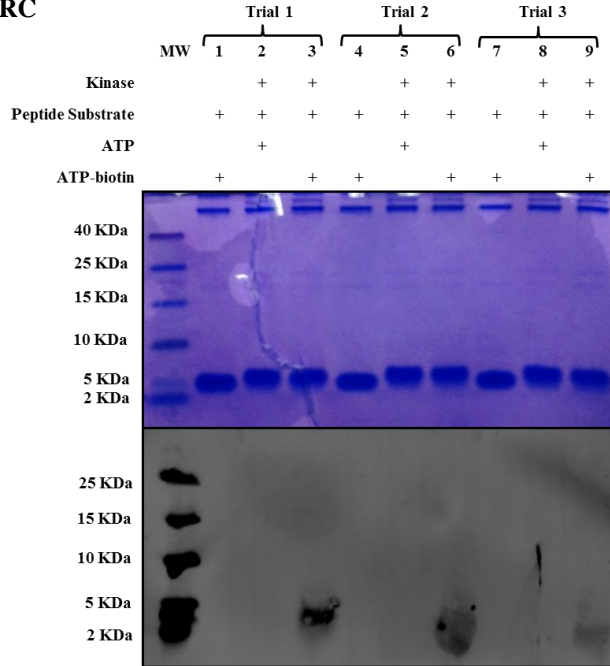
Figure A 2.10: Full gel images for peptide labeling experiment with 10 different kinases. Phosphorylated peptides or biotinylated phosphopeptides were created by incubating ATP or ATP-biotin with AKT1 and AKT(PKB) substrate (CKRPRAASFAE) (A), CAMK4 and Autocamtide (KKALRRQETVDAL-amide) (B), CHK1 and CHKtide (KKKVSRSGLYRSPSMPENLNRPR) (C), FLT1 and IGF1Rtide (KKKSPGEYVNIEFG) (D), GSK3β and GSK3 substrate (YRRAAVPPSPSLSRHSSPHQ(pS)EDEEE) (E), MARK1 and CHKtide (KKKVSRSGLYRSPSMPENLNRPR) (F), MST1 and Axltide (KKSRGDYMTMQIG) (G), PAK1 and PAKtide (RRRLSFAEPG) (H), RSK1 and S6K substrate (KRRRLASLR) (I), or SRC and SRC substrate (KVEKIGEGTYGVVYK-amide) (J), in the manufacturer provide buffer (1X, Promega). Crude reaction mixtures were separated on a 16% Tris-tricine peptide gel and transferred to a PVDF membrane. Peptides are visualized with Coomassie Brilliant Blue (top gel) and biotinylated peptides with SA-Cy5 conjugate (bottom gel) with reaction contents indicated above each lane. Trials 1, 2, and 3 represent three independent trials. Reaction with CAMK4 labeling was seen only with single trial.

2.3 Complete Gel Images for Protein Labeling

(A) Reaction with ASK1

(B) Reaction with Aurora A

(C) Reaction with CDK1

	MW	Trial 1			Trial 2			Trial 3		
		1	2	3	4	5	6	7	8	9
Kinase			+	+		+	+		+	+
Protein Substrate		+	+	+	+	+	+	+	+	+
ATP			+			+			+	
ATP-biotin		+		+	+		+	+		+

← Histone H1

Sypro Ruby

SA-Cy5

← biotinylated
phospho-Histone H1

(D) Reaction with CK1

	MW	Trial 1			Trial 2			Trial 3		
		1	2	3	4	5	6	7	8	9
Kinase			+	+		+	+		+	+
Protein Substrate		+	+	+	+	+	+	+	+	+
ATP			+			+			+	
ATP-biotin		+		+	+		+	+		+

← Casein

Sypro Ruby

← biotinylated
phospho-casein

SA-Cy5
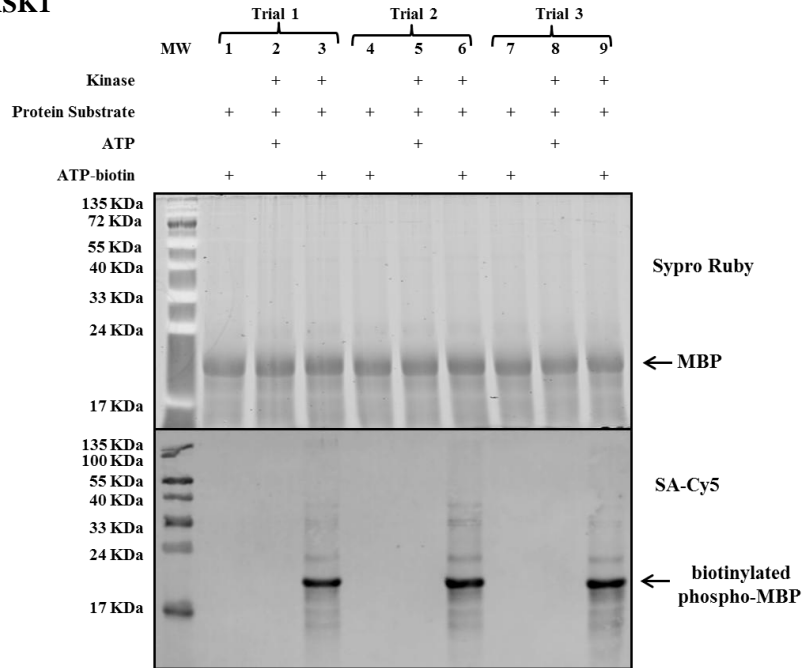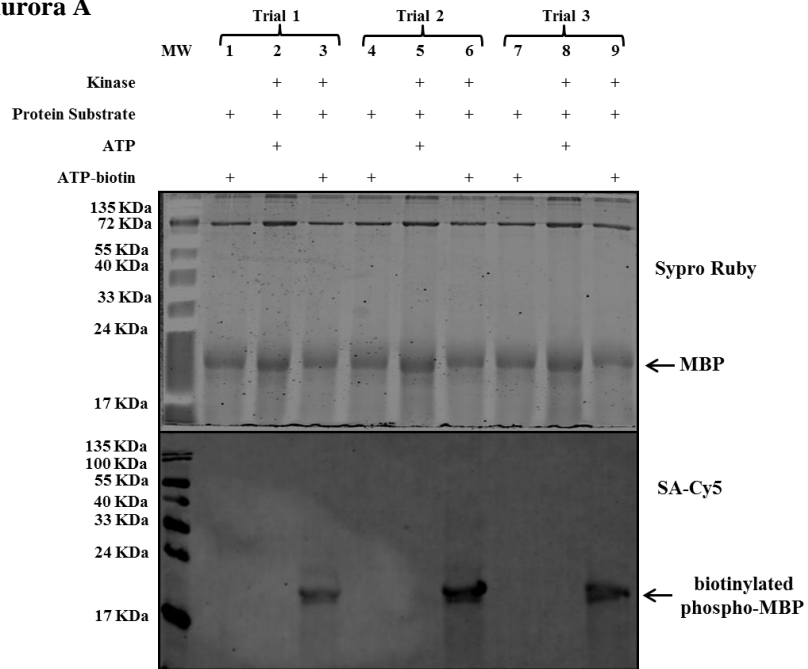
(E) Reaction with DAPK1
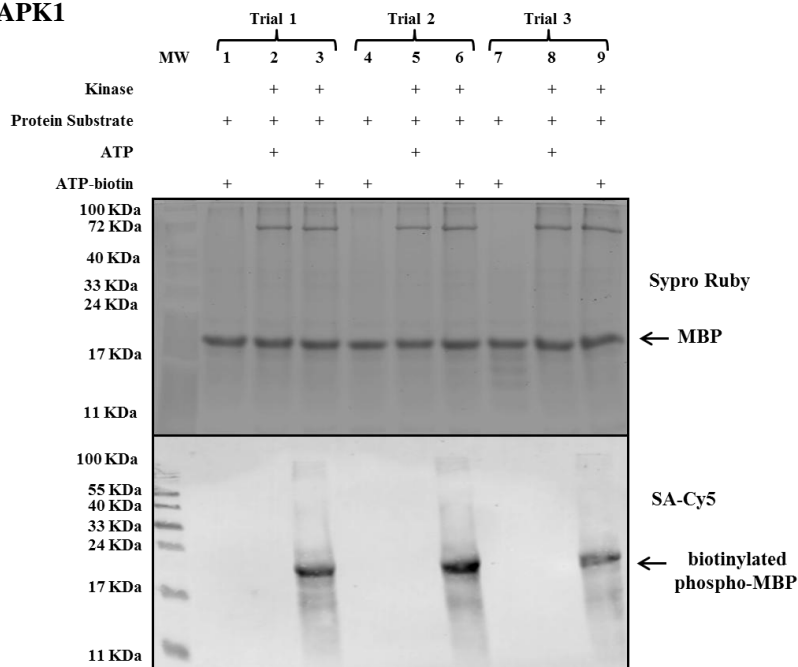
(F) Reaction with ERK1
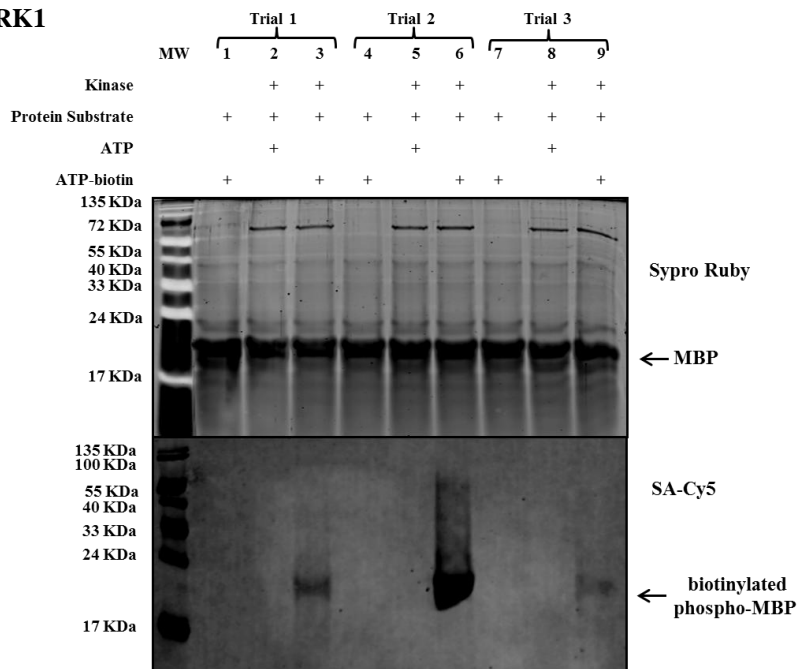
(G) Reaction with GRK5

(H) Reaction with HIPK1
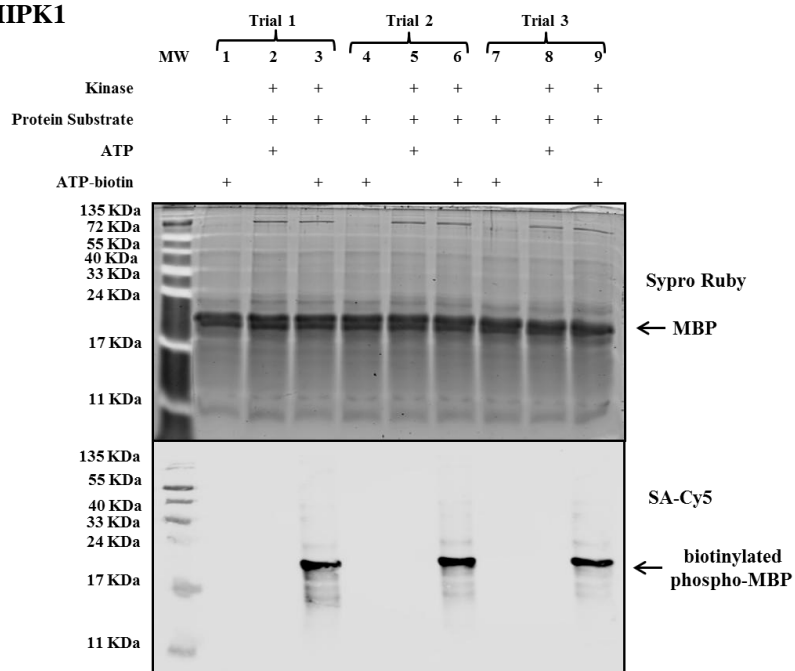
(I) Reaction with JAK3
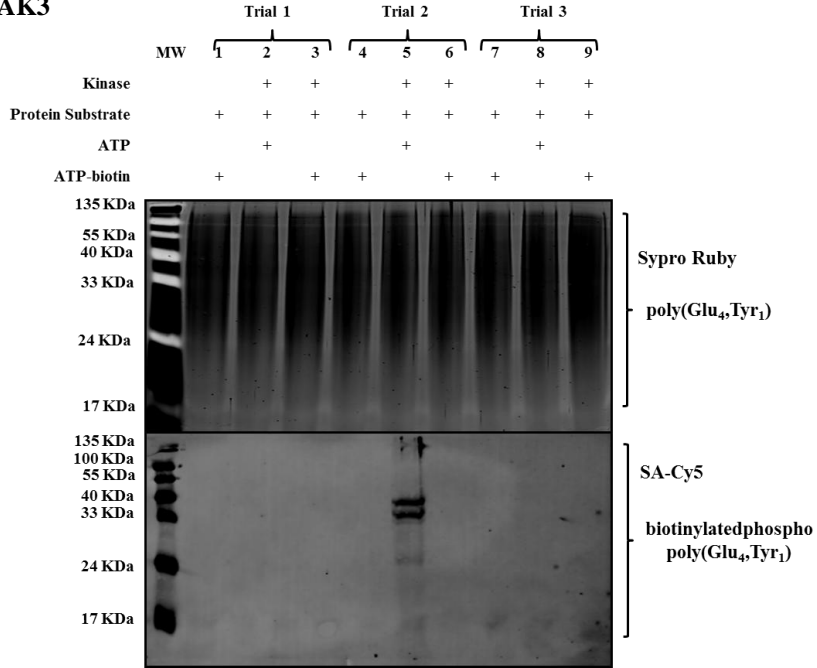
(J) Reaction with MLK1

(K) Reaction with NEK2

		Trial 1			Trial 2			Trial 3	
MW	1	2	3	4	5	6	7	8	9
Kinase		+	+		+	+		+	+
Protein Substrate		+	+	+	+	+	+	+	+
ATP		+			+			+	
ATP-biotin		+		+		+	+		+

135 KDa
72 KDa
40 KDa
33 KDa
24 KDa
17 KDa
11 KDa

Sypro Ruby
← MBP

135 KDa
55 KDa
40 KDa
33 KDa
24 KDa
17 KDa
11 KDa

SA-Cy5
← biotinylated
phospho-MBP

(L) Reaction with TGFβR2

		Trial 1			Trial 2			Trial 3	
MW	1	2	3	4	5	6	7	8	9
Kinase		+	+		+	+		+	+
Protein Substrate		+	+	+	+	+	+	+	+
ATP		+			+			+	
ATP-biotin		+		+		+	+		+

72 KDa
40 KDa
33 KDa
24 KDa
17 KDa
11 KDa

Sypro Ruby
← MBP

100 KDa
55 KDa
40 KDa
33 KDa
24 KDa
17 KDa
11 KDa

SA-Cy5
← biotinylated
phospho-MBP

(M) Reaction with TRKA

Figure A 2.11: Full gel images for protein labeling experiment with 13 different kinases. Phosphorylated proteins or biotinylated phosphoproteins were created by incubating ATP or ATP-biotin with ASK1 and MBP (A), Aurora A and MBP (B), CDK1 and Histone H1 protein (C), CK1 and dephosphorylated Casein protein (D), DAPK1 and MBP (E), ERK1 and MBP (F), GRK5 and Casein protein (G), HIPK1 and MBP (H), JAK3 and poly (Glu$_4$, Tyr$_1$) peptide substrate (I), MLK1 and MBP (J), NEK2 and MBP (K), TGFβR2 and MBP (L), or TRKA and poly (Glu$_4$, Tyr1) peptide substrate (M) in the manufacturer provide buffer (1X, Promega). Crude reaction mixtures were separated on 16% SDS-PAGE and transferred in to PVDF membrane. Proteins are visualized with Sypro Ruby Stain (top gel) and biotinylated proteins with SA-Cy5 conjugate (bottom gel) with reaction contents indicated above each lane. Trial 1, 2, and 3 represented three independent trials. MBP stand for Myelin Basic Protein. Complete gel images for remaining three kinases (Abl, CK2, and PKA) can be found on Appendix 3.2. The experiments with ASK1, CDK1, CK1, GRK5, HIPK1, and MLK1 were performed by graduate student Maheeka Embogama. The experiment with CDK1, CK1, GRK5, MLK1 western blots indicate biotin labeling of BSA, which is a component in the buffer used in kinase reaction. Both JAK3 and TRKA labeling was seen only in a single trial. Molecular weight of protein as follows: MBP (~18 kDa), Casein (~24 kDa), and Histone H1 (~22 kDa).

2.4 Complete HPLC Traces

(A) Reaction with Abl

i

★ Unmodified peptide   ▲ Phosphopeptide   ● acid-cleaved biotin amine

ii

★ Unmodified peptide   ▲ Phosphopeptide   ● acid-cleaved biotin amine
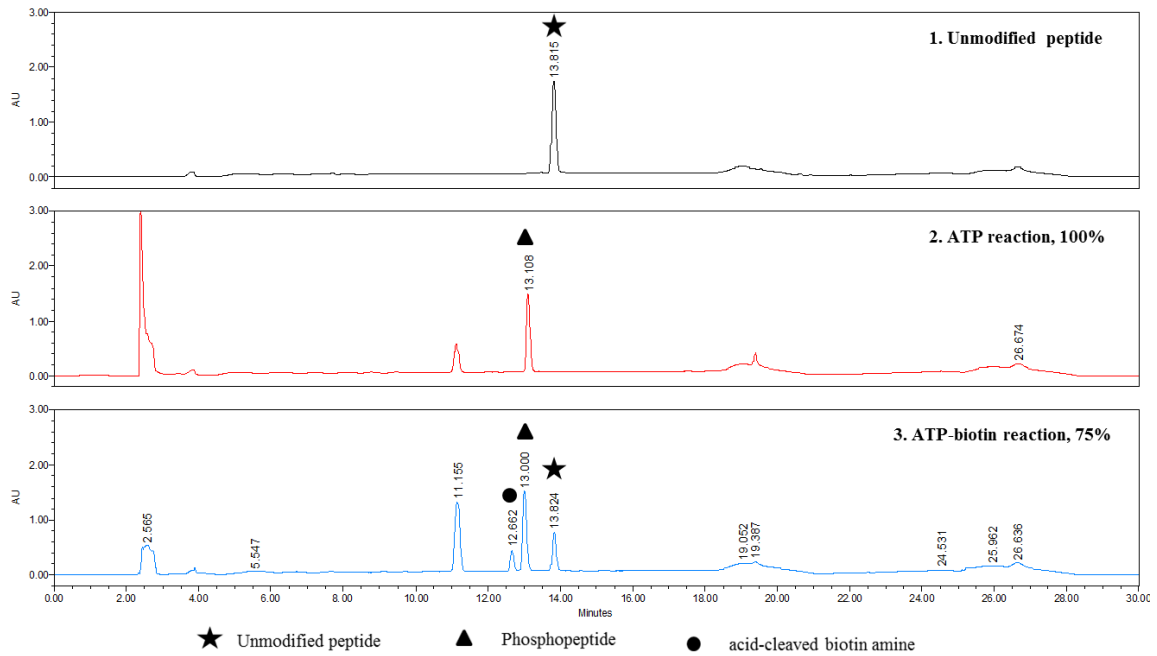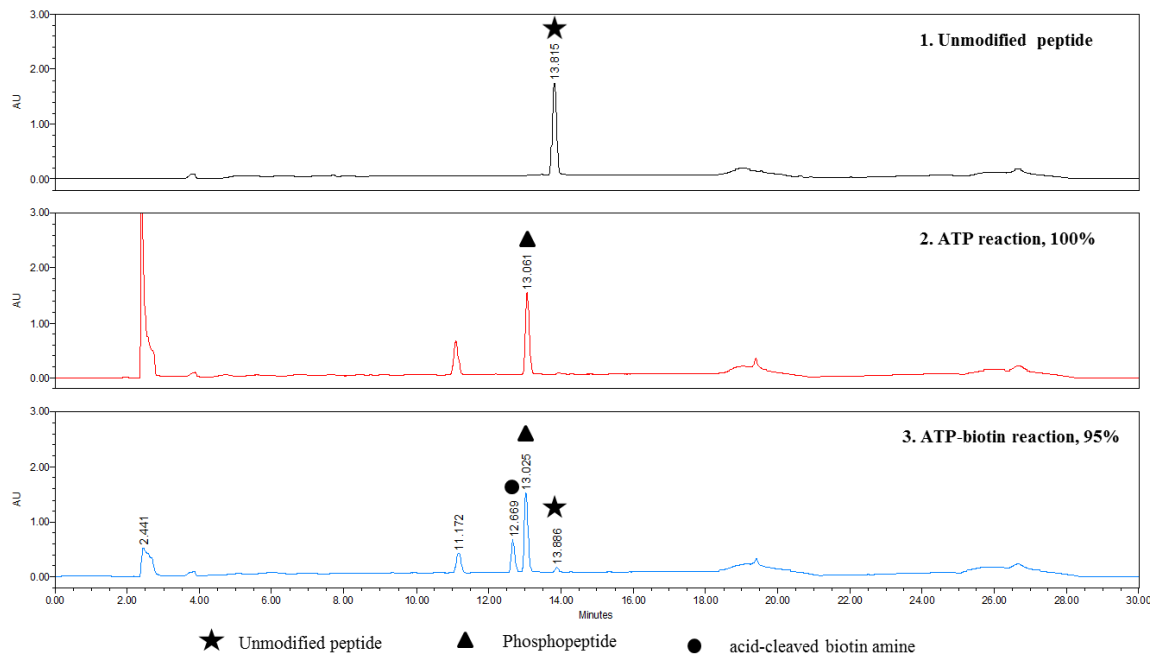
Figure A 2.12: HPLC traces for the peptides (panel 1) after phosphorylation (panel 2), or biotinylation (panel 3). Reactions were performed using Abl enzyme and the Abl peptide substrate (EAIYAAPFAKKK). i, ii, and iii are three independent trials.

(B) Reaction with AKT1
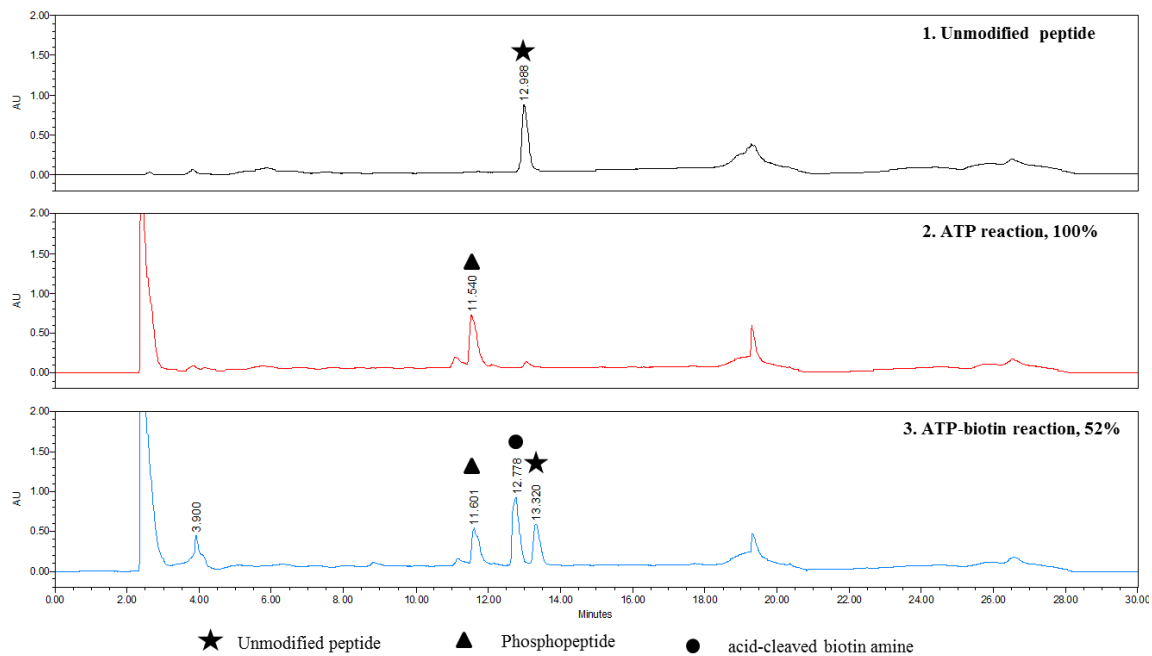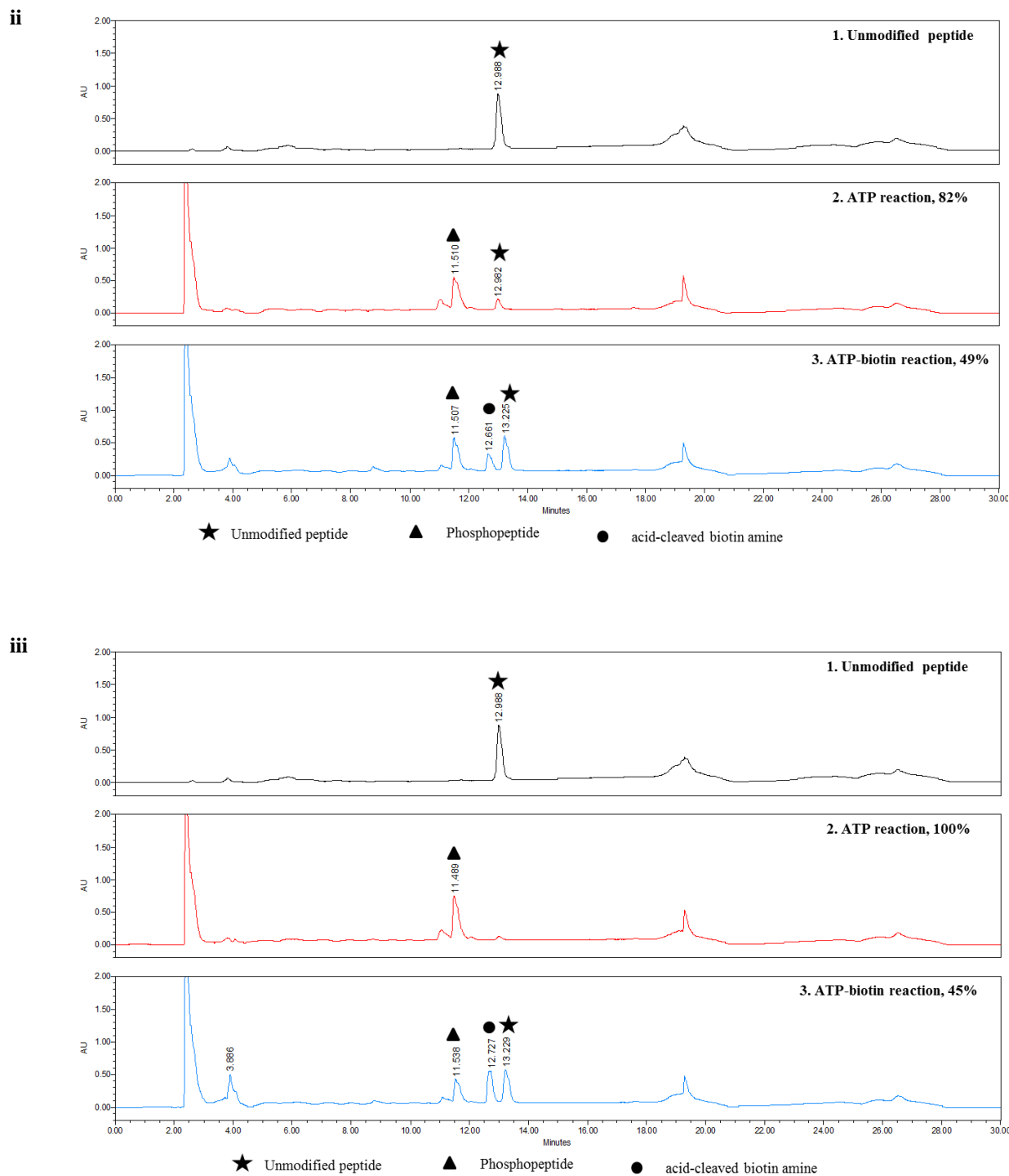
Figure A 2.13: HPLC traces for the peptides (panel 1) after phosphorylation (panel 2), or biotinylation (panel 3). Reactions were performed using AKT1 enzyme and the AKT (PKB) substrate (CKRPRAASFAE). i, ii, and iii are three independent trials.

(C) Reaction with CAMK4

i

★ Unmodified peptide   ▲ Phosphopeptide   ● acid-cleaved biotin amine

ii

★ Unmodified peptide   ▲ Phosphopeptide   ● acid-cleaved biotin amine
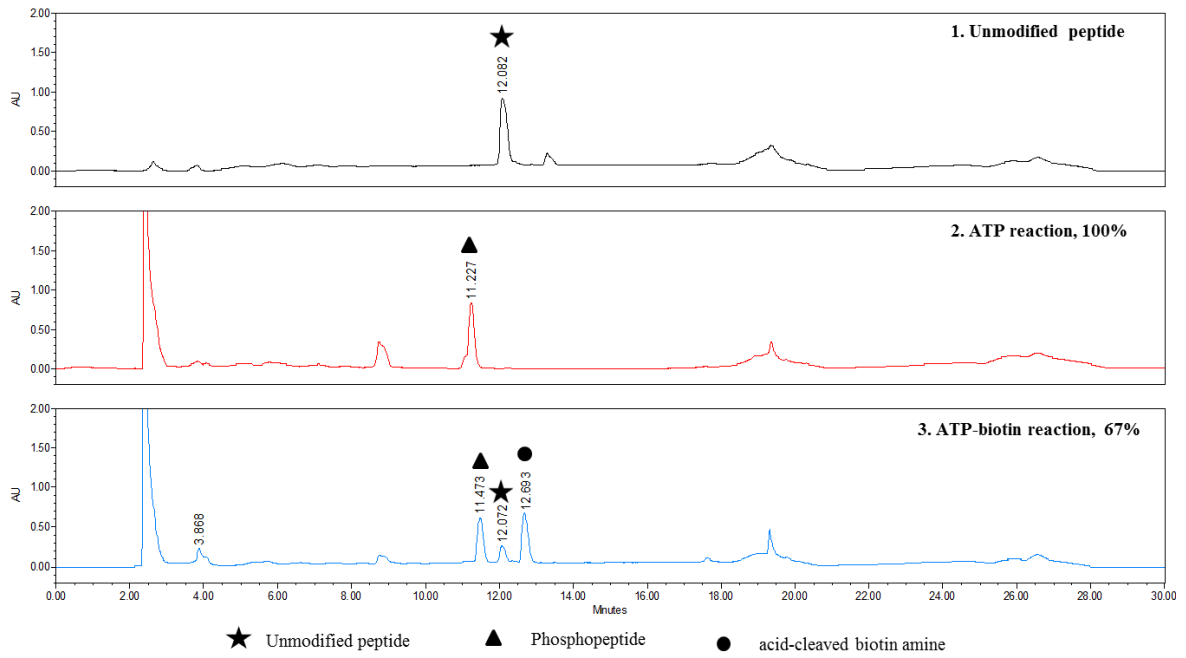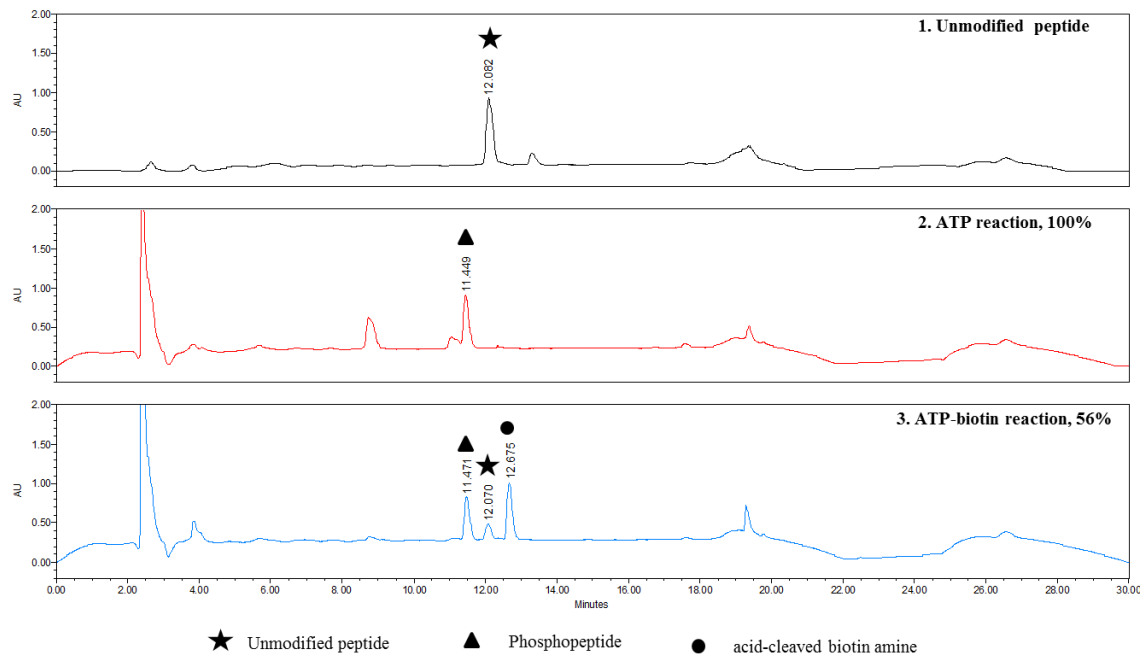
iii
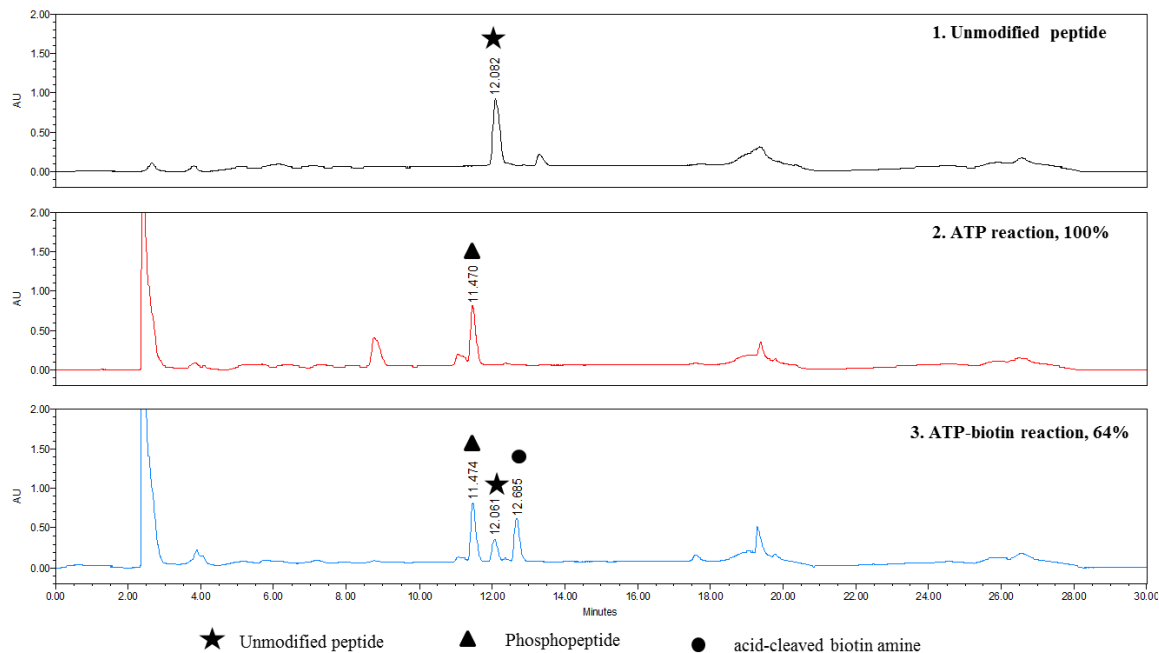
Figure A 2.14: HPLC traces for the peptides (panel 1) after phosphorylation (panel 2), or biotinylation (panel 3). Reactions were performed using CAMK4 enzyme and the Autocamtide (KKALRRQETVDAL-amide). i, ii, and iii are three independent trials.

(D) Reaction with CK2

i
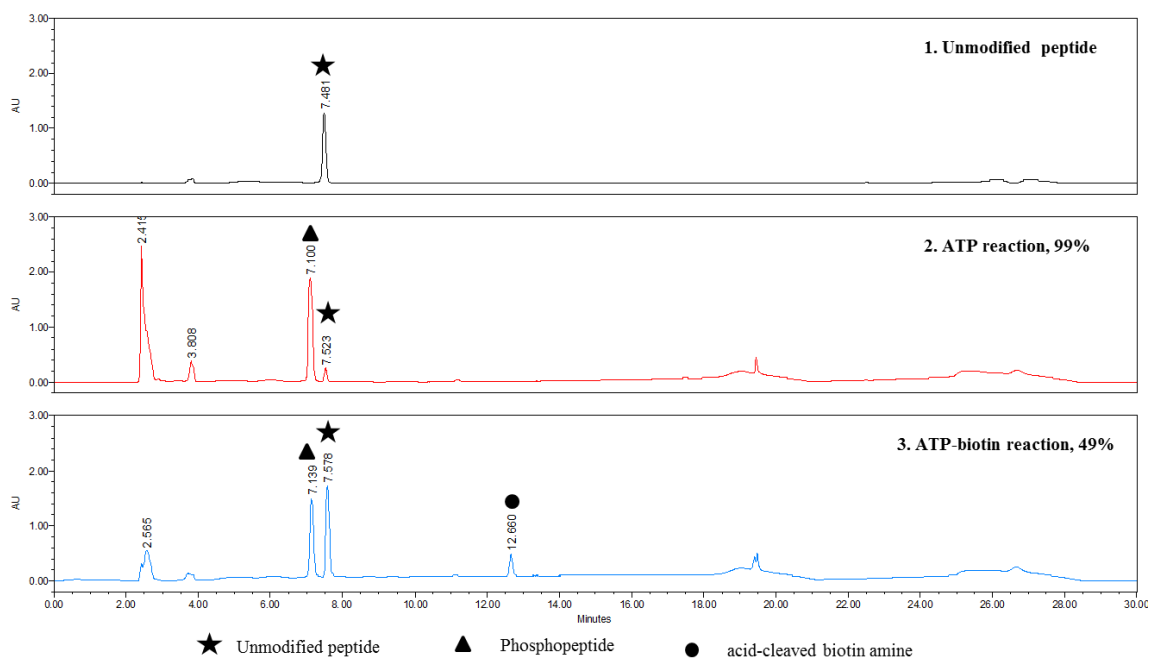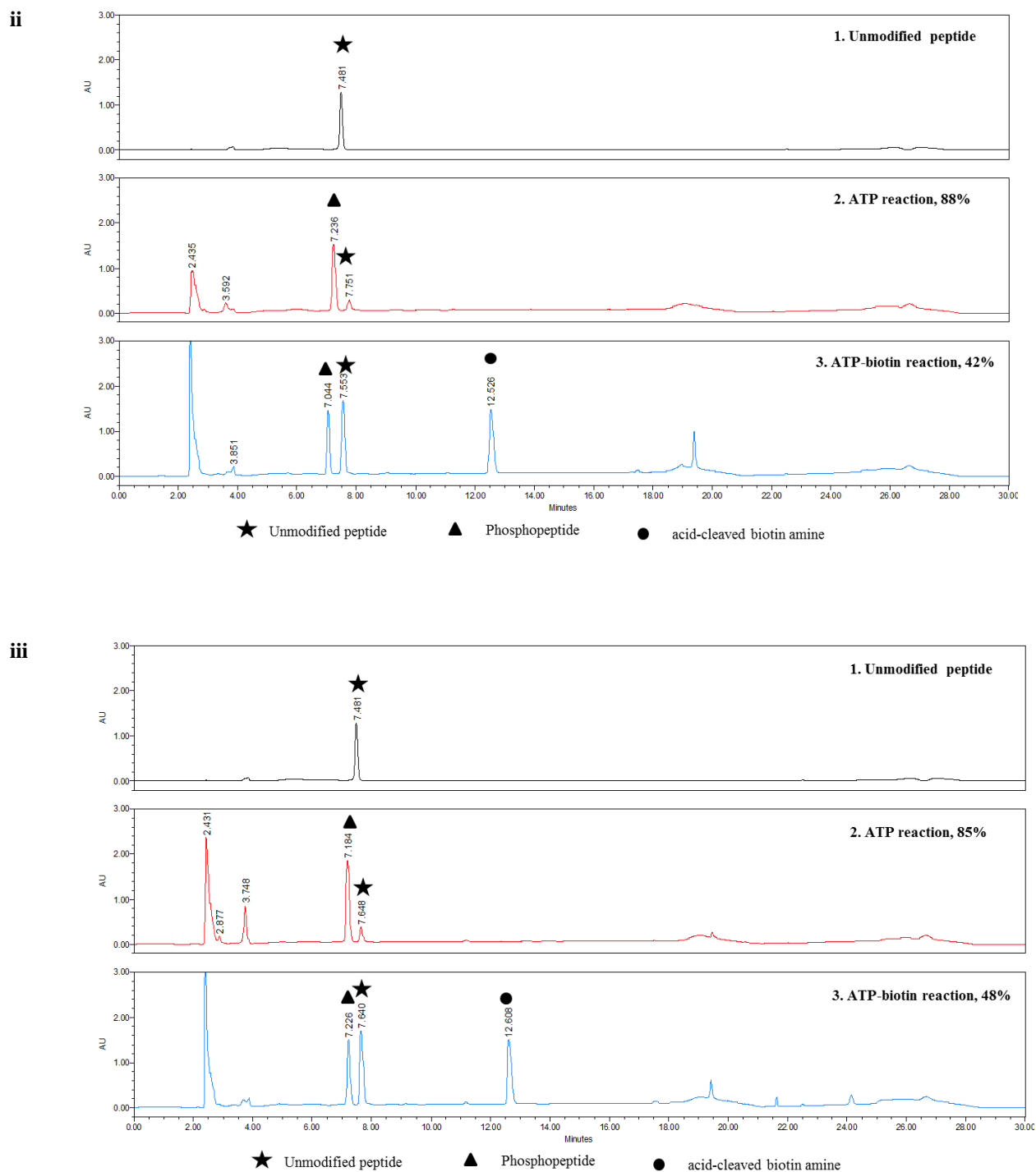
Figure A 2.15: HPLC traces for the peptides (panel 1) after phosphorylation (panel 2), or biotinylation (panel 3). Reactions were performed using CK2 enzyme and the CK2 peptide substrate (RRREEETEEE). i, ii, and iii are three independent trials.

(E) Reaction with FLT1

i

| ★ Unmodified peptide | ▲ Phosphopeptide | ● acid-cleaved biotin amine |

ii

| ★ Unmodified peptide | ▲ Phosphopeptide | ● acid-cleaved biotin amine |
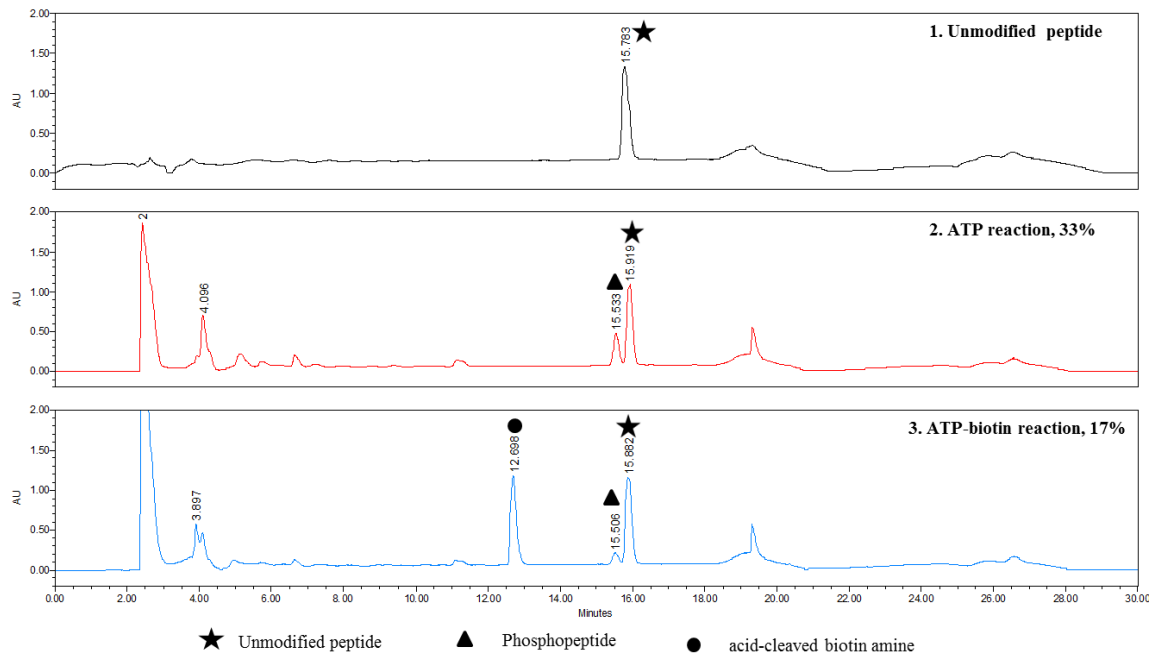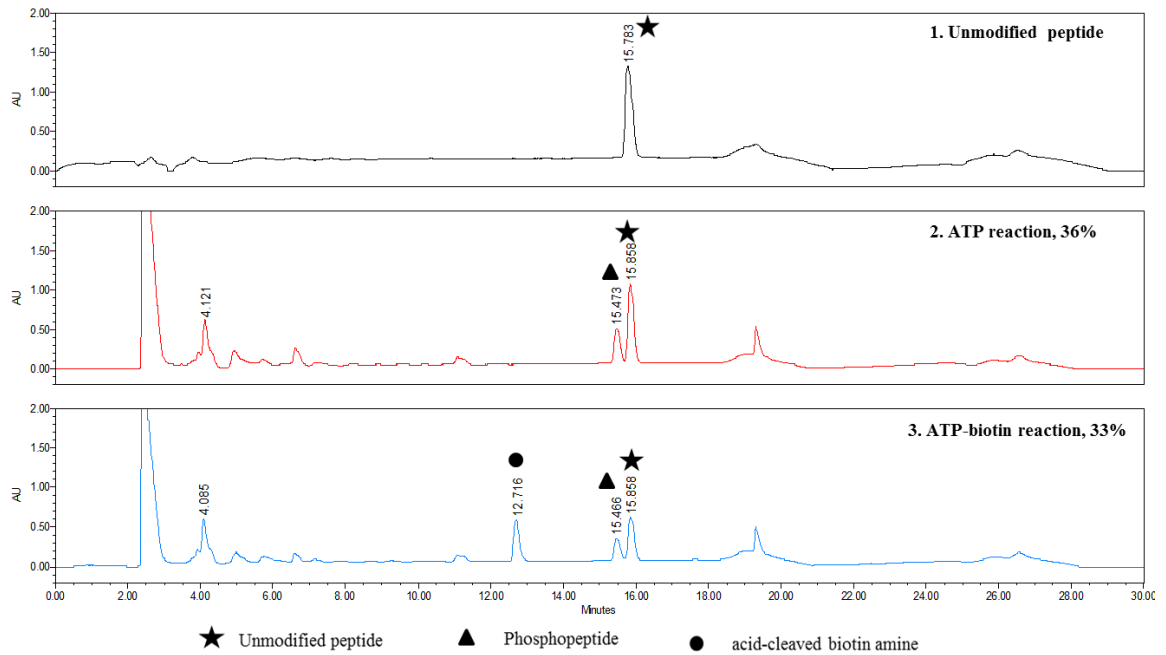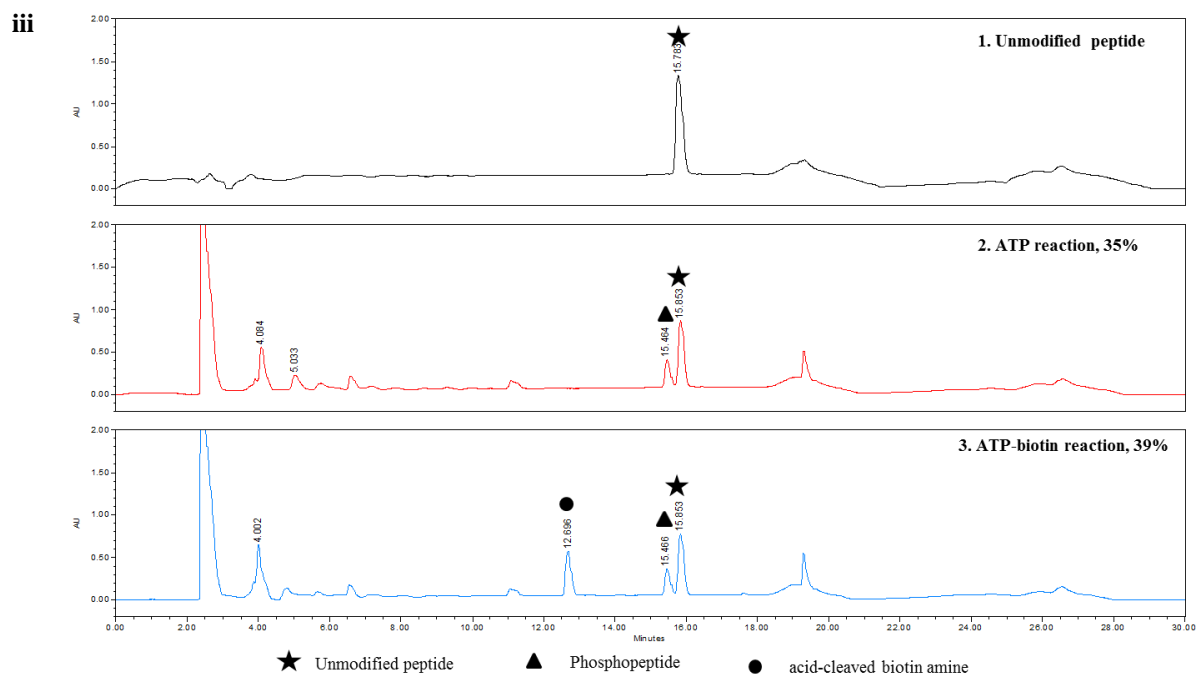
Figure A 2.16: HPLC traces for the peptides (panel 1) after phosphorylation (panel 2), or biotinylation (panel 3). Reactions were performed using FLT1 enzyme and the IGF1Rtide (KKKSPGEYVNIEFG). i, ii, and iii are three independent trials.

(F) Reaction with GSK3β
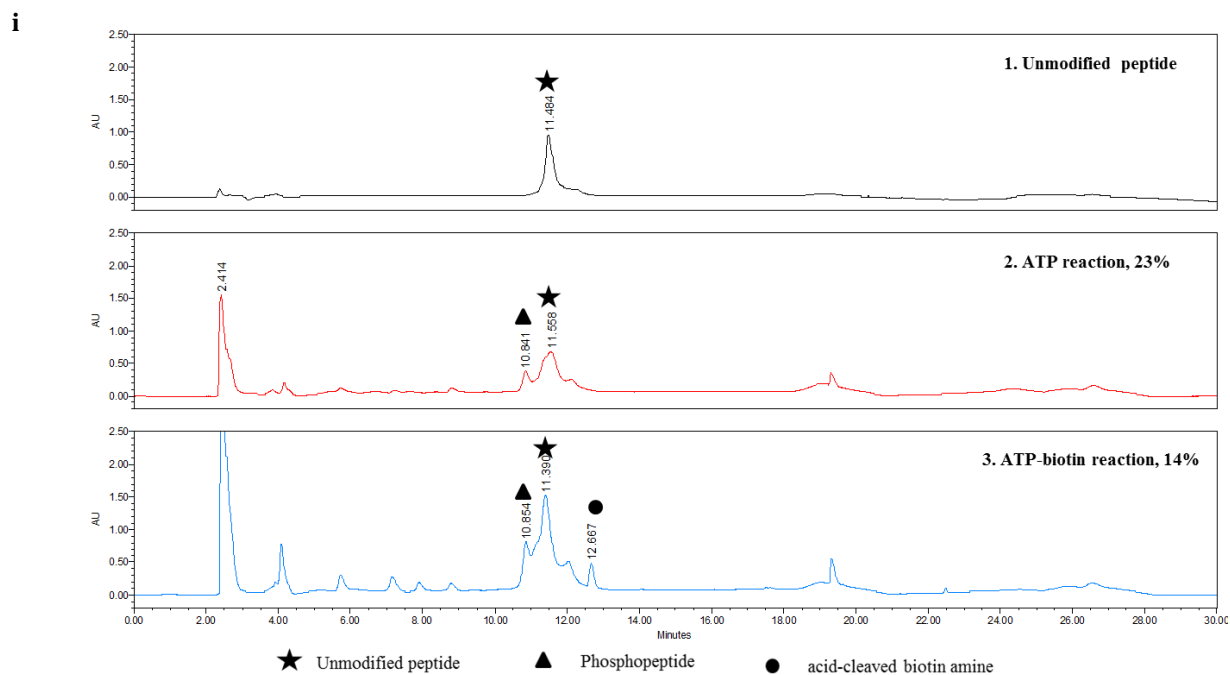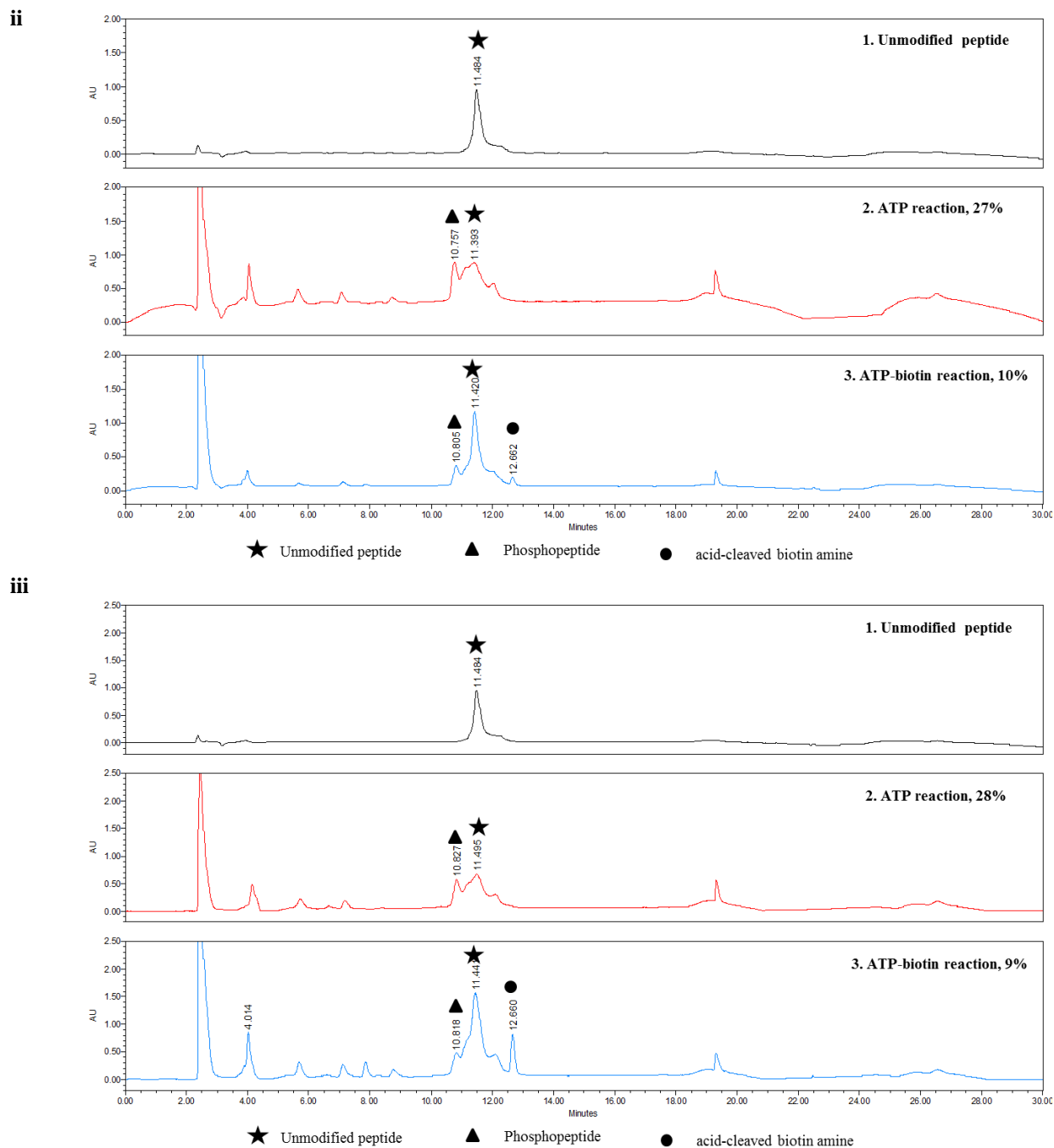
Figure A 2.17: HPLC traces for the peptides (panel 1) after phosphorylation (panel 2), or biotinylation (panel 3). Reactions were performed using GSK3β enzyme and the GSK3 substrate (YRRAAVPPSPSLSRHSSPHQ(pS)EDEEE). i, ii, and iii are three independent trials. Note: Because the starting peptide was already phosphorylated, the separation of mono and di-phosphorylated peptides was poor.

(G) Reaction with PAK1

i

★ Unmodified peptide   ▲ Phosphopeptide   ● acid-cleaved biotin amine

ii

★ Unmodified peptide   ▲ Phosphopeptide   ● acid-cleaved biotin amine
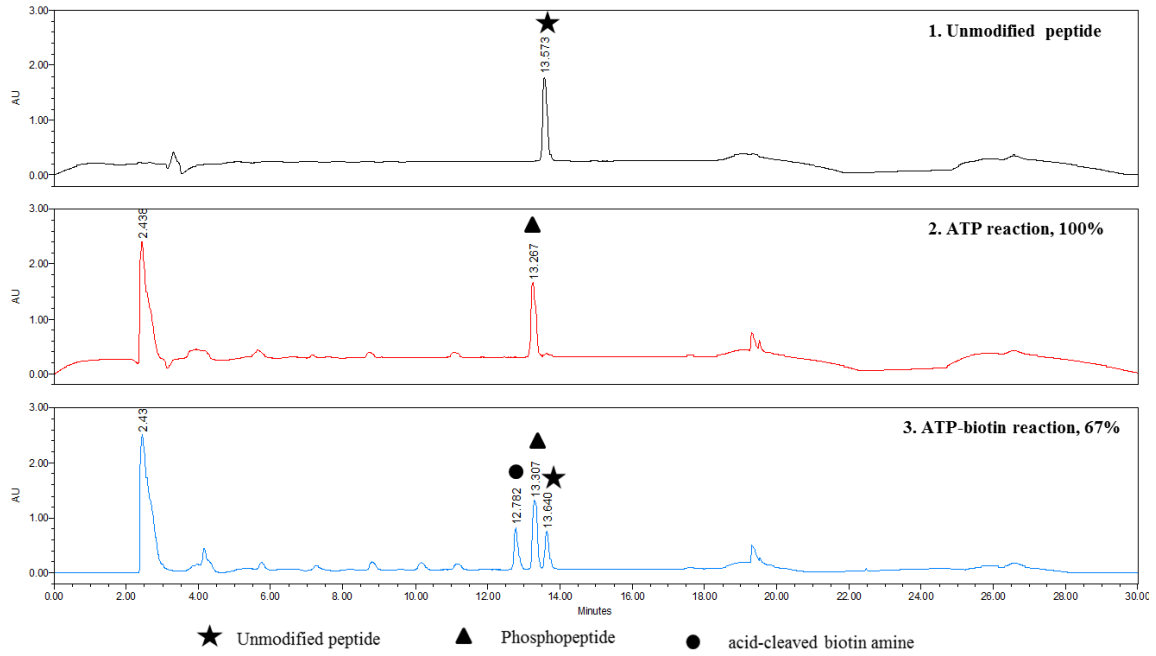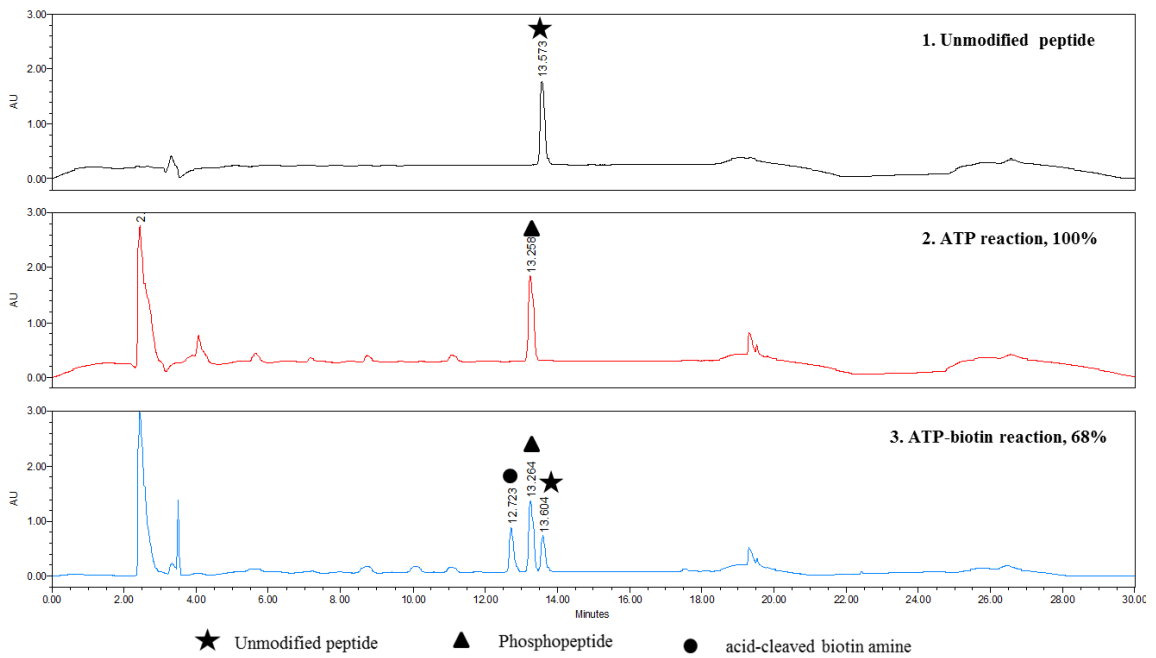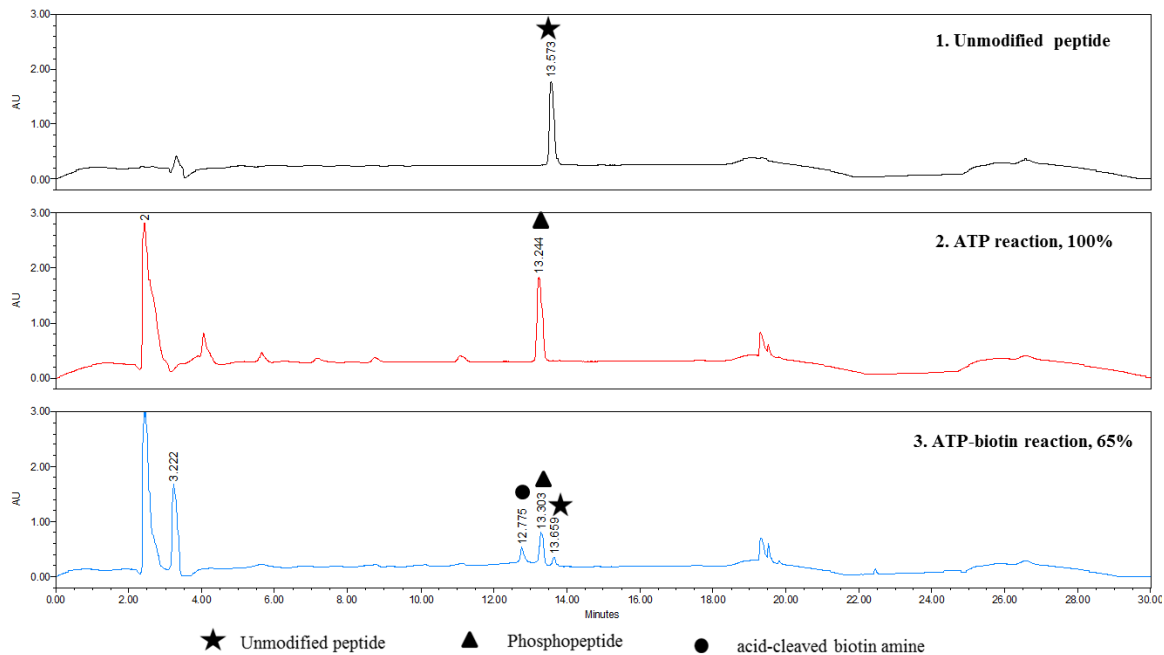
Figure A 2.18: HPLC traces for the peptides (panel 1) after phosphorylation (panel 2), or biotinylation (panel 3). Reactions were performed using PAK1 enzyme and the PAKtide (RRRLSFAEPG). i, ii, and iii are three independent trials.

(H) Reaction with PKA
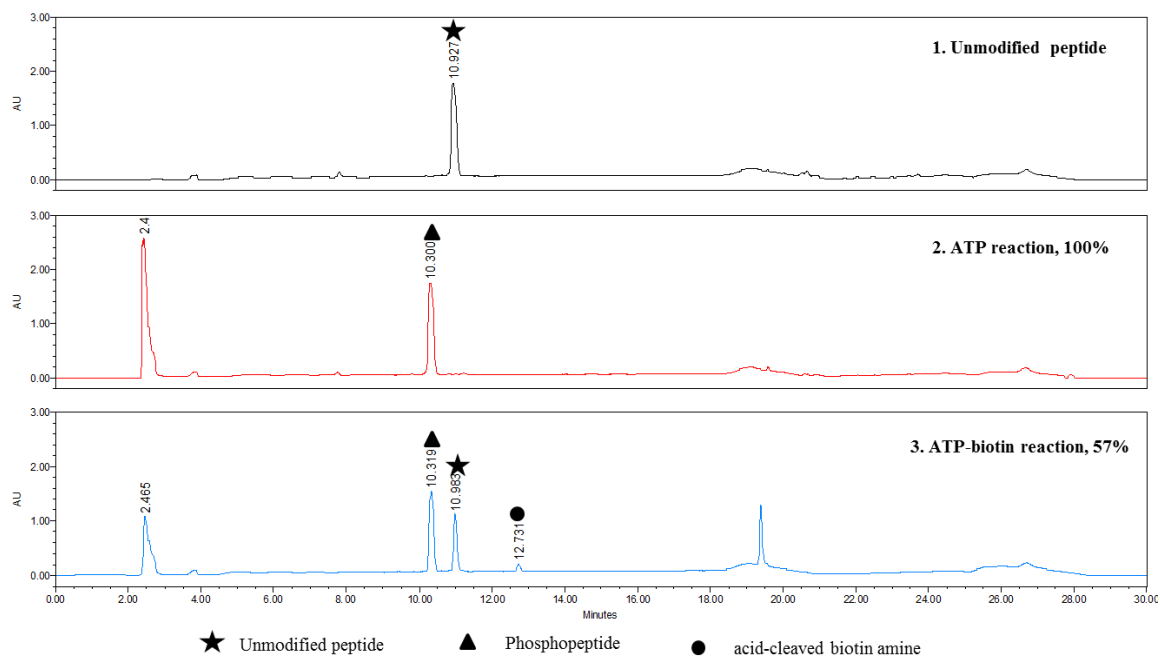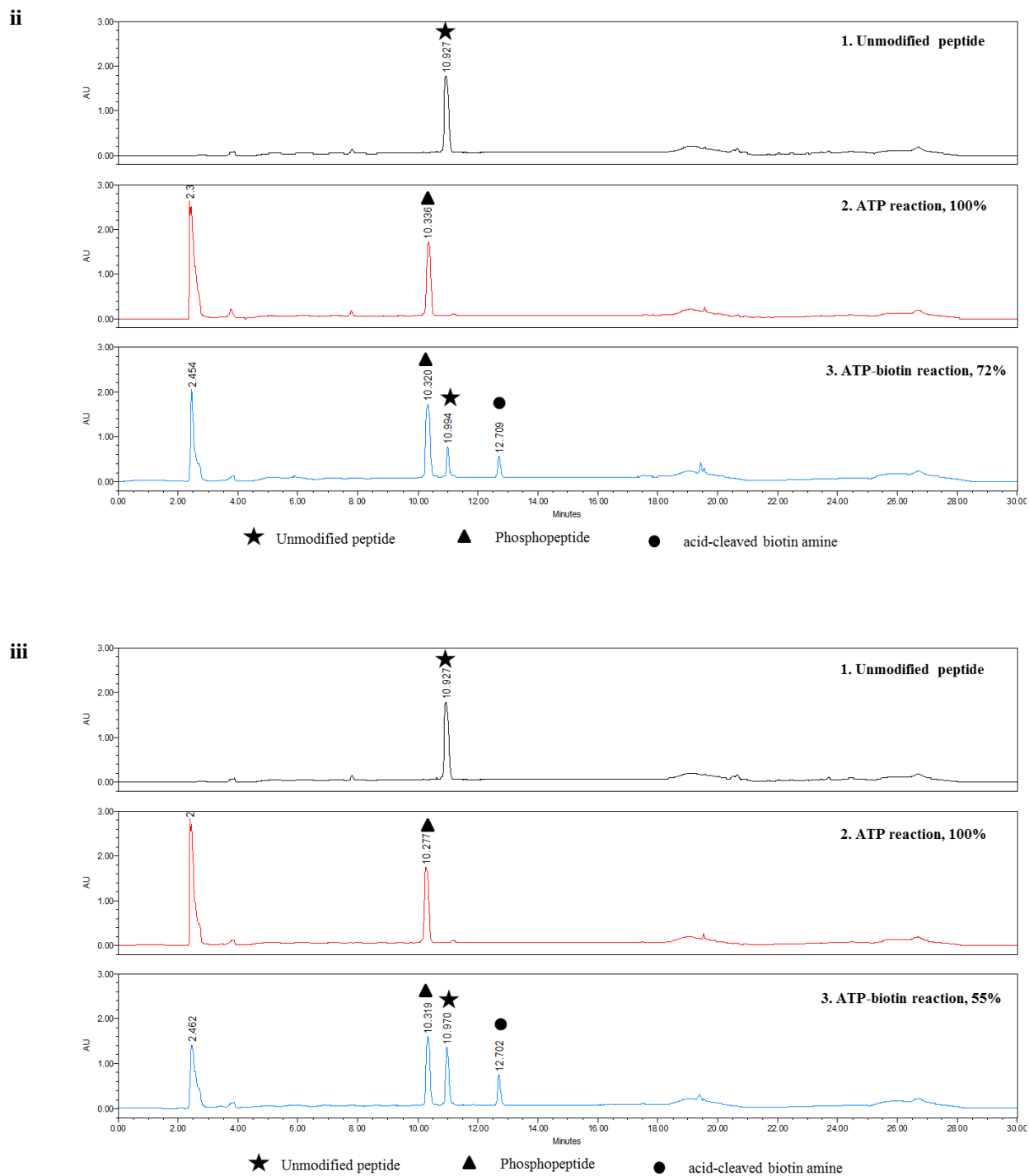
Figure A 2.19: HPLC traces for the peptides (panel 1) after phosphorylation (panel 2), or biotinylation (panel 3). Reactions were performed using PKA enzyme and the kemptide (LRRASLG). i, ii, and iii are three independent trials.

(I) Reaction with RSK1

i

★ Unmodified peptide   ▲ Phosphopeptide   ● acid-cleaved biotin amine

ii

★ Unmodified peptide   ▲ Phosphopeptide   ● acid-cleaved biotin amine
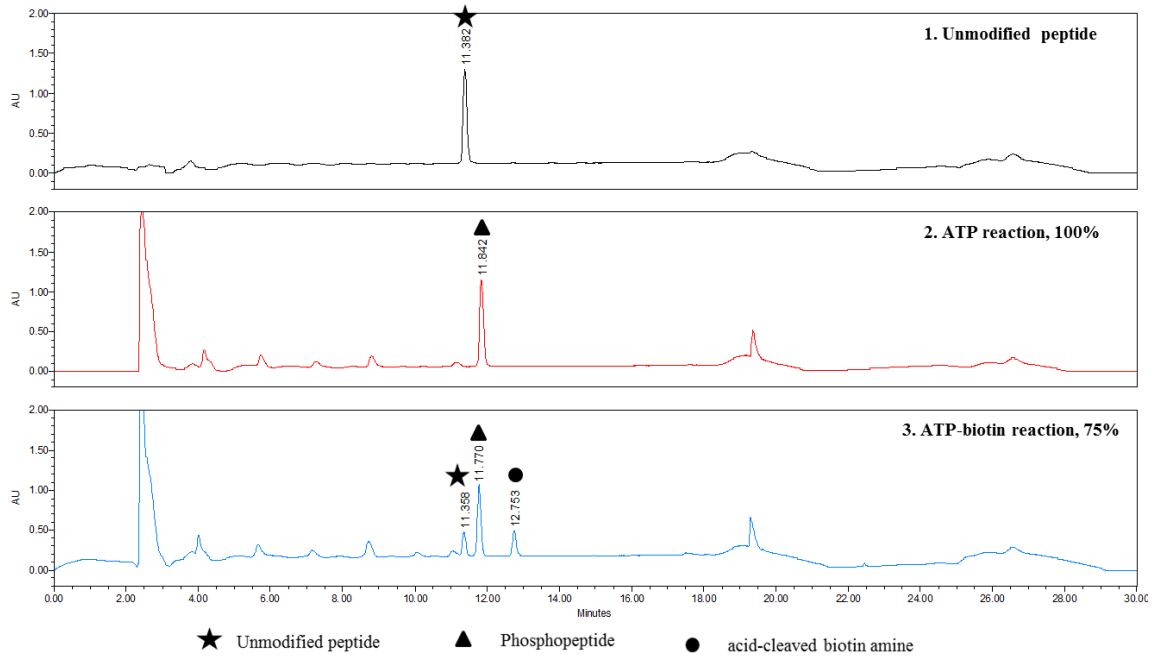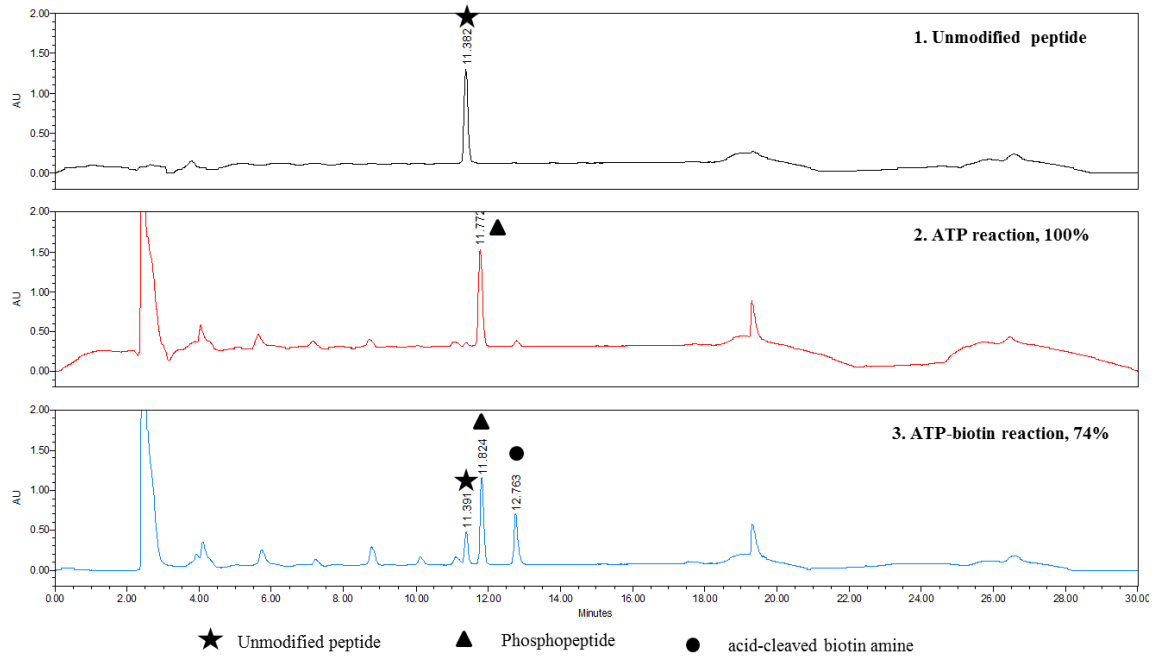
iii
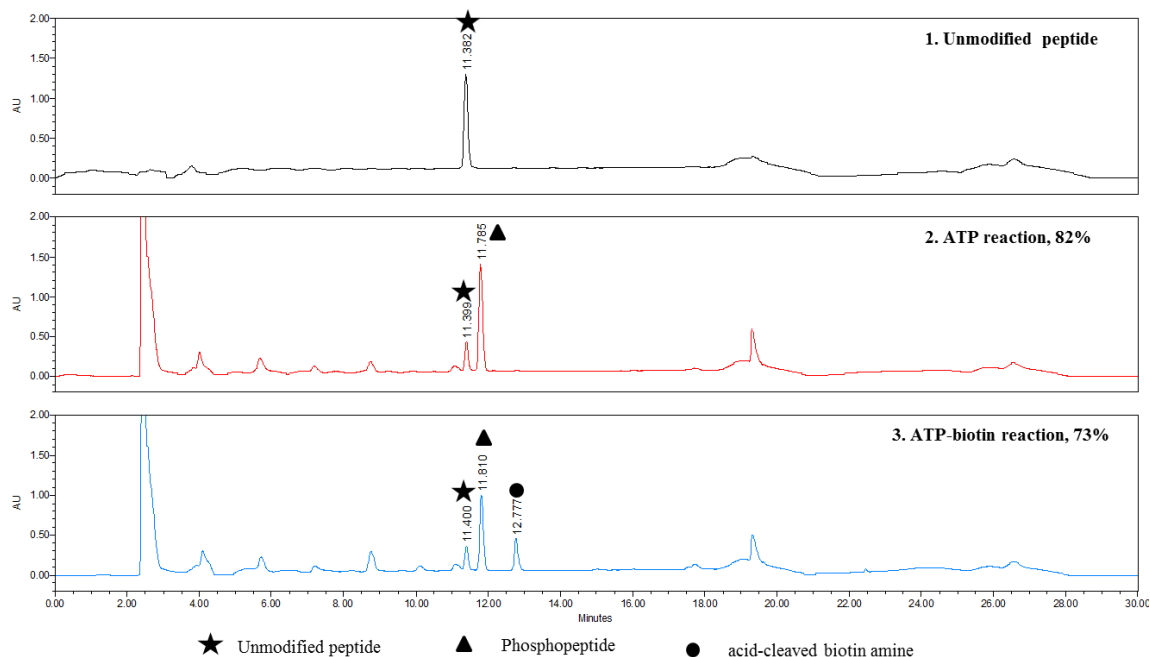
Figure A 2.20: HPLC traces for the peptides (panel 1) after phosphorylation (panel 2), or biotinylation (panel 3). Reactions were performed using RSK1 enzyme and the S6K substrate (KRRRLASLR). i, ii, and iii are three independent trials. Note: phodphopeptide was eluted after the unphosphorylated starting peptide.

(J) Reaction with SRC

i
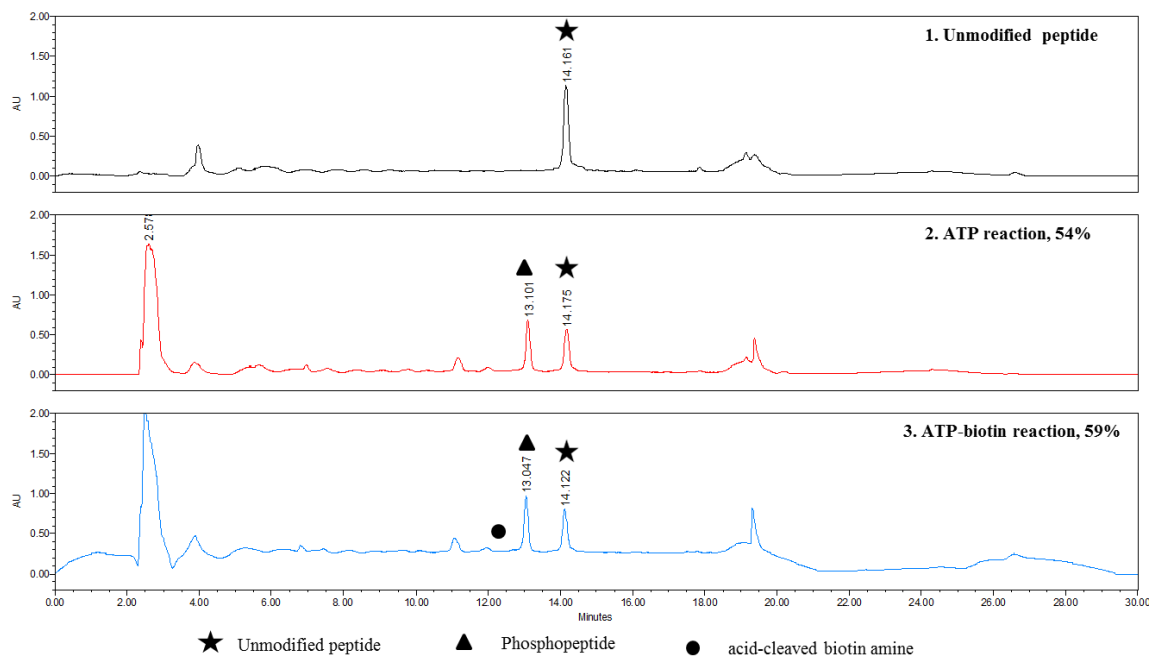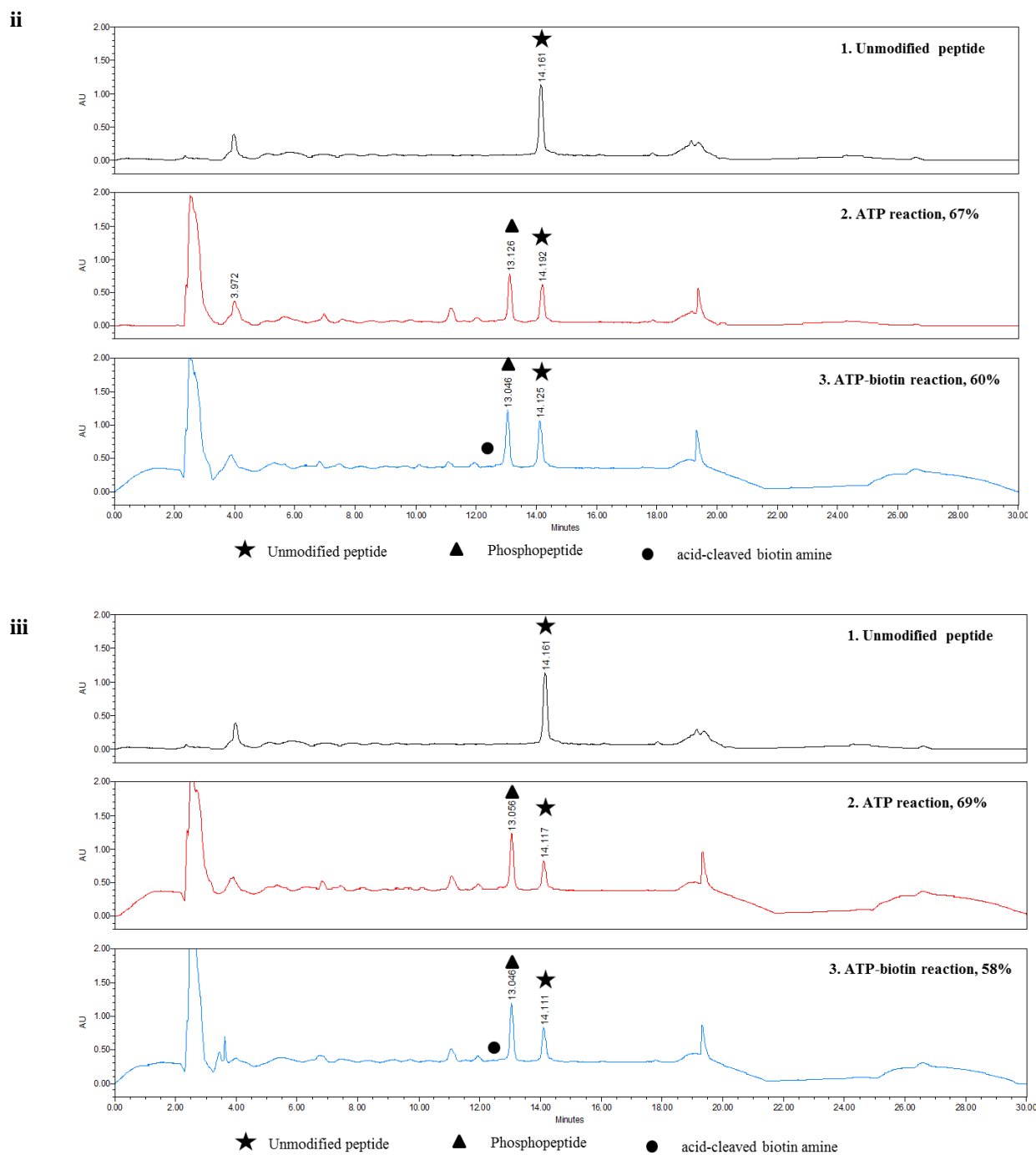
Figure A 2.21: HPLC traces for the peptides (panel 1) after phosphorylation (panel 2), or biotinylation (panel 3). Reactions were performed using SRC enzyme and the SRC peptide substrate (KVEKIGEGTYGVVYK-amide). i, ii, and iii are the three independent trials. Note: biotin-amine peak (t_R~12.6 min) was not observed in the biotinylation reaction (panel 3).

2.5 Complete Gel Images for Protein Quantification

(A) Reaction with ASK1
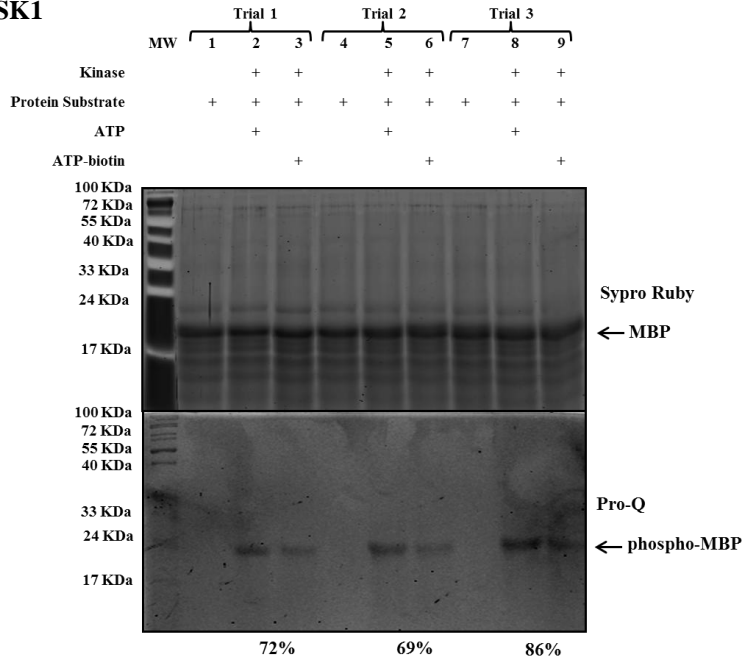
(B) Reaction with Aurora A
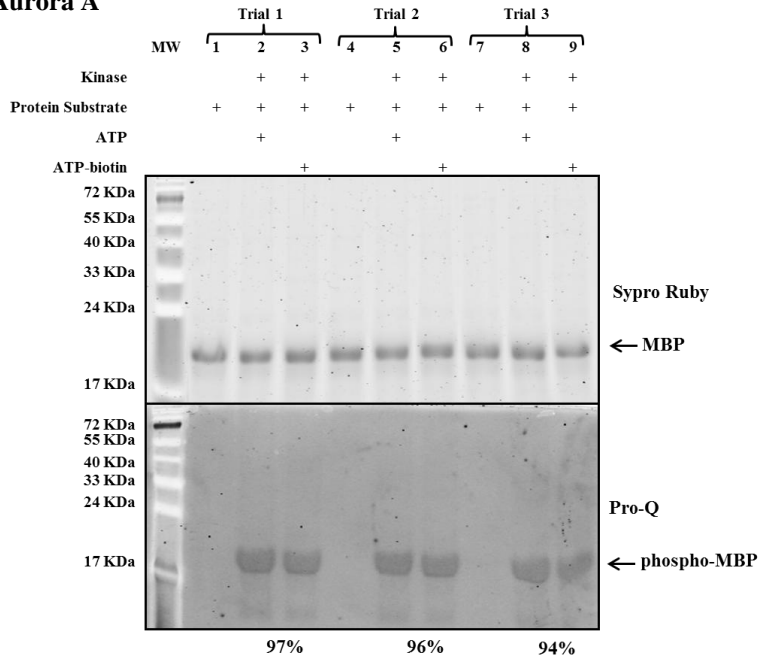
(C) Reaction with CAMK4
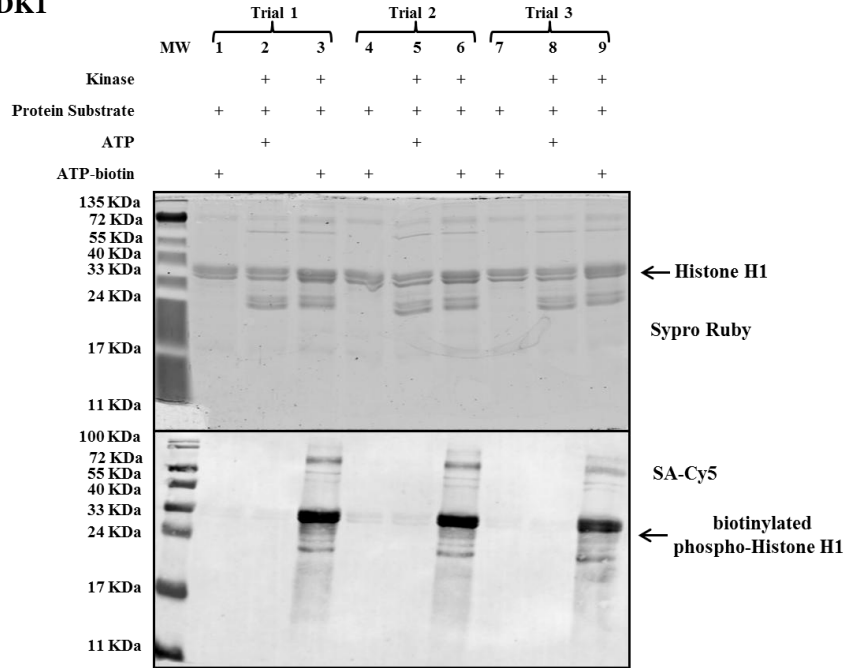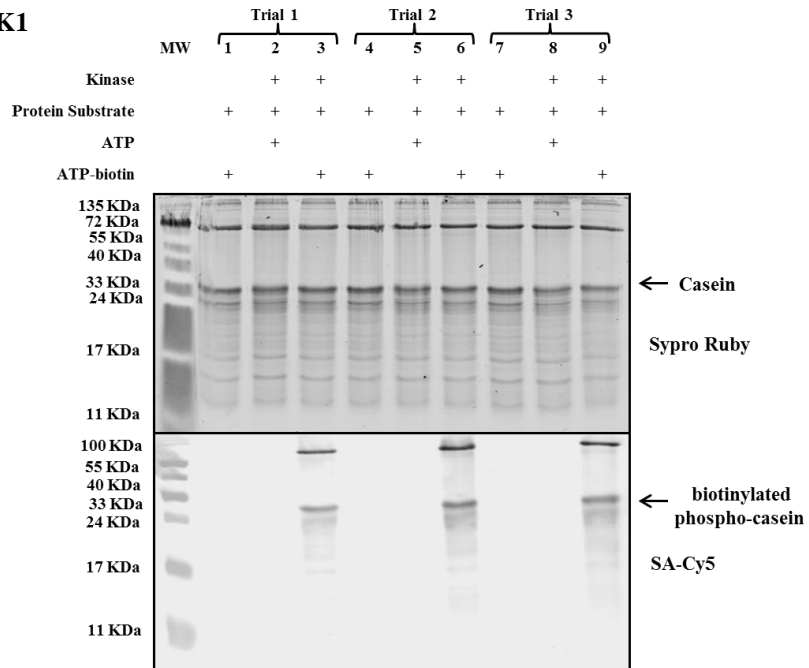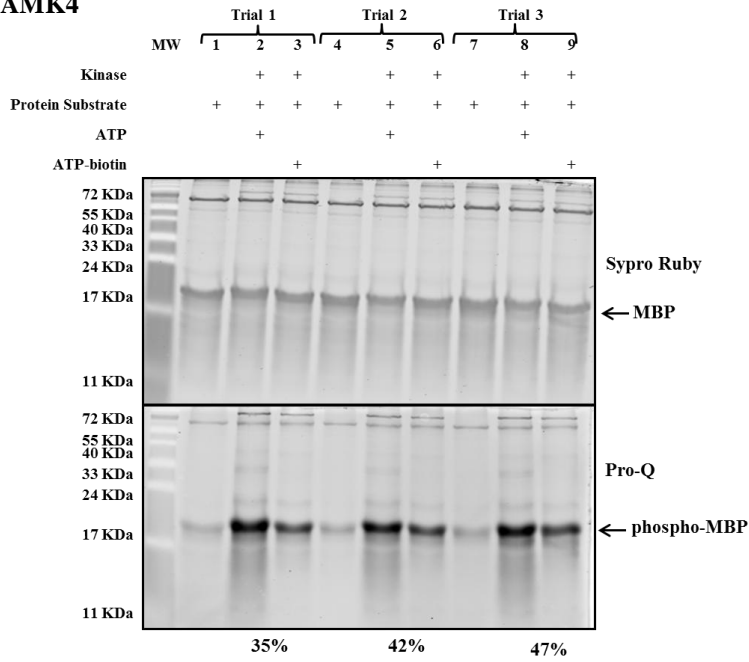

(D) Reaction with CDK1

(E) Reaction with CHK1

		Trial 1			Trial 2			Trial 3	
MW	1	2	3	4	5	6	7	8	9
Kinase		+	+		+	+		+	+
Protein Substrate	+	+	+	+	+	+	+	+	+
ATP		+			+			+	
ATP-biotin			+			+			+

72 KDa
55 KDa
40 KDa
33 KDa
24 KDa
17 KDa
11 KDa

Sypro Ruby
← MBP

40 KDa
24 KDa
17 KDa
11 KDa

Pro-Q
← phospho-MBP

46%   42%   54%

(F) Reaction with CK1

		Trial 1			Trial 2			Trial 3	
MW	1	2	3	4	5	6	7	8	9
Kinase		+	+		+	+		+	+
Protein Substrate	+	+	+	+	+	+	+	+	+
ATP		+			+			+	
ATP-biotin			+			+			+

72 KDa
24 KDa
17 KDa

Sypro Ruby
← Casein

72 KDa
55 KDa
40 KDa
33 KDa
24 KDa
17 KDa

Pro-Q
← phospho-casein

65%   96%   84%
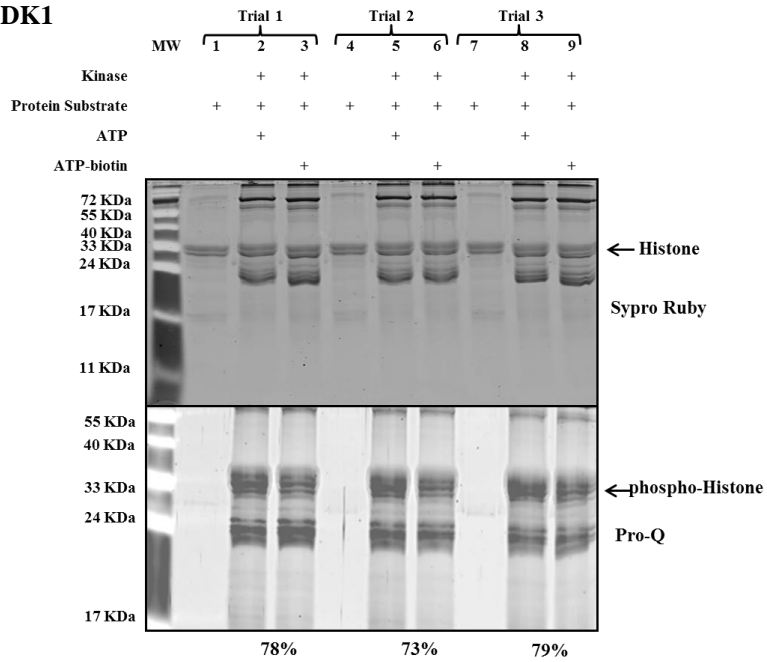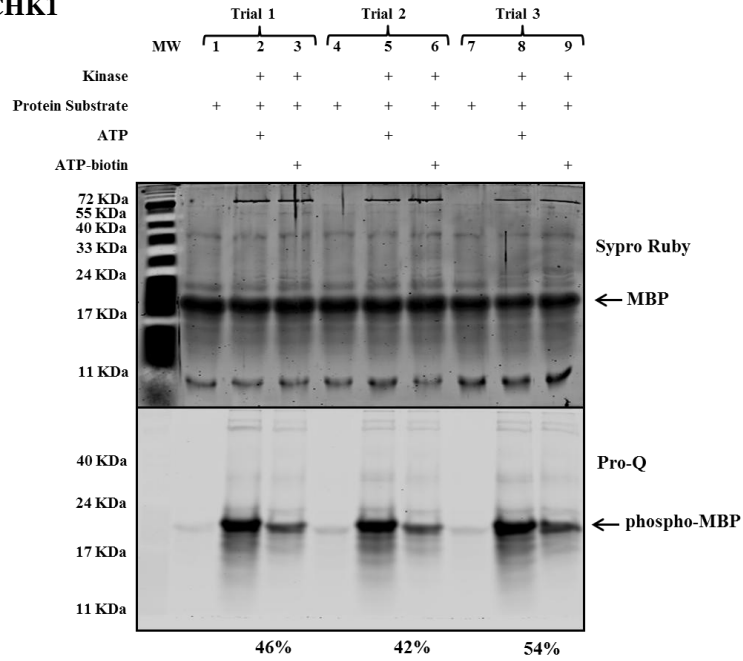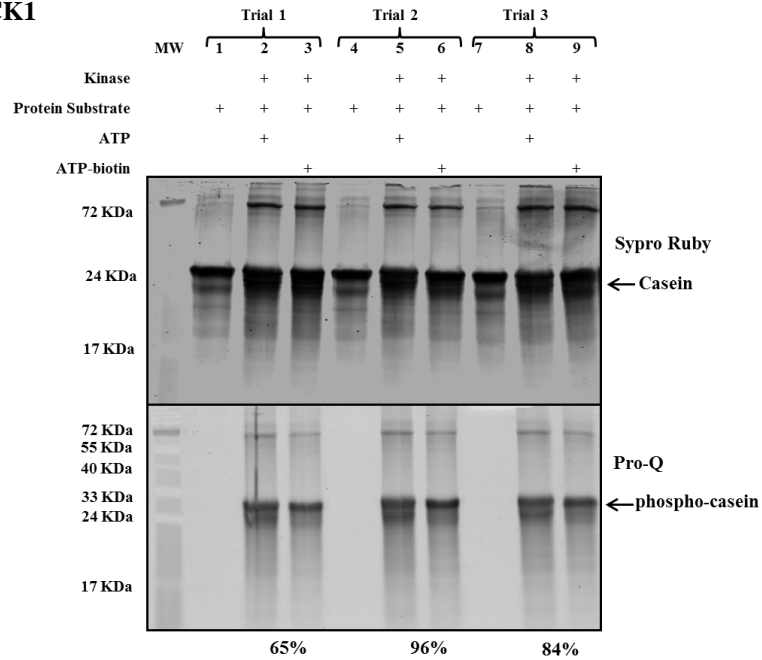
(G) Reaction with DAPK1
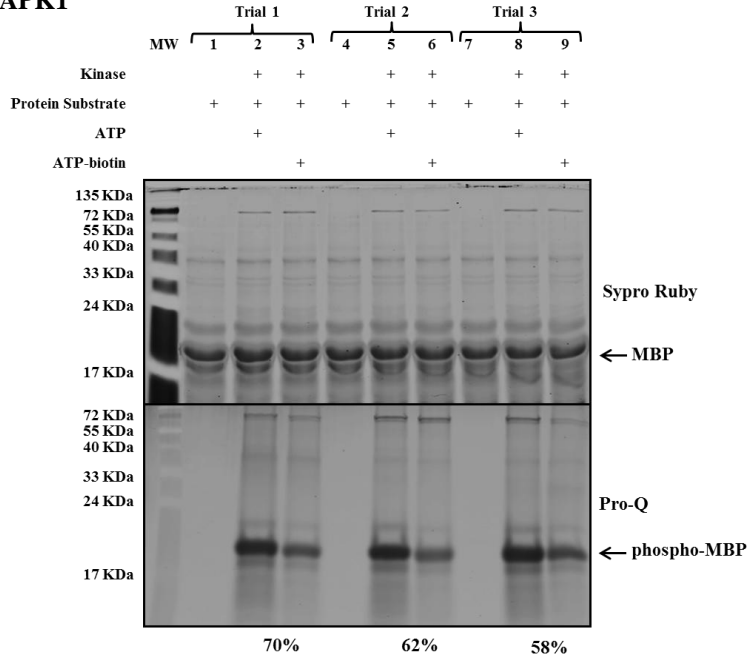
(H) Reaction with ERK1

(I) Reaction with GRK5

| | Trial 1 | Trial 2 | Trial 3 |
| MW | 1 2 3 | 4 5 6 | 7 8 9 |

Kinase: + + / + + / + +
Protein Substrate: + + + / + + + / + + +
ATP: + / + / +
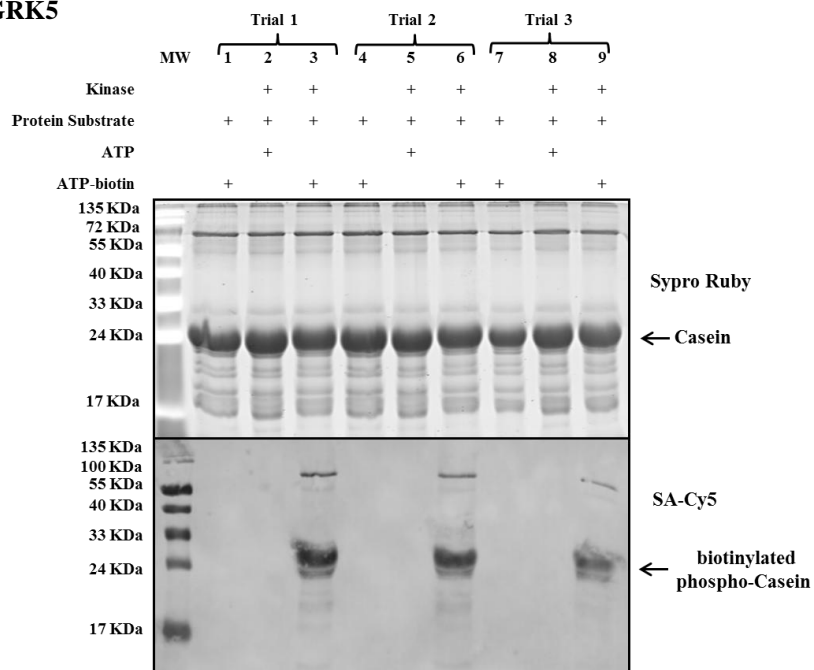ATP-biotin: + / + / +

Sypro Ruby
← Casein

Pro-Q
← phospho-casein

68% 49% 41%

(J) Reaction with HIPK1

| | Trial 1 | Trial 2 | Trial 3 |
| MW | 1 2 3 | 4 5 6 | 7 8 9 |

Kinase: + + / + + / + +
Protein Substrate: + + + / + + + / + + +
ATP: + / + / +
ATP-biotin: + / + / +

Sypro Ruby
← MBP

Pro-Q
← phospho-MBP

47% 44% 42%

(K) Reaction with JAK3

		Trial 1			Trial 2			Trial 3	
MW	1	2	3	4	5	6	7	8	9
Kinase		+	+		+	+		+	+
Protein Substrate	+	+	+	+	+	+	+	+	+
ATP		+			+			+	
ATP-biotin			+			+			+

Sypro Ruby

poly(Glu$_4$,Tyr$_1$)

Pro-Q

biotinylatedphospho
poly(Glu$_4$,Tyr$_1$)

96%   89%   89%

(L) Reaction with MARK1

		Trial 1			Trial 2			Trial 3	
MW	1	2	3	4	5	6	7	8	9
Kinase		+	+		+	+		+	+
Protein Substrate	+	+	+	+	+	+	+	+	+
ATP		+			+			+	
ATP-biotin			+			+			+

Sypro Ruby

← MBP

Pro-Q

← phospho-MBP

50%   63%   82%
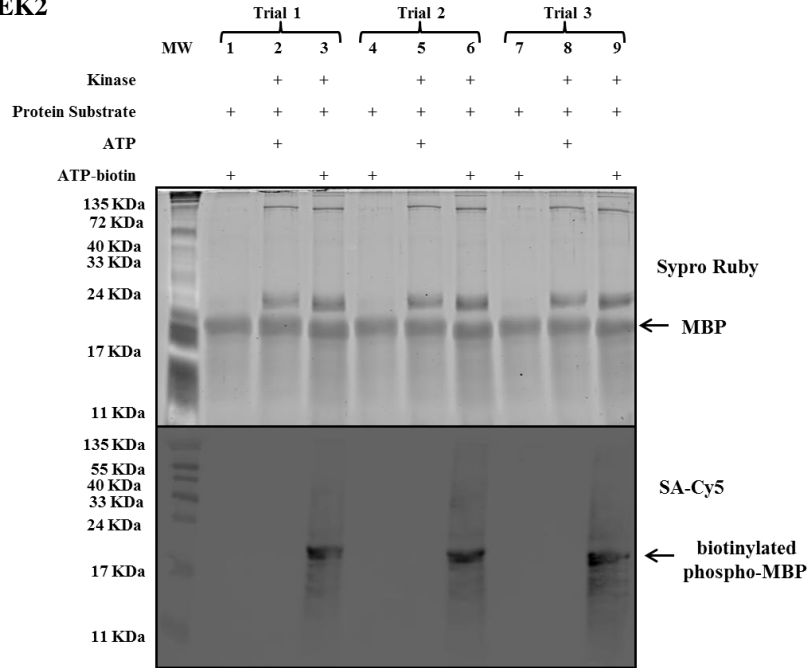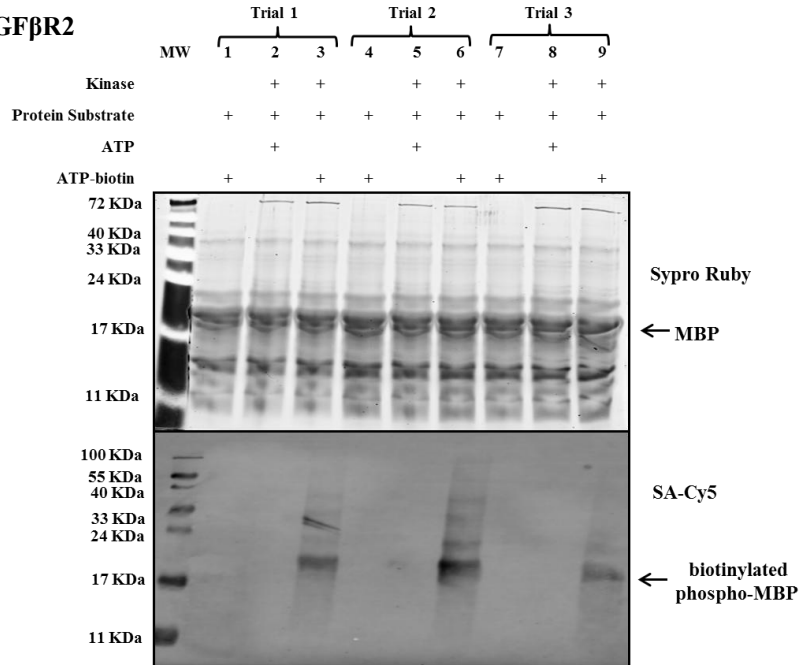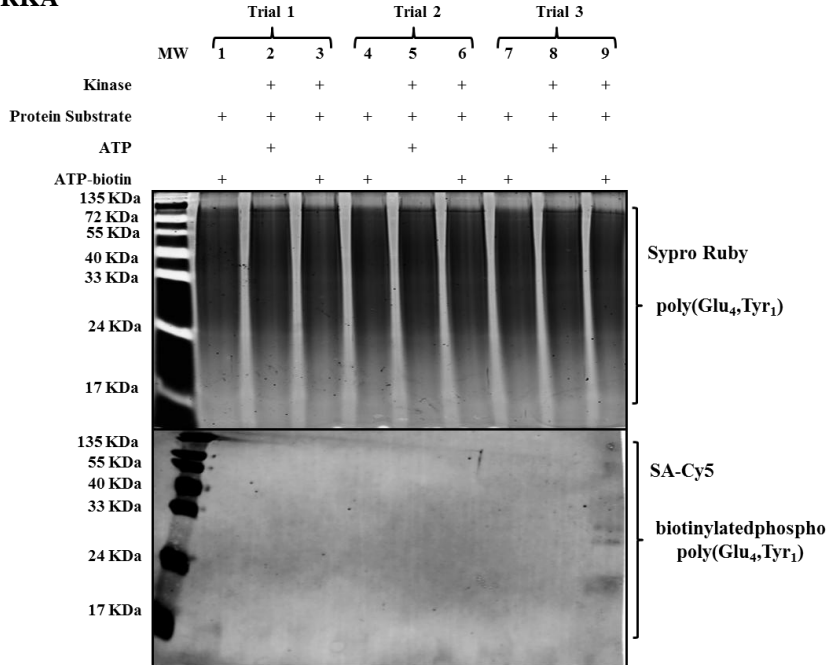
(M) Reaction with MLK1

(N) Reaction with MST1
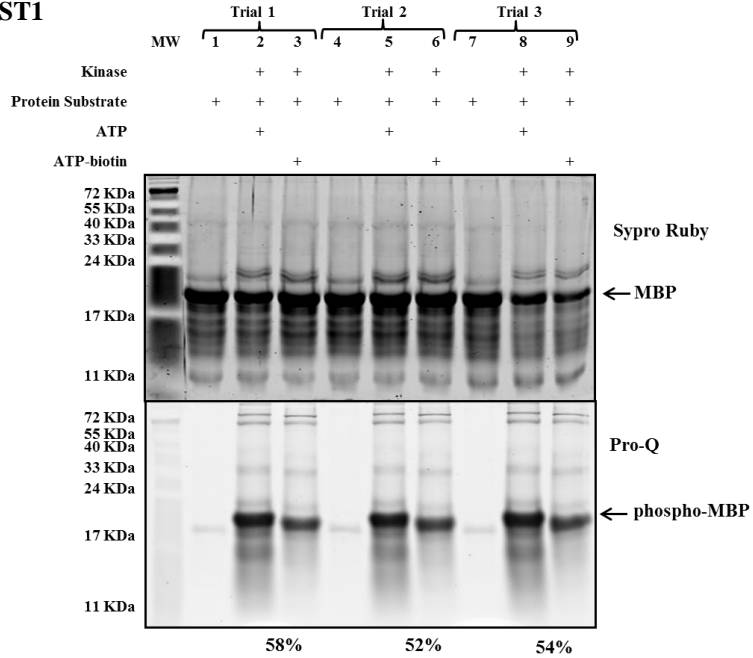
(O) Reaction with NEK2
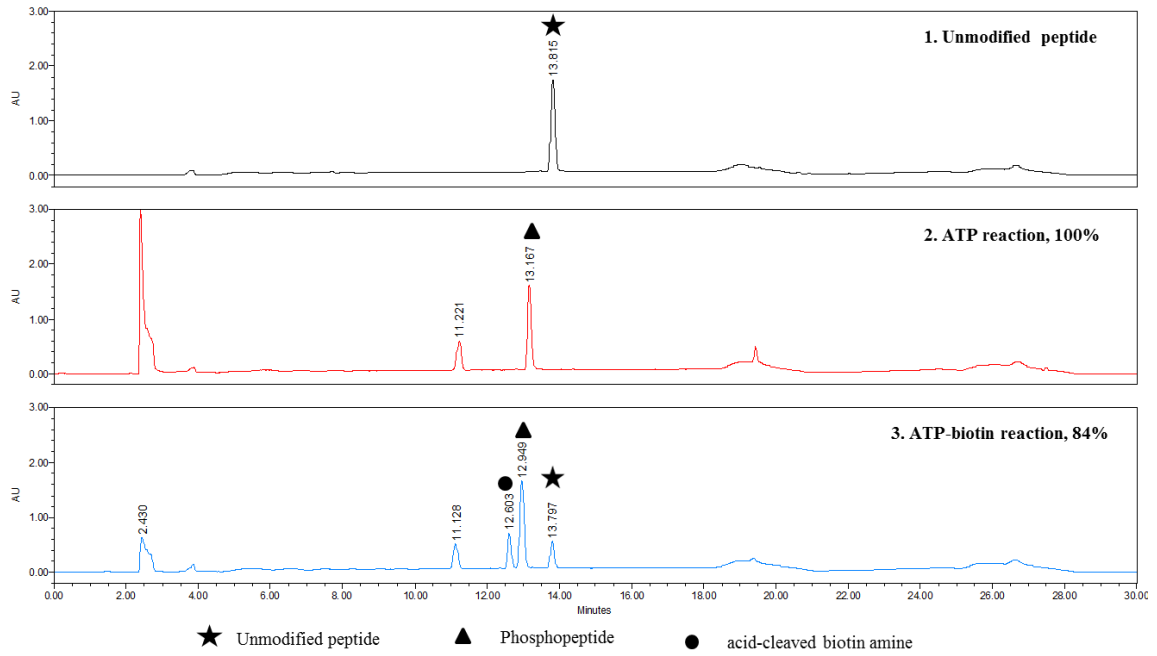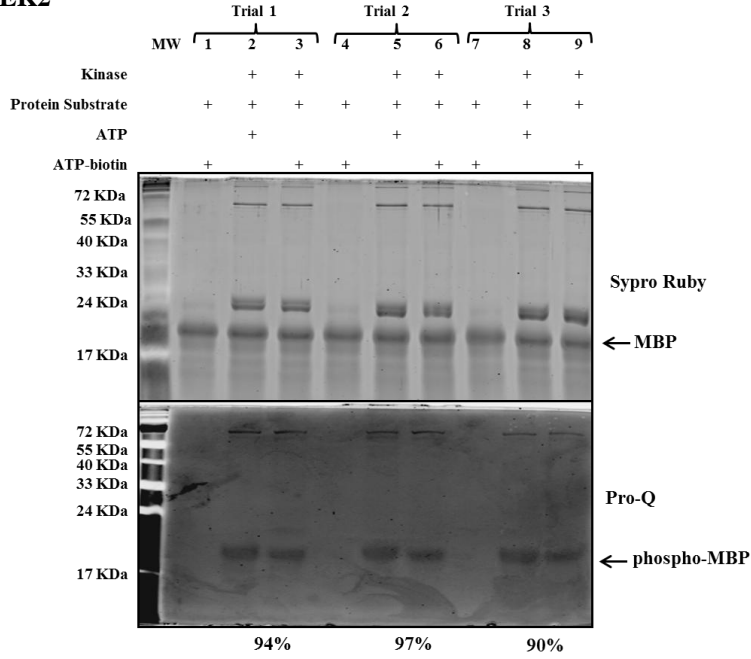

(P) Reaction with TGFβR2
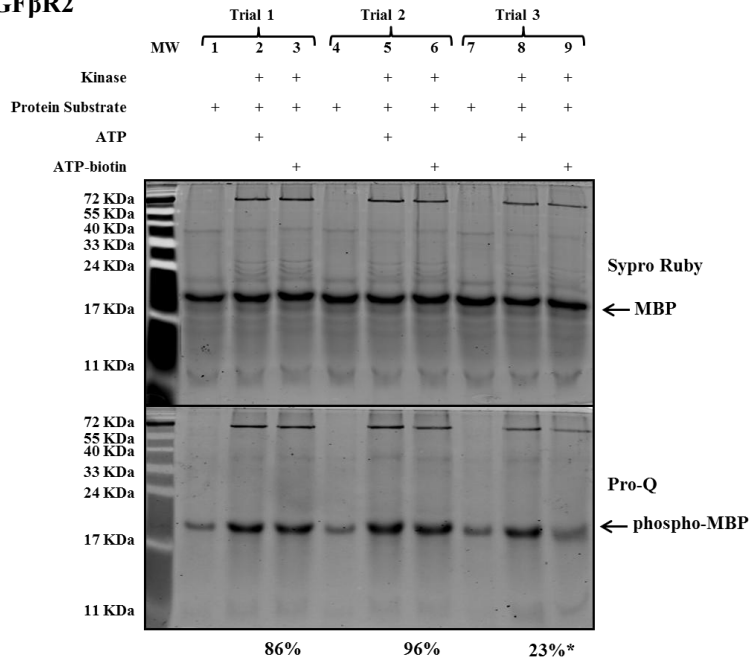
(Q) Reaction with TRKA
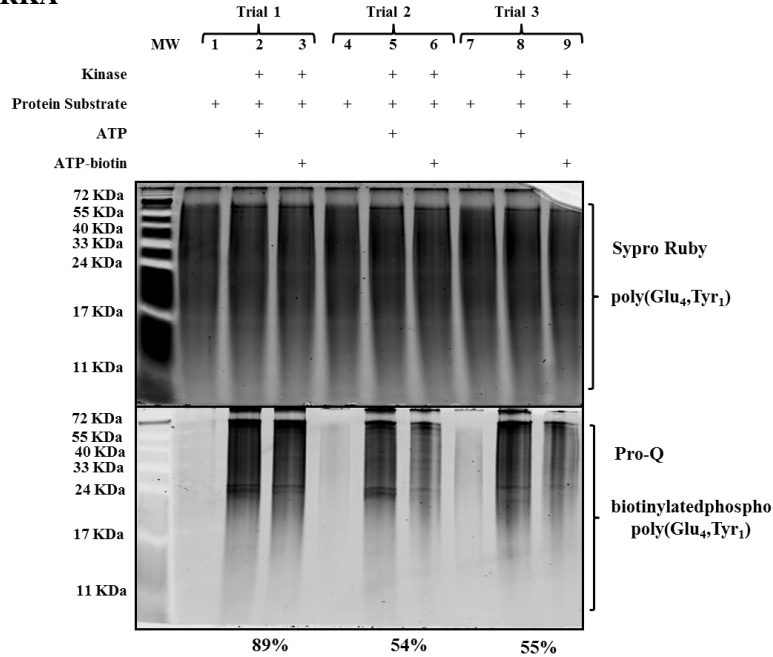
Figure A 2.22: Full gel images for protein quantification experiment with 16 different kinases. Phosphorylated proteins or biotinylated phosphoproteins were created by incubating ATP or ATP-biotin with ASK1 and MBP (A), Aurora A and MBP (B), CAMK4 and MBP (C), CHK1 and MBP (D), CDK1 and Histone H1 protein (E), CK1 and dephosphorylated Casein protein (F), DAPK1 and MBP (G), ERK1 and MBP (H), GRK5 and Casein protein (I), HIPK1 and MBP (J), JAK3 and poly (Glu$_4$, Tyr1) peptide substrate (K), MARK1 and MBP (L), MLK1 and MBP (M), MST1 and MBP (N), NEK2 and MBP (O), TGFβR2 and MBP (P), or TRKA and poly (Glu$_4$, Tyr1) (Q) peptide substrate in the manufacturer provide buffer (1X, Promega). Reaction products were treated with 50% TFA to obtain phosphoproteins for quantification. Crude reaction mixtures were separated on 16% SDS-PAGE. Proteins were visualized with Sypro Ruby Stain (top gel) and phosphoproteins with Pro-Q diamond stain (bottom gel) with reaction contents indicated above each lane. Trial 1, 2, and 3 represent three independent trials. MBP stands for Myelin Basic Protein. Quantification of ERK1 and TGFβR2 was done with only two trials as the other one was outlier. The experiment with CAMK4 was performed by Maheeka Embogama. Sypro Ruby and Pro-Q stains are independent gels load from same crude reaction mixtures.

2.6 Michaelis-Menten Kinetics Plots

(A) Reaction with Abl
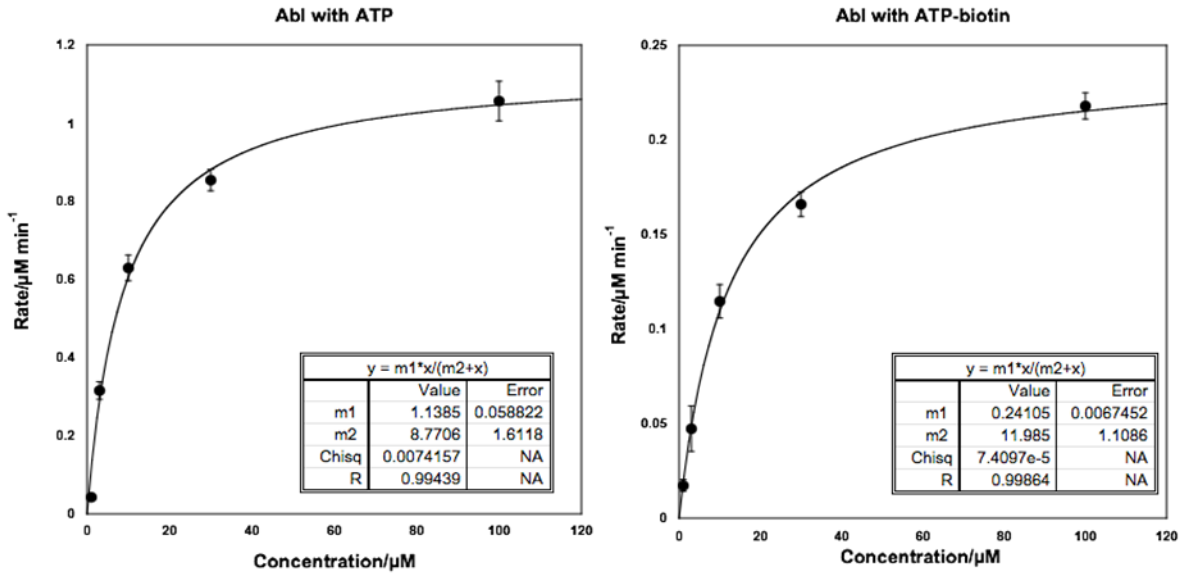
Figure A 2.23: Michaelis-Menten plots for ADP-Glo assay of ATP (left) or ATP-biotin (right) with Abl and Abl peptide (EAIYAAPFAKKK). Average of three independent trials with standard error is shown here. m1=V_{max} and m2=K_M.

(B) Reaction with AKT1
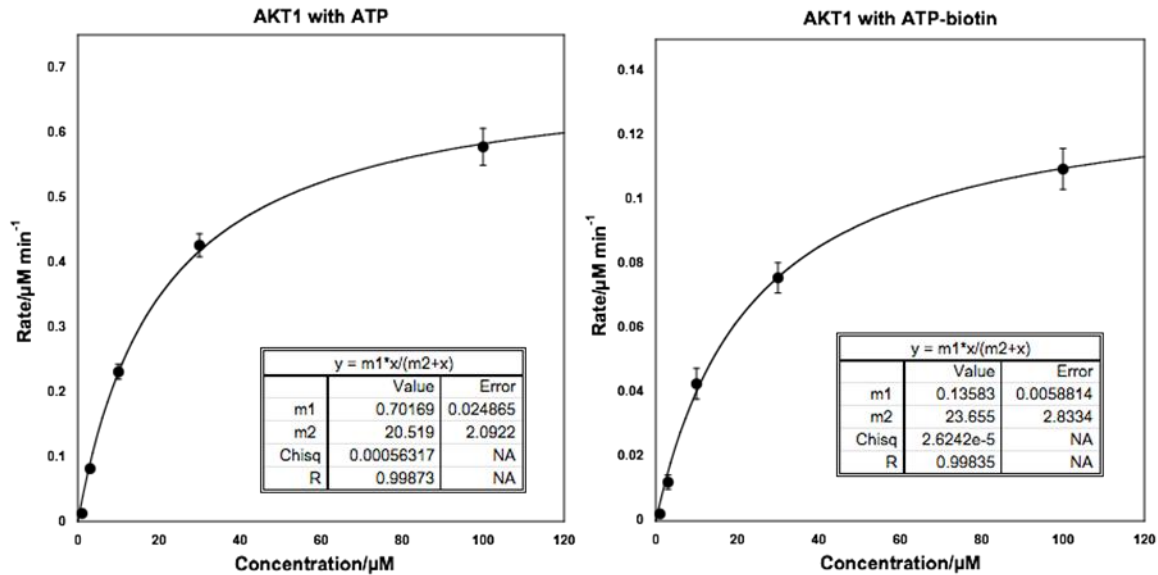
Figure A 2.24: Michaelis-Menten plots for ADP-Glo assay of ATP (left) or ATP-biotin (right) with AKT1 and AKT (PKB) peptide substrate (CKRPRAASFAE). Average of three independent trials with standard error is shown here. m1=V_{max} and m2=K_M.

(C) Reaction with ASK1
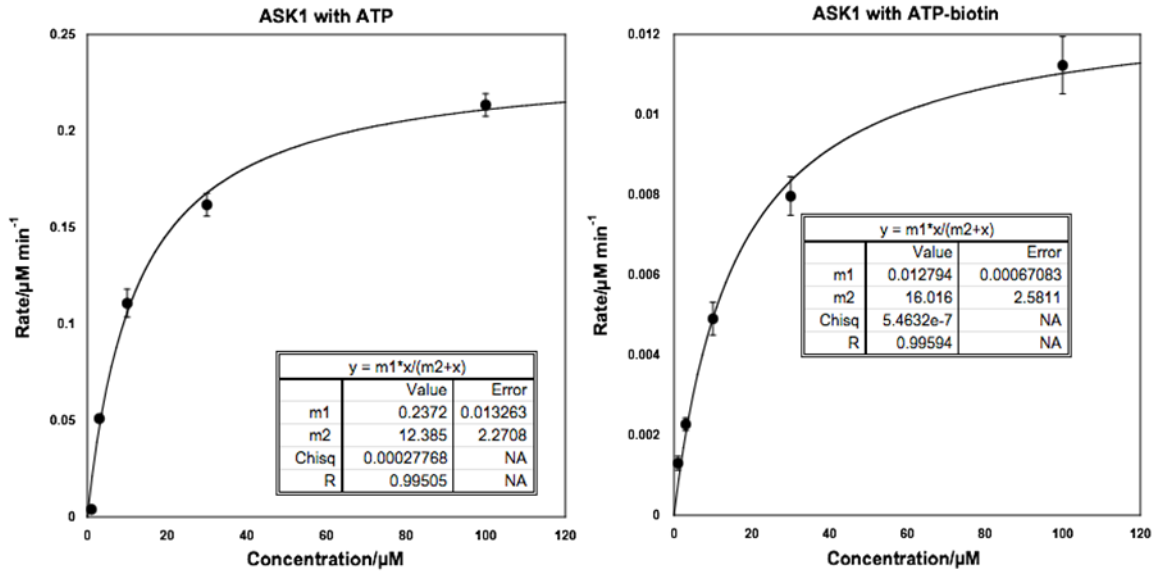
Figure A 2.25: Michaelis-Menten plots for ADP-Glo assay of ATP (left) or ATP-biotin (right) with ASK1 and MBP. Average of three independent trials with standard error is shown here. m1=V_{max} and m2=K_M.

(D) Reaction with Aurora A
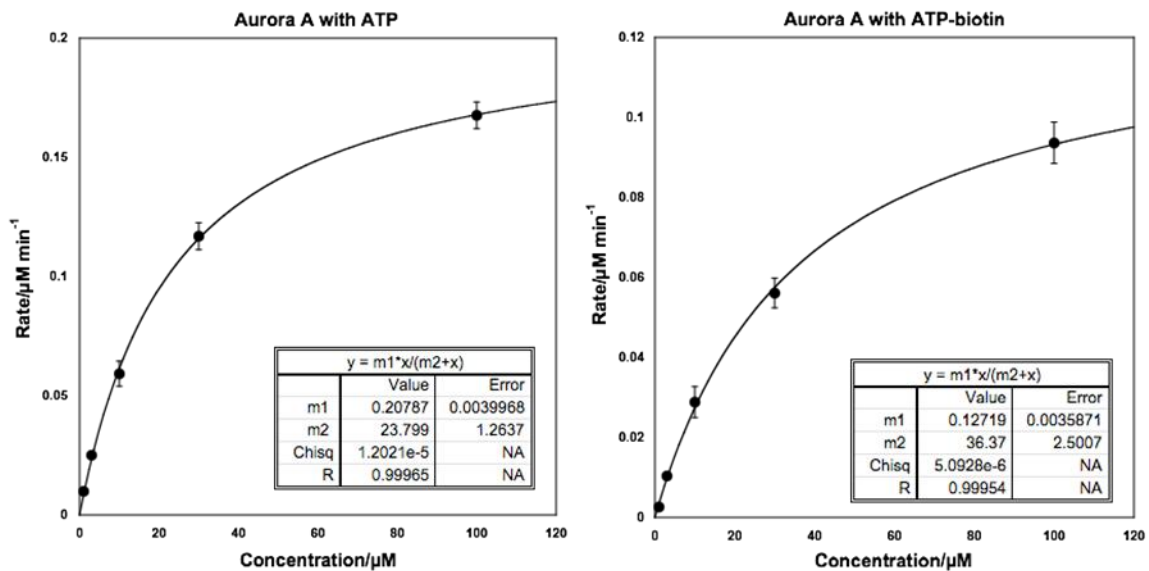
Figure A 2.26: Michaelis-Menten plots for ADP-Glo assay of ATP (left) or ATP-biotin (right) with Aurora A and MBP. Average of three independent trials with standard error is shown here. m1=V_{max} and m2=K_M.

(E) Reaction with CAMK4
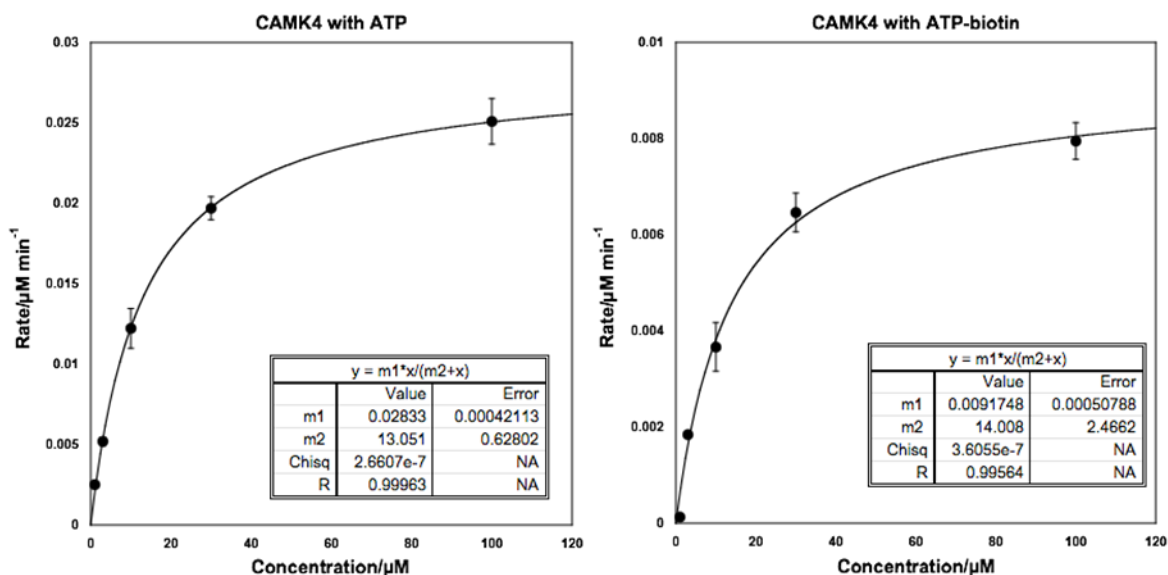
Figure A 2.27: Michaelis-Menten plots for ADP-Glo assay of ATP (left) or ATP-biotin (right) with CAMK4 and Autocamtide (KKALRRQETVDAL-amide). Average of three independent trials with standard error is shown here. m1=V_{max} and m2=K_M.

(F) Reaction with CDK1
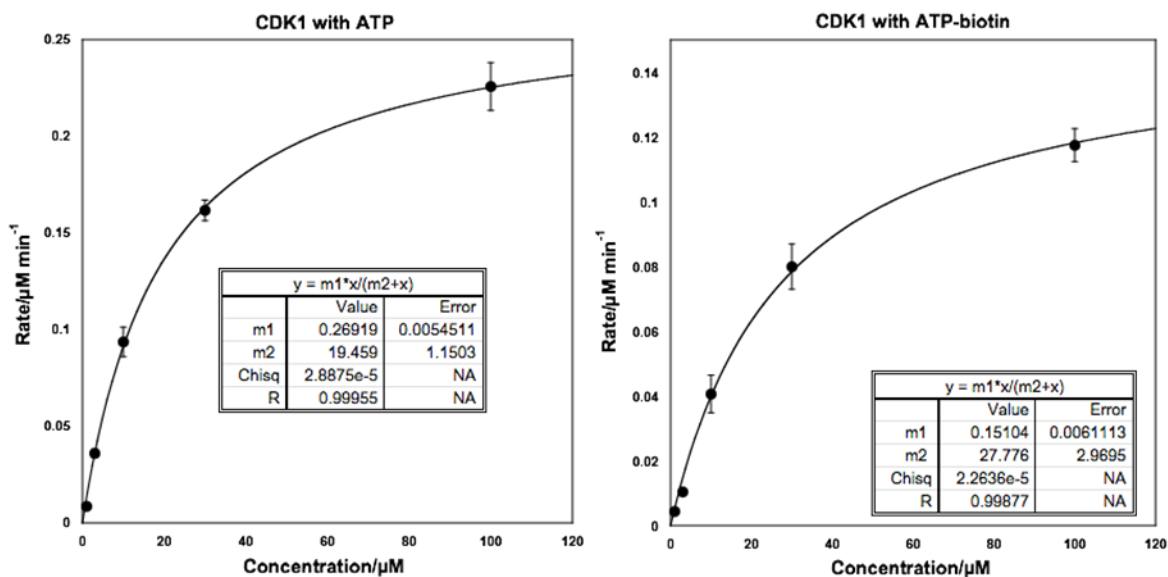
Figure A 2.28: Michaelis-Menten plots for ADP-Glo assay of ATP (left) or ATP-biotin (right) with CDK1 and Histone H1 protein. Average of three independent trials with standard error is shown here. m1=V_{max} and m2=K_M.

(G) Reaction with CHK1
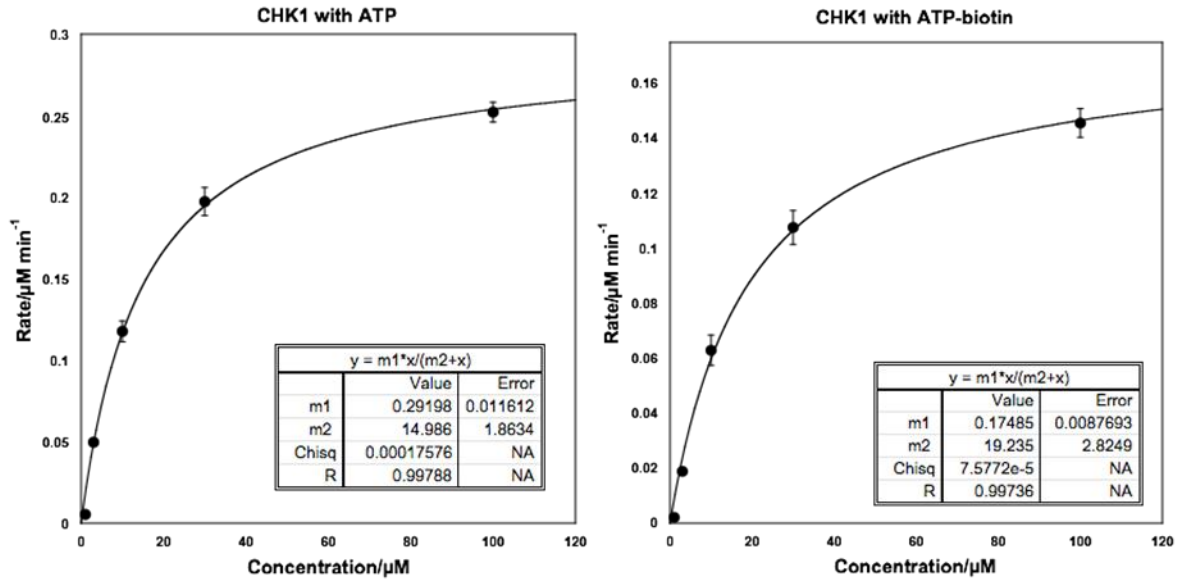
Figure A 2.29: Michaelis-Menten plots for ADP-Glo assay of ATP (left) or ATP-biotin (right) with CHK1 and CHKtide (KKKVSRSGLYRSPSMPENLNRPR). Average of three independent trials with standard error is shown here. m1=V_{max} and m2=K_M.

(H) Reaction with CK1
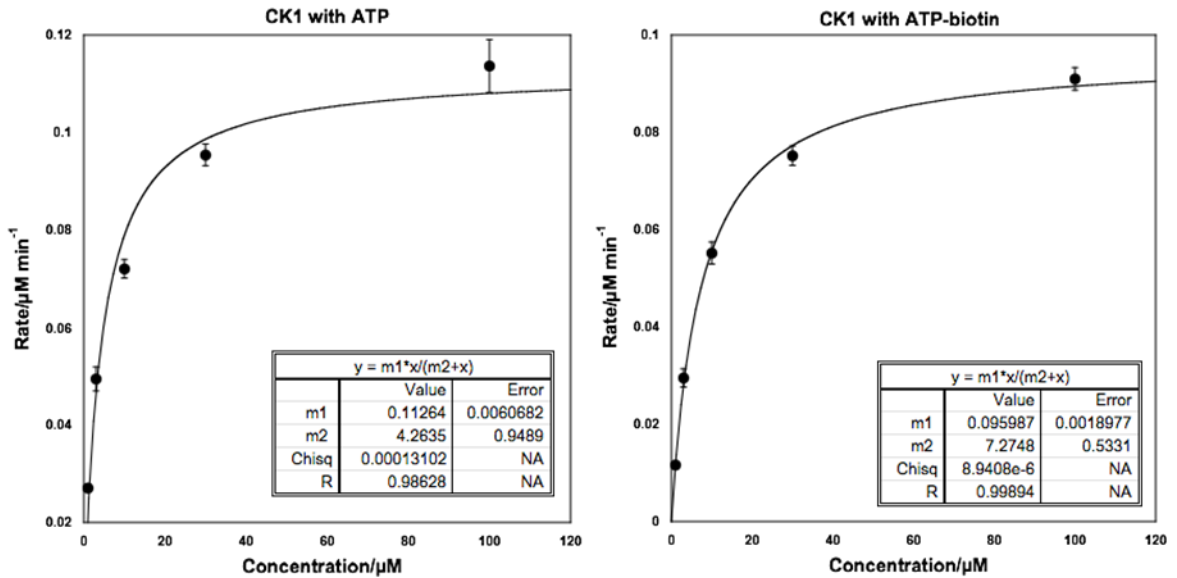
Figure A 2.30: Michaelis-Menten plots for ADP-Glo assay of ATP (left) or ATP-biotin (right) with CK1 and dephosphorylated Casein protein. Average of three independent trials with standard error is shown here. m1=V_{max} and m2=K_M.

(I) Reaction with CK2
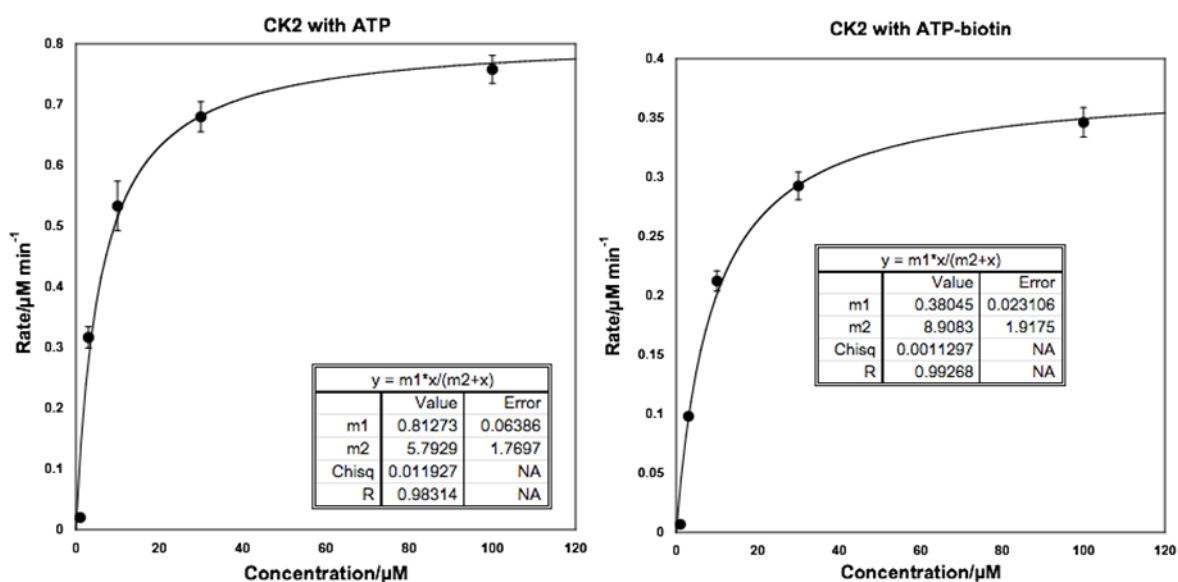
Figure A 2.31: Michaelis-Menten plots for ADP-Glo assay of ATP (left) or ATP-biotin (right) with CK2 and CK2 peptide (RRREEETEEE). Average of three independent trials with standard error is shown here. m1=V_{max} and m2=K_M.

(J) Reaction with DAPK1
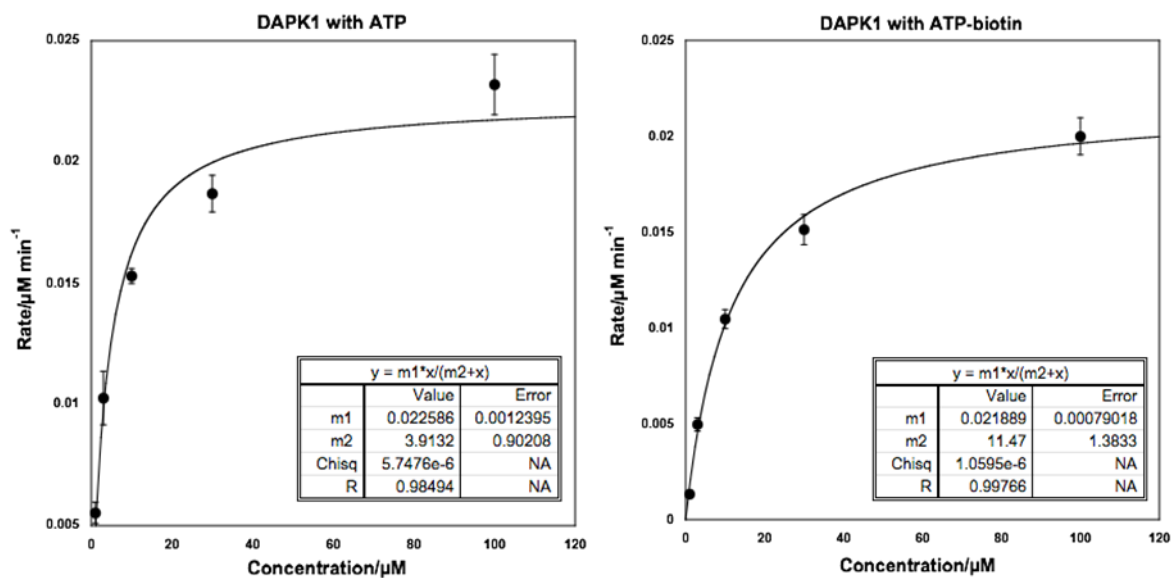
Figure A 2.32: Michaelis-Menten plots for ADP-Glo assay of ATP (left) or ATP-biotin (right) with DAPK1 and MBP. Average of three independent trials with standard error is shown here. m1=V_{max} and m2=K_M.

(K) Reaction with ERK1
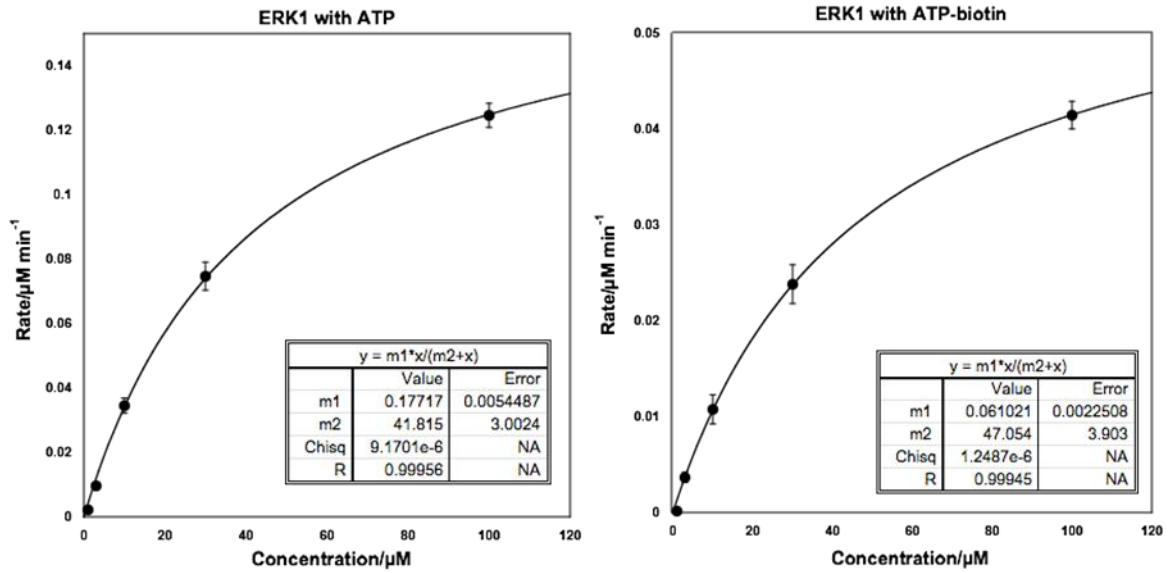
Figure A 2.33: Michaelis-Menten plots for ADP-Glo assay of ATP (left) or ATP-biotin (right) with ERK1 and MBP. Average of three independent trials with standard error is shown here. m1=V_{max} and m2=K_M.

(L) Reaction with FLT1
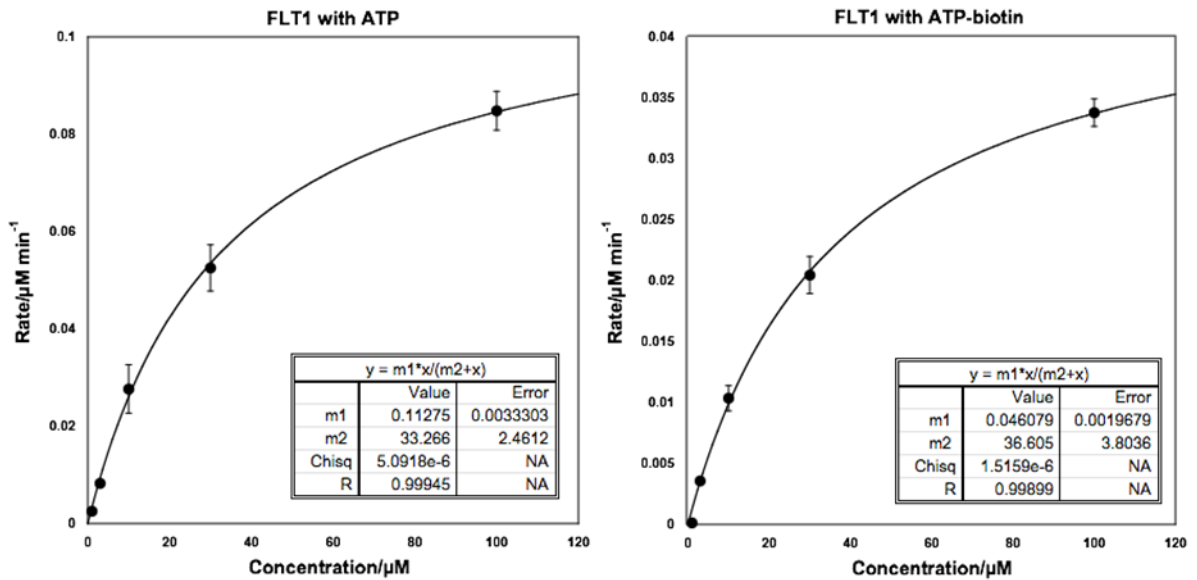
Figure A 2.34: Michaelis-Menten plots for ADP-Glo assay of ATP (left) or ATP-biotin (right) with FLT1 and IGF1Rtide (KKKSPGEYVNIEFG). Average of three independent trials with standard error is shown here. m1=V_{max} and m2=K_M.

(M) Reaction with GRK5

GRK5 with ATP

y = m1*x/(m2+x)		
	Value	Error
m1	0.010578	0.00053104
m2	9.2354	1.6298
Chisq	5.7909e-7	NA
R	0.99387	NA

GRK5 with ATP-biotin

y = m1*x/(m2+x)		
	Value	Error
m1	0.0043763	0.00012979
m2	9.1391	0.95506
Chisq	3.4894e-8	NA
R	0.99794	NA
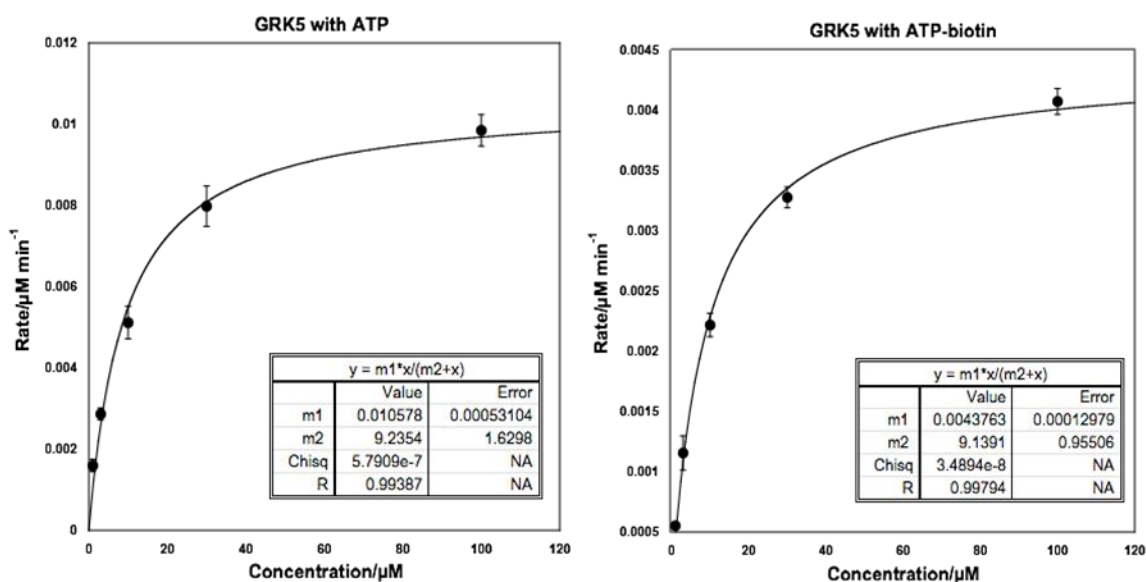
Figure A 2.35: Michaelis-Menten plots for ADP-Glo assay of ATP (left) or ATP-biotin (right) with GRK5 and Casein protein. Average of three independent trials with standard error is shown here. m1=V_{max} and m2=K_M.

(N) Reaction with GSK3β

GSK3 with ATP

y = m1*x/(m2+x)		
	Value	Error
m1	0.10822	0.003309
m2	4.6608	0.57866
Chisq	3.6904e-5	NA
R	0.99617	NA

GSK3 with ATP-biotin

y = m1*x/(m2+x)		
	Value	Error
m1	0.001973	9.3619e-5
m2	11.395	1.8092
Chisq	1.4963e-8	NA
R	0.99581	NA
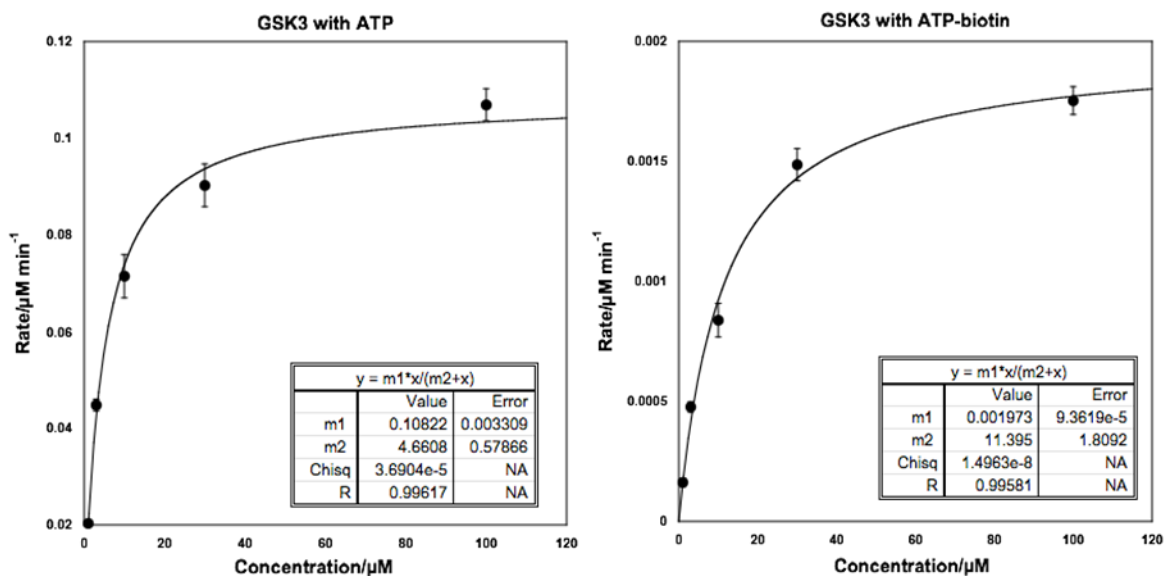
Figure A 2.36: Michaelis-Menten plots for ADP-Glo assay of ATP (left) or ATP-biotin (right) with GSK3β and GSK3 substrate (YRRAAVPPSPSLSRHSSPHQ(pS)EDEEE). Average of three independent trials with standard error is shown here. m1=V_{max} and m2=K_M.

(O) Reaction with HIPK1
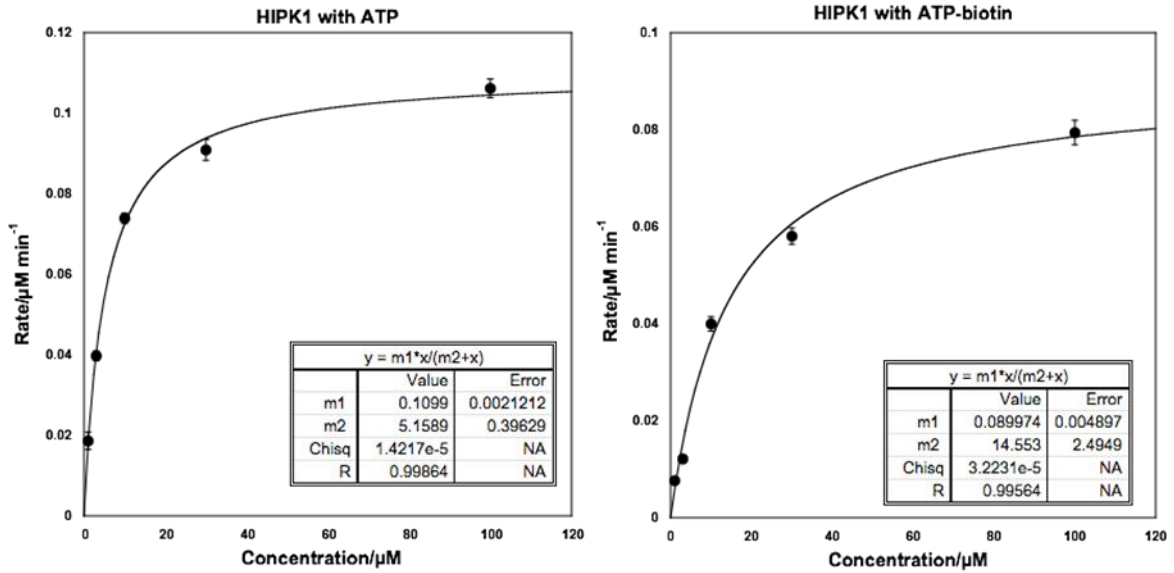
Figure A 2.37: Michaelis-Menten plots for ADP-Glo assay of ATP (left) or ATP-biotin (right) with HIPK1 and MBP. Average of three independent trials with standard error is shown here. m1=V_{max} and m2=K_M.

(P) Reaction with JAK3
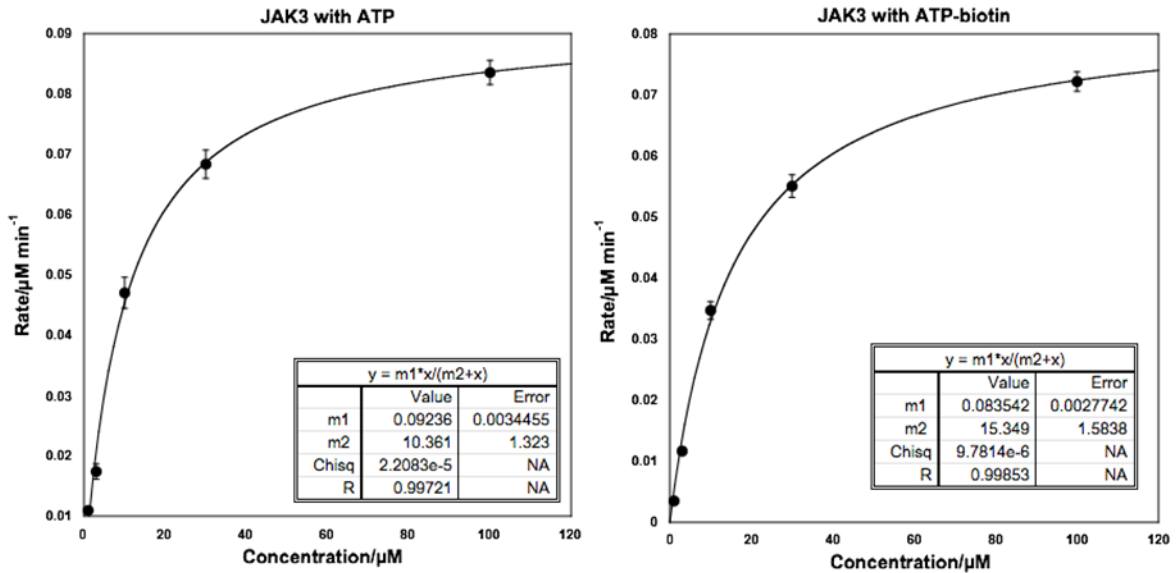
Figure A 2.38: Michaelis-Menten plots for ADP-Glo assay of ATP (left) or ATP-biotin (right) with JAK3 and poly (Glu$_4$, Tyr$_1$) peptide substrate. Average of three independent trials with standard error is shown here. m1=V_{max} and m2=K_M.

(Q) Reaction with MARK1
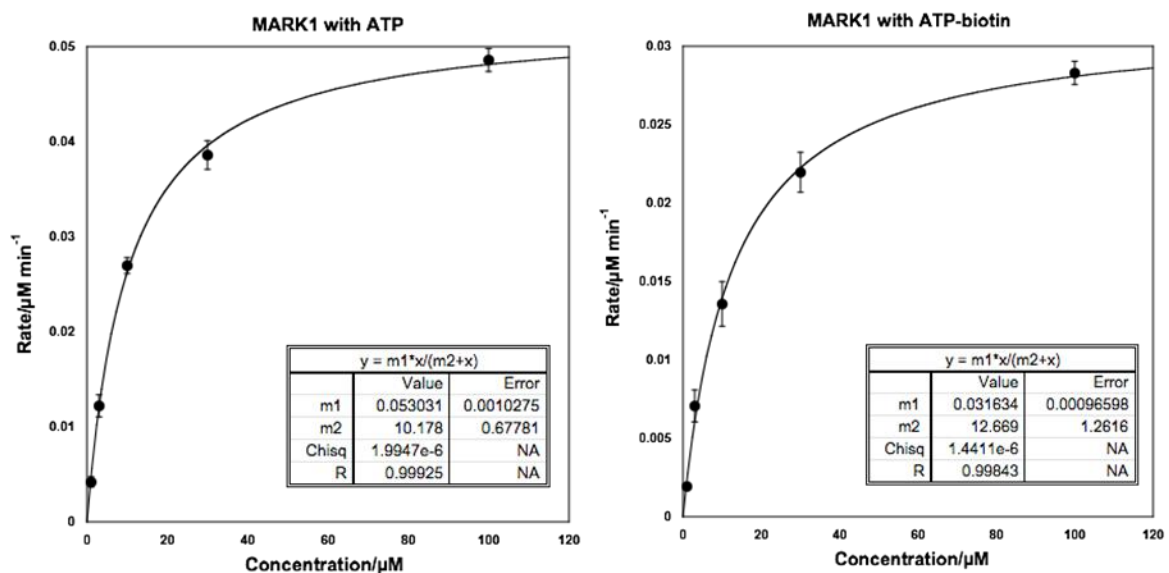
Figure A 2.39: Michaelis-Menten plots for ADP-Glo assay of ATP (left) or ATP-biotin (right) with MARK1 and CHKtide (KKKVSRSGLYRSPSMPENLNRPR). Average of three independent trials with standard error is shown here. m1=V_{max} and m2=K_M.

(R) Reaction with MLK1
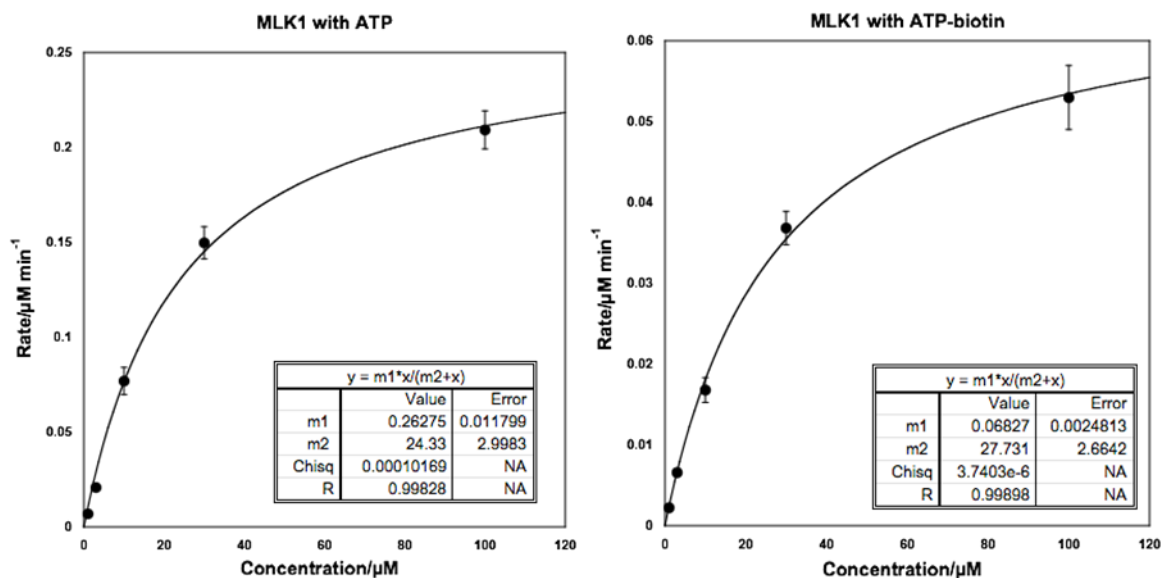
Figure A 2.40: Michaelis-Menten plots for ADP-Glo assay of ATP (left) or ATP-biotin (right) with MLK1 and MBP. Average of three independent trials with standard error is shown here. m1=V_{max} and m2=K_M.

(S) Reaction with MST1
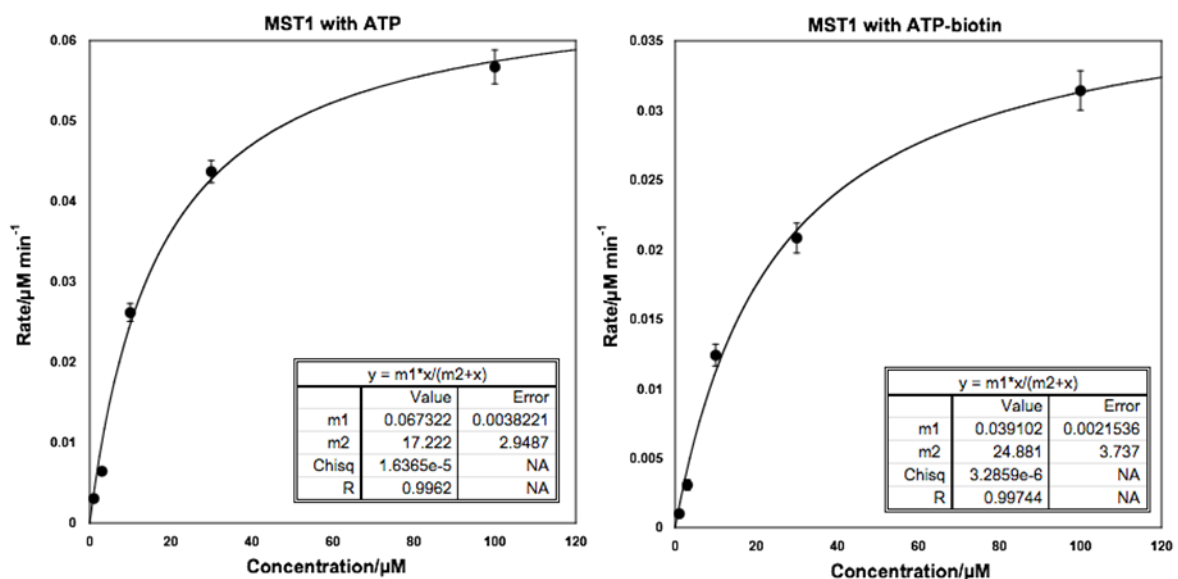
Figure A 2.41: Michaelis-Menten plots for ADP-Glo assay of ATP (left) or ATP-biotin (right) with MST1 and Axltide (KKSRGDYMTMQIG). Average of three independent trials with standard error is shown here. m1=V_{max} and m2=K_M.

(T) Reaction with NEK2
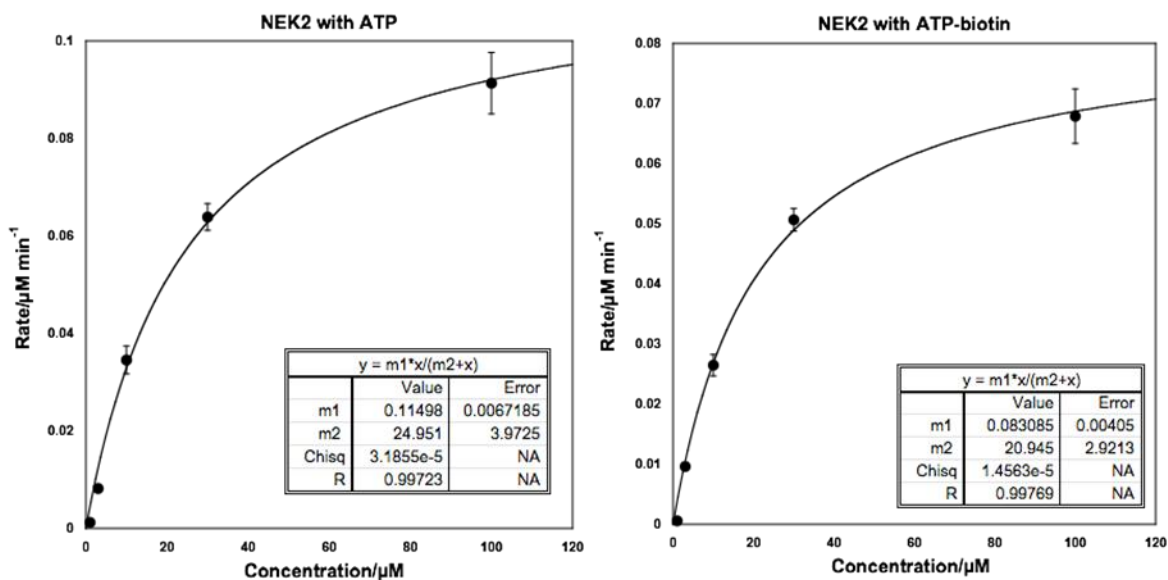
Figure A 2.42: Michaelis-Menten plots for ADP-Glo assay of ATP (left) or ATP-biotin (right) with NEK2 and MBP. Average of three independent trials with standard error is shown here. m1=V_{max} and m2=K_M.

(U) Reaction with PAK1
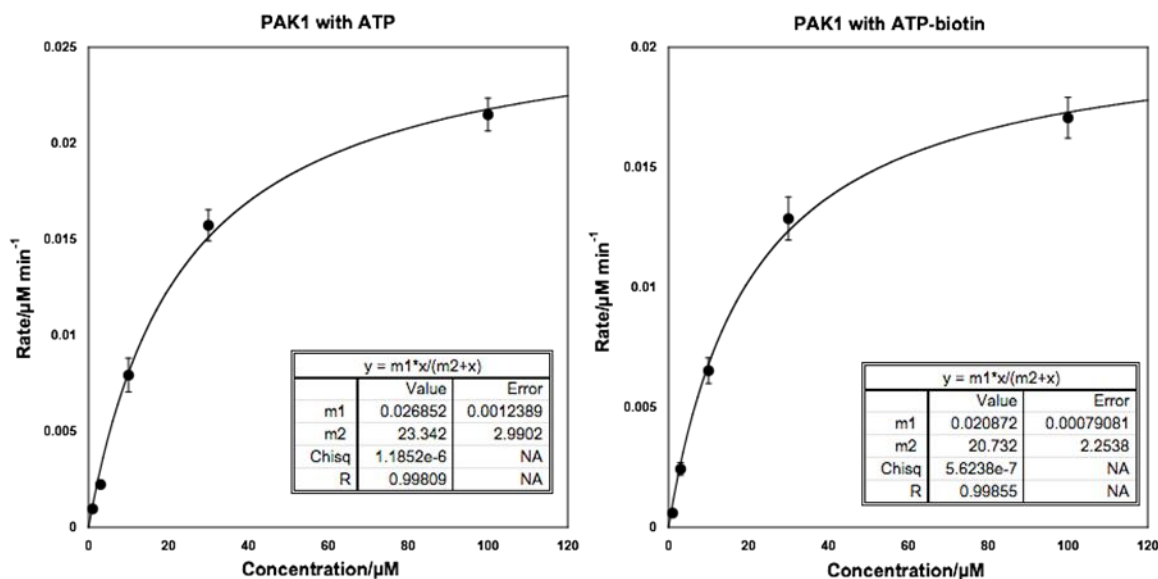
Figure A 2.43: Michaelis-Menten plots for ADP-Glo assay of ATP (left) or ATP-biotin (right) with PAK1 and PAKtide (RRRLSFAEPG). Average of three independent trials with standard error is shown here. m1=V_{max} and m2=K_M.

(V) Reaction with PKA
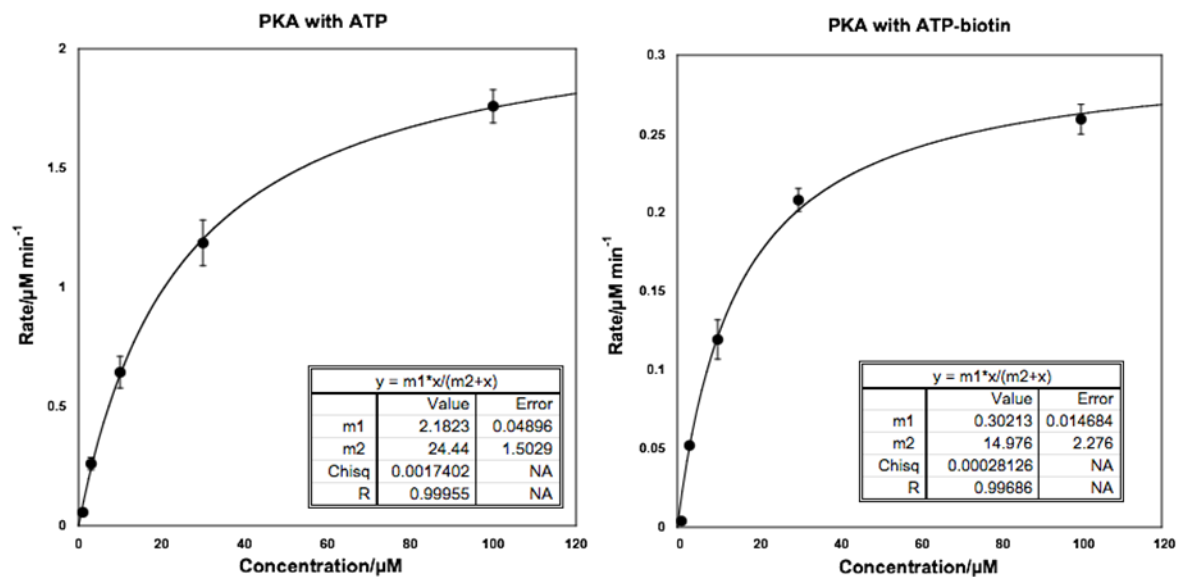
Figure A 2.44: Michaelis-Menten plots for ADP-Glo assay of ATP (left) or ATP-biotin (right) with PKA and kemptide (LRRASLG). Average of three independent trials with standard error is shown here. m1=V_{max} and m2=K_M.

(W) Reaction with RSK1
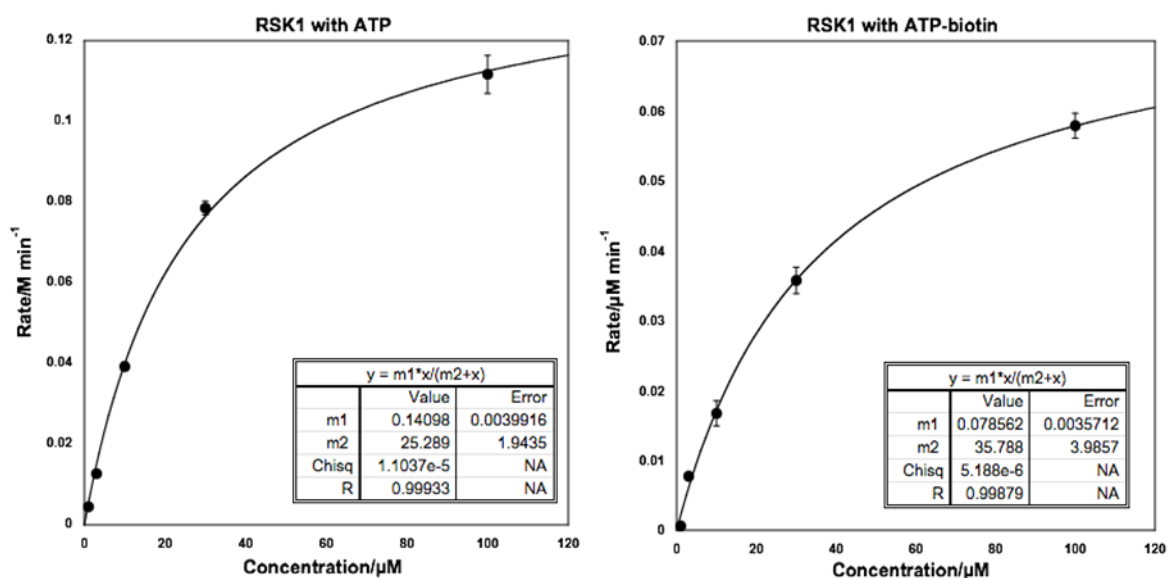
Figure A 2.45: Michaelis-Menten plots for ADP-Glo assay of ATP (left) or ATP-biotin (right) with RSK1 and S6K substrate (KRRRLASLR). Average of three independent trials with standard error is shown here. m1=V_{max} and m2=K_M.

(X) Reaction with SRC
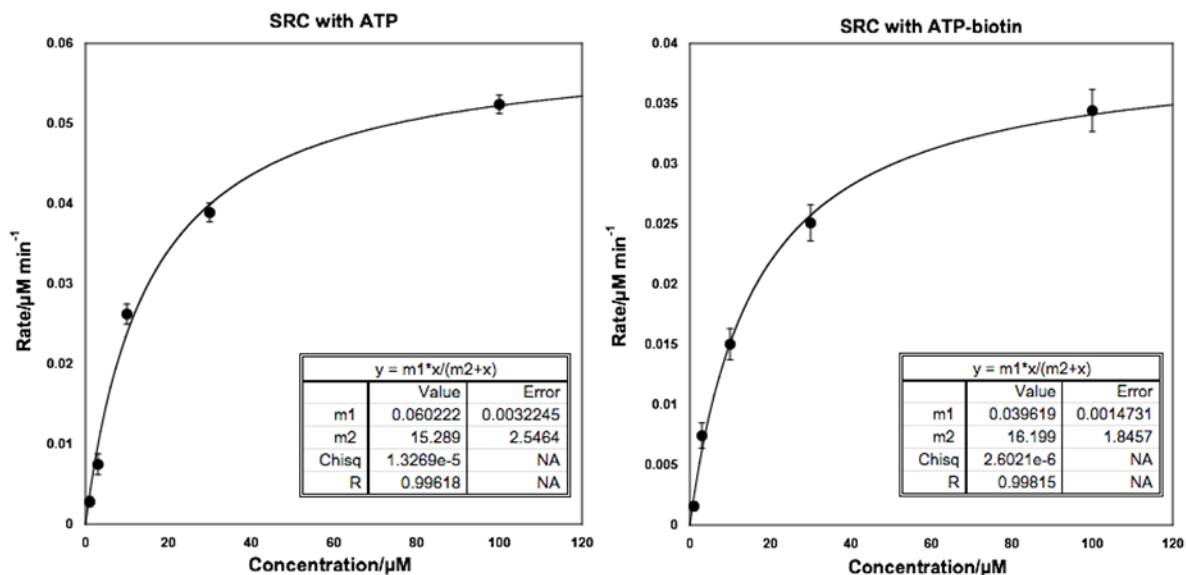
Figure A 2.46: Michaelis-Menten plots for ADP-Glo assay of ATP (left) or ATP-biotin (right) with SRC and SRC substrate (KVEKIGEGTYGVVYK-amide). Average of three independent trials with standard error is shown here. m1=V_{max} and m2=K_M.

(Y) Reaction with TGFβR2
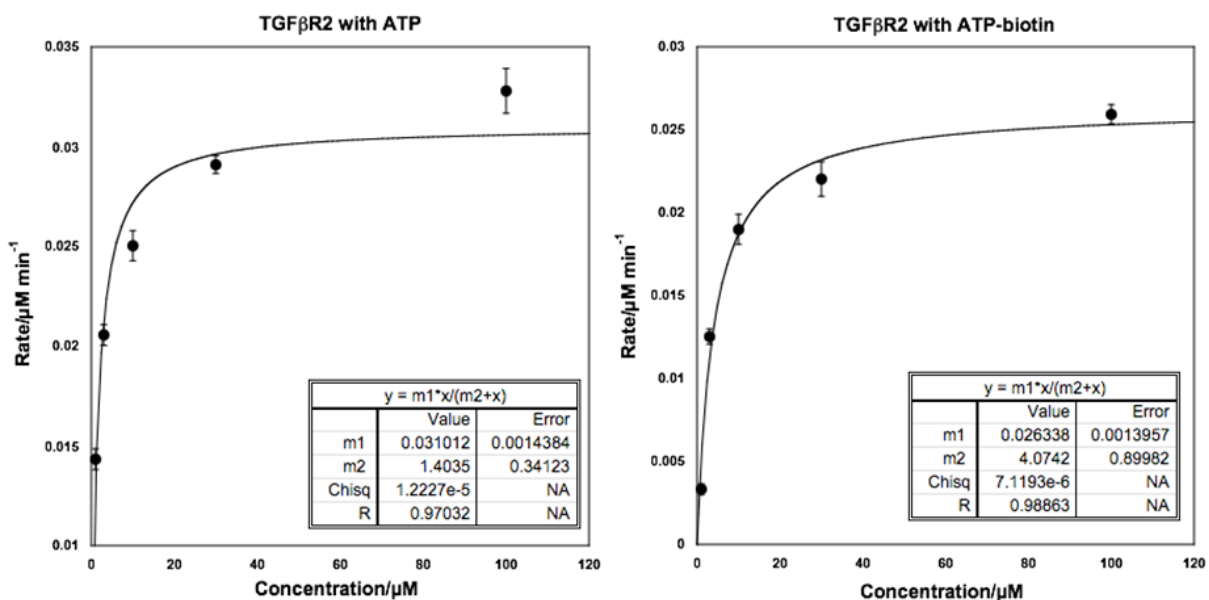
Figure A 2.47: Michaelis-Menten plots for ADP-Glo assay of ATP (left) or ATP-biotin (right) with TGFβR2 and MBP. Average of three independent trials with standard error is shown here. m1=V_{max} and m2=K_M.

(Z) Reaction with TRKA
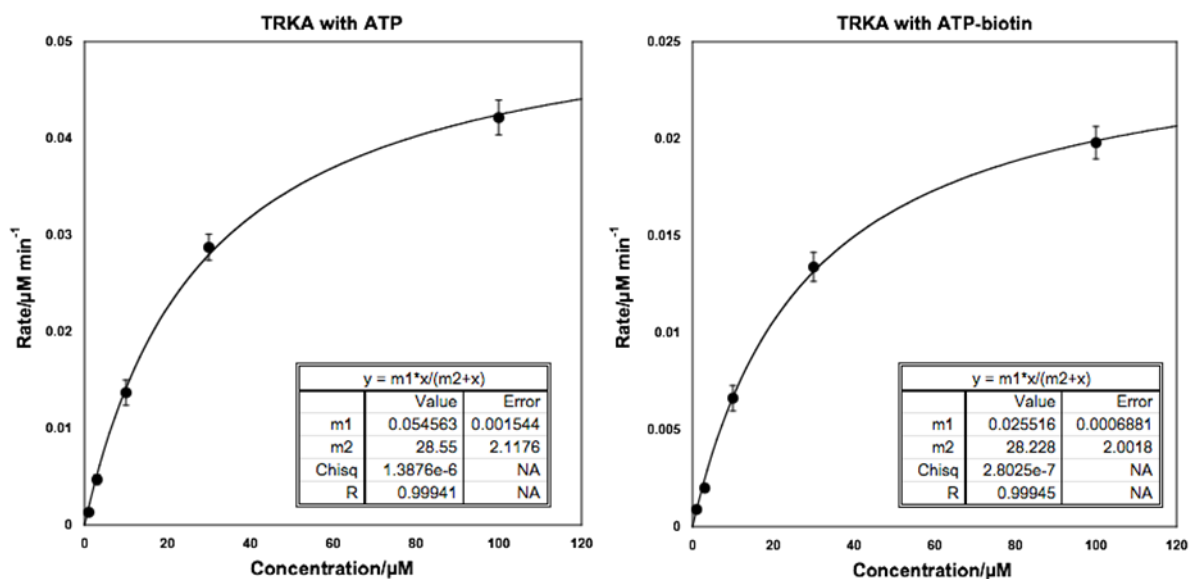
Figure A 2.48: Michaelis-Menten plots for ADP-Glo assay of ATP (left) or ATP-biotin (right) with TRKA and poly (Glu$_4$, Tyr$_1$) peptide substrate. Average of three independent trials with standard error is shown here. m1=V_{max} and m2=K_M.

2.7 Supporting HPLC Traces for Biotinylation
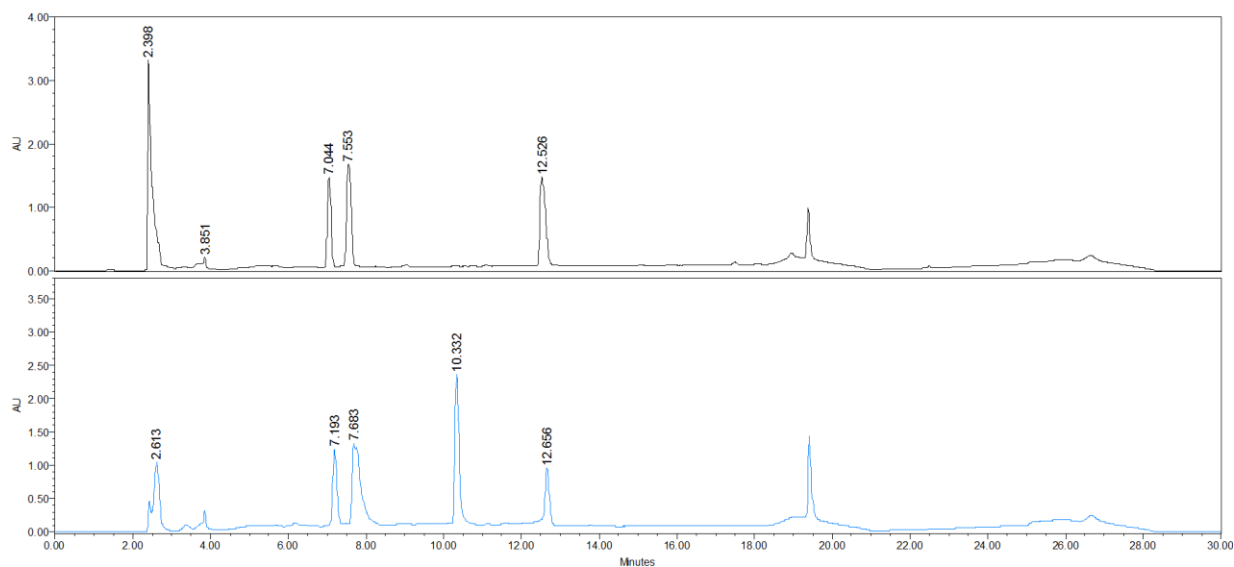
Figure A 2.49: HPLC traces for the CK2 peptides after biotinylation. Reactions were performed using CK2 enzyme and the CK2 peptide substrate (RRREEETEEE) and subjected to HPLC analysis with (top spectra) or without (bottom spectra) heat deactivation and pre-equlibration with buffer. Without these treatments, ATP-biotin remained intact (t_R=10.3), where the biotin-amine linker (t_R=12.6) attached to phosphate on peptide was removed. The peptide appears at 7.6 min, while the phosphopeptide appears at 7.1 min.

2.8 Mechanism for Biotin-amine Cleavage
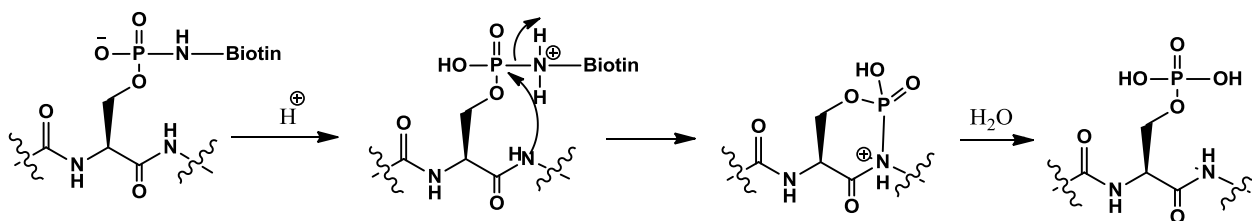
Figure A 2.50: Release of biotin-amine linker attached to phosphate on peptides during pre-equilibration and HPLC analysis at low pH and high pressure. The cleavage is facilitate by neighboring group participating.

2.9 ADP-Glo Assay Controls-HPLC Data
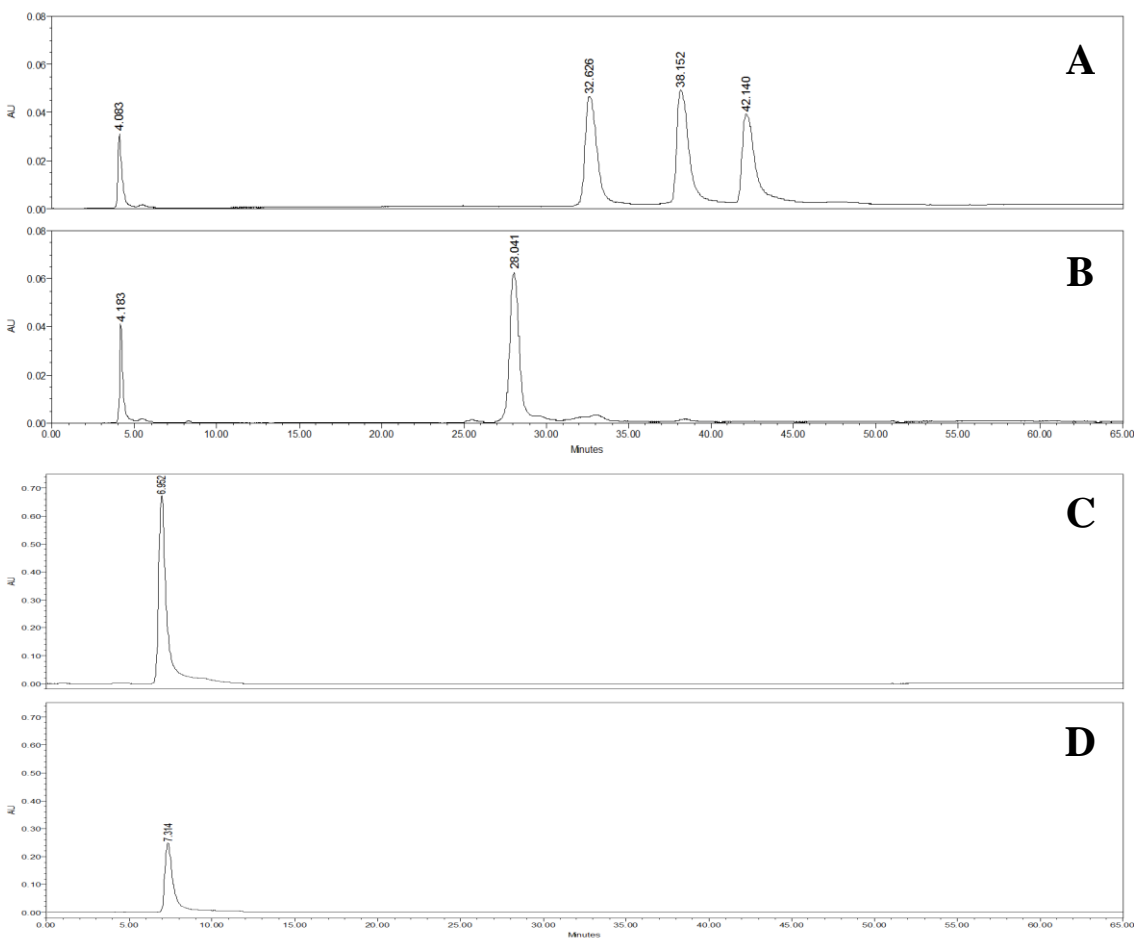
Figure A 2.51: HPLC traces for the ATP (A, t_R=42.1 min) ADP (A, t_R=38.2 min), AMP (A, t_R=32.6 min), ATP-biotin (B, t_R=28.0 min), adenine (C, t_R=6.9 min), and adenosine (D, t_R=7.1 min).

2.10 ADP-Glo Assay Controls-Time dependent Luminescence Data
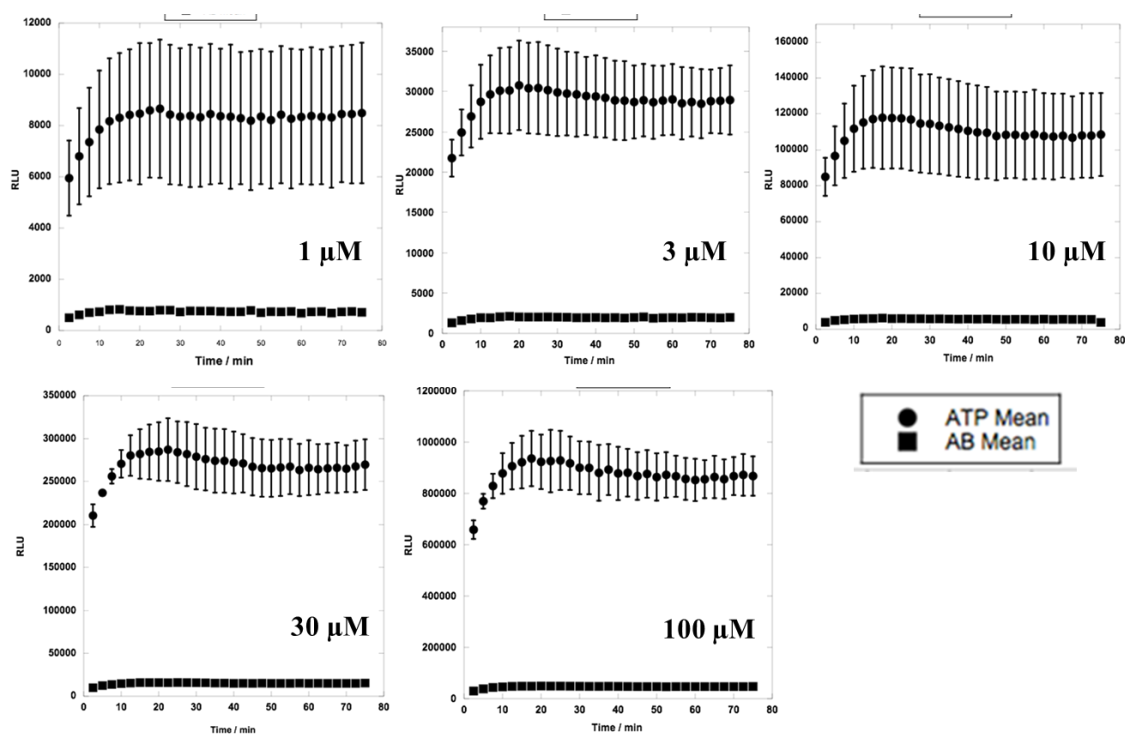
Figure A 2.52: ATP (●) or ATP-biotin (■) incubated with kinase detection reagent and luminescence signal was measure every 2.5 min with five different concentration (1 µM, 3 µM, 10 µM, 30 µM, and 100 µM). Mean of the three independent trials is shown with standard errors.

APPENDIX B

3.1 Complete HPLC Traces
(A) Reaction with PKA and PP1
HPLC trace for reactions performed using PKA and PP1 (Trial 1).
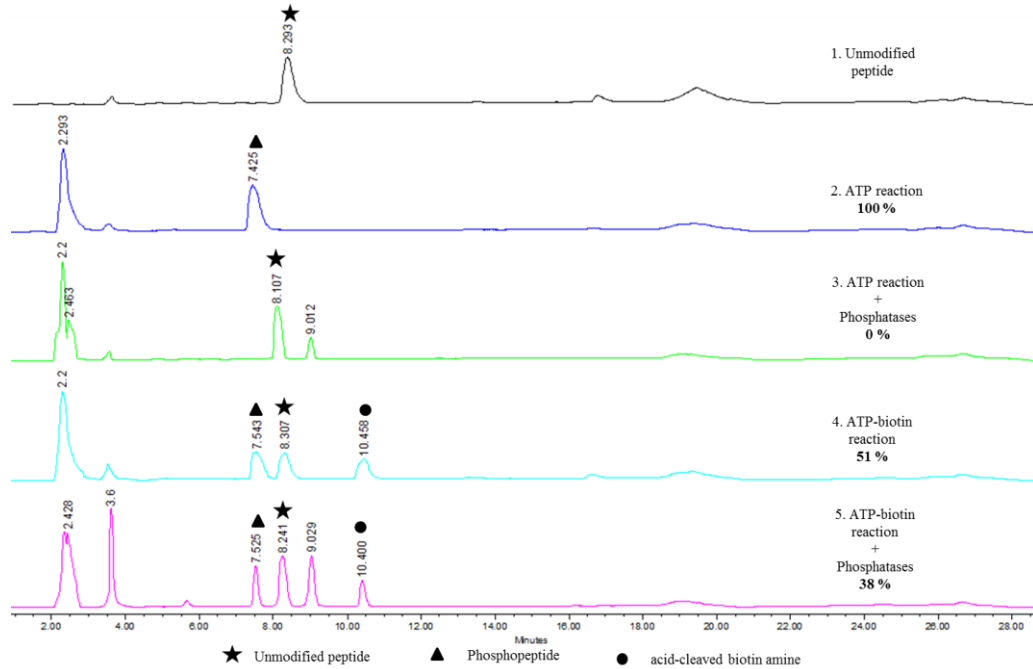
HPLC trace for reactions performed using PKA and PP1 (Trial 2).
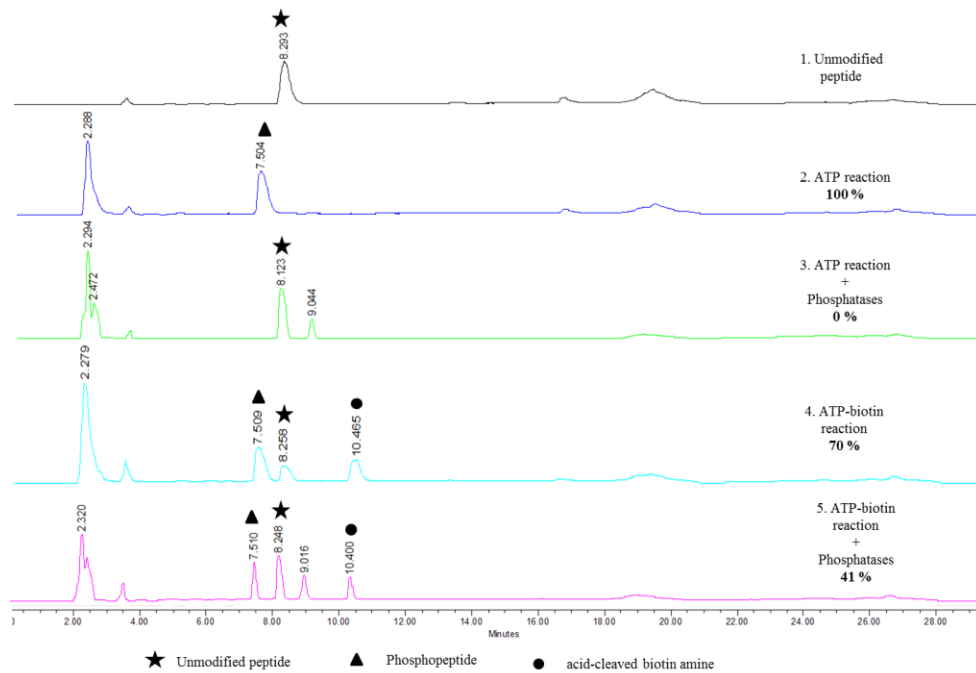
HPLC trace for reactions performed using PKA and PP1 (Trial 3).
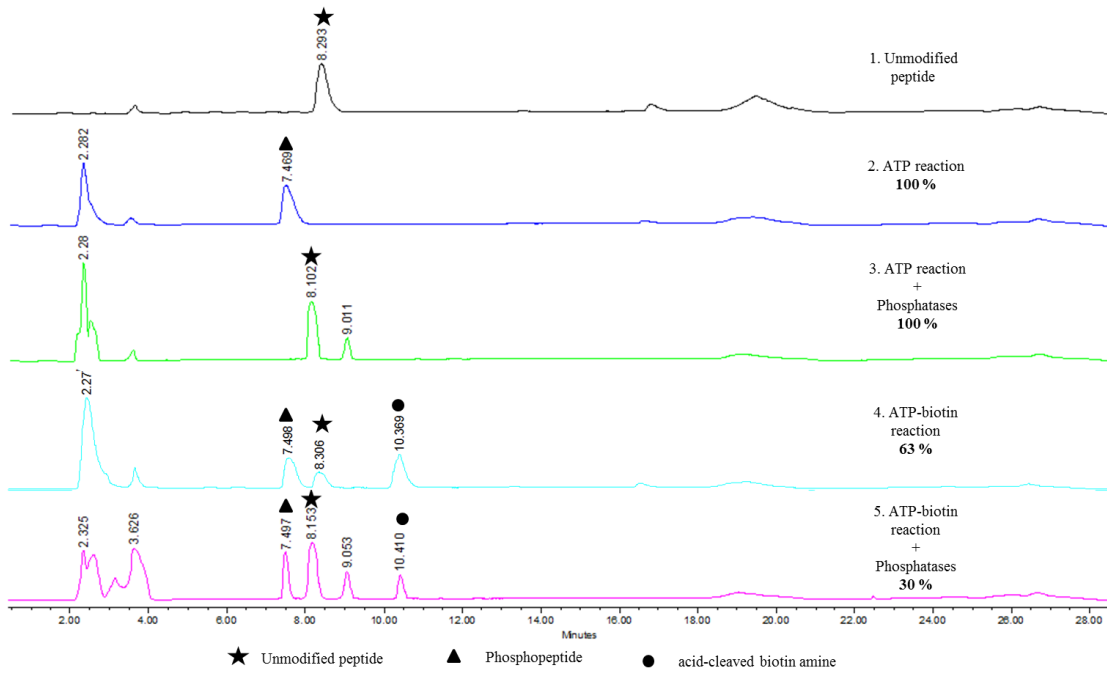
Figure A 3.1: HPLC traces for the peptides (panel 1) after phosphorylation (panel 2), phosphorylation followed by phosphatase treatment (panel 3), biotinylation (panel 4) or biotinylation followed by phosphatase treatment (panel 5). Reactions were performed using PKA, the PKA substrate peptide (LRRASLG), and PP1. All the three independent trials are shown here with the percentage of phosphopeptide in the reaction.

(B) Reaction with CK2 and CIP

HPLC trace for reactions performed using CK2 and CIP (Trial 1).
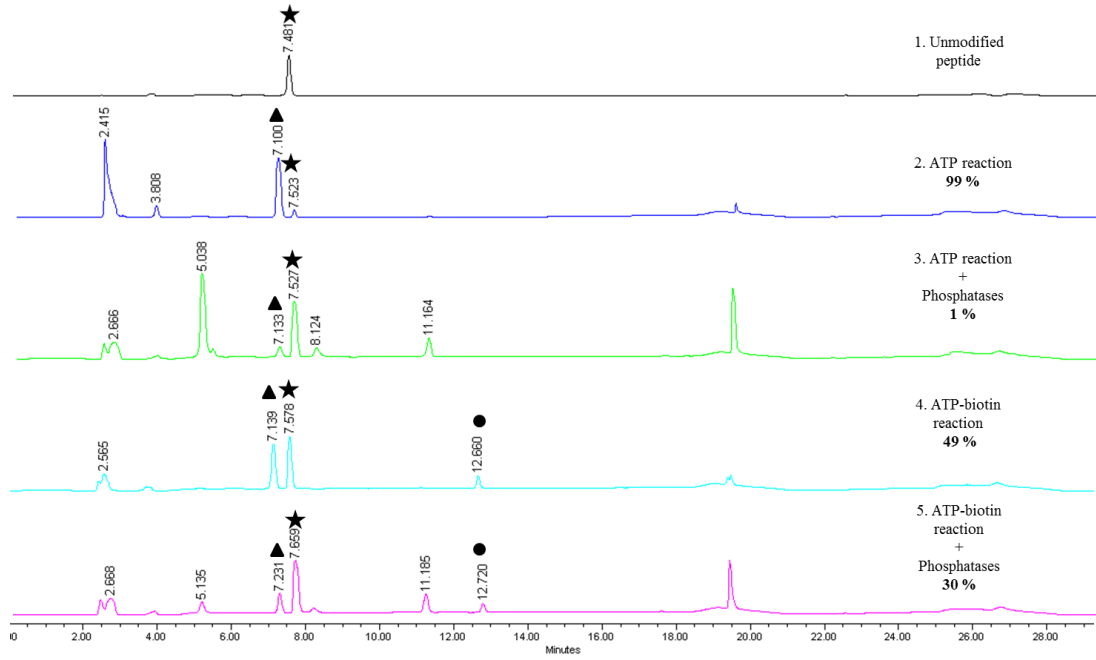
HPLC trace for reactions performed using CK2 and CIP (Trial 2).
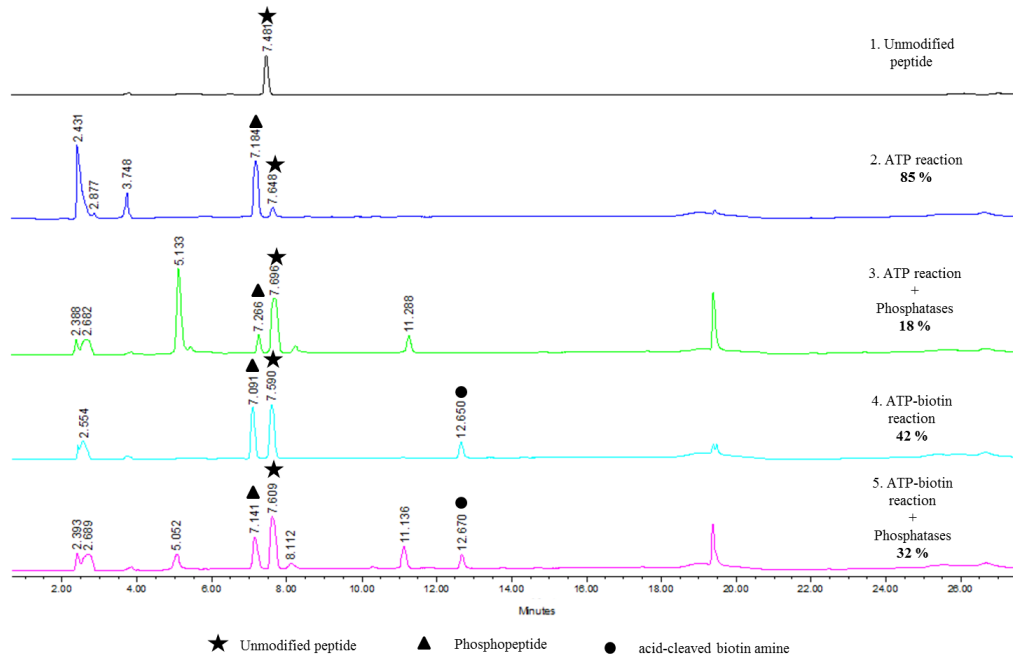
HPLC trace for reactions performed using CK2 and CIP (Trial 3).
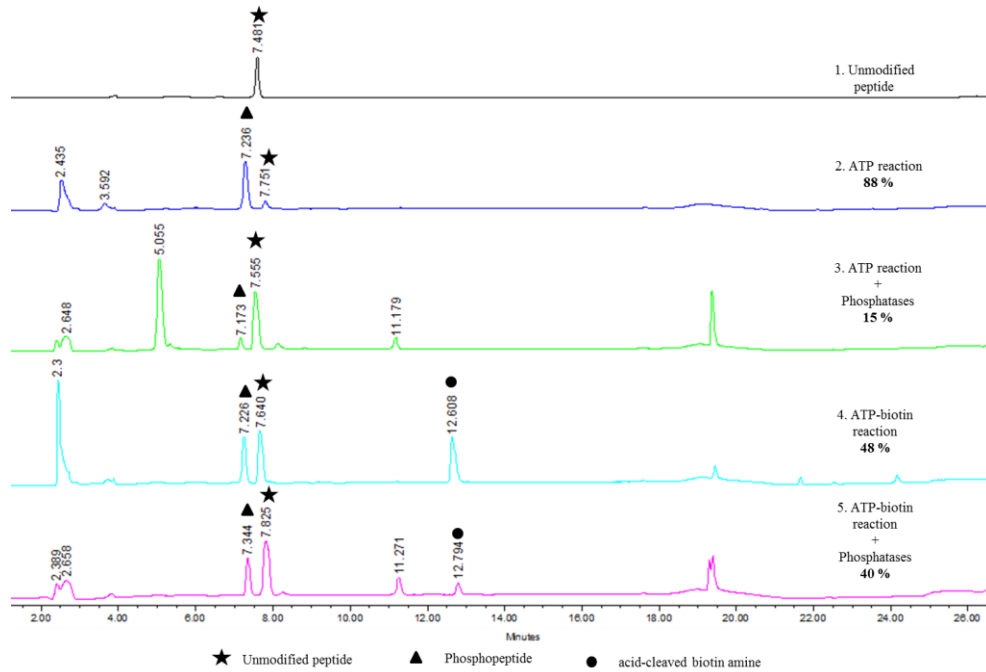
Figure A 3.2: HPLC traces for the peptides (panel 1) after phosphorylation (panel 2), phosphorylation followed by phosphatase treatment (panel 3), biotinylation (panel 4) or biotinylation followed by phosphatase treatment (panel 5). Reactions were performed using CK2, the CK2 peptide (RRREEETEEE), and CIP. A, B, and C are the three independent trials with the percentage of phosphopeptide in the reaction.

(C) Reaction with Abl and TCPTP

HPLC trace for reactions performed using Abl and TCPTP (Trial 1).
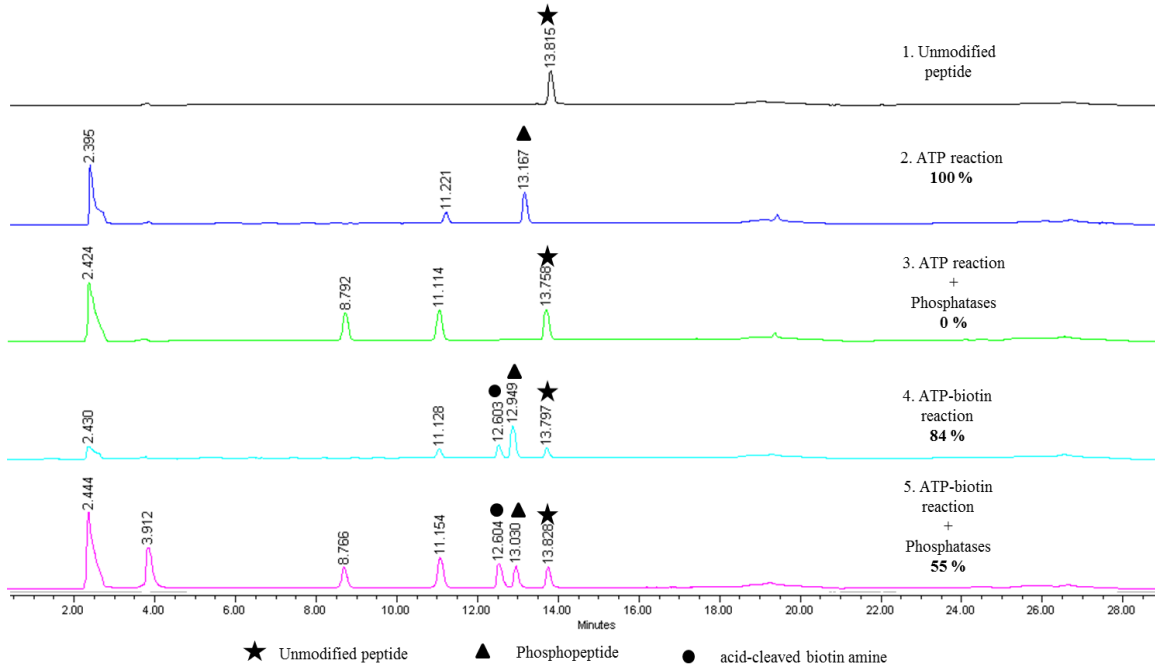
HPLC trace for reactions performed using Abl and TCPTP (Trial 2).
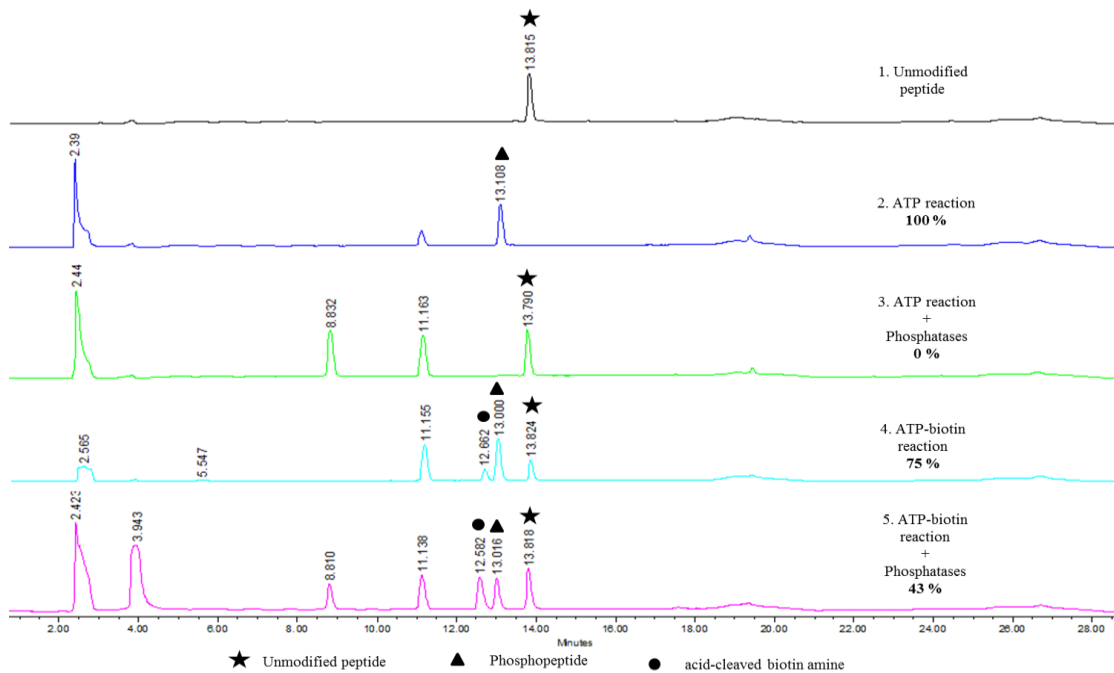
HPLC trace for reactions performed using Abl and TCPTP (Trial 3).
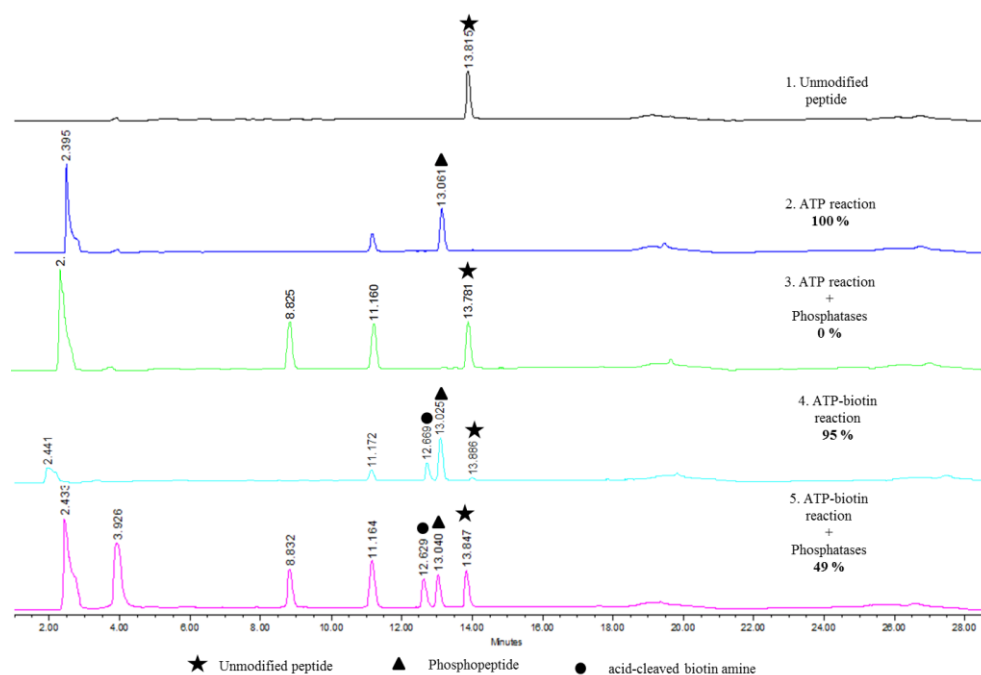
Figure A 3.3: HPLC traces for the peptides (panel 1) after phosphorylation (panel 2), phosphorylation followed by phosphatase treatment (panel 3), biotinylation (panel 4) or biotinylation followed by phosphatase treatment (panel 5). Reactions were performed using Abl, the Abl substrate peptide (EAIYAAPFAKKK), and TC PTP. A, B, and C are the three independent trials with the percentage of phosphopeptide in the reaction.

3.2 Complete Gel Images

(A) Reaction with PKA and PP1

Gel images for reactions performed using PKA and PP1 (Trial 1).

	1	2	3	4	5	6	7	8	9
PP 1	+		+				+		+
MB Protein		+	+	+	+	+	+	+	+
PKA						+	+	+	+
ATP				+		+	+		
ATP-biotin					+			+	+

Gel images for reactions performed using PKA and PP1 (Trial 2).

	1	2	3	4	5	6	7	8	9
PP 1	+		+				+		+
MB Protein		+	+	+	+	+	+	+	+
PKA						+	+	+	+
ATP				+		+	+		
ATP-biotin					+			+	+
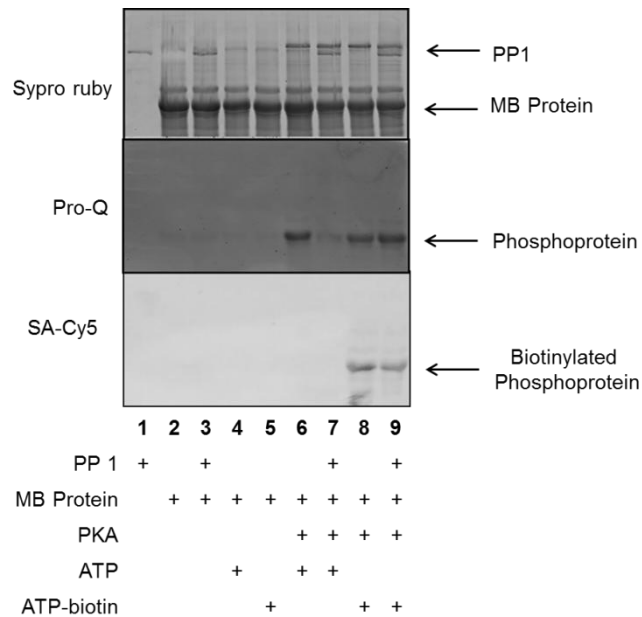
Gel images for reactions performed using PKA and PP1 (Trial 3).

Figure A 3.4: Full gel images for full length protein experiments containing PKA, MBP substrate, and PP1, with reaction contents indicated under each lane. The three independent trials, showing 2%, 5%, and 12% phosphoproteins remain (Pro-Q, lane 7), and 74%, 63%, and 79% biotinylated phosphoproteins remain (SA-Cy5, lane 9) after phosphatase treatment. The ATP kinase reaction (lane 6) is set to 100% in Pro-Q, while the ATP-biotin kinase reaction (lane 8) is set to 100% SA-Cy5.

(B) Reaction with CK2 and CIP

Gel images reactions performed using CK2 and CIP (Trial 1).
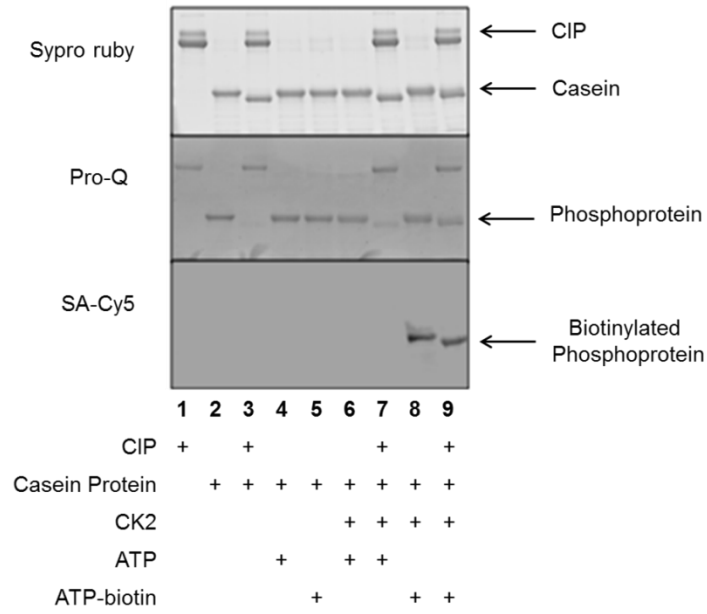
Gel images reactions performed using CK2 and CIP (Trial 2).
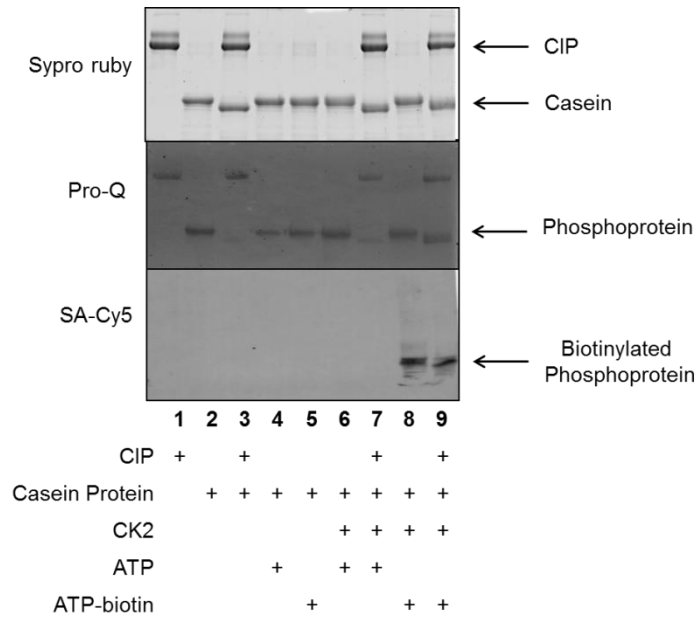
Gel images reactions performed using CK2 and CIP (Trial 3).
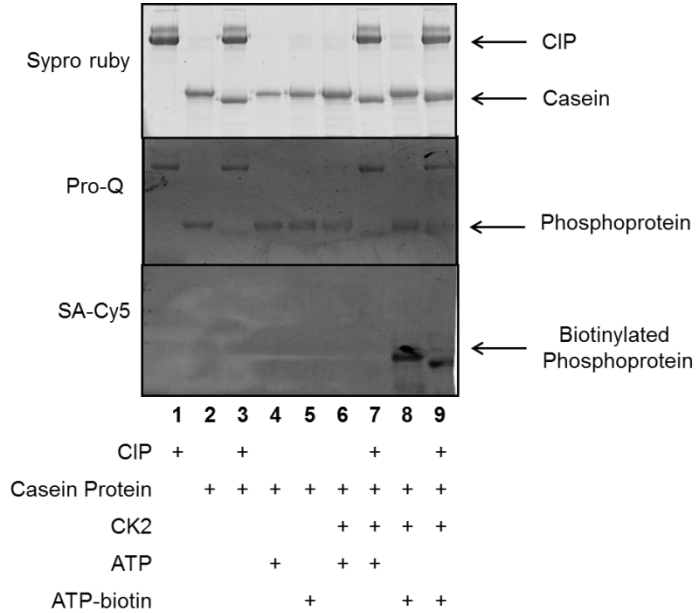
Figure A 3.5: Full gel images for full length protein experiments containing CK2, β-casein substrate, and CIP, with reaction contents indicated under each lane. The three independent trials, showing 9%, 4%, and 5% phosphoproteins remain (Pro-Q, lane 7), and 70%, 108%, and 66% biotinylated phosphoproteins remain (SA-Cy5, lane 9) after phosphatase treatment. The ATP kinase reaction (lane 6) is set to 100% in Pro-Q, while the ATP-biotin kinase reaction (lane 8) is set to 100% SA-Cy5.

(C) Reaction with Abl and TCPTP

Gel images for reactions performed using Abl and TC PTP (Trial 1).
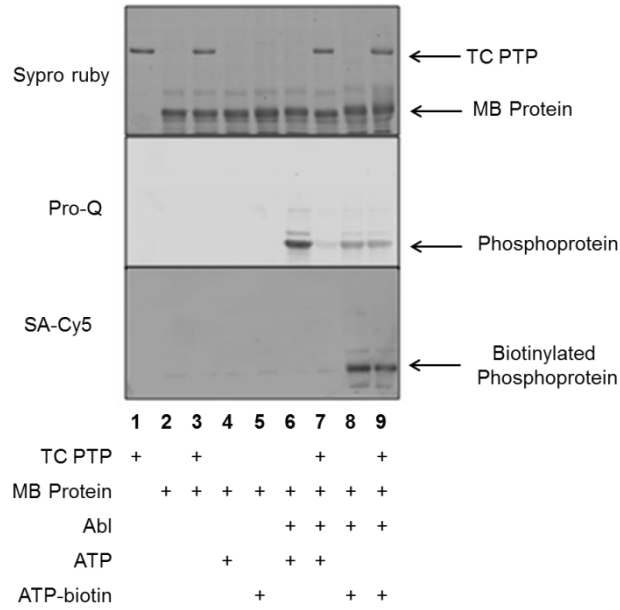
Gel images for reactions performed using Abl and TC PTP (Trial 2).
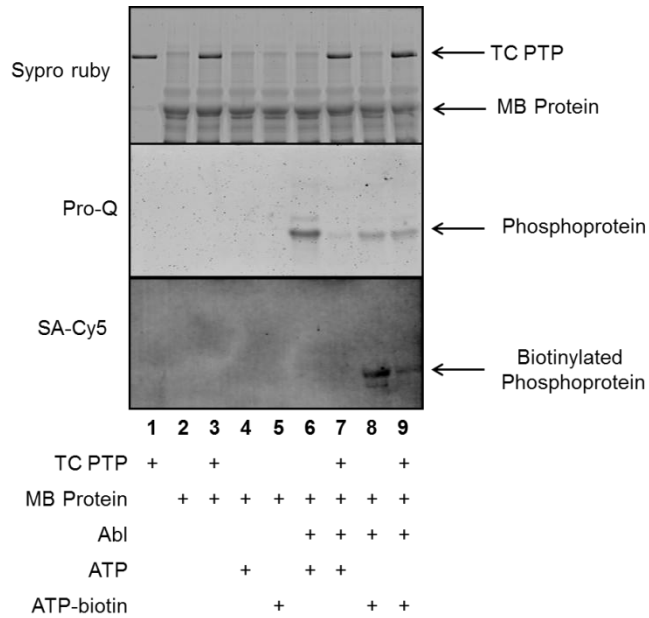
Gel images for reactions performed using Abl and TC PTP (Trial 3).
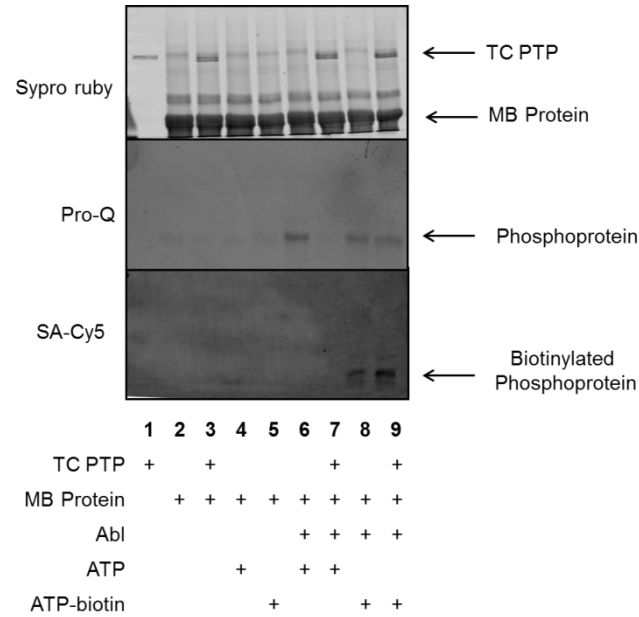
Figure A 3.6: Full gel images for full length protein experiments containing Abl, MBP substrate, and TC PTP, with reaction contents indicated under each lane. The three independent trials, showing 11%, 7%, and 2% phosphoproteins remain (Pro-Q, lane 7), and 70%, 68%, and 111% biotinylated phosphoproteins remain (SA-Cy5, lane 9) after phosphatase treatment. The ATP kinase reaction (lane 6) is set to 100% in Pro-Q, while the ATP-biotin kinase reaction (lane 8) is set to 100% SA-Cy5.

3.3 Gel Images Related to Inhibitors Studies.

Gel images for reactions performed using presence of kinase or phosphatase inhibitors (Trial 1).

		1	2	3	4	5	6	7
ATP			+	+	+			
ATP-biotin						+	+	+
Kinase inhibitor				+			+	
Phosphatase inhibitors					+			+

Gel images for reactions performed using presence of kinase or phosphatase inhibitors (Trial 2).

		1	2	3	4	5	6	7
ATP			+	+	+			
ATP-biotin						+	+	+
Kinase inhibitor				+			+	
Phosphatase inhibitors					+			+
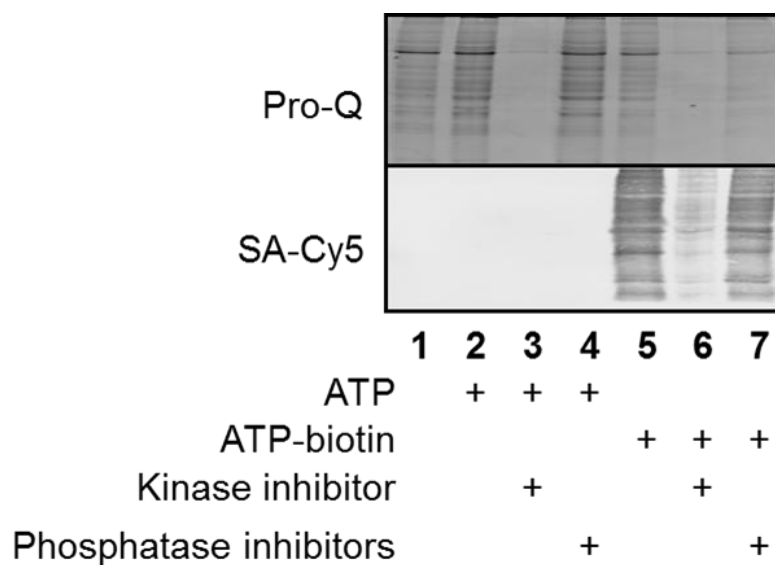
Gel images for reactions performed using presence of kinase or phosphatase inhibitors (Trial 3).

Figure A 3.7: Gel analysis of phosphoproteins (ProQ, top) or biotinylated phosphoproteins (SA-Cy5, bottom) from HeLa cell lysates incubated with ATP or ATP-biotin in the absence or presence of kinase or phosphatase inhibitors. The contents of each reaction are indicated below each lane. Addition of kinase inhibitor showed 15%, 18%, and 22% phosphopeptides (Pro-Q, lane 3), and 31%, 33%, and 16% biotinylated phosphoproteins (SA-Cy5, lane 6). Addition of phosphatase inhibitors showed 136%, 109%, and 110% phosphopeptides (Pro-Q, lane 4), and 83%, 90%, and 69% biotinylated phosphoproteins (SA-Cy5, lane 7). The ATP kinase reaction (lane 2) is set to 100% in Pro-Q, while the ATP-biotin kinase reaction (lane 5) is set to 100% SA-Cy5.

3.4 Quantification of Gel Images Related to Inhibitors Studies

A. Pro-Q Staining

B. SA-Cy5 Staining

	1	2	3	4	5	6	7		1	2	3	4	5	6	7
HeLa lysates	+	+	+	+	+	+	+		+	+	+	+	+	+	+
ATP		+	+	+						+	+	+			
ATP-biotin					+	+	+						+	+	+
Kinase inhibitor			+			+					+			+	
Phosphatase inhibitors				+			+					+			+
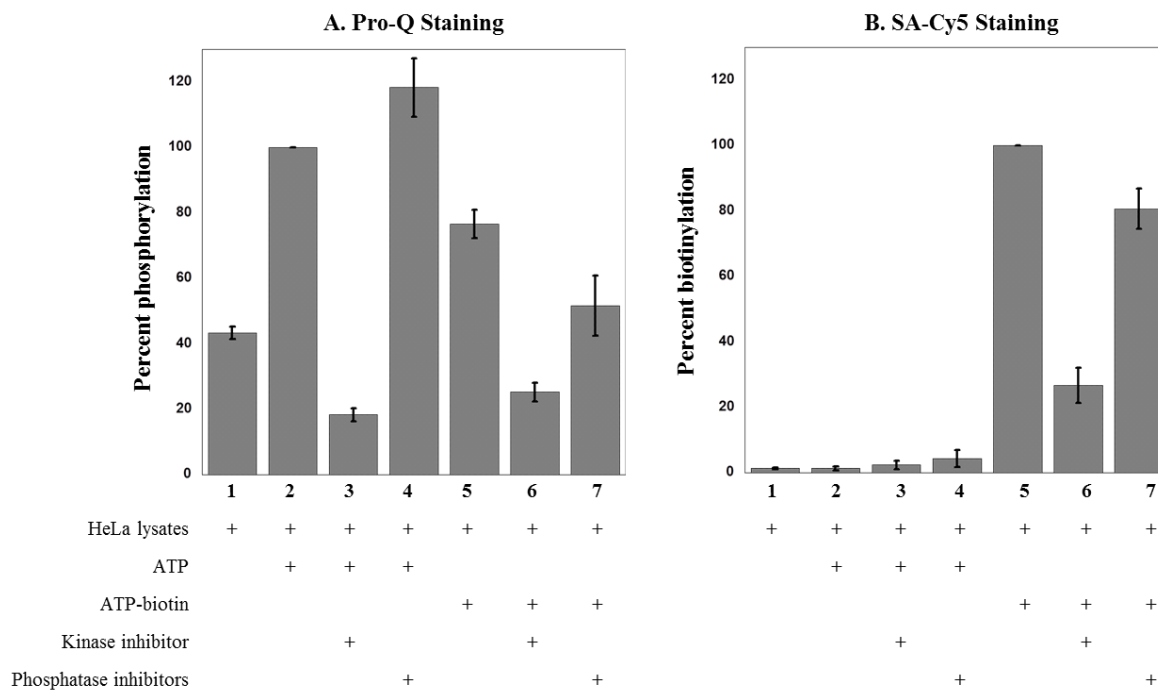
Figure A 3.8: Gel bands were quantified using ImageQuant 5.1 by drawing the same size rectangular shape around comparable bands. The percentage of phosphoproteins or biotinylated phosphoproteins observed after kinase or phosphatase inhibitor treatment was calculated by dividing the protein signal after treatment (Pro-Q, lane 3 or 4 and SA-Cy5, lane 6 or 7) to the protein signal before treatment (Pro-Q, lane 2 and SA-Cy-5, lane 5). The contents of each reaction are indicated below each lane. The ATP kinase reaction (lane 2) is set to 100% in part A, while the ATP-biotin kinase reaction (lane 5) is set to 100% in part B.

3.4 Two-Dimension Gel Images

(A) Gel images for reactions performed using ATP in the presence of phosphatase inhibitors
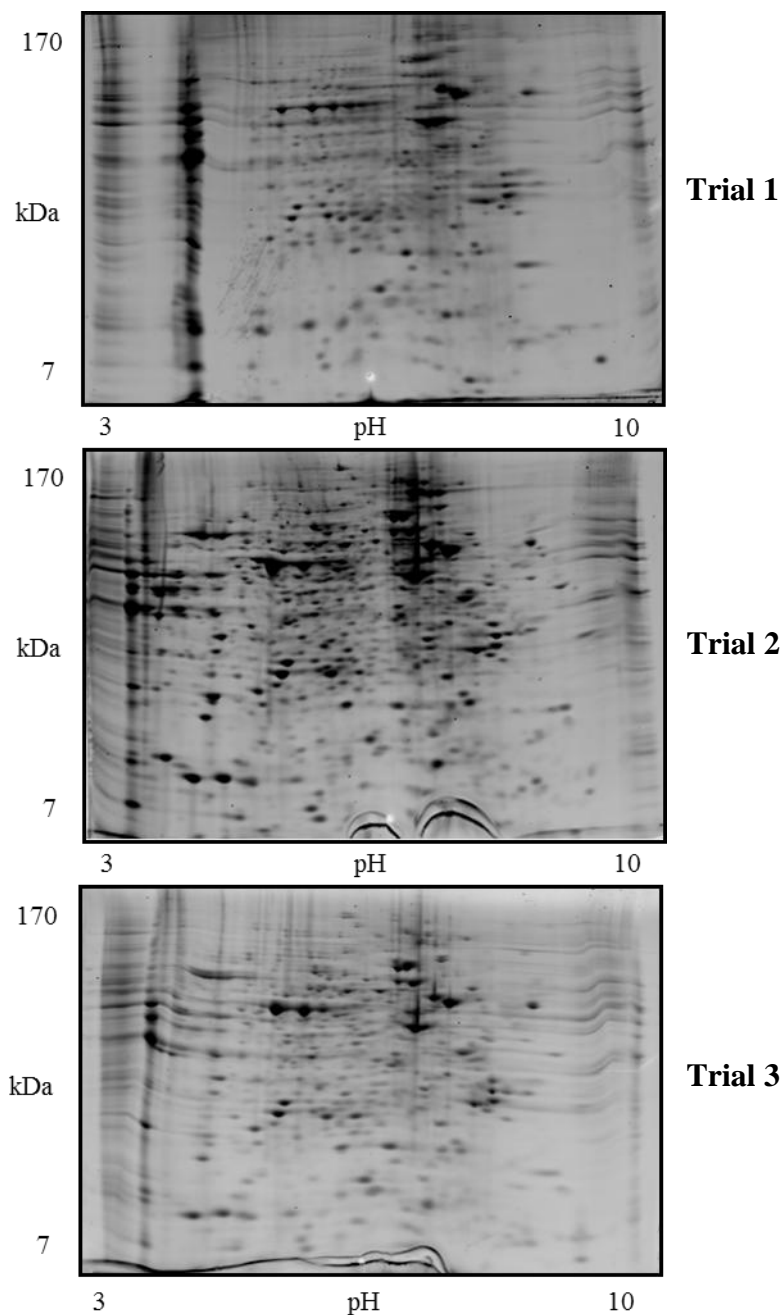
Figure A 3.9: Reaction of HeLa cell lysates and ATP with phosphatase inhibitors (phosphatase inhibitor treated). Proteins were visualized with Pro-Q diamond phosphoprotein stain. All the three independent trials are displayed here.

(B) Gel images for reactions performed using ATP in the absence of phosphatase inhibitors
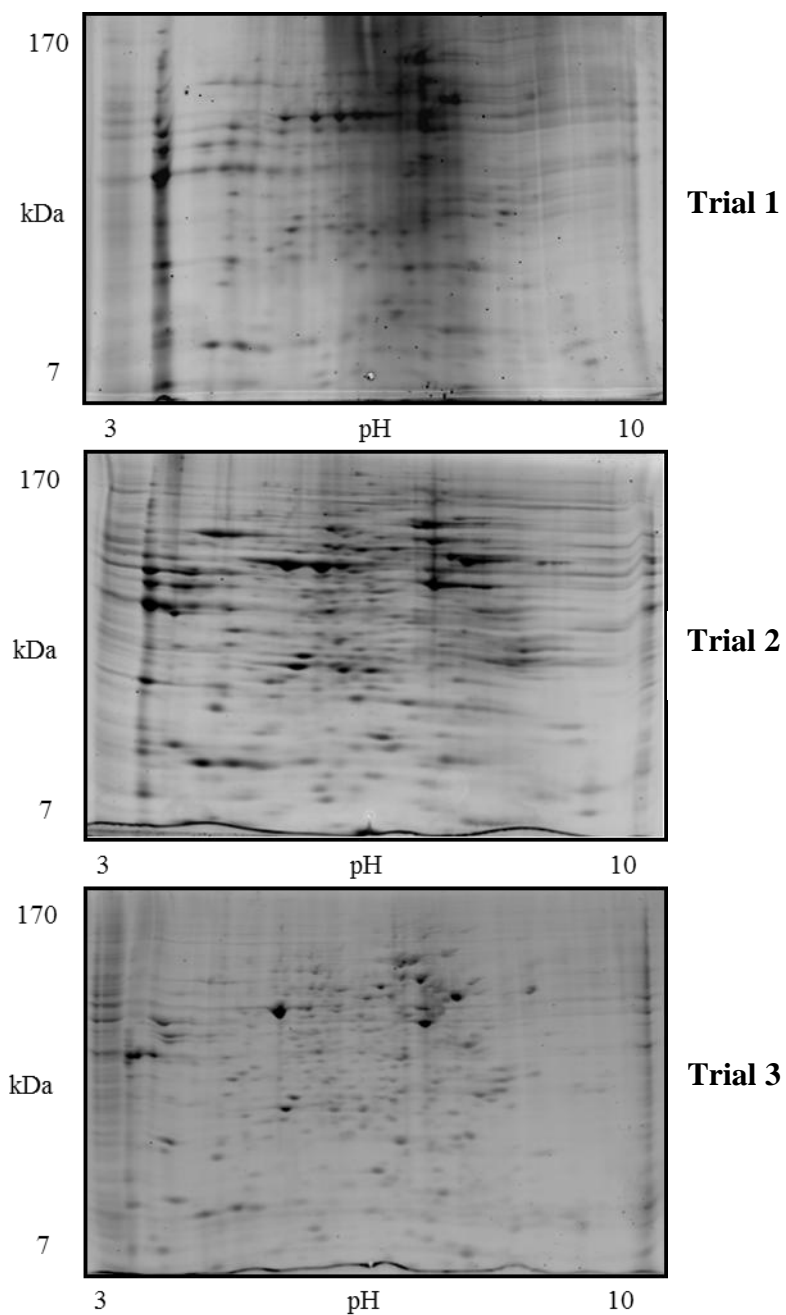
Figure A 3.10: Reaction of HeLa cell lysates and ATP without phosphatase inhibitors (untreated). Proteins were visualized with Pro-Q diamond phosphoprotein stain. All the three independent trials are displayed here.

(C) Gel images for reactions performed using ATP-biotin in the presence of phosphatase inhibitors
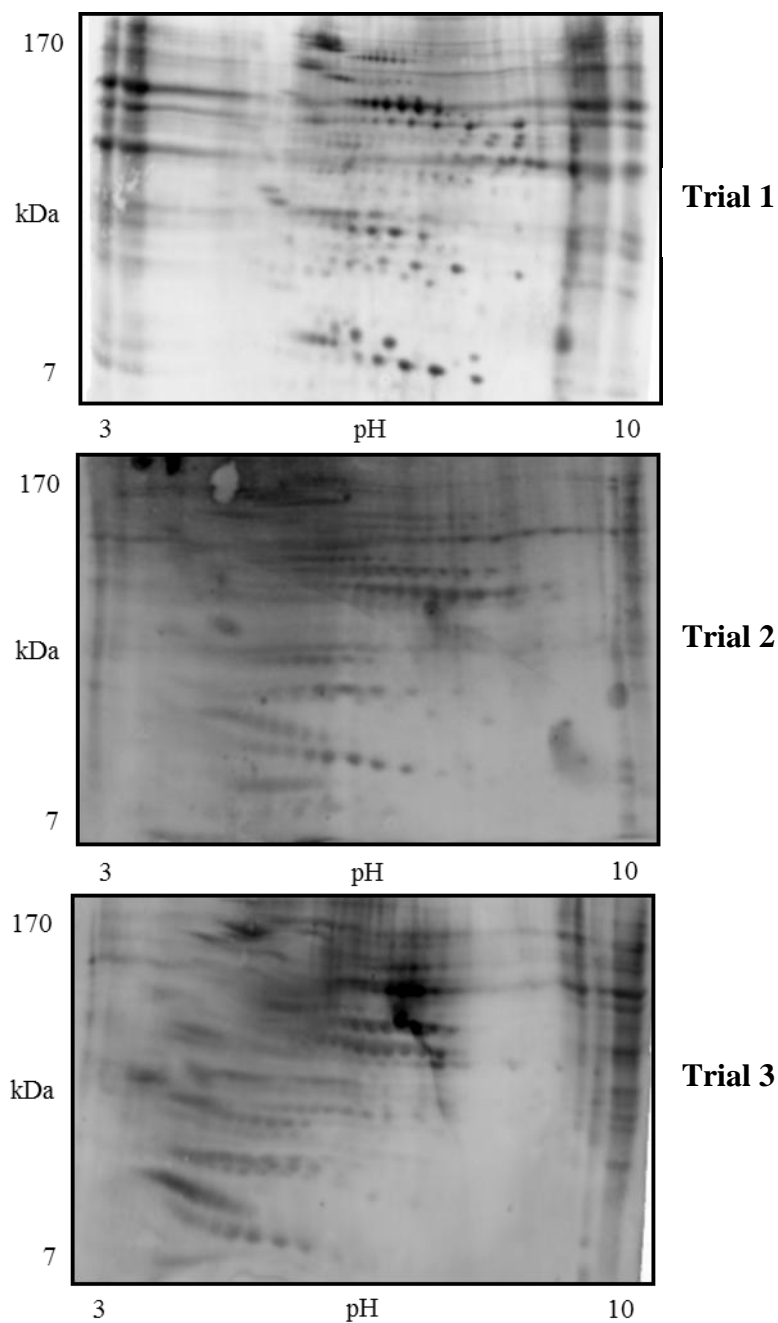
Figure A 3.11: Reaction of HeLa cell lysates and ATP-biotin with phosphatase inhibitors (phosphatase inhibitor treated). Biotinylated proteins were visualized with SA-Cy5. All the three independent trials are displayed here.

(D) Gel images for reactions performed using ATP-biotin in the absence of phosphatase inhibitors
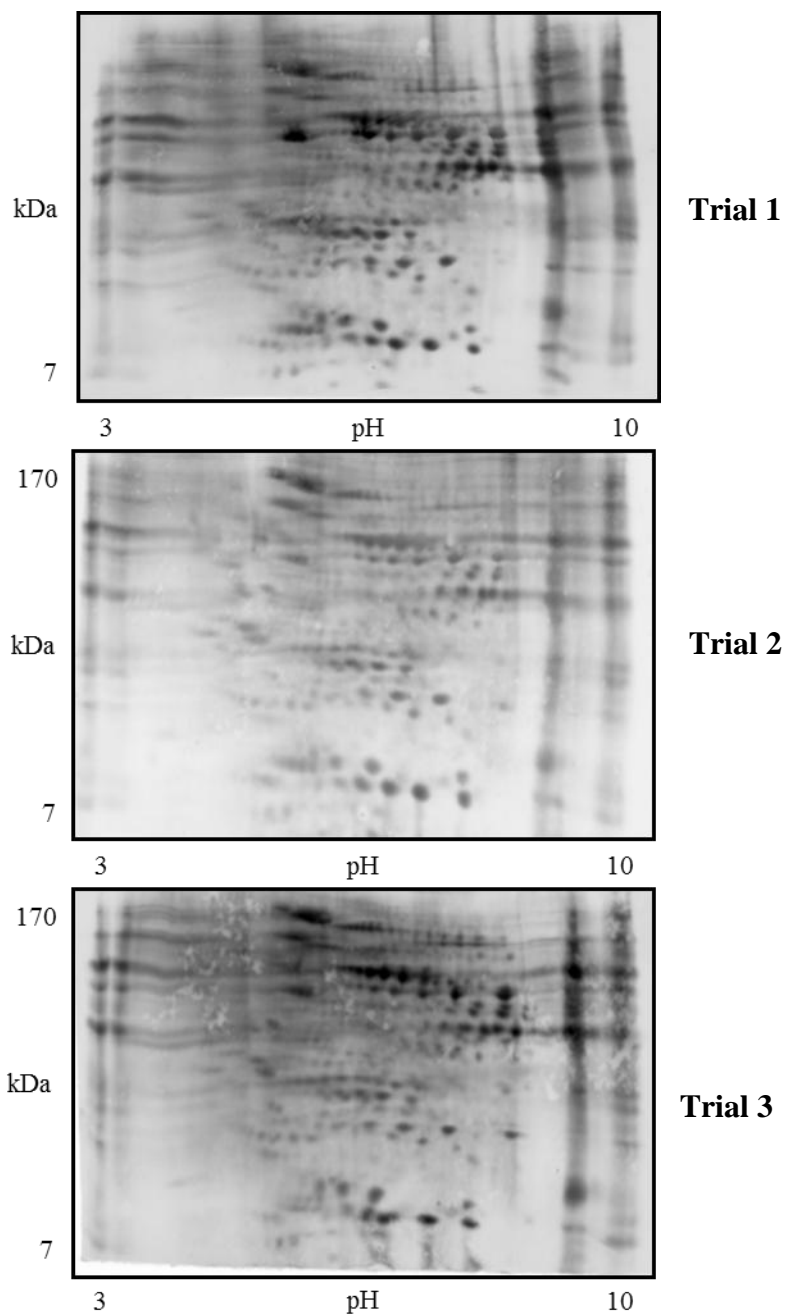
Figure A 3.12: Reaction of HeLa cell lysates and ATP-biotin without phosphatase inhibitors (untreated). Biotinylated proteins were visualized with SA-Cy5. All the three independent trials are displayed here.

APPENDIX C

Table A 4.1: Phosphopeptides identified by MS analysis after kinase-catalyzed biotinylation of casein, followed by purification of the trypsin digestion using NeutrAvidin affinity chromatography and elution with biotin[a]

Accession number	Protein name Peptide sequence	MW (Da)	SC[b]	PP[c]	IS[d]/IDS[e]	LP[f]	IM[g]
gi|30794310	Casein, beta	25,000					
	FQsEEQQQTEDELQDK		4	80	34/44	100	CID

[a] Peptides identified by MS were searched for serine, threonine, or tyrosine residues containing a +508 m/z modification, which is consistent with the presence of a biotinylated phosphate. 99% protein and 80% peptides cutoffs were used to generate the Scaffold coverage which scored above 0.8% FDR threshold. [b]SC=Spectral Count. [c] PP= Peptide probability (written as percentage). [d] IS= Ion Score. [e] IDS= Identity Score. [f]LP= Localization Probability(written as a percentage). [g]IM= Ionization Method. CID=Collision Induced Dissociation.

Annotated spectra from Scaffold

Peptide sequence: FQsEEQQQTEDELQDK
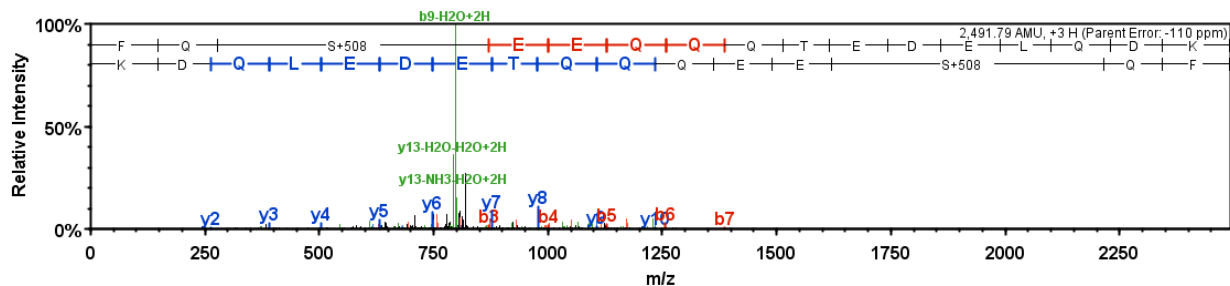
Figure A 4.1: The annotated spectrum of casein proteins identified by MS/MS analysis after ATP-biotin treatment, followed by avidin purification and biotin elution. Only one peptide was observed.

Table A 4.2: Phosphopeptides identified by MS analysis after purification of a trypsin digestion of casein using TiO$_2$ affinity chromatography[a]

Accession number	Proteins/peptides name	MW (Da)	SC[b]	PP[c]	IS[d]/IDS[e]	LP[f]	IM[g]
gi|30794348	**Casein, alpha s1**	**24 500**					
	DIGsEStEDQAMEDIK		2	95	44/46	100,14	CID
	DIGsEsTEDQAMEDIK		1	75	31/46	100,92	CID
	VPQLEIVPNsAEER		16	95	87/48	100	both
	VPQLEIVPNsAEERLHSMK		4	95	88/49	100	both
	YKVPQLEIVPNsAEER		16	95	121/49	100	both
	YKVPQLEIVPNsAEERLHSMK		1	95	53/49	99	ETD
gi|27806963	**Casein, alpha-S2**	**26 000**					
	KTVDMEsTEVFTKK		3	95	111/49	100	ETD
	NAVPITPTLNREQLsTsEENSKK		6	95	74/49	93,87	ETD
	NAVPITPTLNREQLStsEENSKK		1	93	59/49	31,70	ETD
	NAVPITPTLNREQLsTSEENsKK		1	95	65/49	64,94	ETD
	TVDMEsTEVFTK		6	95	77/49	90	both
	TVDMEsTEVFTKK		7	95	91/49	99	both
	TVDmEStEVFTKK		4	95	61/49	33	ETD
	TVDMEsTEVFTKKTK		2	92	43/49	83	ETD
gi|30794310	**Casein, beta**	**25 000**					
	FQsEEQQQTEDELQDK		78	95	108/49	100	both
	FQsEEQQQtEDELQDK		7	94	88/49	100,100	both
	FQSEEQQQtEDELQDK		1	82	34/46	99	CID
	IEKFQsEEQQQTEDELQDK		82	95	77/46	100	both
	IEKFQsEEQQQtEDELQDK		10	95	51/46	100,100	CID
	IEKFQSEEQQQtEDELQDK		1	94	48/49	100	CID
	KIEKFQsEEQQQTEDELQDK		4	95	112/49	100	ETD

[a] Peptides identified by MS were searched for serine, threonine, or tyrosine residues containing a +80 m/z modification, which is consistent with the presence of a phosphate group. 99% protein and 80% peptides cutoffs were used to generate the Scaffold coverage which scored above 0.9% FDR threshold. [b] SC=Spectral Count. [c] PP= Peptide probability (written as percentage). [d] IS= Ion Score. [e] IDS= Identity Score. [f]LP= Localization Probability (written as a percentage, multiple numbers corresponding to the value of each site). [g]IM= Ionization Method. CID=Collision Induced Dissociation, ETD= Electron Transfer Disscociation, both=CID and ETD.

Sequence of Casein Protein

gi|30794310 (100%), 25,098.2 Da
casein beta [Bos taurus]
4 unique peptides, 6 unique spectra, 111 total spectra, 60/224 amino acids (27% coverage)

```
M K V L I L A C L V   A L A L A R E L E E   L N V P G E I V E S   L S S S E E S I T R   I N K K I E K F Q S   E E Q Q Q T E D E L
Q D K I H P F A Q T   Q S L V Y P F P G P   I P N S L P Q N I P   P L T Q T P V V V P   P F L Q P E V M G V   S K V K E A M A P K
Q K E M P F P K Y P   V E P F T E S Q S L   T L T D V E N L H L   P L P L L Q S W M H   Q P H Q P L P P T V   M F P P Q S V L S L
S Q S K V L P V P Q   K A V P Y P Q R D M   P I Q A F L L Y Q E   P V L G P V R G P F   P I I V
```

gi|30794348 (100%), 24,529.4 Da
casein alpha s1 [Bos taurus]
4 unique peptides, 5 unique spectra, 15 total spectra, 37/214 amino acids (17% coverage)

```
M K L L I L T C L V   A V A L A R P K H P   I K H Q G L P Q E V   L N E N L L R F F V   A P F P E V F G K E   K V N E L S K D I G
S E S T E D Q A M E   D I K Q M E A E S I   S S S E E I V P N S   V E Q K H I Q K E D   V P S E R Y L G Y L   E Q L L R L K K Y K
V P Q L E I V P N S   A E E R L H S M K E   G I H A Q Q K E P M   I G V N Q E L A Y F   Y P E L F R Q F Y Q   L D A Y P S G A W Y
Y V P L G T Q Y T D   A P S F S D I P N P   I G S E N S E K T T   M P L W
```

gi|27806963 (100%), 26,019.0 Da
casein alpha-S2 [Bos taurus]
5 unique peptides, 5 unique spectra, 19 total spectra, 48/222 amino acids (22% coverage)

```
M K F F I F T C L L   A V A L A K N T M E   H V S S S E E S I I   S Q E T Y K Q E K N   M A I N P S K E N L   C S T F C K E V V R
N A N E E E Y S I G   S S S E E S A E V A   T E E V K I T V D D   K H Y Q K A L N E I   N Q F Y Q K F P Q Y   L Q Y L Y Q G P I V
L N P W D Q V K R N   A V P I T P T L N R   E Q L S T S E E N S   K K T V D M E S T E   V F T K K T K L T E   E E K N R L N F L K
K I S Q R Y Q K F A   L P Q Y L K T V Y Q   H Q K A M K P W I Q   P K T K V I P Y V R   Y L
```

Figure A 4.2: Primary sequences of casein proteins identified in the TiO$_2$ purification after ATP treatment. Amino acids highlighted in yellow represent peptides observed in the MS/MS analysis, while amino acids in green were modified through either phosphorylation (S or T) or oxidation (M). 99% protein and 80% peptides cutoffs were used to generate the Scaffold coverage, which scored above 0.9% FDR threshold.

Annotated spectra from Scaffold
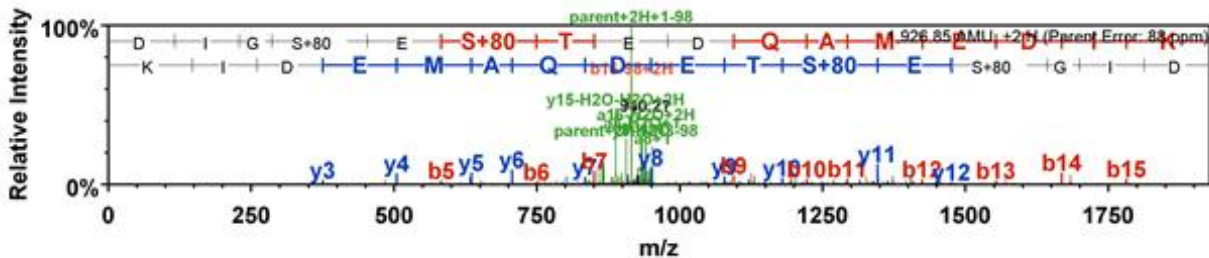
Peptide sequence: DIGsEsTEDQAMEDIK

Peptide sequence: DIG**s**ES**t**EDQAMEDIK
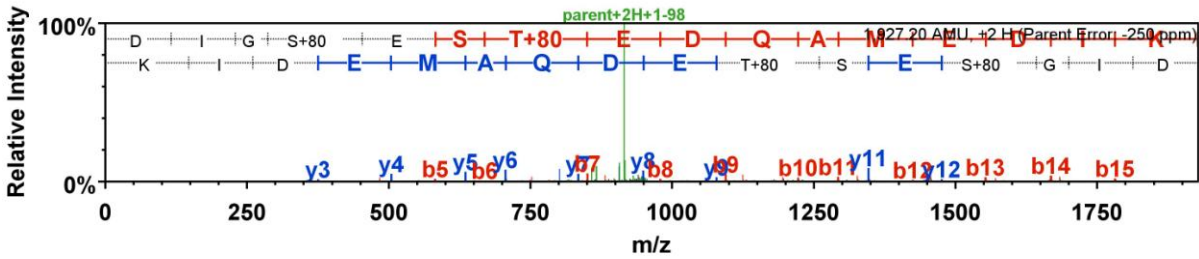
Peptide sequence: VPQLEIVPN**s**AEER
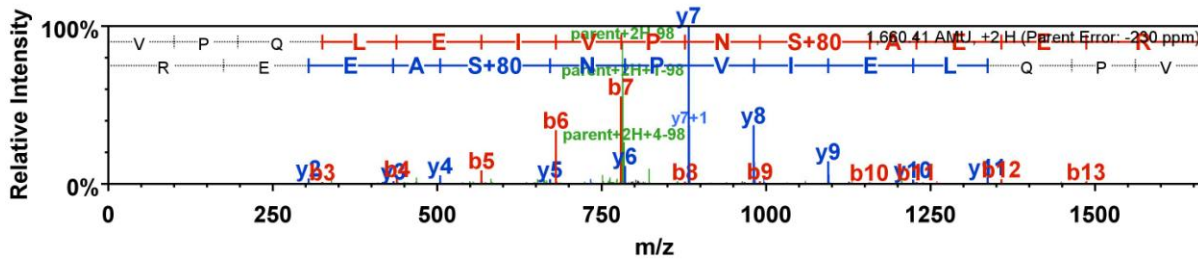
Peptide sequence: VPQLEIVPN**s**AEERLHSMK
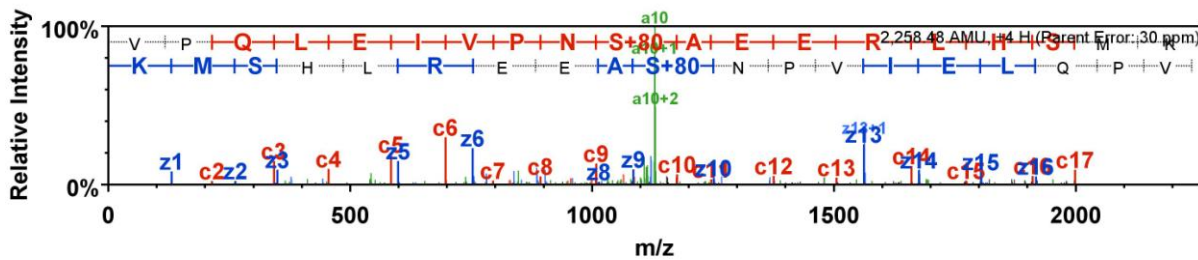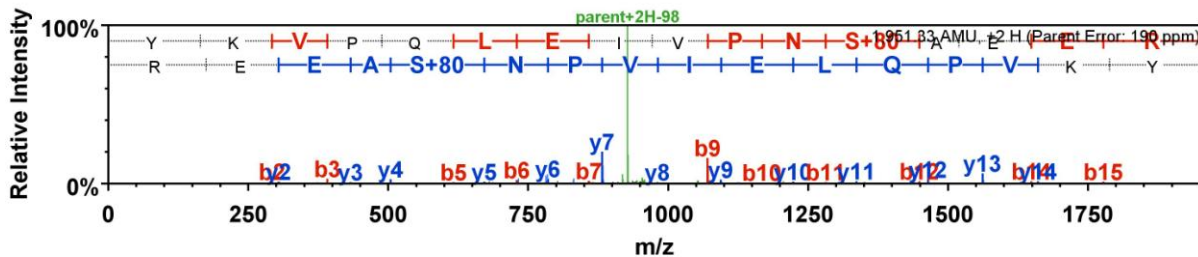
Peptide sequence: YKVPQLEIVPN**s**AEER

Peptide sequence: YKVPQLEIVPN**s**AEERLHSMK
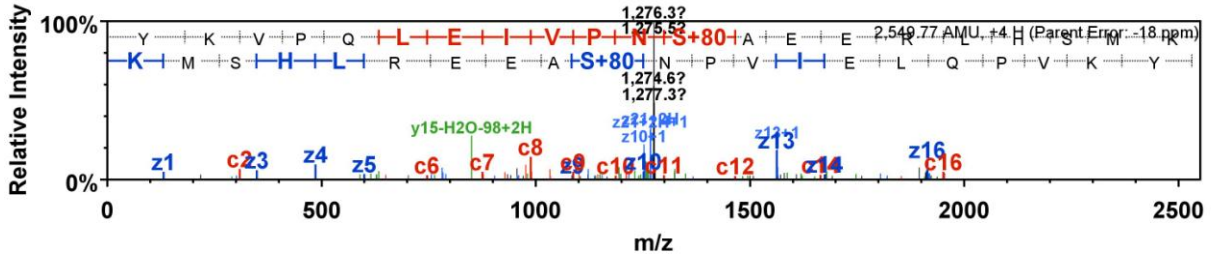
Peptide sequence: NAVPITPTLNREQL**s**T**s**EENSKK
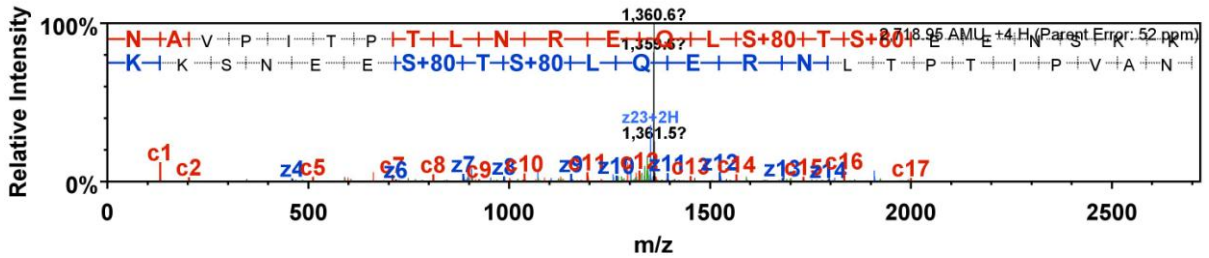
Peptide sequence: NAVPITPTLNREQLS**ts**EENSKK
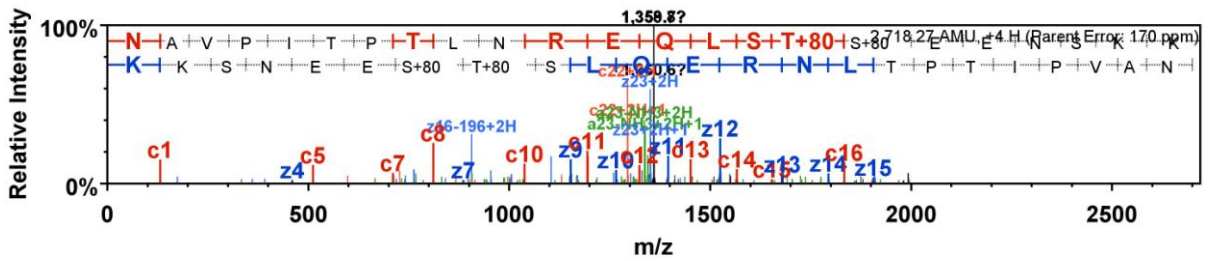
Peptide sequence: NAVPITPTLNREQL**s**TSEEN**s**KK
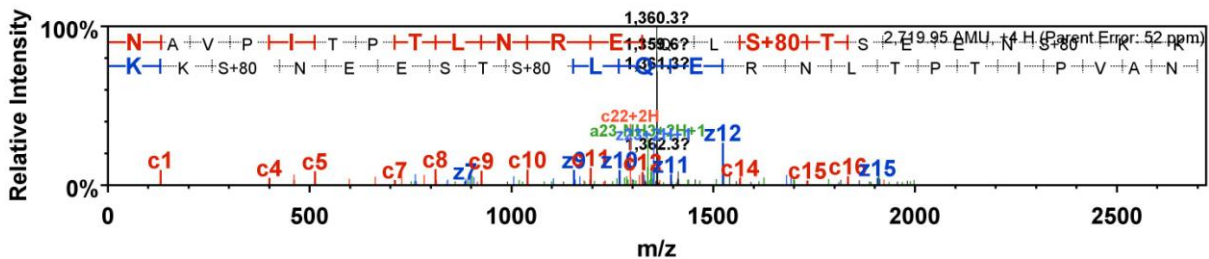
Peptide sequence: KTVDMEsTEVFTKK
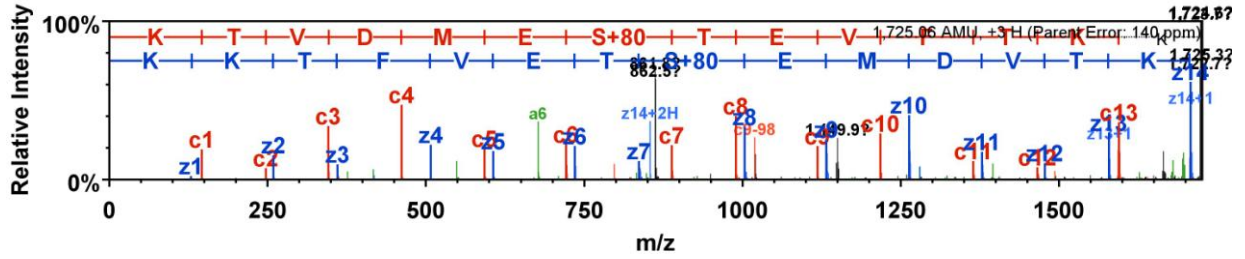
Peptide sequence: TVDMEsTEVFTKK
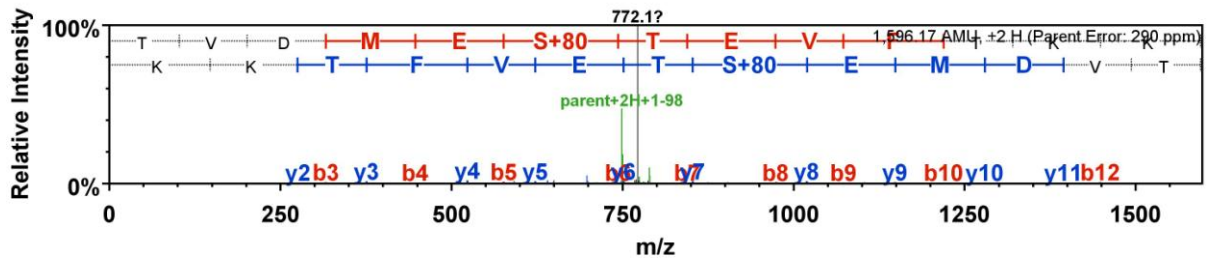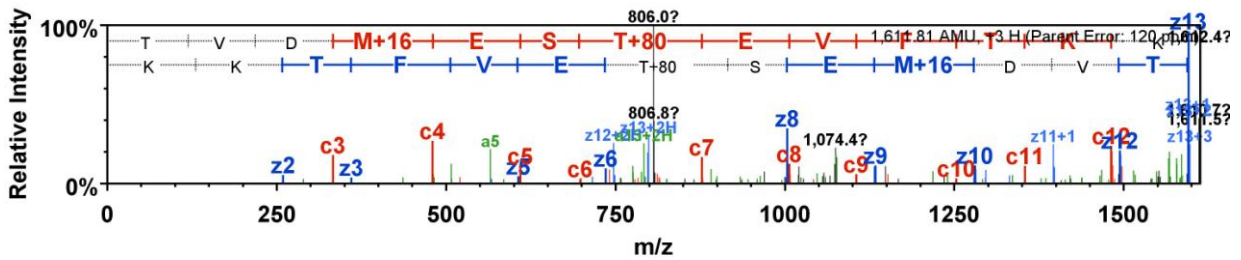
Peptide sequence: TVDmEStEVFTKK
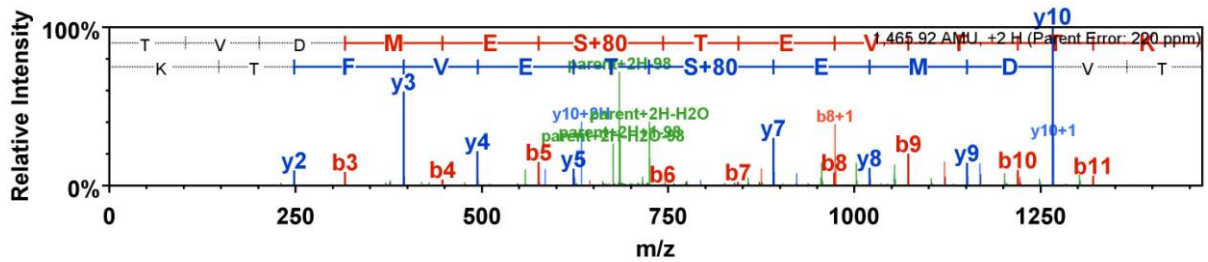
Peptide sequence: TVDMEsTEVFTK

Peptide sequence: TVDME**s**TEVFTKKTK
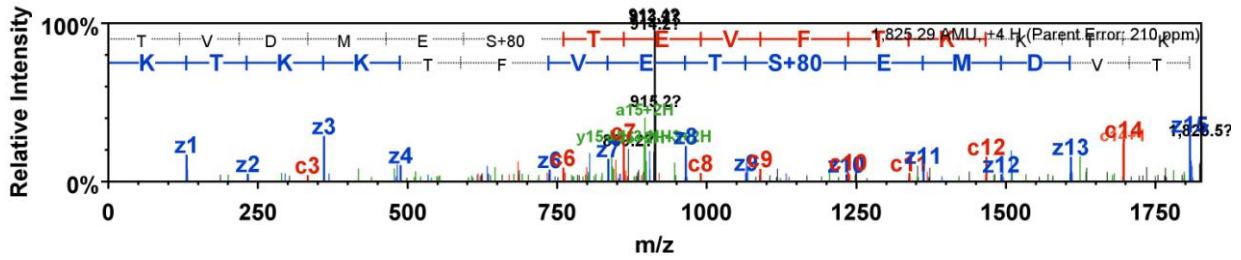
Peptide sequence: FQ**s**EEQQQTEDELQDK
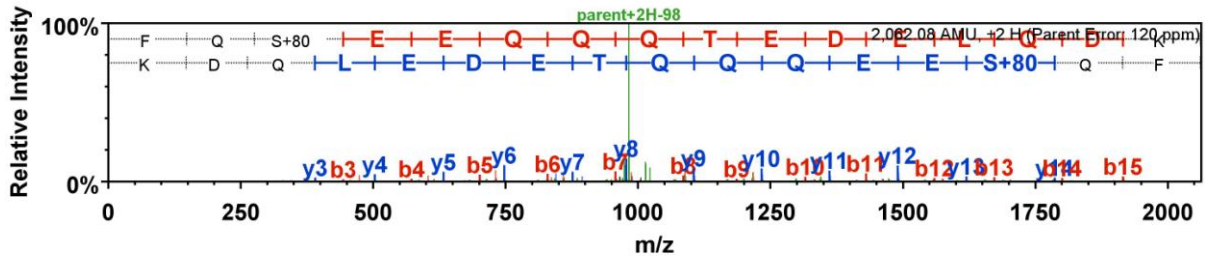
Peptide sequence: FQ**s**EEQQQ**t**EDELQDK
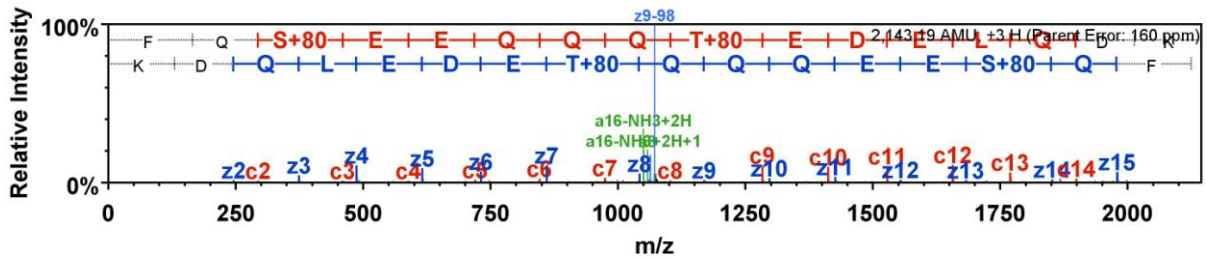
Peptide sequence: FQSEEQQQ**t**EDELQDK
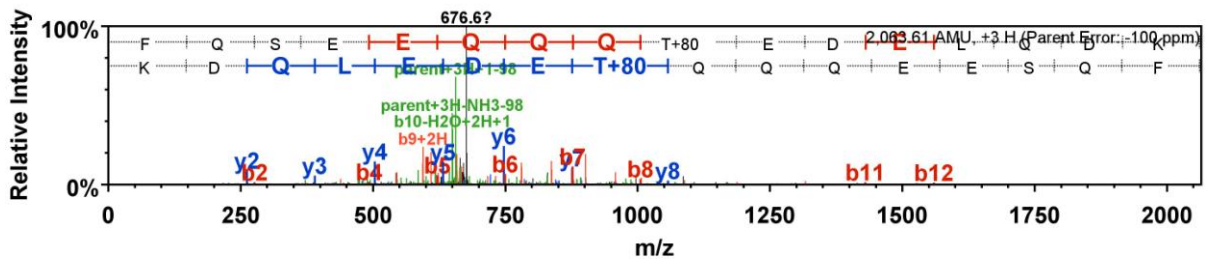
Peptide sequence: IEKFQSEEQQQtEDELQDK
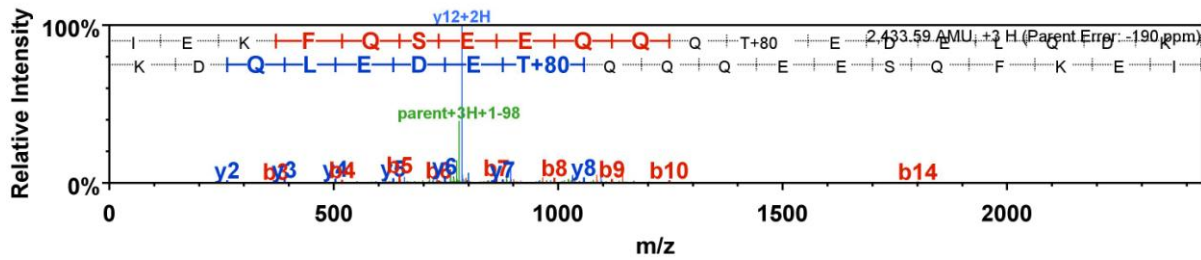
Peptide sequence: IEKFQsEEQQQtEDELQDK
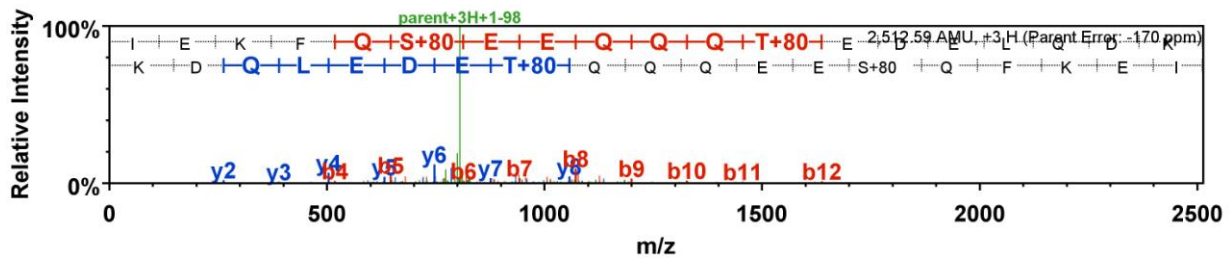
Peptide sequence: IEKFQsEEQQQTEDELQDK
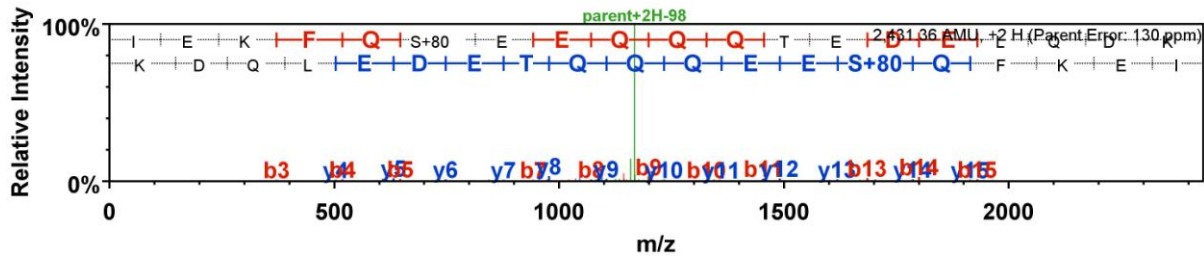
Peptide sequence: KIEKFQsEEQQQTEDELQDK
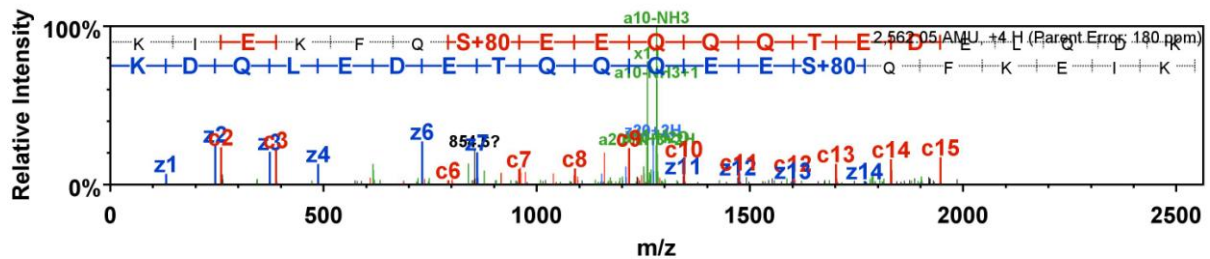
Figure A 4.3: The annotated spectrum of casein proteins identified by MS/MS analysis after ATP treatment, followed by TiO_2 purification. While twelve unique peptide spectra were observed, several had variable phosphorylation states. All 21 spectra representing the observed phosphorylated states are shown.

Table A 4.3: Phosphopeptides identified by MS analysis after kinase-catalyzed biotinylation of casein, followed by purification of the trypsin digestion using NeutrAvidin affinity chromatography and acidic elution[a]

Accession number	Proteins/Peptides name	MW (Da)	SC[b]	PP[c]	IS[d]/IDS[e]	LP[f]	IM[g]
gi|30794348	Casein, alpha s1	24,500					
	VPQLEIVPNsAEER		1	94	42/46	100	CID
	YKVPQLEIVPNsAEER		9	95	62/48	100	both
gi|30794310	Casein, beta	25,000					
	IEKFQsEEQQQtEDELQDK		4	81	37/46	100,100	CID

[a] Peptides identified by MS were searched for serine, threonine, or tyrosine residues containing a +80 m/z modification, which is consistent with the presence of a phosphate group. 99% protein and 80% peptides cutoffs were used to generate the Scaffold coverage which scored above 0.6% FDR threshold. [b] SC=Spectral Count. [c] PP= Peptide probability (written as percentage). [d] IS= Ion Score. [e] IDS= Identity Score. [f] LP= Localization Probability (written as a percentage, multiple numbers corresponding to the value of each site). [g] IM= Ionization Method. CID=Collision Induced Dissociation, ETD= Electron Transfer Disscociation, both=CID and ETD.

Annotated spectra from Scaffold

Peptide sequence: YKVPQLEIVPN**s**AEER
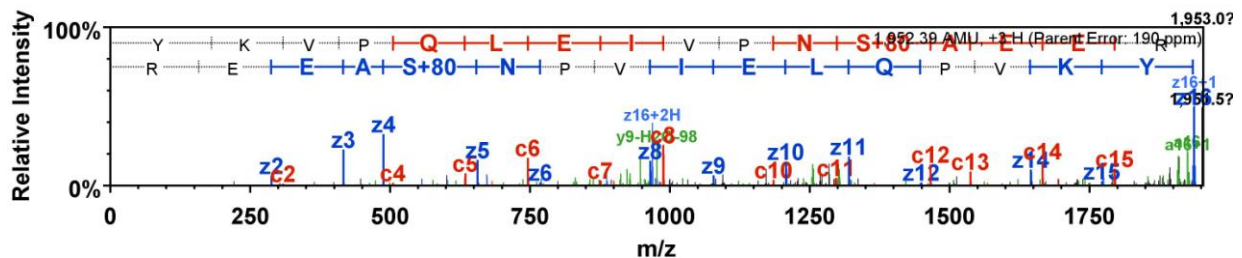
Peptide sequence: VPQLEIVPNsAEER
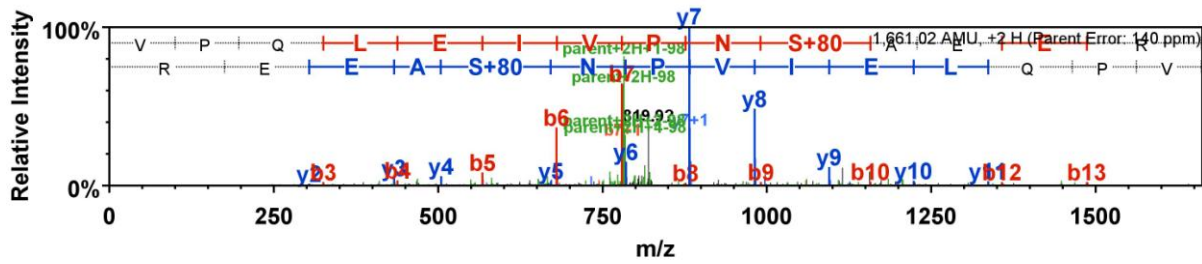
Peptide sequence: IEKFQsEEQQQtEDELQDK
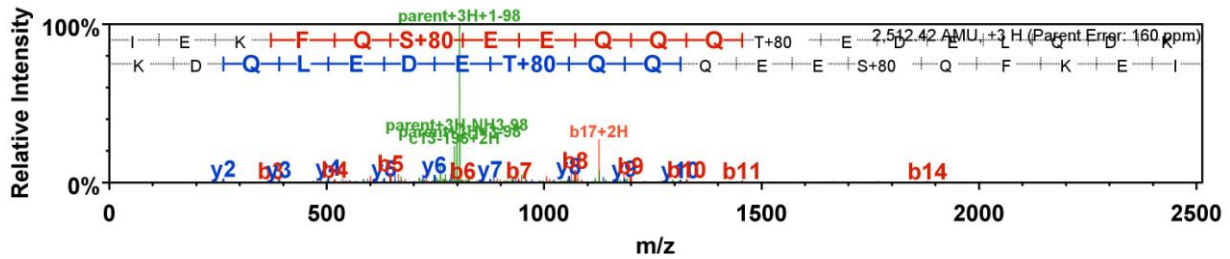
Figure A 4.4: The annotated spectrum of casein proteins identified by MS/MS analysis after ATP-biotin treatment, followed by avidin purification and acidic elution. Three peptides were observed

Table A 4.4: Phosphopeptides identified by MS analysis after kinase-catalyzed biotinylation of casein in the presence of calf intestinal phosphatase, followed by purification of the trypsin digestion using NeutrAvidin affinity chromatography and acidic elution[a]

Accession numbers	Proteins/Peptides name	MW (Da)	SC[b]	PP[c]	IS[d]/IDS[e]	LP[f]	IM[g]
gi|30794348	Casein, alpha s1	24,500					
	DIGSEsTEDQAMEDIK		2	95	50/46	85	CID
	DIGsEsTEDQAMEDIK		13	95	52/46	100,99	CID
	VNELsKDIGsEStEDQAMEDIK		1	56	29/46	100,100,29	CID
	VPQLEIVPNsAEER		17	95	71/46	100	CID
	YKVPQLEIVPNsAEER		26	95	113/46	100	CID
gi|27806963	Casein, alpha-S2	26,000					
	NANEEEYsIGsssEEsAEVATEEVK		2	55	28/46	72,83,87, 79,57	CID
	TVDMEsTEVFTK		3	95	64/46	99	CID
	TVDMEStEVFTK		10	95	64/46	81	CID
	TVDMEsTEVFTKK		11	95	71/46	99	CID
gi|30794310	Casein, beta	25,000					
	FQsEEQQQTEDELQDK		96	95	81/46	100	CID
	FQsEEQQQtEDELQDK		14	95	51/46	100,100	CID
	IEKFQsEEQQQTEDELQDK		47	95	62/46	100	CID
	IEKFQsEEQQQtEDELQDK		16	94	48/46	100,100	CID
gi|27881412	Casein, kappa	21,252					
	sPAQILQWQVLSNTVPAK		1	80	37/46	100	CID

[a] Peptides identified by MS were searched for serine, threonine, or tyrosine residues containing a +80 m/z modification, which is consistent with the presence of a phosphate group. 99% protein and 55% peptides cutoffs were used to generate the Scaffold coverage which scored above 0.8% FDR threshold. [b] SC=Spectral Count. [c] PP= Peptide probability (written as percentage). [d] IS= Ion Score. [e] IDS= Identity Score. [f] LP= Localization Probability (written as a percentage, multiple numbers corresponding to the value of each site). [g] IM= Ionization Method. CID=Collision Induced Dissociation.

Sequence of Casein Protein

gi|30794348 (100%), 24,529.4 Da
casein alpha s1 [Bos taurus]
8 unique peptides, 13 unique spectra, 68 total spectra, 79/214 amino acids (37% coverage)

```
M K L L I L T C L V   A V A L A R P K H P   I K H Q G L P Q E V   L N E N L L R F F V   A P F P E V F G K E   K V N E L S K D I G
S E S T E D Q A M E   D I K Q M E A E S I   S S S E E I V P N S   V E Q K H I Q K E D   V P S E R Y L G Y L   E Q L L R L K K Y K
V P Q L E I V P N S   A E E R L H S M K E   G I H A Q Q K E P M   I G V N Q E L A Y F   Y P E L F R Q F Y Q   L D A Y P S G A W Y
Y V P L G T Q Y T D   A P S F S D I P N P   I G S E N S E K T T   M P L W
```

gi|27806963 (100%), 26,019.0 Da
casein alpha-S2 [Bos taurus]
9 unique peptides, 12 unique spectra, 27 total spectra, 86/222 amino acids (39% coverage)

```
M K F F I F T C L L   A V A L A K N T M E   H V S S S E E S I I   S Q E T Y K Q E K N   M A I N P S K E N L   C S T F C K E V V R
N A N E E E Y S I G   S S S E E S A E V A   T E E V K I T V D D   K H Y Q K A L N E I   N Q F Y Q K F P Q Y   L Q Y L Y Q G P I V
L N P W D Q V K R N   A V P I T P T L N R   E Q L S T S E E N S   K K T V D M E S T E   V F T K K T K L T E   E E K N R L N F L K
K I S Q R Y Q K F A   L P Q Y L K T V Y Q   H Q K A M K P W I Q   P K T K V I P Y V R   Y L
```

gi|30794310 (100%), 25,098.2 Da
casein beta [Bos taurus]
2 unique peptides, 4 unique spectra, 88 total spectra, 19/224 amino acids (8% coverage)

```
M K V L I L A C L V   A L A L A R E L E E   L N V P G E I V E S   L S S S E E S I T R   I N K K I E K F Q S
E E Q Q Q T E D E L   Q D K I H P F A Q T   Q S L V Y P F P G P   I P N S L P Q N I P   P L T Q T P V V V P
P F L Q P E V M G V   S K V K E A M A P K   Q K E M P F P K Y P   V E P F T E S Q S L   T L T D V E N L H L
P L P L L Q S W M H   Q P H Q P L P P T V   M F P P Q S V L S L   S Q S K V L P V P Q   K A V P Y P Q R D M
P I Q A F L L Y Q E   P V L G P V R G P F   P I I V
```

gi|27881412 (100%), 21,269.5 Da
casein kappa [Bos taurus]
5 unique peptides, 8 unique spectra, 64 total spectra, 77/190 amino acids (41% coverage)

```
M M K S F F L V V T   I L A L T L P F L G   A Q E Q N Q E Q P I   R C E K D E R F F S   D K I A K Y I P I Q   Y V L S R Y P S Y G
L N Y Y Q Q K P V A   L I N N Q F L P Y P   Y Y A K P A A V R S   P A Q I L Q W Q V L   S N T V P A K S C Q   A Q P T T M A R H P
H P H L S F M A I P   P K K N Q D K T E I   P T I N T I A S G E   P T S T P T T E A V   E S T V A T L E D S   P E V I E S P P E I
N T V Q V T S T A V
```

Figure A 4.5: Primary sequences of casein proteins identified in the Avidin purification after ATP-biotin treatment in the presence of CIP. Amino acids highlighted in yellow represent peptides observed in the MS/MS analysis, while amino acids in green were modified through either phosphorylation (S or T) or oxidation (M). 99% protein and 55% peptides cutoffs were used to generate the Scaffold coverage, which scored above 0.8% FDR threshold.

Annotated spectra from Scaffold

Peptide sequence: DIG**s**E**s**TEDQAMEDIK
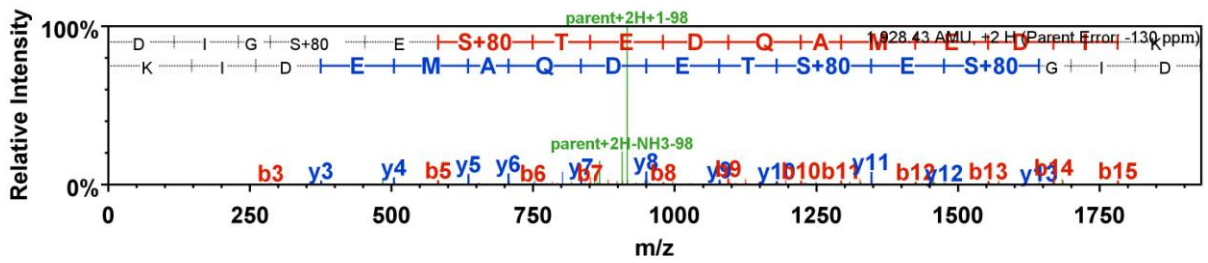
Peptide sequence: DIGSE**s**TEDQAMEDIK
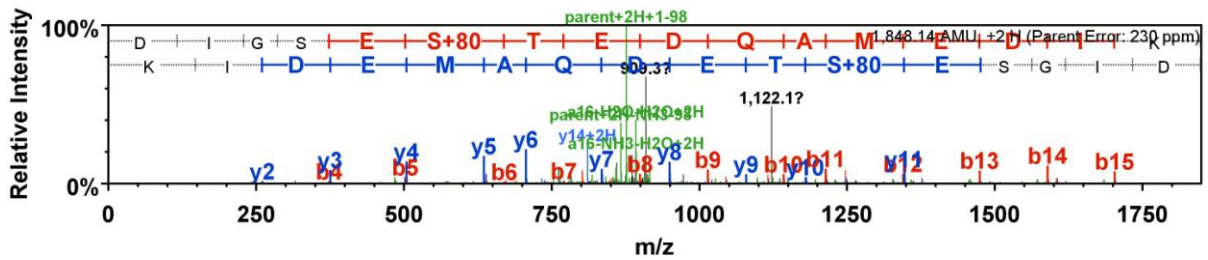
Peptide sequence: VNEL**s**KDIG**s**ES**t**EDQAMEDIK
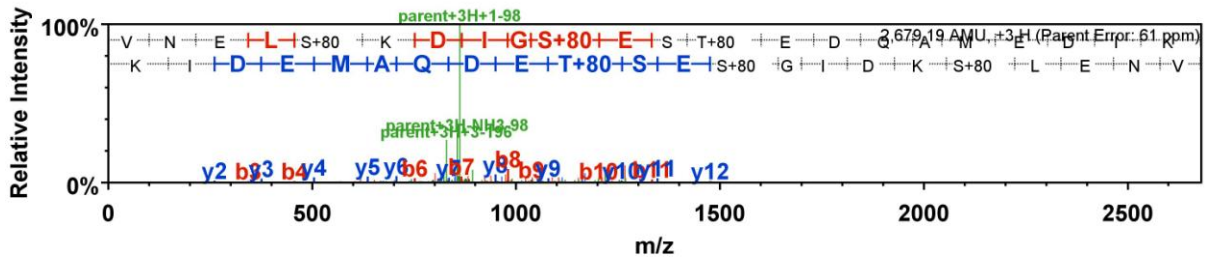
Peptide sequence: VPQLEIVPN**s**AEER
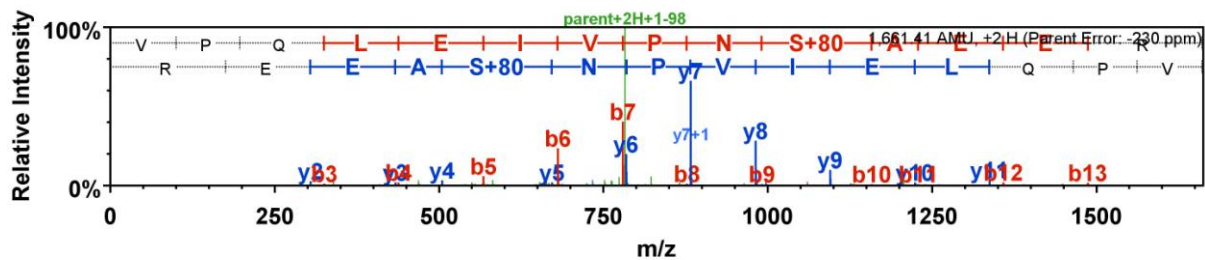
Peptide sequence: YKVPQLEIVPN**s**AEER
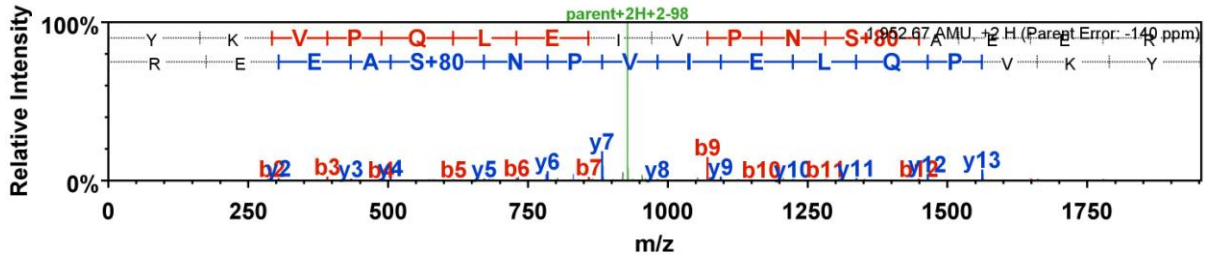
Peptide sequence: NANEEEY**s**IG**sss**EE**s**AEVATEEVK
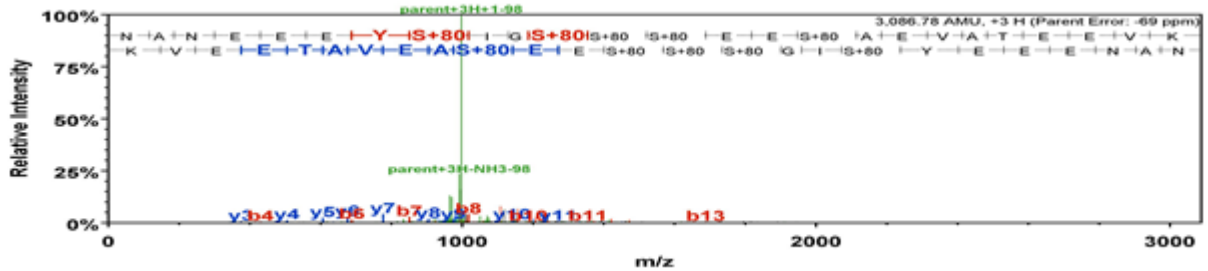
Peptide sequence: TVDME**s**TEVFTKK
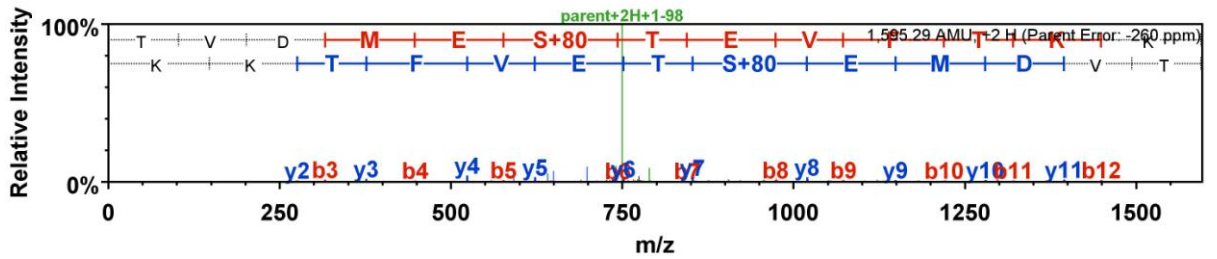
Peptide sequence: TVDMES**t**EVFTK
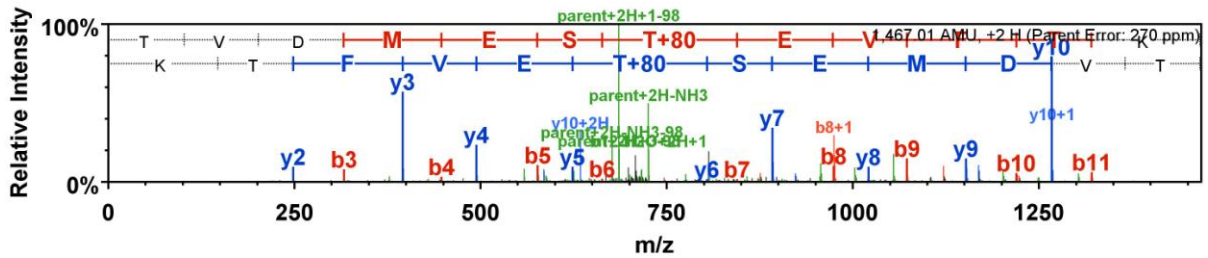
Peptide sequence: TVDME**s**TEVFTK
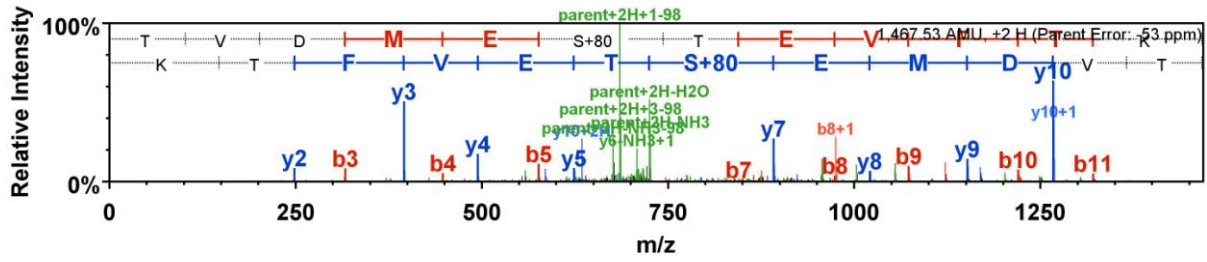
Peptide sequence: **s**PAQILQWQVLSNTVPAK
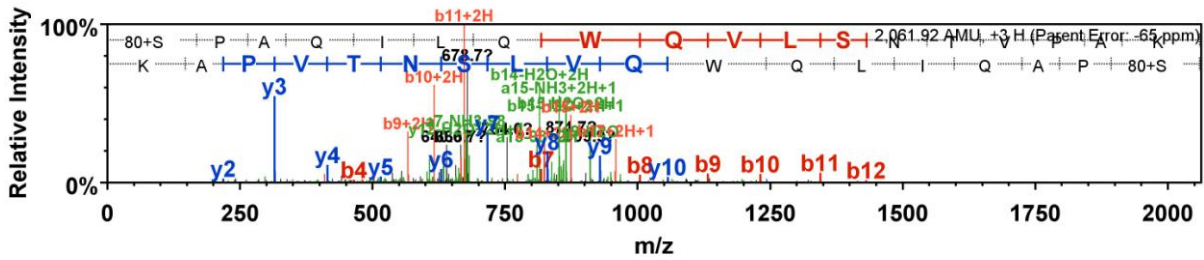
Peptide sequence: FQ**s**EEQQQTEDELQDK
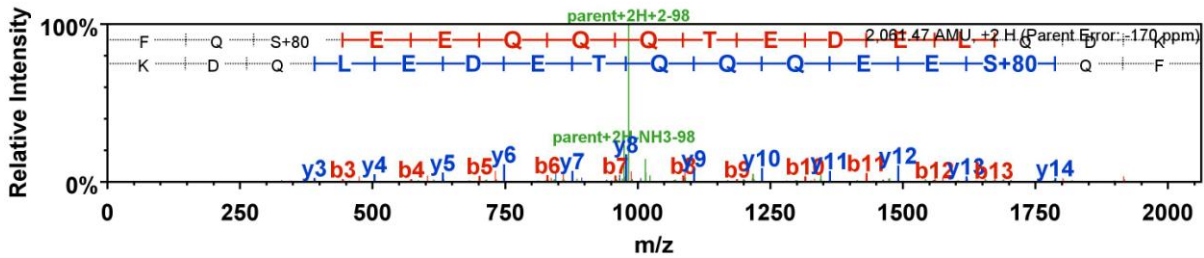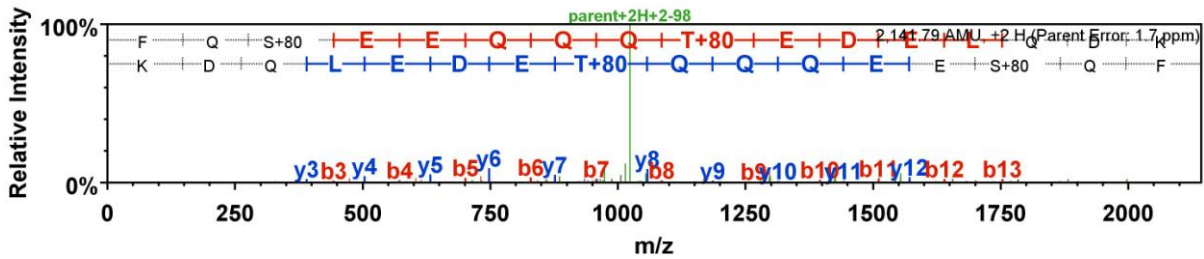
Peptide sequence: FQ**s**EEQQQ**t**EDELQDK

Peptide sequence: IEKFQsEEQQQTEDELQDK
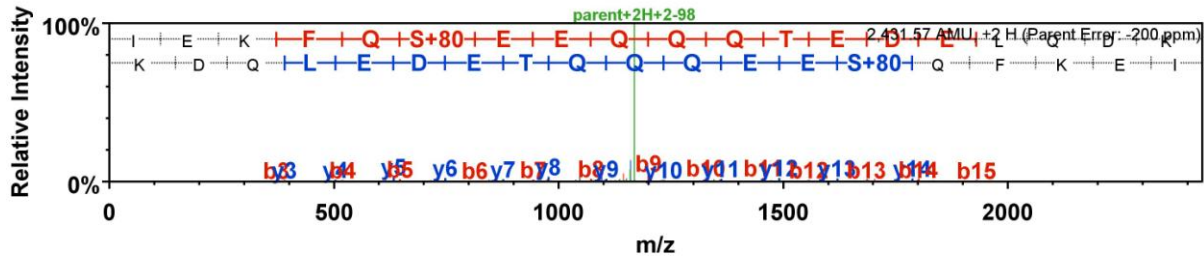
Peptide sequence: IEKFQsEEQQQtEDELQDK
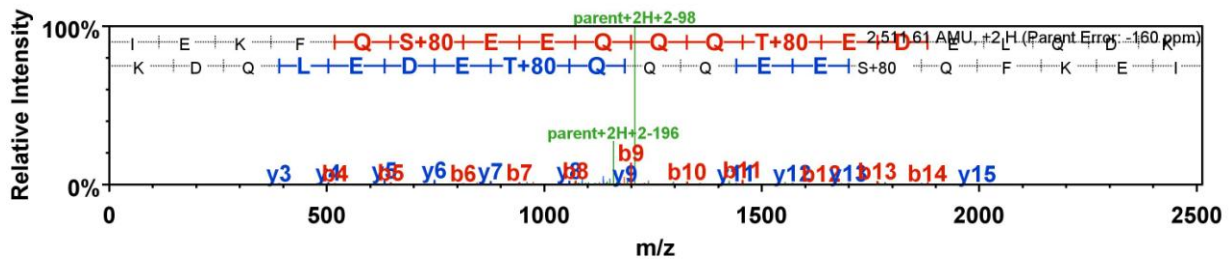
Figure A 4.6: The annotated spectrum of casein proteins identified by MS/MS analysis after ATP-biotin treatment in the presence of CIP, followed by avidin purification and acidic elution. While ten unique peptide spectra were observed, several had variable phosphorylation states. All 14 spectra representing the observed phosphorylated states are shown.

Table A 4.5: Phosphopeptides identified by MS analysis after kinase-catylzed biotinylation of HeLa cell lysates and subsequent purification of the trypsin digestion using NeutrAvidin affinity chromatography and acidic elution[a]

Accession numbers	Proteins/peptides name	MW (Da)	SC[b]	PP[c]	IS[d]/IDS[e]	LP[f]	IM[g]
DECR_HUMAN	2,4-dienoyl-CoA reductase, mitochondrial	36,069					
	GAAFLSITTIYAETGSGFVVPSASAKAGVEAMsK		1	95	69/43	15	CID
PRS4_HUMAN	26S protease regulatory subunit 4	49,186					
	MGQsQSGGHGPGGGK		1	91	22/43	98	CID
RT28_HUMAN	28S ribosomal protein S28, mitochondrial	20,843					
	NVEsFASmLR		2	95	43/43	100	CID
RS12_HUMAN	40S ribosomal protein S12	14,515					
	aEEGIAAGGVMDVNTALQEVLKtALIHDGLAR		13	95	82/43	100	CID
RS15A_HUMAN	40S ribosomal protein S15a	14,840					
	QFGFIVLtTSAGImDHEEAR		1	95	43/43	100	CID
RS17L_HUMAN	40S ribosomal protein S17	15,551					
	DNYVPEVSALDQEIIEVDPDtKEMLK		1	95	40/43	100	CID
RS24_HUMAN	40S ribosomal protein S24	15,424					
	tHFGGGKTtGFGMIYDSLDYAK		6	95	57/43	97,70	CID
RLA0_HUMAN	60S acidic ribosomal protein P0	34,274					
	NVASVcLQIGYPTVASVPHsIINGYKR		1	93	45/43	49	CID
RLA2_HUMAN	60S acidic ribosomal protein P2	11,666					
	YVASYLLAALGGNSsPSAK		2	95	58/43	100	CID
RL11_HUMAN	60S ribosomal protein L11	20,253					
	YDPSIGIYGLDFYVVLGRPGFsIADKK		1	95	37/43	100	CID
RL12_HUMAN	60S ribosomal protein L12	17,819					
	VVYLRctGGEVGATSALAPK		23	95	71/43	99	CID
RL14_HUMAN	60S ribosomal protein L14	23,432					
	APGtKGtAAAAAAAAAAK		7	90	59/43	100, 100	CID
6PGD_HUMAN	6-phosphogluconate dehydrogenase, decarboxylating	53,142					
	ALYAsKIISYAQGFmLLR		2	95	51/43	81	CID
ACTS_HUMAN	Actin, alpha skeletal muscle	42,052					
	KDLYANNVmsGGTTmYPGIADR		3	95	33/43	100	CID
KAD2_HUMAN	Adenylate kinase 2, mitochondrial	26,479					
	AtMDAGKLVSDEMVVELIEK		5	95	65/43	99	CID

AKA12_HUMAN	A-kinase anchor protein 12	191,474					
	GsVEEPKPEEPK		1	95	47/43	100	CID
AKP8L_HUMAN	A-kinase anchor protein 8-like	71,650					
	AVLsERDLYR		3	95	39/43	87	CID
APLP1_HUMAN	Amyloid-like protein 1	72,176					
	EAVsGLLImGAGGGSLIVLSMLLLRR		1	95	41/43	45	CID
ANR16_HUMAN	Ankyrin repeat domain-containing protein 16	39,284					
	FLLQsGLK		2	95	53/43	91	CID
ANXA1_HUMAN	Annexin A1	38,716					
	amVsEFLKQAWFIENEEQEYVQTVK		3	95	44/43	100	CID
ANXA2_HUMAN	Annexin A2	38,606					
	ELAsALKsALSGHLETVILGLLK		1	95	51/43	100, 100	CID
ANXA3_HUMAN	Annexin A3	36,377					
	HYGYSLysAIKSDTSGDYEITLLK		3	94	56/42	42,92	CID
AP2A2_HUMAN	AP-2 complex subunit alpha-2	103,963					
	QLsNPQQEVQNIFK		1	95	56/43	89	CID
AATM_HUMAN	Aspartate aminotransferase, mitochondrial	47,519					
	YyDPKtcGFDFTGAVEDISK		9	95	72/43	55,90	CID
ABCE1_HUMAN	ATP-binding cassette sub-family E member 1	67,316					
	NTVANsPQTLLAGmNKFLSQLEITFR		1	91	43/43	43	CID
ACTBL_HUMAN	Beta-actin-like protein 2	42,004					
	MTQIMFEAFNTPAMyVAIQAVLSLYASGR		38	95	57/43	100	CID
	cPEAIFQPSFLGIEsSGIHETTFNSImK		1	95	30/43	100	CID
	EKMTQIMFEAFNtPAMYVAIQAVLSLYASGR		9	95	43/43	99	CID
BMP4_HUMAN	Bone morphogenetic protein 4	46,555					
	FLFNLsSIPENEVISSAELR		1	95	40/43	98	CID
KCC4_HUMAN	Calcium/calmodulin-dependent protein kinase type IV	51,926					
	tEIGVLLR		3	93	43/42	100	CID
CATB_HUMAN	Cathepsin B	37,821					
	NGPVEGAFSVYSDFLLYKsGVYQHVTGEmMGGHAIR		1	93	49/42	11	CID
CIDEA_HUMAN	Cell death activator CIDE-A	24,688					
	GVmASsLQELISK		1	95	46/43	63	CID
CENP1_HUMAN	CENPB DNA-binding domain-containing protein 1	21,053					
	SIIEEGEytPQVSLt		1	95	32/43	57,34,72	CID
CE350_HUMAN	Centrosome-associated protein 350	350,933					
	DNKAtSPGPtDLEtR		1	95	33/43	43,27,39	CID

CHKB_HUMAN	**Choline/ethanolamine kinase**	45,272					
	EPVLsAAIATK		2	95	46/43	71	CID
COPE_HUMAN	**Coatomer subunit epsilon**	34,483					
	LVLQYAPsA		1	90	40/43	95	CID
COF1_HUMAN	**Cofilin-1**	18,503					
	asGVAVSDGVIK		2	95	51/43	100	CID
COF2_HUMAN	**Cofilin-2**	18,737					
	StLGEKLGGNVVVSLEGKPL			95	56/43	42	CID
CO9A2_HUMAN	**Collagen alpha-2(IX) chain**	65,131					
	AAAtASPR		1	95	42/42	100	CID
CO6A6_HUMAN	**Collagen alpha-6(VI) chain**	247,178					
	mIsAGLPGEMGSPGEPGPPGR		2	95	30/43	29	CID
C1T9A_HUMAN	**Complement C1q and tumor necrosis factor-related protein 9A**	34,682					
	DAYMSsEDQASGGIVLQLK		1	95	33/43	34	CID
CSN1_HUMAN	**COP9 signalosome complex subunit 1**	55,538					
	MAAAFNTTVAALEDELTQLILEGLIsAR		1	95	53/43	76	CID
	IPPAIKsANsELGGIWSVGQR		3	92	48/43	100,100	CID
KCRB_HUMAN	**Creatine kinase B-type**	42,645					
	LAVEALSSLDGDLAGRyyALK		1	95	38/43	100,100	CID
CD11A_HUMAN	**Cyclin-dependent kinase 11A**	91,363					
	EYGsPLK		1	91	39/42	100	CID
CDK12_HUMAN	**Cyclin-dependent kinase 12**	164,159					
	WSDSSKQDDSPSGASYGQDyDLsPsR		1	94	30/43	100,100,100	CID
UCRI_HUMAN	**Cytochrome b-c1 complex subunit Rieske, mitochondrial**	29,668					
	GFSYLVtGVttVGVAYAAKNAVTQFVSSmSASADVLALAK		2	95	76/42	34,37.39	CID
CCHL_HUMAN	**Cytochrome c-type heme lyase**	30,602					
	DYQFtILDVRPALDSLSAVWDR		1	94	53/43	35	CID
ERCC6_HUMAN	**DNA excision repair protein ERCC-6**	168,419					
	VPVQEIDDDFFPSsGEEAEAASVGEGGGGGRK		1	95	30/43	32	CID
DUS4_HUMAN	**Dual specificity protein phosphatase 4**	42,954					
	LmNRDENGGGAGGSGSHGTLGLPsGGK		1	95	32/43	43	CID
DYM_HUMAN	**Dymeclin**	75,939					
	AAAsPELsSPLANQSLLLLLVLANLTDASDAPNPYRQAImSFK		4	95	39/42	23,21	CID
TRI23_HUMAN	**E3 ubiquitin-protein ligase TRIM23**	64,066					
	QDEFMQPIPtIGFNVETVEYK		1	95	49/43	76	CID

EXOS1_HUMAN	**Exosome complex component CSL4**	**21,452**					
	LcNLEEGSPGSGTYTRHGyIFsSLAGcLmK		1	91	50/43	31,38	CID
GNA1_HUMAN	**Glucosamine 6-phosphate N-acetyltransferase**	**20,749**					
	LNcyKItLEcLPQNVGFYK		3	95	36/43	100,100	CID
G3P_HUMAN	**Glyceraldehyde-3-phosphate dehydrogenase**	**36,053**					
	LtGMAFRVPTANVSVVDLTcR		8	95	72/43	99	CID
GRAP1_HUMAN	**GRIP1-associated protein 1**	**95,991**					
	SGLEELVLSEMNsPsR		1	95	50/43	45,63	CID
HSP72_HUMAN	**Heat shock-related 70 kDa protein 2**	**70,023**					
	SENVQDLLLLDVTPLSLGIEtAGGVmtPLIK		1	95	29/43	77,80	CID
HELQ_HUMAN	**Helicase POLQ-like**	**124,136**					
	LyLSFVLYTLLK		1	95	57/43	100	CID
ROA2_HUMAN	**Heterogeneous nuclear ribonucleoproteins A2/B1**	**37,430**					
	DyFEEyGKIDTIEIITDR		3	92	52/43	93,99	CID
HNRPC_HUMAN	**Heterogeneous nuclear ribonucleoproteins C1/C2**	**33,671**					
	SMNsRVFIGNLNTLVVK		2	95	51/43	78	CID
H14_HUMAN	**Histone H1.4**	**21,867**					
	sEtAPAAPAAPAPAEK		1	95	40/43	100, 100	CID
H1X_HUMAN	**Histone H1x**	**22,488**					
	NQPGKYsQLVVETIR		6	95	62/43	21	CID
SETD2_HUMAN	**Histone-lysine N-methyltransferase SETD2**	**287,597**					
	KsSEFLK		1	95	48/42	45	CID
HSDL2_HUMAN	**Hydroxysteroid dehydrogenase-like protein 2**	**45,397**					
	tAQPHPKLLGtIYTAAEEIEAVGGK		5	95	75/43	99, 100	CID
K1C17_HUMAN	**Keratin, type I cytoskeletal 17**	**48,107**					
	TIEELQNKILtATVDNANILLQIDNAR		15	95	56/43	98	CID
K1C18_HUMAN	**Keratin, type I cytoskeletal 18**	**48,059**					
	NHEEEVKGLQAQIAsSGLTVEVDAPK		5	93	44/43	100	CID
K2C1_HUMAN	**Keratin, type II cytoskeletal 1**	**66,040**					
	MsGEcAPNVSVSVSTSHTTISGGGSR		2	95	31/43	43	CID
K2C6A_HUMAN	**Keratin, type II cytoskeletal 6A**	**60,046**					
	AIGGGLSSVGGGSSTIKyTTtSSssR		2	93	56/43	42,57,57,81	CID
K2C7_HUMAN	**Keratin, type II cytoskeletal 7**	**51,387**					
	TLNETELtELQsQISDTSVVLSmDNSR		17	95	61/43	99,87	CID
K2C79_HUMAN	**Keratin, type II cytoskeletal 79**	**57,836**					
	QTYSTKGGFSSNSASGGsGsQAR		1	95	28/43	78,83	CID

LARP1_HUMAN	**La-related protein 1**	**123,513**					
	GEGSDsKESPK		1	95	35/43	100	CID
LIPM_HUMAN	**Lipase member M**	**48,234**					
	EFLyQTR		1	90	40/43	76	CID
LDH6B_HUMAN	**L-lactate dehydrogenase A-like 6B**	**41,944**					
	LMISSIVQYsPHcKLIIVSNPVDILTYVAWK		1	95	91/43	18	CID
LDHB_HUMAN	**L-lactate dehydrogenase B chain**	**36,639**					
	GytNWAIGLSVADLIESMLK		2	95	43/43	100,100	CID
	IHPVstMVKGMYGIENEVFLSLPcILNAR		5	95	66/43	79,73	CID
LONF1_HUMAN	**LON peptidase N-terminal domain and RING finger protein 1**	**86,726**					
	mSsPAVARTsPGGSR		1	95	49/43	67,63	CID
L12R1_HUMAN	**Loss of heterozygosity 12 chromosomal region 1 protein**	**22,223**					
	MGsEQSSEAESRPNDLNSSVTPSPAK		1	95	34/43	77	CID
GMPPB_HUMAN	**Mannose-1-phosphate guanyltransferase beta**	**39,834**					
	ALILVGGyGtR		1	95	28/43	43,21	CID
MA7D3_HUMAN	**MAP7 domain-containing protein 3**	**98,431**					
	ESMEAsPEAmVK		1	95	33/43	45	CID
MALD1_HUMAN	**MARVEL domain-containing protein 1**	**18,915**					
	WLmVNVAHDVLAAALYGAATGImSDQmQRHsycNLK		1	95	46/42	99,99	CID
MARE1_HUMAN	**Microtubule-associated protein RP/EB family member 1**	**30,000**					
	mAVNVYStsVTSDNLSRHDmLAWINESLQLNLTK		1	95	54/42	41,23	CID
M4K2_HUMAN	**Mitogen-activated protein kinase kinase kinase kinase 2**	**91,558**					
	VVRNPYtGATFLLAALPTSLLLLQWyEPLQK		1	95	25/43	54,62	CID
MYL6_HUMAN	**Myosin light polypeptide 6**	**16,930**					
	HVLVTLGEKmtEEEVEmLVAGHEDSNGcINYEAFVR		1	95	45/43	98	CID
ML12B_HUMAN	**Myosin regulatory light chain 12B**	**19,780**					
	NAFAcFDEEATGTIQEDYLRELLttMGDR		1	95	46/43	71,73	CID
MTMRC_HUMAN	**Myotubularin-related protein 12**	**86,150**					
	LINssDELQDNFR		1	95	56/43	99,99	CID
MTMR8_HUMAN	**Myotubularin-related protein 8**	**78,921**					
	SVTLGtVVGSsK		3	95	46/43	100,50	CID
NAA10_HUMAN	**N-alpha-acetyltransferase 10**	**26,459**					
	GLAAEDSGGDsK		1	95	31/43	100	CID
NPHP3_HUMAN	**Nephrocystin-3**	**150,870**					
	NLAVLSyEGGDFEK		1	95	29/43	43	CID

AHNK_HUMAN	**Neuroblast differentiation-associated protein AHNAK**	**629,104**					
	AGAISASGPELQGAGHsKLQVTMPGIK		1	95	30/43	100	CID
NPM_HUMAN	**Nucleophosmin**	**32,576**					
	VtLATLKmsVQPTVsLGGFEITPPVVLR		3	95	51/43	100,100,100	CID
NDKB_HUMAN	**Nucleoside diphosphate kinase B**	**17,298**					
	ymNSGPVVAmVWEGLNVVK		2	95	41/43	88	CID
	YmNsGPVVAmVWEGLNVVK		1	95	69/43	13	CID
O10P1_HUMAN	**Olfactory receptor 10P1**	**34,743**					
	mAGENHTTLPEFLLLGFsDLK		1	95	33/43	21	CID
OR6B1_HUMAN	**Olfactory receptor 6B1**	**35,301**					
	LALGSWAIGFGIsLAK		3	91	46/43	44	CID
PPIA_HUMAN	**Peptidyl-prolyl cis-trans isomerase A**	**18,013**					
	MVNPtVFFDIAVDGEPLGR		8	95	48/43	100	CID
PAL4G_HUMAN	**Peptidyl-prolyl cis-trans isomerase A-like 4G**	**18,166**					
	HtGSGILSMANAGPNTNGSQFFIcTAK		1	92	45/43	88	CID
PPIF_HUMAN	**Peptidyl-prolyl cis-trans isomerase F, mitochondrial**	**22,040**					
	AcSKGsGDPSSSSSSGNPLVYLDVDANGKPLGR		3	95	72/43	78	CID
PEX19_HUMAN	**Peroxisomal biogenesis factor 19**	**32,807**					
	ETLsGLAKNAtDLQNSSmSEEELTK		2	95	51/43	60,83	CID
PGK1_HUMAN	**Phosphoglycerate kinase 1**	**44,615**					
	AsLsKLGDVYVNDAFGTAHR		13	95	58/43	100,100	CID
	TGQATVASGIPAGWMGLDcGPEsSK		5	95	34/43	83	CID
PFD2_HUMAN	**Prefoldin subunit 2**	**16,648**					
	SSGsGAGKGAVSAEQVIAGFNR		1	95	35/43	25	CID
PFD3_HUMAN	**Prefoldin subunit 3**	**22,659**					
	NLSTAtKNLDSLEEDLDFLR		1	95	48/43	28	CID
PAWR_HUMAN	**PRKC apoptosis WT1 regulator protein**	**36,568**					
	mATGGYRtsSGLGGSTTDFLEEWK		1	95	66/43	47,47	CID
PROF1_HUMAN	**Profilin-1**	**15,054**					
	mAGWNAyIDNLmADGTcQDAAIVGYK		20	95	46/43	100	CID
PDCD5_HUMAN	**Programmed cell death protein 5**	**14,285**					
	EAEmRNsILAQVLDQSAR		1	95	53/43	100	CID
PHB2_HUMAN	**Prohibitin-2**	**33,298**					
	TIAtsQNRIYLtADNLVLNLQDESFTR		2	95	59/43	41,84,45	CID
PSME2_HUMAN	**Proteasome activator complex subunit 2**	**27,402**					
	AFYAELYHIISsNLEKIVNPK		1	90	49/43	100	CID

PSA2_HUMAN	Proteasome subunit alpha type-2	25,899					
	GysFsLttFSPSGKLVQIEYALAAVAGGAPSVGIK		1	95	53/43	92,86,84,73	CID
PSA5_HUMAN	Proteasome subunit alpha type-5	26,411					
	LFQVEYAIEAIKLGSTAIGIQtsEGVcLAVEK		1	95	60/43	95,95	CID
PSB7_HUMAN	Proteasome subunit beta type-7	29,966					
	FRPDMEEEEAKNLVsEAIAAGIFNDLGSGSNIDLcVISK		6	95	89/42	43	CID
AHNK2_HUMAN	Protein AHNAK2	616,628					
	VEVTSPNLDVsLPSmEVDIQAPGAKLDStR		1	91	22/43	82	CID
	smEASVDVtAPK		1	95	53/43	100100	CID
DPY30_HUMAN	Protein dpy-30 homolog	11,250					
	MEPEQMLEGQtQVAENPHSEYGLTDNVER		1	95	22/43	100	CID
MIDA_HUMAN	Protein midA homolog, mitochondrial	49,239					
	DHVEVcPDAGVIIEELSQRIALtGGAALVADyGHDGtK		1	95	31/43	63,90,85	CID
MUTED_HUMAN	Protein Muted homolog	21,610					
	msGGGTETPVGcEAAPGGGsK		1	95	33/43	99,99	CID
PPR29_HUMAN	Protein phosphatase 1 regulatory subunit 29	89,689					
	RDSTYsQLSPR		3	95	42/43	23	CID
VPRBP_HUMAN	Protein VPRBP	169,011					
	DENsQLVAIVLR		1	90	43/43	100	CID
PLP2_HUMAN	Proteolipid protein 2	16,691					
	MADsERLsAPGcWAAcTNFSR		18	95	60/43	100100	CID
PSYR_HUMAN	Psychosine receptor	39,335					
	yLAVVYPLK		1	95	56/43	100	CID
ASXL3_HUMAN	Putative Polycomb group protein ASXL3	241,919					
	EAAAAAAVAAAASIVsGAmGsPGEGGKtR		1	95	31/43	23,27,67	CID
CAF17_HUMAN	Putative transferase CAF17, mitochondrial	38,156					
	yLQGVPEGVRDLPPGVALPLESNLAFMNGVSFTK		1	94	27/43	100,	CID
CX069_HUMAN	Putative uncharacterized protein CXorf69	9,236					
	EALGSGHYVGGsIRSMAAAALSGLAVR		1	95	25/43	19	CID
VSIG7_HUMAN	Putative V-set and immunoglobulin domain-containing protein 7	13,301					
	ILFLVVIAAGAQSQVQLmQsGAEVKKPGASVR		1	95	36/43	31	CID
RB11B_HUMAN	Ras-related protein Rab-11B	24,489					
	NNLSFIETSALDSTNVEEAFKNILtEIyR		4	95	63/43	94,83	CID
RAB21_HUMAN	Ras-related protein Rab-21	24,348					
	HVSIQEAESYAESVGAKHyHTSAK		1	95	58/43	32	CID

RFC2_HUMAN	**Replication factor C subunit 2**	**39,158**					
	yRPVKLNEIVGNEDTVSR		1	95	51/43	100	CID
RTBDN_HUMAN	**Retbindin**	**24,615**					
	mDcRVHmRPIGLTWVLQLtLAWILLEAcGGsRPLQAR		1	95	32/42	80,96	CID
RHG23_HUMAN	**Rho GTPase-activating protein 23**	**162,197**					
	LsPPAAPEERPAADTRSIVSGYSTLSTmDR		1	95	35/43	78	CID
ARHGI_HUMAN	**Rho guanine nucleotide exchange factor 18**	**130,784**					
	GTLLsDGsPALSR		1	93	44/43	73,78	CID
PRPS2_HUMAN	**Ribose-phosphate pyrophosphokinase 2**	**34,770**					
	LLsAGAtKVYAILTHGIFSGPAISR		2	95	42/43	86,58	CID
RYR2_HUMAN	**Ryanodine receptor 2**	**564,570**					
	SSTLQQLIsETmVR		1	95	41/43	47	CID
SALL4_HUMAN	**Sal-like protein 4**	**112,231**					
	SSLPstFIR		2	95	52/43	100,100	CID
PP1RA_HUMAN	**Serine/threonine-protein phosphatase 1 regulatory subunit 10**	**99,059**					
	LSHDNmEEKVPWVcPRPLVLPSPLVTPGsNsQER		1	95	28/43	82,80	CID
SPB6_HUMAN	**Serpin B6**	**42,623**					
	TYIGEIFTQILVLPYVGKELNMIImLPDEttDLR		1	95	53/42	21,19	CID
MTAP_HUMAN	**S-methyl-5'-thioadenosine phosphorylase**	**31,236**					
	AEsFMFRtWGADVINmTTVPEVVLAK			95	51/43	100,100	CID
STMN1_HUMAN	**Stathmin**	**17,303**					
	ASGQAFELILsPR		2	95	54/43	100	CID
SMC5_HUMAN	**Structural maintenance of chromosomes protein 5**	**128,810**					
	YVVKTSFYsNK		2	95	32/43	100	CID
	YVVKTSFySNK		4	95	29/43	81	CID
SODC_HUMAN	**Superoxide dismutase [Cu-Zn]**	**15,935**					
	DGVADVSIEDSVISLSGDHcIIGRtLVVHEK		1	95	57/43	91	CID
TCPH_HUMAN	**T-complex protein 1 subunit eta**	**59,368**					
	QQLLIGAyAKALEIIPR		1	95	39/43	100	CID
THEM5_HUMAN	**Thioesterase superfamily member 5**	**27,678**					
	GLKLPSGLAVsSDK		1	95	30/43	100	CID
THIO_HUMAN	**Thioredoxin**	**11,737**					
	QIESKtAFQEALDAAGDK		9	95	63/43	79	CID
ELOC_HUMAN	**Transcription elongation factor B polypeptide 1**	**12,473**					
	mDGEEKtYGGcEGPDAmYVK		2	95	51/43	29	CID
	EHALtSGTIKAmLSGPGQFAENETNEVNFR		2	95	65/43	24	CID

BTF3_HUMAN	**Transcription factor BTF3**	22,168					
	VQAsLAANTFTLTGHAEtKQLtEmLPSILNQLGADSLTSLR		3	95	80/42	100,64,69	CID
TFR1_HUMAN	**Transferrin receptor protein 1**	84,874					
	mmDQARsAFSNLFGGEPLSYTR		2	95	45/43	65	CID
TAGL2_HUMAN	**Transgelin-2**	22,392					
	ENFQNWLKDGtVLcELINALYPEGQAPVK		2	95	51/43	100	CID
T200A_HUMAN	**Transmembrane protein 200A**	54,358					
	SsMALGPGAGQLLSPGAARR		1	95	31/43	100	CID
TPIS_HUMAN	**Triosephosphate isomerase**	30,791					
	VVLAYEPVWAIGTGKtAtPQQAQEVHEK		2	90	51/43	96,86	CID
UBP36_HUMAN	**Ubiquitin carboxyl-terminal hydrolase 36**	122,653					
	tGSSSLPGRPSVIPDHSKK		2	95	37/43	100	CID
UB2D2_HUMAN	**Ubiquitin-conjugating enzyme E2 D2**	16,736					
	SQWSPALTISKVLLsIcsLLcDPNPDDPLVPEIAR		1	95	33/43	30,30	CID
CL043_HUMAN	**Uncharacterized protein C12orf43**	28,171					
	LFFtSVPGGREK		1	95	50/43	100	CID
MYO1F_HUMAN	**Unconventional myosin-If**	124,847					
	SSQAPtRAAPAPPR		1	95	33/43	100	CID
SC22B_HUMAN	**Vesicle-trafficking protein SEC22b**	24,594					
	VLLtmIARVADGLPLAASmQEDEQSGR		4	95	48/43	100	CID
WEE2_HUMAN	**Wee1-like protein kinase 2**	62,926					
	LFLQsGGK		2	93	43/42	100	CID
ZBT7A_HUMAN	**Zinc finger and BTB domain-containing protein 7A**	61,440					
	aGGVDGPIGIPFPDHsSDILSGLNEQR		1	95	32/43	72	CID

Total phosphoproteins	147
Spectral count	447
Number of different phosphopeptides	153
Number of multiply phosphorylated peptides	135
Number of singly phosphorylated peptides	312
Number of each phosphorylated amino acid observed	256(pS), 234(pT), 66(pY)
Number of unique phosphorylated amino acids	304

[a] Peptides identified by MS were searched for serine, threonine, or tyrosine residues containing a +80 m/z modification, which is consistent with the presence of a phosphate group. 50% protein and 80% peptides cutoffs were used to generate the Scaffold coverage which scored above 1.1% FDR threshold. [b] SC=Spectral Count. [c] PP= Peptide probability (written as percentage). [d] IS= Ion Score. [e] IDS= Identity Score. [f] LP= Localization Probability (written as a percentage, multiple numbers corresponding to the value of each site). [g] IM= Ionization Method. CID=Collision Induced Dissociation.

Table A 4.6: Phosphopeptides identified by MS analysis after purification of a HeLa cell lysate trypsin digestion using TiO$_2$ affinity chromatography [a]

Accession	Protein/peptide name	MW (Da)	SC[b]	PP[c]	IS[d]/IDS[e]	LP[f]	IM[g]
U5S1_HUMAN	116 kDa U5 small nuclear ribonucleoprotein component	109,420					
	mDTDLYDEFGNYIGPELDsDEDDDELGRETK		3	95	82/46	51	CID
RS27_HUMAN	40S ribosomal protein S27	9,443					
	PLAKDLLHPsPEEEK		1	87	49/48	100	ETD
RLA0L_HUMAN	60S acidic ribosomal protein P0-like	34,347					
	EESEEsDEDmGFGLFD		9	95	65/46	100	CID
RLA2_HUMAN	60S acidic ribosomal protein P2	11,647					
	EESEEsDDDMGFGLFD		4	95	68/46	100	CID
	KEESEEsDDDMGFGLFD		34	95	7846	100	CID
RL17_HUMAN	60S ribosomal protein L17	21,379					
	VRYsLDPENPTK		3	95	63/48	100	both
	VRySLDPENPTK		1	88	49/48	100	ETD
RL3_HUMAN	60S ribosomal protein L3	46,092					
	HGsLGFLPR		1	89	33/45	100	CID
MEPCE_HUMAN	7SK snRNA methylphosphate capping enzyme	74,338					
	tsSKsEAGARGGGQGsK		1	84	50/48	92,71, 81,82	ETD
ANLN_HUMAN	Actin-binding protein anillin	124,184					
	TPIsPLKTGVSKPIVK		1	89	50/48	29	ETD
CAP1_HUMAN	Adenylyl cyclase-associated protein 1	51,838					
	EMNDAAMFyTNR		1	86	35/46	100	CID
	SGPKPFSAPKPQTsPSPK		6	95	63/48	92	ETD
AK1C1_HUMAN	Aldo-keto reductase family 1 member C1	36,771					
	dAGLAKSIGVsNFNR		1	95	58/48	32	ETD
ANR53_HUMAN	Ankyrin repeat domain-containing protein 53	59,514					
	AtALsKTPEQR		1	79	46/47	100,100	CID
AGAP2_HUMAN	Arf-GAP with GTPase, ANK repeat and PH domain-containing protein 2	124,659					
	gSKSSAGTGAsVsAAAtAAAAGGGGSTASTSGGVGAGAGAR		1	94	63/49	22,32, 22	ETD
ARGL1_HUMAN	Arginine and glutamate-rich protein 1	33,199					
	ASsPPDRIDIFGR		1	84	47/48	100	ETD
ABCF1_HUMAN	ATP-binding cassette sub-family F member 1	95,910					
	LSVPTsDEEDEVPAPKPR		3	95	56/48	99	both
ACLY_HUMAN	ATP-citrate synthase	120,825					

	AKPAMPQDSVPsPR		1	86	48/48	100	ETD
ATN1_HUMAN	**Atrophin-1**	**124,756**					
	ASPGGVStSSSDGKAEK		1	86	49/48	12	ETD
SYEP_HUMAN	**Bifunctional aminoacyl-tRNA synthetase**	**170,575**					
	EYIPGQPPLSQSSDSsPTRNSEPAGLETPEAK		1	84	36	26	CID
UIMC1_HUMAN	**BRCA1-A complex subunit RAP80**	**79,709**					
	vKEVSEsRNLEK		1	82	52/48	50	ETD
BRD4_HUMAN	**Bromodomain-containing protein 4**	**152,199**					
	LNLPDYyKIIK		1	95	6048	94	ETD
CLCA4_HUMAN	**Calcium-activated chloride channel regulator 4**	**101,267**					
	KIEAtRcSAGIsGR		1	82	46/48	63,67	ETD
KAP0_HUMAN	**cAMP-dependent protein kinase type I-alpha regulatory subunit PE=1 SV=1**	**42,964**					
	TDSREDEIsPPPPNPVVK		1	83	36/46	99	CID
KAP2_HUMAN	**cAMP-dependent protein kinase type II-alpha regulatory subunit**	**45,501**					
	AATIVATSEGsLWGLDR		1	79	46/48	26	CID
CSKI2_HUMAN	**Caskin-2**	**126,768**					
	GLLQGEALsEGGRR		1	84	47/48	100	ETD
CTNA1_HUMAN	**Catenin alpha-1**	**100,055**					
	TPEELDDsDFETEDFDVR		2	95	76/46	45	ETD
CHD8_HUMAN	**Chromodomain-helicase-DNA-binding protein 8**	**290,503**					
	SQEILSQGNPFmGVSATAVSsssAGGQPPQSAPK		1	86	68/48	27,26,65	ETD
CTF18_HUMAN	**Chromosome transmission fidelity protein 18 homolog**	**107,366**					
	GDAAssPAPAAsVGsSQGGARK		1	95	51/48	83,84,76,65	ETD
CCD46_HUMAN	**Coiled-coil domain-containing protein 46**	**112,733**					
	SSQIIAELQttIsSLK		1	95	58/46	57,66,23	ETD
COHA1_HUMAN	**Collagen alpha-1(XVII) chain**	**150,404**					
	rGSSySSsmsTGGGGAGsLGAGGAFGEAAGDR		1	85	57/49	54,41,67,29	ETD
CNTP4_HUMAN	**Contactin-associated protein-like 4**	**145,259**					
	GsVTGAVLK		1	83	53/46	100	ETD
CORO7_HUMAN	**Coronin-7**	**100,588**					
	DGALVGtAcKDKQLR		1	92	54/48	100	ETD
CXXC5_HUMAN	**CXXC-type zinc finger protein 5**	**32,960**					
	sLRRSRPLSHYSSFGSSGGSGGGsMmGGEsADK		1	86	70/49	48,37	ETD
CNGB3_HUMAN	**Cyclic nucleotide-gated cation channel beta-3**	**92,235**					
	LFKtLLGGTGKASLAR		1	79	45/48	99	ETD

DC1L1_HUMAN	Cytoplasmic dynein 1 light intermediate chain 1	56,562					
	DFQEYVEPGEDFPAsPQRR		1	95	39/46	99	ETD
CYTSA_HUMAN	Cytospin-A	124,587					
	StcPsAAPsASAPAMTTVENKsK		1	95	44/49	62,63,60,60	ETD
DSC3_HUMAN	Desmocollin-3	99,953					
	gWITIDEIsGSIITSK		1	84	48/48	81	ETD
DNMT1_HUMAN	DNA (cytosine-5)-methyltransferase 1	183,151					
	LVMAGETtNSRGQR		1	79	47/48	17	ETD
MCM2_HUMAN	DNA replication licensing factor MCM2	101,880					
	AIPELDAYEAEGLALDDEDVEELTAsQR		1	93	40/46	98	CID
	GLLYDsDEEDEERPARK		1	80	36/46	89	CID
	GLLYDsDEEDEERPAR		1	81	32/46	99	CID
	RGLLYDsDEEDEERPAR		1	95	55/46	23	CID
DMRT1_HUMAN	Doublesex- and mab-3-related transcription factor 1	39,455					
	AGGFGKASGALVGAASGSSAGGsSRGGGSGSGASDLGAGSK		1	95	75/49	13	ETD
HUWE1_HUMAN	E3 ubiquitin-protein ligase HUWE1	481,874					
	GSGTAsDDEFENLR		1	95	49/46	100	CID
EF1B_HUMAN	Elongation factor 1-beta	24,746					
	YGPADVEDTTGSGATDSKDDDDIDLFGsDDEEESEEAK		8	95	98/45	99	CID
EF1D_HUMAN	Elongation factor 1-delta	31,104					
	KPATPAEDDEDDDIDLFGsDNEEEDKEAAQLR		2	95	57/46	95	both
ENPL_HUMAN	Endoplasmin	92,454					
	EEsDDEAAVEEEEEEKKPK		2	95	45/46	100	CID
	VEEEPEEEPEETAEDTTEDTEQDEDEEMDVGtDEEEETAK		1	95	102/45	27	CID
EIF2A_HUMAN	Eukaryotic translation initiation factor 2A	64,973					
	SDKsPDLAPTPAPQSTPR		4	89	51/48	92	both
EIF3B_HUMAN	Eukaryotic translation initiation factor 3 subunit B	92,465					
	ALENGDADEPSFsDPEDFVDDVsEEELLGDVLK		5	95	55/46	78, 100	CID
EIF3C_HUMAN	Eukaryotic translation initiation factor 3 subunit C	105,329					
	QPLLLsEDEEDTKR		1	94	56/48	100	ETD
EIF3G_HUMAN	Eukaryotic translation initiation factor 3 subunit G	35,594					
	GIPLATGDtSPEPELLPGAPLPPPKEVINGNIK		2	95	48/46	71	CID
EIF3J_HUMAN	Eukaryotic translation initiation factor 3 subunit J	29,045					
	aAAAAAAGDSDsWDADAFSVEDPVR		15	95	115/46	100	CID
IF4G3_HUMAN	Eukaryotic translation initiation factor 4	176,638					

gamma 3

	DITEEIMSGGGsR		1	92	53/48	39	ETD
IF2P_HUMAN	**Eukaryotic translation initiation factor 5B**	138,813					
	NKPGPNIEsGNEDDDASFK		2	93	39/46	100	CID
FAS_HUMAN	**Fatty acid synthase**	273,409					
	QGVQVQVstSNISSLEGAR		2	95	60/49	79,95	ETD
FBSP1_HUMAN	**F-box/SPRY domain-containing protein 1**	30,615					
	aAPAPGAGAAsGGAGcSGGGAGAGAGSGsGAAGAGGR		1	86	71/49	38,42	ETD
FOXK1_HUMAN	**Forkhead box protein K1**	75,439					
	EGsPIPHDPEFGSK		1	81	45/48	100	ETD
FREM2_HUMAN	**FRAS1-related extracellular matrix protein 2**	351,137					
	TGTDLsK		1	95	65/49	96	ETD
F16A2_HUMAN	**FTS and Hook-interacting protein**	105,552					
	DGAGLGLSGGsPGAstPVLLTR		1	90	52/49	45,37,66	ETD
GRIN3_HUMAN	**G protein-regulated inducer of neurite outgrowth 3**	82,420					
	LsDscGsIsKADHSGSLDPTNK		1	80	47/49	68,88,78,57	ETD
CXA3_HUMAN	**Gap junction alpha-3 protein**	47,411					
	asKASRASsGR		1	89	50/47	95, 100	ETD
GLYG2_HUMAN	**Glycogenin-2**	55,166					
	IVVLItPQVssLLR		1	88	38/46	100,100,100	CID
GCC2_HUMAN	**GRIP and coiled-coil domain-containing protein 2**	184,642					
	KtVETLQQQLsK		1	95	60/48	88,65	ETD
RAD_HUMAN	**GTP-binding protein RAD**	33,227					
	MtLNGGGSGAGGsR		1	81	50/48	96,46	ETD
HS90A_HUMAN	**Heat shock protein HSP 90-alpha**	84,645					
	ESEDKPEIEDVGsDEEEEK		2	95	49/46	100	CID
	ESEDKPEIEDVGsDEEEEKK		2	95	49/46	100	both
	EEKESEDKPEIEDVGsDEEEEKK		2	92	76/46	100	both
	ESEDKPEIEDVGsDEEEEKKDGDK		1	95	48/46	100	ETD
HSP72_HUMAN	**Heat shock-related 70 kDa protein 2**	70,005					
	lyQGGPGGGsGGGGSGAsGGPtIEEVD		1	95	64/49	85,98,97,99	ETD
HDGF_HUMAN	**Hepatoma-derived growth factor**	26,771					
	AGDLLEDsPKRPK		8	95	66/46	100	both
HNRPU_HUMAN	**Heterogeneous nuclear ribonucleoprotein U**	90,567					
	LQAALDDEEAGGRPAMEPGNGsLDLGGDSAGR		5	95	54/46	100	CID
HNRL2_HUMAN	**Heterogeneous nuclear ribonucleoprotein U-like protein 2**	85,087					

	sGDETPGSEVPGDKAAEEQGDDQDSEK		1	95	51/46	100	CID
H1X_HUMAN	**Histone H1x**	**22,470**					
	sVELEEALPVTTAEGMAK		6	95	96/46	100	CID
RBBP7_HUMAN	**Histone-binding protein RBBP7**	**47,802**					
	asKEMFEDTVEER		4	95	58/46	100	CID
CUX1_HUMAN	**Homeobox protein cut-like 1**	**164,172**					
	TSAScSPAPESPMSSsEsVK		1	81	49/49	92,16	ETD
HXA3_HUMAN	**Homeobox protein Hox-A3**	**46,351**					
	vEmANLLNLtER		1	79	45/48	100	CID
HXB3_HUMAN	**Homeobox protein Hox-B3**	**44,323**					
	ESRQTsK		1	79	45/47	43	CID
CDC37_HUMAN	**Hsp90 co-chaperone Cdc37**	**44,450**					
	vDYSVWDHIEVsDDEDETHPNIDTASLFR		1	85	37/46	73	CID
LV001_HUMAN	**Ig lambda chain V region 4A**	**12,362**					
	ALIYSTsNK		2	95	44/45	38	CID
IGS10_HUMAN	**Immunoglobulin superfamily member 10**	**290,823**					
	TSALMEAEVGKHTsstsKR		1	81	49/49	70,82,70,93	ETD
INT3_HUMAN	**Integrator complex subunit 3**	**118,056**					
	GAAAAAAASGAAGGGGGGGAGAGAPGGGRLLLSTsLDAK		1	85	49/49	25	ETD
HABP4_HUMAN	**Intracellular hyaluronan-binding protein 4**	**45,767**					
	GGRsPAGASGHRAGAGGR		1	89	50/48	99	ETD
KLD10_HUMAN	**Kelch domain-containing protein 10**	**49,081**					
	RGGGAAGAGGGGSGAGGGsGGSGGR		1	95	63/48	44	ETD
K2C1_HUMAN	**Keratin, type II cytoskeletal 1**	**66,022**					
	GGGGGGYGSGGSSYGSGGGsYGsGGGGGGGR		1	95	47/49	20	ETD
K22E_HUMAN	**Keratin, type II cytoskeletal 2 epidermal**	**65,416**					
	GGSIsGGGyGsGGGK		1	82	46/48	96,100,100	ETD
K2C6A_HUMAN	**Keratin, type II cytoskeletal 6A**	**60,028**					
	sLyGLGGSKRISIGGGScAIsGGYGsR		1	95	55/49	62,26,25	ETD
KLF3_HUMAN	**Krueppel-like factor 3**	**38,811**					
	RASPGLSMPssSPPIK		1	81	48/48	34,38	ETD
LMNA_HUMAN	**Lamin-A/C**	**74,123**					
	SGAQASSTPLSPtRITR		3	95	88/48	100	both
LARP1_HUMAN	**La-related protein 1**	**123,495**					
	GLSAsLPDLDSENWIEVK		4	95	48/46	82	CID
BAT2_HUMAN	**Large proline-rich protein BAT2**	**228,848**					

	GGGtGGPNHPPAPRGR		1	92	53/48	100	ETD
LSG1_HUMAN	Large subunit GTPase 1 homolog	75,208					
	yILKDyVsGK		1	81	51/48	100,100,100	ETD
LMBL3_HUMAN	Lethal(3)malignant brain tumor-like protein 3	88,319					
	MtESASstSGQEFDVFSVmDWKDGVGtLPGSDLK		1	91	37/45	93,91,84,83	CID
LRFN2_HUMAN	Leucine-rich repeat and fibronectin type-III domain-containing protein 2	84,715					
	NELLDFtASLAR		1	80	47/48	50	ETD
LA_HUMAN	Lupus La protein	46,821					
	FAsDDEHDEHDENGATGPVKR		2	95	98/49	100	ETD
KDM2B_HUMAN	Lysine-specific demethylase 2B	152,599					
	ESDHSRsssPtAGPSTEGAEGPEEK		1	86	68/49	63,53,79,66	ETD
KDM3B_HUMAN	Lysine-specific demethylase 3B	191,594					
	GGNAsGEPGLDQR		2	93	54/47	100	ETD
MISSL_HUMAN	MAPK-interacting and spindle-stabilizing protein-like	24,251					
	sDEFSLADALPEHsPAK		2	95	54/46	100	CID
MED1_HUMAN	Mediator of RNA polymerase II transcription subunit 1	168,464					
	LAsPmKPVPGtPPSSKAKSPISSGSGGSHmSGTSSSsGMK		1	83	81/49	34,34,21	ETD
ICLN_HUMAN	Methylosome subunit pICln	26,197					
	FEEESKEPVADEEEEDsDDDVEPITEFR		9	95	78/46	100	CID
MFAP1_HUMAN	Microfibrillar-associated protein 1	51,941					
	SLAALDALNtDDENDEEEYEAWKVR		1	95	62/46	99	CID
MAP4_HUMAN	Microtubule-associated protein 4	120,988					
	DMEsPTKLDVTLAK		5	95	100/48	96	both
	DMSPLSETEMALGKDVtPPPETEVVLIK		1	95	43/46	93	CID
MTUS2_HUMAN	Microtubule-associated tumor suppressor candidate 2	150,178					
	IDQNtVVTR		1	79	45/47	97	CID
MUC16_HUMAN	Mucin-16	2,353,421					
	IEmEStFSVAHGLKGTSTSQDPIVSTEK		1	90	55/49	13	ETD
MBNL1_HUMAN	Muscleblind-like protein 1	41,799					
	AAQYQVNQAAAAQAAATAAAMtQsAVKsLK		1	82	46/49	70,66,41	ETD
MEF2A_HUMAN	Myocyte-specific enhancer factor 2A	54,794					
	NRQVTFtK		1	79	45/47	50	CID
NAT10_HUMAN	N-acetyltransferase 10	115,690					
	aIEEQmVAAKDVVMEPTMKTLsDDLDEAAK		1	91	57/49	90	ETD
SIRT1_HUMAN	NAD-dependent deacetylase sirtuin-1	81,665					

	aDEAALALQPGGsPSAAGADR		1	95	66/46	99	CID
NACA_HUMAN	**Nascent polypeptide-associated complex subunit alpha**	**23,365**					
	VQGEAVSNIQENTQTPTVQEEsEEEEVDETGVEVK		4	95	96/45	98	CID
NEO1_HUMAN	**Neogenin**	**159,999**					
	sGSAPQSPGAsIR		1	95	56/47	16	ETD
CHL1_HUMAN	**Neural cell adhesion molecule L1-like protein**	**135,042**					
	LtVNssNsIK		1	90	51/48	100,100,99,99	ETD
AHNK_HUMAN	**Neuroblast differentiation-associated protein AHNAK**	**629,086**					
	GGVTGsPEASISGSKGDLK		2	90	52/48	86	ETD
	GKGGVTGsPEASISGSKGDLK		2	95	59/48	38	ETD
	LKsEDGVEGDLGETQSR		2	95	62/48	100	ETD
	DIDISsPEFK		1	95	37/46	100	CID
	GKGGVTGSPEAsISGSKGDLK		1	83	36/46	24	CID
NIBL1_HUMAN	**Niban-like protein 1**	**82,666**					
	AAPEAsSPPASPLQHLLPGK		1	85	48/48	29	ETD
	AKQVVSVVQDEEVGLPFEASPEsPPPASPDGVTEIR		1	88	37/45	21	ETD
NCOA1_HUMAN	**Nuclear receptor coactivator 1**	**156,739**					
	VNPsVNPSISPAHGVAR		1	82	47/48	79	ETD
NUCKS_HUMAN	**Nuclear ubiquitous casein and cyclin-dependent kinases substrate**	**27,279**					
	EMLMEDVGsEEEQEEEDEAPFQEK		3	95	49/46	100	CID
NUCL_HUMAN	**Nucleolin**	**76,598**					
	KEDsDEEEDDDsEEDEEDDEDEDEDEDEIEPAAmK		7	95	96/48	100,100	CID
	AAAAAPAsEDEDDEDDDEDDEDDDDDEEDDsEEEAMETTPAK		1	95	76/45	100,100	CID
	AIRLELQGPRGsPNAR		4	95	85/48	100	ETD
	LELQGPRGsPNAR		3	95	78/45	100	ETD
NPM_HUMAN	**Nucleophosmin**	**32,557**					
	cGSGPVHISGQHLVAVEEDAEsEDEEEEDVK		9	95	61/46	100	CID
NPM3_HUMAN	**Nucleoplasmin-3**	**19,325**					
	aAGTAAALAFLsQESR		6	95	72/46	100	CID
NP1L4_HUMAN	**Nucleosome assembly protein 1-like 4**	**42,806**					
	EFITGDVEPTDAESEWHsENEEEEK		1	95	43/46	53	CID
OSB10_HUMAN	**Oxysterol-binding protein-related protein 10**	**83,953**					
	GVSSRSAAAGLGGGGSRssPGsVAAsPSGGGGR		1	95	56/49	46,46,31,82	ETD
OSBL8_HUMAN	**Oxysterol-binding protein-related protein 8**	**101,181**					
	tPMVSVPKmK		1	82	51/47	99	ETD
PHAR3_HUMAN	**Phosphatase and actin regulator 3**	**62,536**					
	tSsVERGKER		1	83	46/47	85,81	ETD

PAIRB_HUMAN	Plasminogen activator inhibitor 1 RNA-binding protein	44,948					
	TDKSSAsAPDVDDPEAFPALA		3	95	53/46	100	CID
	SSAsAPDVDDPEAFPALA		1	82	32/46	76	CID
DDX46_HUMAN	Probable ATP-dependent RNA helicase DDX46	117,348					
	AALGLQDsDDEDAAVDIDEQIESMFNSK		1	79	35/46	100	ETD
SYTC2_HUMAN	Probable threonyl-tRNA synthetase 2, cytoplasmic	92,631					
	NELSGTLsGLTR		1	93	54/47	14	ETD
PA2G4_HUMAN	Proliferation-associated protein 2G4	43,769					
	sGEDEQQEQTIAEDLVVTK		8	95	86/49	100	both
TEBP_HUMAN	Prostaglandin E synthase 3	18,680					
	DWEDDsDEDMSNFDR		6	95	78/46	100	CID
DEK_HUMAN	Protein DEK	42,658					
	EEsEEEEDEDDEEEEEEEKEK		2	95	43/46	100	CID
	sAsAPAAEGEGTPTQPASEKEPEMPGPR		1	79	36/46	43	CID
PDIA6_HUMAN	Protein disulfide-isomerase A6	48,104					
	DGELPVEDDIDLsDVELDDLGKDEL		8	95	79/46	100	CID
DOP1_HUMAN	Protein dopey-1	277,342					
	MTIAASAsLTTINLGATKNLR		1	84	50/49	18	ETD
DPY30_HUMAN	Protein dpy-30 homolog	11,232					
	iVENEKINAEKsSK		1	80	46/48	77	ETD
MUTED_HUMAN	Protein Muted homolog	21,592					
	MsGGGtEtPVGcEAAPGGGsKKR		1	95	44/49	100,99,99,99	ETD
PP14C_HUMAN	Protein phosphatase 1 regulatory subunit 14C	17,825					
	MsVAtGsSETAGGASGGGAR		1	81	46/48	100,27,66	ETD
PP1R7_HUMAN	Protein phosphatase 1 regulatory subunit 7	41,548					
	IRAIENIDtLTNLEsLFLGKNK		1	90	51/49	73,58	ETD
SHSA7_HUMAN	Protein shisa-7	56,197					
	sPALPPDPtAR		1	80	44/47	99	ETD
SYS1_HUMAN	Protein SYS1 homolog	17,598					
	EIPLNsAPK		1	89	35/45	100	CID
PTMA_HUMAN	Prothymosin alpha	12,185					
	sDAAVDTSSEITTK		2	95	46/46	100	CID
HS902_HUMAN	Putative heat shock protein HSP 90-alpha A2	39,348					
	ESKDKPEIEDVGsDEEEEKK		2	95	101/49	100	ETD
PSG7_HUMAN	Putative pregnancy-specific beta-1-glycoprotein 7	46,984					
	ENKDVSTFtcEPK		1	91	52/48	54	ETD

RBM15_HUMAN	**Putative RNA-binding protein 15**	107,175					
	GGEDSTsR		1	79	45/46	33	CID
RB15B_HUMAN	**Putative RNA-binding protein 15B**	97,190					
	GGKAsGDPGAsGmsPR		1	85	50/48	100,100,100	ETD
S22AX_HUMAN	**Putative solute carrier family 22 member ENSG00000182157**	58,972					
	gPALLDAAIPRLGPTRAPAEALGVLsPSYLAPLTR		1	95	61/49	23	ETD
CE060_HUMAN	**Putative uncharacterized protein C5orf60**	39,233					
	GKASPTsFHVSPR		1	79	45/48	26	CID
G3BP1_HUMAN	**Ras GTPase-activating protein-binding protein 1**	52,145					
	SSsPAPADIAQTVQEDLR		18	95	113/48	96	both
	YQDEVFGGFVTEPQEEsEEEVEEPEER		6	95	84/48	100	both
RL3R1_HUMAN	**Relaxin-3 receptor 1**	51,107					
	mQMADAATIAtmNKAAGGDK		1	81	47/48	34	ETD
RTN2_HUMAN	**Reticulon-2**	59,247					
	IPGTGALAsAAAAVsGsK		1	88	50/48	74,71,82	ETD
RTN4_HUMAN	**Reticulon-4**	129,917					
	mEDLDQSPLVSSSDsPPRPQPAFK		6	95	81/46	100	CID
RTL1_HUMAN	**Retrotransposon-like protein 1**	155,161					
	kEPPSGPLQEMEELPtDLLQDmEEPSSGPR		1	95	55/49	37	ETD
RBM14_HUMAN	**RNA-binding protein 14**	69,474					
	sPPRASYVAPLTAQPATYR		1	95	43/46	23	CID
SEPR_HUMAN	**Seprase**	87,697					
	TINIPyPK		1	82	32/45	100	CID
SEPT2_HUMAN	**Septin-2**	41,470					
	IYHLPDAEsDEDEDFKEQTR		3	95	63/49	100	both
SRRM1_HUMAN	**Serine/arginine repetitive matrix protein 1**	102,319					
	KETEsEAEDNLDDLEK		3	95	68/48	100	ETD
	EKtPELPEPSVK		3	95	57/46	100	both
SRRM2_HUMAN	**Serine/arginine repetitive matrix protein 2**	299,604					
	MALPPQEDATAsPPRQK		1	79	45/48	96	CID
	VKPEtPPRQSHSGSIsPYPK		3	95	7049	99,64	ETD
	SATRPsPsPERSSTGPEPPAPTPLLAER		2	95	60/46	99,98	CID
	VSGRTsPPLLDR		1	86	48/47	100	ETD
DCLK1_HUMAN	**Serine/threonine-protein kinase DCLK1**	82,208					
	KHFNtGPKPNStAAGVsVIAtTALDK		1	95	57/49	37,37,49,97	ETD
ICK_HUMAN	**Serine/threonine-protein kinase ICK**	71,412					
	SSGtMSVIsK		1	86	36/46	33,41	CID

OXSR1_HUMAN	Serine/threonine-protein kinase OSR1	58,005						
	LHKTEDGGWEWsDDEFDEESEEGK		1	90	38/46	100	CID	
TAOK2_HUMAN	Serine/threonine-protein kinase TAO2	138,237						
	MLLARHsLDQDLLR		1	95	49/46	100	CID	
SDCG1_HUMAN	Serologically defined colon cancer antigen 1	122,940						
	IASKEEsSNSSDsK		1	91	51/48	29,71	ETD	
SMAP_HUMAN	Small acidic protein	20,315						
	SAsPDDDLGSSNWEAADLGNEER		15	95	117/46	58	CID	
UTP20_HUMAN	Small subunit processome component 20 homolog	318,378						
	aAPPTAGsmAlEK		1	95	40/46	71	CID	
SC6A8_HUMAN	Sodium- and chloride-dependent creatine transporter 1	70,506						
	sAENGIYSVSGDEKK		1	87	49/48	73	ETD	
SKA3_HUMAN	Spindle and kinetochore-associated protein 3	46,343						
	yNSNLATPIAIK		1	92	53/47	91	ETD	
SF3A1_HUMAN	Splicing factor 3A subunit 1	88,868						
	FGESEEVEMEVEsDEEDDKQEK		1	95	48/46	100	CID	
SFR19_HUMAN	Splicing factor, arginine/serine-rich 19	139,255						
	RRSGAASSSSsSR		1	84	46/47	17	ETD	
STMN1_HUMAN	Stathmin	17,285						
	ASGQAFELILsPR		1	95	68/46	100	CID	
STUB1_HUMAN	STIP1 homology and U box-containing protein 1	34,839						
	LGAGGGsPEKSPSAQELK		1	94	59/48	92	ETD	
SPEG_HUMAN	Striated muscle preferentially expressed protein kinase	354,268						
	DmGALTctARNR		1	88	49/48	88	ETD	
SMC4_HUMAN	Structural maintenance of chromosomes protein 4	147,170						
	TEsPATAAETASEELDNR		7	95	77/46	47	both	
SUN2_HUMAN	SUN domain-containing protein 2	80,294						
	VDQMEGGAAGPsAsVR		1	81	50/49	100,100	ETD	
SMCE1_HUMAN	SWI/SNF-related matrix-associated actin-dependent regulator of chromatin subfamily E member 1	46,632						
	eAAEQAERSQSsIVPEEEQAANK		1	95	52/49	64	ETD	
TTBK2_HUMAN	Tau-tubulin kinase 2	137,397						
	fLEtcLEKMQKDTsAGK		1	95	56/49	100,35	ETD	
ERCC2_HUMAN	TFIIH basal transcription factor complex helicase subunit	86,894						

	GFtIIIEPFDDR		1	87	49/48	100	ETD
SMCA4_HUMAN	**Transcription activator BRG1**	**184,632**					
	DSDAGssTPTTSTR		1	79	45/48	25,25	CID
SOX11_HUMAN	**Transcription factor SOX-11**	**46,663**					
	MDPSAKPSASQsPEKSAAGGGGGSAGGGAGGAK		1	83	82/49	19	ETD
TIF1B_HUMAN	**Transcription intermediary factor 1-beta**	**88,531**					
	aASAAAASAAAASAASGsPGPGEGSAGGEKR		22	95	146/46	98	both
	FSAVLVEPPPMSLPGAGLSsQELSGGPGDGP		2	95	51/46	32	CID
P66A_HUMAN	**Transcriptional repressor p66-alpha**	**68,045**					
	TVSAGKGSATsNWKK		1	87	49/48	14	ETD
TYY1_HUMAN	**Transcriptional repressor protein YY1**	**44,694**					
	DIDHETVVEEQIIGENsPPDYSEYMTGK		1	87	37/46	93	CID
TLE3_HUMAN	**Transducin-like enhancer protein 3**	**83,399**					
	VSPAHsPPENGLDK		1	91	52/48	96	ETD
TMCO7_HUMAN	**Transmembrane and coiled-coil domain-containing protein 7**	**120,731**					
	AARQAVGsGAQETcGLDR		1	89	52/48	91	ETD
TMCC1_HUMAN	**Transmembrane and coiled-coil domains protein 1**	**72,035**					
	SGQEMtAVMQsGRPR		1	84	48/48	50,59	ETD
TRIO_HUMAN	**Triple functional domain protein**	**346,885**					
	lssGKADGHVK		1	79	45/47	100,100	CID
NSUN2_HUMAN	**tRNA (cytosine-5-)-methyltransferase NSUN2**	**86,455**					
	AGEPNsPDAEEANsPDVTAGcDPAGVHPPR		1	95	66/46	99,99	CID
TBA1B_HUMAN	**Tubulin alpha-1B chain**	**50,134**					
	DYEEVGVDsVEGEGEEEGEEY		2	95	83/46	100	CID
	TIGGGDDsFNTFFSETGAGK		1	95	41/46	99	CID
	TIGGGDDsFNTFFSETGAGKHVPR		1	95	55/46	66	CID
PTN18_HUMAN	**Tyrosine-protein phosphatase non-receptor type 18**	**50,465**					
	TLSAsAAEVAPR		1	93	53/48	74	ETD
U520_HUMAN	**U5 small nuclear ribonucleoprotein 200 kDa helicase**	**244,496**					
	EEAsDDDMEGDEAVVR		2	95	65/46	100	CID
UBP2L_HUMAN	**Ubiquitin-associated protein 2-like**	**114,516**					
	RYPSSISSsPQKDLTQAK		3	95	77/49	99	ETD
CF174_HUMAN	**Uncharacterized protein C6orf174**	**103,184**					
	NSGSGVAGGGSGGGGsyWK		1	81	46/48	66,46	ETD
K0753_HUMAN	**Uncharacterized protein KIAA0753**	**109,390**					
	LsyAVHLAR		1	91	34/46	100 100	CID

			SC	PP	IS/IDS	LP	IM
	AQRVNsTTEANIHLKDGssVNtAK		1	95	51/49	87,40,40,55	ETD
CF035_HUMAN	**UPF0463 transmembrane protein C6orf35**	**14,741**					
	GGIFLGTVAAAGmLAGFITTLsLAKKK		1	84	50/49	15	ETD
CB029_HUMAN	**UPF0760 protein C2orf29**	**55,200**					
	GGAsGPGSGSGGPGGPAGRmsLTPK		1	95	69/49	28,28	ETD
YRDC_HUMAN	**YrdC domain-containing protein, mitochondrial**	**29,310**					
	LFRPPsPAPAAPGAR		1	95	58/48	100	ETD
ZC3HF_HUMAN	**Zinc finger CCCH domain-containing protein 15**	**48,586**					
	DVDETGITVAsLER		1	95	49/46	100	CID
Z512B_HUMAN	**Zinc finger protein 512B**	**97,246**					
	LPGSSKsGPGKDGSR		1	89	50/48	21	ETD
Z804A_HUMAN	**Zinc finger protein 804A**	**136,872**					
	StTVTVR		2	84	33/45	22	CID
ZKSC2_HUMAN	**Zinc finger protein with KRAB and SCAN domains 2**	**110,922**					
	KENVGNVVSLGSAVStsNKItR		1	81	47/49	65,65,54	ETD
ZXDC_HUMAN	**Zinc finger protein ZXDC**	**89,970**					
	GAGSNAGASQStQR		1	91	51/48	14	ETD
ZRAB2_HUMAN	**Zinc finger Ran-binding domain-containing protein 2**	**37,387**					
	EEsDGEYDEFGR		1	95	42/46	100	CID
	EVEDKEsEGEEEDEDEDLSK		1	95	41/46	100	CID

Total phosphoproteins	188
Spectral count	490
Number of different phosphopeptides	220
Number of multiply phosphorylated peptides	72
Number of singly phosphorylated peptides	418
Number of each phosphorylated amino acid observed	521(pS), 68(pT), 9(pY)
Number of unique phosphorylated amino acids	309

[a] Peptides identified by MS were searched for serine, threonine, or tyrosine residues containing a +80 m/z modification, which is consistent with the presence of a phosphate group. 50% protein and 79% peptides cutoffs were used to generate the Scaffold coverage which scored above 1.3% FDR threshold. [b] SC=Spectral Count. [c] PP= Peptide probability (written as percentage). [d] IS= Ion Score. [e] IDS= Identity Score. [f] LP= Localization Probability (written as a percentage, multiple numbers corresponding to the value of each site). [g] IM= Ionization Method. CID=Collision Induced Dissociation, ETD= Electron Transfer Disscociation, both=CID and ETD.

Gel image for Avidin Purification with Casein Model Study
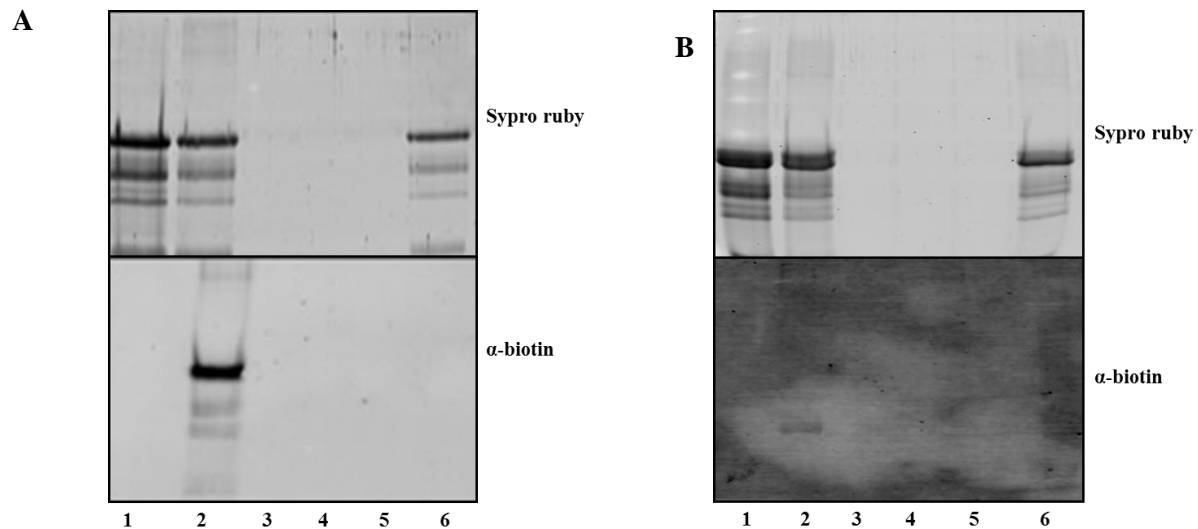
Figure A 4.7: ATP-biotin reaction. B-casein (lane 1) were biotinylated with CK2 and ATP-biotin (lane 2), load onto an avidin column (lane 3), washed (lane 4 and 5) and eluted with acid (lane 6). All proteins were visualized with sypro ruby stain (top) and anti-biotin (bottom). Two trials are shown here.

Table A 4.7: Phosphopeptides identified by MS analysis after kinase-catylzed biotinylation of casein and subsequent purification of the full-length proteins using NeutrAvidin affinity chromatography and acidic elution[a]

Accession number	Proteins/peptides name	MW (Da)	SP[b]	PP[c]	IS[d]/IDS[e]	LP[f]	IM[g]
gi|30794348	casein alpha s1	24,500					
	VPQLEIVPNsAEER		8	95	58/46	100	CID
	YKVPQLEIVPNsAEER		11	95	69/46	100	CID
gi|27806963	casein alpha-S2	26,000					
	NmAINPsKENLcSTFcK		9	95	67/46	100	CID
	TVDmEsTEVFTK		5	95	54/46	99	CID
gi|30794310	casein beta	25,000					
	FQsEEQQQTEDELQDK		11	95	88/46	100	CID
	FQsEEQQQtEDELQDK		9	95	53/46	100,100	CID
	IEKFQsEEQQQTEDELQDK		8	95	65/46	100	CID
	IEKFQsEEQQQtEDELQDK		8	95	55/46	100,100	CID

Total phosphoproteins	3
Total phosphopeptides	69
Number of different phosphopeptides	6
Number of multiply phosphorylated peptides	17
Number of singly phosphorylated peptides	52
Number of each phosphorylated amino acid observed	69(pS),17(pT)
Number of unique phosphorylated amino acids	5

[a] The full length proteins isolated after affinity chromatography were digested with trypsin prior to MS analysis. Peptides identified by MS were searched for serine, threonine, or tyrosine residues containing a +80 m/z modification, which is consistent with the presence of a phosphate group. 99% protein and 90% peptides cutoffs were used to generate the Scaffold coverage which scored above 0.6% FDR threshold. [b] SC=Spectral Count. [c] PP= Peptide probability (written as percentage). [d] IS= Ion Score. [e] IDS= Identity Score. [f] LP= Localization Probability (written as a percentage). [g] IM= Ionization Method.

Gel image for Avidin Purification with HeLa Cell Lysates
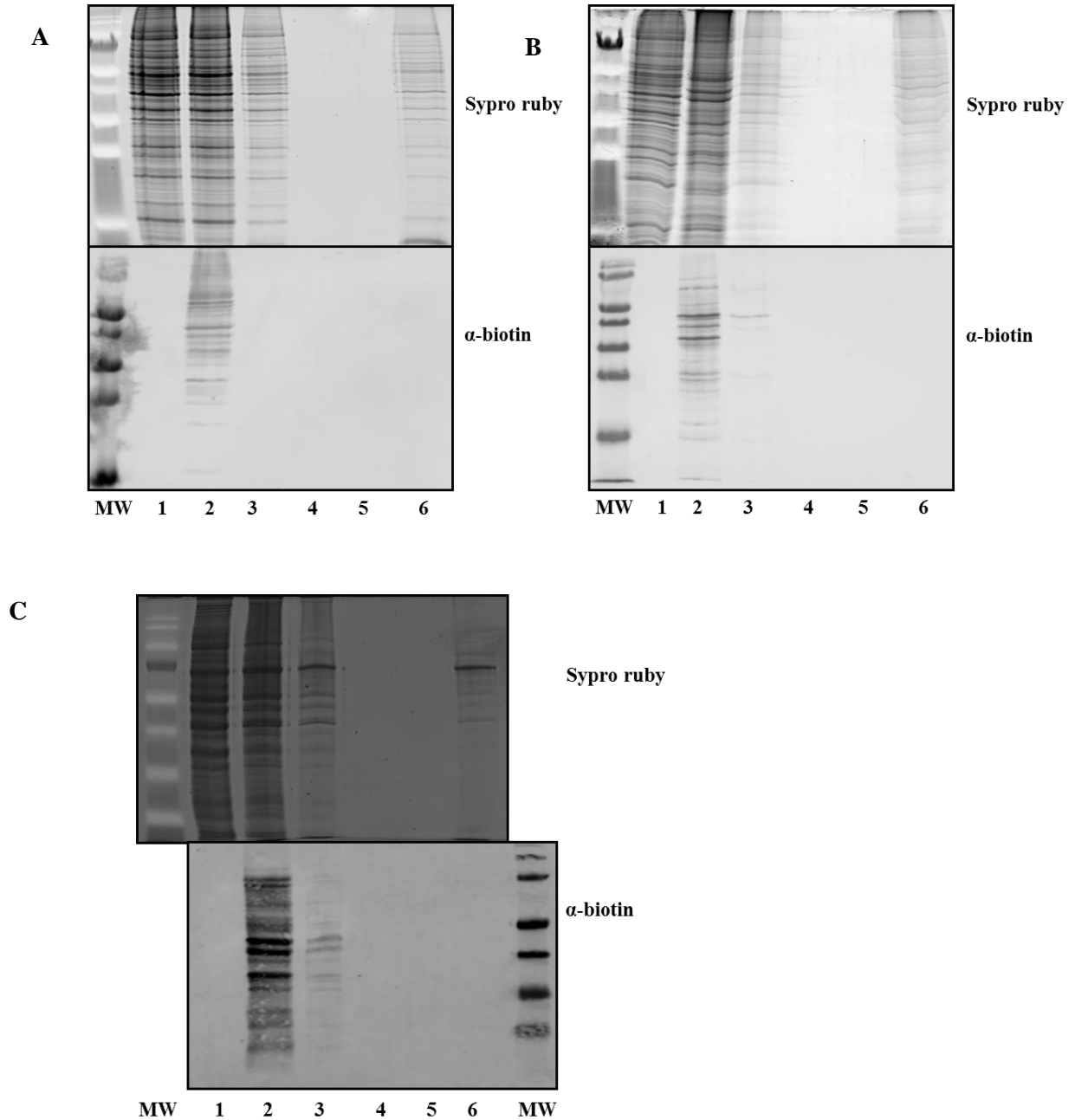
Figure A 4.8: ATP-biotin reaction. HeLa cell lysates (lane 1) were biotinylated with ATP-biotin (lane 2), load onto an avidin column (lane 3), washed (lane 4 and 5) and eluted with acid (lane 6). All proteins were visualized with sypro ruby stain (top) and anti-biotin (bottom). All the three trials are shown here.

Table A 4.8: Phosphopeptides identified by MS analysis after kinase-cataylzed biotinylation of HeLa cell lysates and subsequent purification of the full length proteins using NeutrAvidin affinity chromatography and acidic elution[a]

Accession numbers	Proteins/peptides name	MW (Da)	SC[b]	PP[c]	IS[d]/IDS[e]	LP[f]	IM[g]
RS3_HUMAN	40S ribosomal protein S3	26,671					
	ELAEDGYSGVEVRVtPtR		1	93	39/43	100,99	CID
RL12_HUMAN	60S ribosomal protein L12	17,801					
	VVyLRcTGGEVGATSALAPK		11	95	52/43	100	CID
RL14_HUMAN	60S ribosomal protein L14	23,414					
	APGtKGtAAAAAAAAAAK		1	82	34/43	100,100	CID
RL18_HUMAN	60S ribosomal protein L18	21,617					
	tNRPPLsLSRMIR		1	82	34/43	98,14	CID
F263_HUMAN	6-phosphofructo-2-kinase/fructose-2,6-biphosphatase 3	59,592					
	IGGDSGLSsR		1	95	44/43	100	CID
6PGD_HUMAN	6-phosphogluconate dehydrogenase, decarboxylating	53,124					
	ALYAsKIISYAQGFmLLR		4	95	46/43	59	CID
ACACB_HUMAN	Acetyl-CoA carboxylase 2	276,526					
	GSGmIAGESSLAyEEIVTIsLVtcR		1	65	30/43	92,100,100	CID
ARPC5_HUMAN	Actin-related protein 2/3 complex subunit 5	16,303					
	ALAAGGVGSIVRVLtAR		1	82	36/43	96	CID
ENOA_HUMAN	Alpha-enolase	47,152					
	AGytDKVVIGMDVAASEFFR		56	95	43/43	100,100	CID
ALMS1_HUMAN	Alstrom syndrome protein 1	460,940					
	SSLDFQVVQPSLPDSNTITQDLKTIPSQNSQIVtsR		1	93	38/42	18,18	CID
AN13A_HUMAN	Ankyrin repeat domain-containing protein 13A	67,602					
	QGWTVLHEAVstGDPEMVYtVLQHR		1	87	36/43	51,51,51	CID
AP1B1_HUMAN	AP-1 complex subunit beta-1	104,621					
	AAMIWIVGEyAER		1	54	17/43	100	CID
APOC3_HUMAN	Apolipoprotein C-III	10,834					
	AsEAEDAsLLsFmQGYMK		1	71	31/43	98,79,86	CID
ARRD1_HUMAN	Arrestin domain-containing protein 1	45,963					
	VtcIGScGVSNK		1	90	37/43	100	CID
BIRC6_HUMAN	Baculoviral IAP repeat-containing protein 6	530,237					
	VALGAsRK		1	95	41/42	100	CID
E41L1_HUMAN	Band 4.1-like protein 1	98,487					

			1	93	40/43	25	CID
E41L3_HUMAN	**Band 4.1-like protein 3**	**120,662**					
	yTMSRSLDGEVGTGQyATTK		1	94	40/43	21,58	CID
ACTBL_HUMAN	**Beta-actin-like protein 2**	**41,986**					
	TTGIVmDSGDGVtHIVPIyEGYALPHAILR		10	95	42/43	92,99	CID
KCMA1_HUMAN	**Calcium-activated potassium channel subunit alpha-1**	**137,546**					
	mANGGGGGGGSsGGGGGGGGSSLR		2	92	38/43	90	CID
CNN1_HUMAN	**Calponin-1**	**33,153**					
	GAsQAGmTAPGtK		1	92	40/43	100,85	CID
CPSM_HUMAN	**Carbamoyl-phosphate synthase [ammonia], mitochondrial**	**164,925**					
	EyGVKVLGtsVESImATEDR		4	95	41/43	99,100,100	CID
CBX3_HUMAN	**Chromobox protein homolog 3**	**20,794**					
	GLDPERIIGATDSsGELMFLmK		1	55	28/43	33	CID
COF2_HUMAN	**Cofilin-2**	**18,719**					
	StLGEKLGGNVVVSLEGKPL		7	95	46/43	36	CID
COCA1_HUMAN	**Collagen alpha-1(XII) chain**	**333,127**					
	GmTsSEPISImEK		1	95	41/43	29	CID
KCRB_HUMAN	**Creatine kinase B-type**	**42,627**					
	LAVEALSSLDGDLAGRyyALK		1	95	40/43	100,100	CID
CLC5A_HUMAN	**C-type lectin domain family 5 member A**	**21,504**					
	GKGstLAIVNtPEK		1	85	36/43	100,100,100	CID
CCDB1_HUMAN	**Cyclin-D1-binding protein 1**	**40,244**					
	LNEAAVTVSREATtLTIVFSQLPLPSPQETQK		1	93	38/43	47	CID
DYHC1_HUMAN	**Cytoplasmic dynein 1 heavy chain 1**	**532,388**					
	LVEAISRDLSsQLLK		2	90	38/43	45	CID
SERA_HUMAN	**D-3-phosphoglycerate dehydrogenase**	**56,633**					
	ILQDGGLQVVEKQNLsK		2	55	28/43	100	CID
RPA2_HUMAN	**DNA-directed RNA polymerase I subunit RPA2**	**128,215**					
	ISFtILDAVISPPtVPK		1	95	45/43	11,98	CID
ALG6_HUMAN	**Dolichyl pyrophosphate Man9GlcNAc2 alpha-1,3-glucosyltransferase**	**58,166**					
	IIQYLFLIsVItmVLLTLmtVtLDPPQK		1	86	35/43	67,67,67,67	CID
DYDC2_HUMAN	**DPY30 domain-containing protein 2**	**20,569**					
	EMEmtEMLK		2	95	45/43	100	CID
MARH7_HUMAN	**E3 ubiquitin-protein ligase MARCH7**	**78,035**					
	sNFSSRESEssR		1	58	17/43	97,51,51	CID

EF2_HUMAN	**Elongation factor 2**	95,322					
	cLyAsVLTAQPR		1	71	31/43	100,100	CID
IF4A1_HUMAN	**Eukaryotic initiation factor 4A-I**	46,137					
	SGSsRVLITTDLLAR		3	88	37/43	24	CID
MCA3_HUMAN	**Eukaryotic translation elongation factor 1 epsilon-1**	19,793					
	aAAAELSLLEKsLGLSK		6	90	40/43	65	CID
EIF3A_HUMAN	**Eukaryotic translation initiation factor 3 subunit A**	166,557					
	mstRVLLAtLsIPITPER		1	89	36/43	71,71,71,97	CID
IF4B_HUMAN	**Eukaryotic translation initiation factor 4B**	69,136					
	GFGyAEFEDLDSLLsALsLNEEsLGNR		1	55	28/43	80,80,80,80	CID
XPO7_HUMAN	**Exportin-7**	123,895					
	AtEPHmLETytPEVTK		1	55	28/43	99,61,61	CID
FLNA_HUMAN	**Filamin-A**	280,711					
	sQGDAsKVtAQGPGLEPSGNIANK		1	72	31/43	100,100,100	CID
ALDOC_HUMAN	**Fructose-bisphosphate aldolase C**	39,438					
	VLAAVYKALSDHHVYLEGTLLKPNmVtPGHAcPIK		1	62	31/43	21	CID
SYUG_HUMAN	**Gamma-synuclein**	13,312					
	EQANAVSEAVVsSVNTVATK		1	60	30/43	52	CID
GNPI1_HUMAN	**Glucosamine-6-phosphate isomerase 1**	32,651					
	VPtMALTVGVGTVmDAR		1	58	29/43	30	CID
G6PI_HUMAN	**Glucose-6-phosphate isomerase**	63,130					
	TITDVINIGIGGSDLGPLMVTEALKPySSGGPR		1	58	29/43	13	CID
G3P_HUMAN	**Glyceraldehyde-3-phosphate dehydrogenase**	36,035					
	LtGMAFRVPTANVSVVDLTcR		5	95	44/43	98	CID
CLCN7_HUMAN	**H(+)/Cl(-) exchange transporter 7**	88,663					
	FDSEKMAYTIHEIPVFIAmGVVGGVLGAVFNALNyWLtMFR		1	88	35/42	86,86	CID
HSP7C_HUMAN	**Heat shock cognate 71 kDa protein**	70,882					
	VssKNsLESYAFNmK		4	95	42/43	100,100,100	CID
HMGB3_HUMAN	**High mobility group protein B3**	22,963					
	IKsTNPGISIGDVAK		5	78	33/42	49	CID
HSDL2_HUMAN	**Hydroxysteroid dehydrogenase-like protein 2**	45,379					
	tAQPHPKLLGtIYTAAEEIEAVGGK		1	82	34/43	63,86	CID
INT9_HUMAN	**Integrator complex subunit 9**	73,798					
	FGDVVHFmELWGKSSLNTVIFTEPDFsyLEALAPYQPLAMK		1	90	38/42	29,29	CID

K1C16_HUMAN	Keratin, type I cytoskeletal 16	51,251					
	ISSVLAGGscR		1	55	29/43	100	CID
K2C1_HUMAN	Keratin, type II cytoskeletal 1	66,022					
	GGSGGGGGGssGGR		1	61	29/43	100,100	CID
K22E_HUMAN	Keratin, type II cytoskeletal 2 epidermal	65,416					
	yGSGGGSKGGSISGGGyGsGGGK		2	62	30/43	80,93,100	CID
K2C7_HUMAN	Keratin, type II cytoskeletal 7	51,369					
	TLNETELtELQsQISDTSVVLSmDNSR		2	95	44/43	22,74	CID
K2C8_HUMAN	Keratin, type II cytoskeletal 8	53,688					
	sLDmDSIIAEVK		4	81	33/43	100	CID
BAG6_HUMAN	Large proline-rich protein BAG6	119,389					
	LINLVGEsLR		1	91	36/43	100	CID
LRC59_HUMAN	Leucine-rich repeat-containing protein 59	34,913					
	AGsKGGNLR		1	95	39/42	100	CID
LIPM_HUMAN	Lipase member M	48,216					
	EFLyQTR		4	95	41/42	100	CID
MUC16_HUMAN	Mucin-16	2,353,421					
	SQSSVLADSsPMcttsTmGDTSVLTSTPAFLETR		2	91	37/43	23,23	CID
NPM_HUMAN	Nucleophosmin	32,557					
	VTLATLKmsVQPtVsLGGFEITPPVVLR		6	95	45/43	100,100,100	CID
NDKB_HUMAN	Nucleoside diphosphate kinase B	17,280					
	YmNsGPVVAmVWEGLNVVK		12	95	52/43	82	CID
OR2A5_HUMAN	Olfactory receptor 2A5	35,191					
	AFSTcSsHLcmVGLFFGSAIVMymAPKSR		1	93	41/43	29,29	CID
PACRL_HUMAN	PACRG-like protein	27,135					
	MQKsEGsGGtQLK		1	95	54/43	100,100,100	CID
PDZD2_HUMAN	PDZ domain-containing protein 2	301,623					
	AEYsQGKsSLMSDsR		1	87	36/43	93,98,18	CID
PAL4G_HUMAN	Peptidylprolyl cis-trans isomerase A-like 4G	18,148					
	HTGSGILsMANAGPNTNGSQFFIcTAK		2	95	48/43	78	CID
PRDX2_HUMAN	Peroxiredoxin-2	21,874					
	LsEDyGVLKTDEGIAYR		4	89	38/43	100,100	CID
PRDX5_HUMAN	Peroxiredoxin-5, mitochondrial	22,068					
	ETDLLLDDsLVSIFGNR		1	92	38/43	94	CID
PHLP_HUMAN	Phosducin-like protein	34,264					

	ttLDDKLLGEK			1	95	38/43	100,100	CID

P3C2G_HUMAN	**Phosphatidylinositol-4-phosphate 3-kinase C2 domain-containing subunit gamma**	165,701					
	SKtVFVGAINIR		1	93	39/43	54	CID

PKHO2_HUMAN	**Pleckstrin homology domain-containing family O member 2**	53,332					
	EVAsAAsDGLLR		1	95	41/43	100,100	CID

PARP1_HUMAN	**Poly [ADP-ribose] polymerase 1**	113,070					
	AESSDKLyR		1	62	29/43	100,100	CID
	LTVNPGtK		1	61	33/43	100	CID

PK1L2_HUMAN	**Polycystic kidney disease protein 1-like 2**	272,556					
	WLIsmAVsFVESmFVtQPLK		1	87	37/43	100,98,85	CID

PFD2_HUMAN	**Prefoldin subunit 2**	16,630					
	SsGSGAGKGAVSAEQVIAGFNR		13	95	47/43	54	CID

PR40A_HUMAN	**Pre-mRNA-processing factor 40 homolog A**	108,789					
	YsALAKLSEK		1	90	37/43	46	CID

PRP16_HUMAN	**Pre-mRNA-splicing factor ATP-dependent RNA helicase PRP16**	140,488					
	ymtDGILLR		2	95	38/43	100,100	CID

SAP_HUMAN	**Proactivator polypeptide**	58,094					
	NStKQEILAALEK		2	75	33/43	51	CID
	HEVPAKsDVycEVcEFLVK		1	95	42/43	100,100	CID

NSD2_HUMAN	**Probable histone-lysine N-methyltransferase NSD2**	152,241					
	TTVsMPR		1	95	42/42	20	CID

AT8B2_HUMAN	**Probable phospholipid-transporting ATPase ID**	137,426					
	LNLKPDLsDtVR		1	95	39/43	100,100	CID

PDC6I_HUMAN	**Programmed cell death 6-interacting protein**	96,007					
	LALAsLGYEK		1	95	46/43	100	CID

PDCD5_HUMAN	**Programmed cell death protein 5**	14,267					
	EAEmRNsILAQVLDQSAR		5	95	50/43	100	CID

PSB1_HUMAN	**Proteasome subunit beta type-1**	26,473					
	AMtTGAIAAmLSTILYSR		1	62	30/43	57	CID

AF17_HUMAN	**Protein AF-17**	112,059					
	HSSGGGGGGAGGGGGSmGGGGSGFIsGRR		4	76	32/43	55	CID
	TSRHssGGGGGGGAGGGGGsmGGGGsGFISGR		3	87	36/43	87,87,95,41	CID

PSYR_HUMAN	**Psychosine receptor**	39,317					
	yLAVVYPLK		1	95	56/43	100	CID

MGAL1_HUMAN	**Putative maltase-glucoamylase-like protein**	73,914					

FLJ16351

	NMNNTGmFAHDEPPAyK		1	91	39/43	74	CID

GDIB_HUMAN	**Rab GDP dissociation inhibitor beta**	50,648					
	mLLYTEVtR		1	71	32/43	100	CID

RADI_HUMAN	**Radixin**	68,548					
	mPKPINVRVTtMDAELEFAIQPNTTGK		5	95	51/43	54	CID

RANB3_HUMAN	**Ran-binding protein 3**	60,192					
	LNDMAstDDGTLQsR		1	66	31/43	91,92,59	CID

ABCA4_HUMAN	**Retinal-specific ATP-binding cassette transporter**	255,933					
	tHPERIAGR		1	95	48/43	100	CID

RGAG1_HUMAN	**Retrotransposon gag domain-containing protein 1**	144,263					
	APIsGAmsmPLtR		2	74	17/43	100,100,100	CID

PRPS2_HUMAN	**Ribose-phosphate pyrophosphokinase 2**	34,752					
	LLsAGAtKVYAILTHGIFSGPAISR		1	95	53/43	94,83	CID

SRSF2_HUMAN	**Serine/arginine-rich splicing factor 2**	25,459					
	yGRVGDVYIPR		3	92	39/43	100	CID

SPA9_HUMAN	**Serpin A9**	46,540					
	STPAsQVySLNTDFAFR		1	85	35/43	32,93	CID

SH2B3_HUMAN	**SH2B adapter protein 3**	63,208					
	mNGPALQPSSPsSAPSASPAAAPR		1	95	44/43	65	CID

UTP20_HUMAN	**Small subunit processome component 20 homolog**	318,378					
	DmSSIYsmYSTLLAHK		1	84	34/43	17	CID

SPEE_HUMAN	**Spermidine synthase**	33,807					
	QNQDAFDVIITDSSDPMGPAESLFKEsYYQLmK		1	79	32/43	14	CID

GRP75_HUMAN	**Stress-70 protein, mitochondrial**	73,663					
	EGSGSSGtGEQKEDQK		1	63	29/43	49	CID

SODM_HUMAN	**Superoxide dismutase [Mn], mitochondrial**	24,705					
	yQEALAKGDVTAQIALQPALK		1	51	28/43	84	CID

TLN1_HUMAN	**Talin-1**	269,747					
	GISmSSsKLLLAAK		1	73	17/43	25	CID

TCPA_HUMAN	**T-complex protein 1 subunit alpha**	60,327					
	sQmESmLISGYALNcVVGSQGmPKR		1	95	40/43	44	CID

TCPB_HUMAN	**T-complex protein 1 subunit beta**	57,472					
	ILLSsGRDAsLMVTNDGATILK		1	85	35/43	94,15	CID

THIO_HUMAN	**Thioredoxin**	11,719	

	QIEsKTAFQEALDAAGDK		7	95	61/43	73	CID
	QIESKtAFQEALDAAGDK		8	95	56/43	77	CID
ELOC_HUMAN	**Transcription elongation factor B polypeptide 1**	**12,455**					
	EHALtSGTIKAmLSGPGQFAENETNEVNFR		1	95	41/43	23	CID
TAF4B_HUMAN	**Transcription initiation factor TFIID subunit 4B**	**91,072**					
	DNLLASGTssLtAtK		6	95	44/43	92,90,90,70	CID
TIF1A_HUMAN	**Transcription intermediary factor 1-alpha**	**116,813**					
	QLEHVMHFSKWAVSSGSSTALLysK		1	88	37/43	26,26	CID
TIF1B_HUMAN	**Transcription intermediary factor 1-beta**	**88,531**					
	HQEHILRFAsWALESDNNTALLLSK		1	95	40/43	100	CID
TFR1_HUMAN	**Transferrin receptor protein 1**	**84,856**					
	mmDQARsAFSNLFGGEPLSYTR		3	95	44/43	58	CID
TKT_HUMAN	**Transketolase**	**67,861**					
	QAFtDVATGSLGQGLGAAcGmAYtGK		1	75	31/43	42,48	CID
TM14C_HUMAN	**Transmembrane protein 14C**	**11,547**					
	NVWVFLATSGTLAGImGmRFYHsGK		1	89	36/43	21	CID
TPD54_HUMAN	**Tumor protein D54**	**22,220**					
	LGLstLGELKQNLSR		2	67	30/43	100,100	CID
UBN2_HUMAN	**Ubinuclein-2**	**146,074**					
	LTNSSsTGtVGK		1	95	42/43	21,100	CID
UBP36_HUMAN	**Ubiquitin carboxyl-terminal hydrolase 36**	**122,635**					
	tGSSSLPGRPSVIPDHSKK		5	95	43/43	82	CID
UBP42_HUMAN	**Ubiquitin carboxyl-terminal hydrolase 42**	**145,211**					
	ssNVLTLSLKR		1	88	36/43	100,100	CID
CF062_HUMAN	**Uncharacterized protein C6orf62**	**27,066**					
	DSsYSLESSLELLQK		1	93	38/43	25	CID
CI066_HUMAN	**Uncharacterized protein C9orf66**	**31,167**					
	sALETSAFPPSKPK		2	91	37/43	100	CID
URB2_HUMAN	**Unhealthy ribosome biogenesis protein 2 homolog**	**170,531**					
	SLDsstPLPIVR		1	91	37/43	100,100,100	CID
CA227_HUMAN	**UPF0732 protein C1orf227**	**11,338**					
	mAsINRTIEImK		28	95	57/43	100	CID
WBP11_HUMAN	**WW domain-binding protein 11**	**69,982**					
	tsAyGPPTRAVsILPLLGHGVPR		1	50	27/43	87,87,89,69	CID
ZNF90_HUMAN	**Zinc finger protein 90**	**69,041**					

AFISSsLLYKHK	1	90	36/43	27	CID

Total phosphoproteins	118
Total phosphopeptides	341
Number of different phosphopeptides	126
Number of multiply phosphorylated peptides	131
Number of singly phosphorylated peptides	182
Number of each phosphorylated amino acid observed	223(S), 185(T), 109(Y)
Number of unique phosphorylated amino acids	237

[a] The full length proteins isolated after affinity chromatography were digested with trypsin prior to MS analysis. Peptides identified by MS were searched for serine, threonine, or tyrosine residues containing a +80 m/z modification, which is consistent with the presence of a phosphate group. 90% protein and 55% peptides cutoffs were used to generate the Scaffold coverage which scored above 0.8% FDR threshold. [b] SC=Spectral Count. [c] PP= Peptide probability(written as percentage). [d] IS= Ion Score. [e] IDS= Identity Score. [f] LP= Localization Probability (written as a percentage, multiple numbers corresponding to the value of each site). [g] IM= Ionization Method. CID=Collision Induced Dissociation, ETD= Electron Transfer Disscociation, both=CID and ETD.

Gel image for ATP control reaction
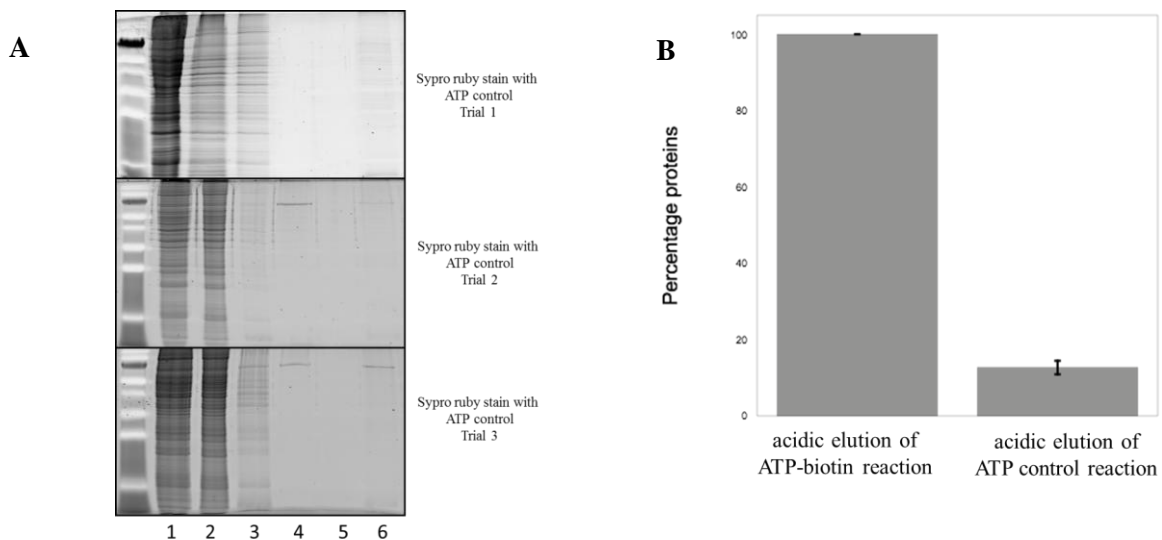
Figure A 4.9: (A) Control experiment with ATP. Hela cell lysates (lane 1) were phosphorylated with ATP, load onto an avidin column (lane 2), washed (lane 3, 4 and 5) and eluted with acid (lane 6). All proteins were visualized with sypro ruby stain. (B) Quantification of elution lanes (lane 6) of ATP reactions and ATP-biotin (images shown in Figure A 4.8, lane 6), showing that 13% protein signal was observed in the ATP control reaction compared to the ATP-biotin reaction (Figure A 4.8, lane 6 set to 100%).

REFERENCES

1.   Manning, G., Plowman, G. D., Hunter, T., and Sudarsanam, S. (2002) Evolution of protein kinase signaling from yeast to man, *Trends in biochemical sciences 27*, 514-520.

2.   Walsh, C. T., Garneau-Tsodikova, S., and Gatto, G. J., Jr. (2005) Protein posttranslational modifications: the chemistry of proteome diversifications, *Angewandte Chemie 44*, 7342-7372.

3.   Levene, P. A., Alsberg, C. L.,. (1906) The Cleavage Products of Vitellin, *J. Biol. Chem. 2*, 127-133.

4.   Burnett, G., and Kennedy, E. P. (1954) The enzymatic phosphorylation of proteins, *The Journal of biological chemistry 211*, 969-980.

5.   Hunter, T. (1995) Protein kinases and phosphatases: the Yin and Yang of protein phosphorylation and signaling, *Cell (Cambridge, Massachusetts) 80*, 225-236.

6.   Cohen, P. (2002) Timeline: Protein kinases - the major drug targets of the twenty-first century?, *Nature Reviews Drug Discovery 1*, 309-315.

7.   Barford, D. (1995) Protein phosphatases, *Curr Opin Struct Biol 5*, 728-734.

8.   Parang, K., Till, J. H., Ablooglu, A. J., Kohanski, R. A., Hubbard, S. R., and Cole, P. A. (2001) Mechanism-based design of a protein kinase inhibitor, *Nature Structural Biology 8*, 37-41.

9.   Lawrence, D. S. (2003) Chemical Probes of Signal-Transducing Proteins, *Accounts of Chemical Research 36*, 401-409.

10.   Hof, P., Pluskey, S., Dhe-Paganon, S., Eck, M. J., and Shoelson, S. E. (1998) Crystal structure of the tyrosine phosphatase SHP-2, *Cell 92*, 441-450.

11.   Bode, A. M., and Dong, Z. (2004) Post-translational modification of p53 in tumorigenesis, *Nature reviews. Cancer 4*, 793-805.

12.   Olsson, A., Manzl, C., Strasser, A., and Villunger, A. (2007) How important are post-translational modifications in p53 for selectivity in target-gene transcription and tumour suppression?, *Cell death and differentiation 14*, 1561-1575.

13.   Shieh, S. Y., Ikeda, M., Taya, Y., and Prives, C. (1997) DNA damage-induced phosphorylation of p53 alleviates inhibition by MDM2, *Cell 91*, 325-334.

14.   Chehab, N. H., Malikzay, A., Stavridi, E. S., and Halazonetis, T. D. (1999) Phosphorylation of Ser-20 mediates stabilization of human p53 in response to DNA damage, *Proc Natl Acad Sci U S A 96*, 13777-13782.

15.   Saito, S., Yamaguchi, H., Higashimoto, Y., Chao, C., Xu, Y., Fornace, A. J., Jr., Appella, E., and Anderson, C. W. (2003) Phosphorylation site interdependence of human p53 post-translational modifications in response to stress, *The Journal of biological chemistry 278*, 37536-37544.

16.   Dumaz, N., and Meek, D. W. (1999) Serine15 phosphorylation stimulates p53 transactivation but does not directly influence interaction with HDM2, *Embo J 18*, 7002-7010.

17.   Fiscella, M., Ullrich, S. J., Zambrano, N., Shields, M. T., Lin, D., Lees-Miller, S. P., Anderson, C. W., Mercer, W. E., and Appella, E. (1993) Mutation of the serine 15 phosphorylation site of human p53 reduces the ability of p53 to inhibit cell cycle progression, *Oncogene 8*, 1519-1528.

18.   Chrivia, J. C., Kwok, R. P., Lamb, N., Hagiwara, M., Montminy, M. R., and Goodman, R. H. (1993) Phosphorylated CREB binds specifically to the nuclear protein CBP, *Nature 365*, 855-859.

19.   Parker, D., Ferreri, K., Nakajima, T., LaMorte, V. J., Evans, R., Koerber, S. C., Hoeger, C., and Montminy, M. R. (1996) Phosphorylation of CREB at Ser-133 induces complex formation with CREB-binding protein via a direct mechanism, *Mol Cell Biol 16*, 694-703.

20.   Johnson, L. N., and Barford, D. (1993) The effects of phosphorylation on the structure and function of proteins, *Annual review of biophysics and biomolecular structure 22*, 199-232.

21.   Yoon, S. O., Soltoff, S. P., and Chao, M. V. (1997) A dominant role of the juxtamembrane region of the TrkA nerve growth factor receptor during neuronal cell differentiation, *The Journal of biological chemistry 272*, 23231-23238.

22.   Lewis, T. S., Shapiro, P. S., and Ahn, N. G. (1998) Signal transduction through MAP kinase cascades, *Advances in cancer research 74*, 49-139.

23.   Heisterkamp, N., Jenster, G., ten Hoeve, J., Zovich, D., Pattengale, P. K., and Groffen, J. (1990) Acute leukaemia in bcr/abl transgenic mice, *Nature 344*, 251-253.

24.   Daley, G. Q., Van Etten, R. A., and Baltimore, D. (1990) Induction of chronic myelogenous leukemia in mice by the P210bcr/abl gene of the Philadelphia chromosome, *Science 247*, 824-830.

25.   Kelliher, M. A., McLaughlin, J., Witte, O. N., and Rosenberg, N. (1990) Induction of a chronic myelogenous leukemia-like syndrome in mice with v-abl and BCR/ABL, *Proc Natl Acad Sci U S A 87*, 6649-6653.

26.   Faderl, S., Talpaz, M., Estrov, Z., and Kantarjian, H. M. (1999) Chronic myelogenous leukemia: biology and therapy, *Annals of internal medicine 131*, 207-219.

27.   Hehlmann, R., Hochhaus, A., Baccarani, M., and European, L. (2007) Chronic myeloid leukaemia, *Lancet 370*, 342-350.

28.   Capdeville, R., Buchdunger, E., Zimmermann, J., and Matter, A. (2002) Glivec (STI571, imatinib), a rationally developed, targeted anticancer drug, *Nature reviews. Drug discovery 1*, 493-502.

29.   Munstermann, U., Fritz, G., Seitz, G., Lu, Y. P., Schneider, H. R., and Issinger, O. G. (1990) Casein kinase II is elevated in solid human tumours and rapidly proliferating non-neoplastic tissue, *European journal of biochemistry / FEBS 189*, 251-257.

30.   Chang, H. W., Aoki, M., Fruman, D., Auger, K. R., Bellacosa, A., Tsichlis, P. N., Cantley, L. C., Roberts, T. M., and Vogt, P. K. (1997) Transformation of chicken cells by the gene encoding the catalytic subunit of PI 3-kinase, *Science 276*, 1848-1850.

31.   Irby, R. B., Mao, W., Coppola, D., Kang, J., Loubeau, J. M., Trudeau, W., Karl, R., Fujita, D. J., Jove, R., and Yeatman, T. J. (1999) Activating SRC mutation in a subset of advanced human colon cancers, *Nature genetics 21*, 187-190.

32.   Zdychova, J., and Komers, R. (2005) Emerging role of Akt kinase/protein kinase B signaling in pathophysiology of diabetes and its complications, *Physiological research / Academia Scientiarum Bohemoslovaca 54*, 1-16.

33.   Mendelsohn, J., and Baselga, J. (2003) Status of epidermal growth factor receptor antagonists in the biology and treatment of cancer, *Journal of clinical oncology : official journal of the American Society of Clinical Oncology 21*, 2787-2799.

34.   Blume-Jensen, P., and Hunter, T. (2001) Oncogenic kinase signalling, *Nature 411*, 355-365.

35.   Karin, M., and Hunter, T. (1995) Transcriptional control by protein phosphorylation: signal transmission from the cell surface to the nucleus, *Current biology : CB 5*, 747-757.

36.   Garber, K. (2006) The second wave in kinase cancer drugs, *Nat Biotechnol 24*, 127-130.

37.   Manning, G., Whyte, D. B., Martinez, R., Hunter, T., and Sudarsanam, S. (2002) The protein kinase complement of the human genome, *Science 298*, 1912-1934.

38.   Adams, J. A. (2001) Kinetic and catalytic mechanisms of protein kinases, *Chemical Reviews (Washington, D. C.) 101*, 2271-2290.

39.   Parang, K., Kohn, J. A., Saldanha, S. A., and Cole, P. A. (2002) Development of photo-crosslinking reagents for protein kinase-substrate interactions, *FEBS Lett 520*, 156-160.

40.   Hanks, S. K. (1987) Homology probing: identification of cDNA clones encoding members of the protein-serine kinase family, *Proc Natl Acad Sci U S A 84*, 388-392.

41.   Hanks, S. K., Quinn, A. M., and Hunter, T. (1988) The protein kinase family: conserved features and deduced phylogeny of the catalytic domains, *Science 241*, 42-52.

42.   Niefind, K., Putter, M., Guerra, B., Issinger, O. G., and Schomburg, D. (1999) GTP plus water mimic ATP in the active site of protein kinase CK2, *Nat Struct Biol 6*, 1100-1103.

43.   Helms, V., and McCammon, J. A. (1997) Kinase conformations: a computational study of the effect of ligand binding, *Protein Sci 6*, 2336-2343.

44.   Ablooglu, A. J., Till, J. H., Kim, K., Parang, K., Cole, P. A., Hubbard, S. R., and Kohanski, R. A. (2000) Probing the catalytic mechanism of the insulin receptor kinase with a tetrafluorotyrosine-containing peptide substrate, *The Journal of biological chemistry 275*, 30394-30398.

45.   Cole, P. A., Courtney, A. D., Shen, K., Zhang, Z., Qiao, Y., Lu, W., and Williams, D. M. (2003) Chemical approaches to reversible protein phosphorylation, *Acc Chem Res 36*, 444-452.

46.   Knighton, D. R., Zheng, J. H., Ten Eyck, L. F., Ashford, V. A., Xuong, N. H., Taylor, S. S., and Sowadski, J. M. (1991) Crystal structure of the catalytic subunit of cyclic adenosine monophosphate-dependent protein kinase, *Science 253*, 407-414.

47.   Grant, B. D., and Adams, J. A. (1996) Pre-steady-state kinetic analysis of cAMP-dependent protein kinase using rapid quench flow techniques, *Biochemistry 35*, 2022-2029.

48.   Wu, J. J., Afar, D. E. H., Phan, H., Witte, O. N., and Lam, K. S. (2002) Recognition of Multiple Substrate Motifs by the c-ABL Protein Tyrosine Kinase, *Comb. Chem. High Throughput Screen. 5*, 83-91.

49.   Meggio, F., Marin, O., and Pinna, L. A. (1994) Substrate Specificity of protein kinase CK2, *Cell. Mol. Biol. Res. 40*, 401-409.

50.   Kemp, B. E., Graves, D. J., Benjamini, E., and Krebs, E. G. (1977) Role of multiple basic residues in determining the substrate specificity of cyclic AMP-dependent protein kinase, *The Journal of biological chemistry 252*, 4888-4894.

51.   Olsen, J. V., Blagoev, B., Gnad, F., Macek, B., Kumar, C., Mortensen, P., and Mann, M. (2006) Global, in vivo, and site-specific phosphorylation dynamics in signaling networks, *Cell 127*, 635-648.

52.   Charron, G., Zhang, M. M., Yount, J. S., Wilson, J., Raghavan, A. S., Shamir, E., and Hang, H. C. (2009) Robust fluorescent detection of protein fatty-acylation with chemical reporters, *Journal of the American Chemical Society 131*, 4967-4975.

53.   Du, J., Jiang, H., and Lin, H. (2009) Investigating the ADP-ribosyltransferase activity of sirtuins with NAD analogues and 32P-NAD, *Biochemistry 48*, 2878-2890.

54.   Duckworth, B. P., Zhang, Z., Hosokawa, A., and Distefano, M. D. (2007) Selective labeling of proteins by using protein farnesyltransferase, *Chembiochem : a European journal of chemical biology 8*, 98-105.

55.   Grammel, M., Luong, P., Orth, K., and Hang, H. C. (2011) A chemical reporter for protein AMPylation, *Journal of the American Chemical Society 133*, 17103-17105.

56.   Hang, H. C., Geutjes, E. J., Grotenbreg, G., Pollington, A. M., Bijlmakers, M. J., and Ploegh, H. L. (2007) Chemical probes for the rapid detection of Fatty-acylated proteins in Mammalian cells, *Journal of the American Chemical Society 129*, 2744-2745.

57.   Hang, H. C., Wilson, J. P., and Charron, G. (2011) Bioorthogonal chemical reporters for analyzing protein lipidation and lipid trafficking, *Acc Chem Res 44*, 699-708.

58.   Heal, W. P., Wickramasinghe, S. R., Leatherbarrow, R. J., and Tate, E. W. (2008) N-Myristoyl transferase-mediated protein labelling in vivo, *Organic & biomolecular chemistry 6*, 2308-2315.

59.   Hwang, Y., Thompson, P. R., Wang, L., Jiang, L., Kelleher, N. L., and Cole, P. A. (2007) A selective chemical probe for coenzyme A-requiring enzymes, *Angewandte Chemie 46*, 7621-7624.

60.   Jeger, S., Zimmermann, K., Blanc, A., Grunberg, J., Honer, M., Hunziker, P., Struthers, H., and Schibli, R. (2010) Site-specific and stoichiometric modification of antibodies by bacterial transglutaminase, *Angewandte Chemie 49*, 9995-9997.

61.   Jiang, H., Kim, J. H., Frizzell, K. M., Kraus, W. L., and Lin, H. (2010) Clickable NAD analogues for labeling substrate proteins of poly(ADP-ribose) polymerases, *Journal of the American Chemical Society 132*, 9363-9372.

62.   Kostiuk, M. A., Corvi, M. M., Keller, B. O., Plummer, G., Prescher, J. A., Hangauer, M. J., Bertozzi, C. R., Rajaiah, G., Falck, J. R., and Berthiaume, L. G. (2008) Identification of palmitoylated mitochondrial proteins using a bio-orthogonal azido-palmitate analogue, *FASEB journal : official publication of the Federation of American Societies for Experimental Biology 22*, 721-732.

63.   La Clair, J. J., Foley, T. L., Schegg, T. R., Regan, C. M., and Burkart, M. D. (2004) Manipulation of carrier proteins in antibiotic biosynthesis, *Chemistry & biology 11*, 195-201.

64.   Lee, B. W., Sun, H. G., Zang, T., Kim, B. J., Alfaro, J. F., and Zhou, Z. S. (2010) Enzyme-catalyzed transfer of a ketone group from an S-adenosylmethionine analogue: a tool for the functional analysis of methyltransferases, *Journal of the American Chemical Society 132*, 3642-3643.

65.   Lewallen, D. M., Steckler, C. J., Knuckley, B., Chalmers, M. J., and Thompson, P. R. (2012) Probing adenylation: using a fluorescently labelled ATP probe to directly label and immunoprecipitate VopS substrates, *Mol Biosyst 8*, 1701-1706.

66.   Lin, C. W., and Ting, A. Y. (2006) Transglutaminase-catalyzed site-specific conjugation of small-molecule probes to proteins in vitro and on the surface of living cells, *Journal of the American Chemical Society 128*, 4542-4543.

67.   Luo, M. (2012) Current chemical biology approaches to interrogate protein methyltransferases, *ACS chemical biology 7*, 443-463.

68.   Martin, B. R., and Cravatt, B. F. (2009) Large-scale profiling of protein palmitoylation in mammalian cells, *Nature methods 6*, 135-138.

69.   Rashidian, M., Song, J. M., Pricer, R. E., and Distefano, M. D. (2012) Chemoenzymatic reversible immobilization and labeling of proteins without prior purification, *Journal of the American Chemical Society 134*, 8455-8467.

70.   Sprung, R., Nandi, A., Chen, Y., Kim, S. C., Barma, D., Falck, J. R., and Zhao, Y. (2005) Tagging-via-substrate strategy for probing O-GlcNAc modified proteins, *J Proteome Res 4*, 950-957.

71.   Vocadlo, D. J., Hang, H. C., Kim, E. J., Hanover, J. A., and Bertozzi, C. R. (2003) A chemical approach for identifying O-GlcNAc-modified proteins in cells, *Proc Natl Acad Sci U S A 100*, 9116-9121.

72.   Yang, Y. Y., Ascano, J. M., and Hang, H. C. (2010) Bioorthogonal chemical reporters for monitoring protein acetylation, *Journal of the American Chemical Society 132*, 3640-3641.

73.   Yu, M., de Carvalho, L. P., Sun, G., and Blanchard, J. S. (2006) Activity-based substrate profiling for Gcn5-related N-acetyltransferases: the use of chloroacetyl-coenzyme A to identify protein substrates, *Journal of the American Chemical Society 128*, 15356-15357.

74.   Cassel, D., and Glaser, L. (1982) Resistance to phosphatase of thiophosphorylated epidermal growth factor receptor in A431 membranes, *Proc Natl Acad Sci U S A 79*, 2231-2235.

75.   Facemyer, K. C., and Cremo, C. R. (1992) A new method to specifically label thiophosphorylatable proteins with extrinsic probes. Labeling of serine-19 of the regulatory light chain of smooth muscle myosin, *Bioconjugate Chem. 3*, 408-413.

76.   Sun, I. Y., Johnson, E. M., and Allfrey, V. G. (1980) Affinity purification of newly phosphorylated protein molecules. Thiophosphorylation and recovery of histones H1, H2B, and H3 and the high mobility group protein HMG-1 using adenosine 5'-O-(3-thiotriphosphate) and cyclic AMP-dependent protein kinase, *The Journal of biological chemistry 255*, 742-747.

77.   Cole, P. A., Burn, P., Takacs, B., and Walsh, C. T. (1994) Evaluation of the catalytic mechanism of recombinant human Csk (C-terminal Src kinase) using nucleotide analogs and viscosity effects, *The Journal of biological chemistry 269*, 30880-30887.

78.   Grace, M. R., Walsh, C. T., and Cole, P. A. (1997) Divalent ion effects and insights into the catalytic mechanism of protein tyrosine kinase Csk, *Biochemistry 36*, 1874-1881.

79.   Sondhi, D., Xu, W., Songyang, Z., Eck, M. J., and Cole, P. A. (1998) Peptide and protein phosphorylation by protein tyrosine kinase Csk: insights into specificity and mechanism, *Biochemistry 37*, 165-172.

80.   Sun, I. Y., and Allfrey, V. G. (1982) In vivo thiophosphorylation of chromosomal proteins. Recovery and analysis of HeLa histones and derivative phosphopeptides, *The Journal of biological chemistry 257*, 1347-1353.

81.   Kwon, S. W., Kim, S. C., Jaunbergs, J., Falck, J. R., and Zhao, Y. (2003) Selective enrichment of thiophosphorylated polypeptides as a tool for the analysis of protein phosphorylation, *Mol Cell Proteomics 2*, 242-247.

82.   Allen, J. J., Li, M., Brinkworth, C. S., Paulson, J. L., Wang, D., Hubner, A., Chou, W. H., Davis, R. J., Burlingame, A. L., Messing, R. O., Katayama, C. D., Hedrick, S. M., and Shokat, K. M. (2007) A semisynthetic epitope for kinase substrates, *Nature methods 4*, 511-516.

83.   Blethrow Justin, D., Glavy Joseph, S., Morgan David, O., and Shokat Kevan, M. (2008) Covalent capture of kinase-specific phosphopeptides reveals Cdk1-cyclin B substrates, *Proc Natl Acad Sci U S A 105*, 1442-1447.

84.   Hiriyanna, K. T., Baedke, D., Baek, K. H., Forney, B. A., Kordiyak, G., and Ingebritsen, T. S. (1994) Thiophosphorylated substrate analogs are potent active site-directed inhibitors of protein-tyrosine phosphatases, *Analytical biochemistry 223*, 51-58.

85.   Mulkey, R. M., Endo, S., Shenolikar, S., and Malenka, R. C. (1994) Involvement of a calcineurin/inhibitor-1 phosphatase cascade in hippocampal long-term depression, *Nature 369*, 486-488.

86. Endo, S., Critz, S. D., Byrne, J. H., and Shenolikar, S. (1995) Protein phosphatase-1 regulates outward K+ currents in sensory neurons of Aplysia californica, *Journal of neurochemistry 64*, 1833-1840.

87. Allen, J. J., Lazerwith, S. E., and Shokat, K. M. (2005) Bio-orthogonal affinity purification of direct kinase substrates, *Journal of the American Chemical Society 127*, 5288-5289.

88. Raaf, J., Brunstein, E., Issinger, O.-G., and Niefind, K. (2008) The CK2alpha /CK2beta Interface of Human Protein Kinase CK2 Harbors a Binding Pocket for Small Molecules, *Chemistry & Biology (Cambridge, MA, United States) 15*, 111-117.

89. Yde, C. W., Ermakova, I., Issinger, O.-G., and Niefind, K. (2005) Inclining the Purine Base Binding Plane in Protein Kinase CK2 by Exchanging the Flanking Side-chains Generates a Preference for ATP as a Cosubstrate, *Journal of Molecular Biology 347*, 399-414.

90. Zheng, J., Knighton, D. R., Ten Eyck, L. F., Karlsson, R., Xuong, N., Taylor, S. S., and Sowadski, J. M. (1993) Crystal structure of the catalytic subunit of cAMP-dependent protein kinase complexed with magnesium-ATP and peptide inhibitor, *Biochemistry 32*, 2154-2161.

91. Green, K. D., and Pflum, M. K. H. (2007) Kinase-Catalyzed Biotinylation for Phosphoprotein Detection, *J. Am. Chem. Soc. 129*, 10-11.

92. Green, K. D., and Pflum, M. K. H. (2009) Exploring kinase cosubstrate promiscuity: monitoring kinase activity through dansylation, *Chembiochem : a European journal of chemical biology 10*, 234-237.

93. Suwal, S., and Pflum, M. K. H. (2010) Phosphorylation-Dependent Kinase-Substrate Cross-Linking, *Angewandte Chemie, International Edition 49*, 1627-1630, S1627/1621-S1627/1613.

94.   Senevirathne, C., Green, K. D., and Pflum, M. K. H. (2009) Kinase-Catalyzed Biotinylation of Peptides, Proteins, and Lysates, In *Current Protocols in Chemical Biology*, John Wiley & Sons, Inc.

95.   Cook, P. F., Neville, M. E., Jr., Vrana, K. E., Hartl, F. T., and Roskoski, R., Jr. (1982) Adenosine cyclic 3',5'-monophosphate dependent protein kinase: kinetic mechanism for the bovine skeletal muscle catalytic subunit, *Biochemistry 21*, 5794-5799.

96.   Cheng, K. Y., Noble, M. E., Skamnaki, V., Brown, N. R., Lowe, E. D., Kontogiannis, L., Shen, K., Cole, P. A., Siligardi, G., and Johnson, L. N. (2006) The role of the phospho-CDK2/cyclin A recruitment site in substrate recognition, *The Journal of biological chemistry 281*, 23167-23179.

97.   Wilke, K. E., Francis, S., and Carlson, E. E. (2012) Activity-based probe for histidine kinase signaling, *Journal of the American Chemical Society 134*, 9150-9153.

98.   Attwood, P. V., Piggott, M. J., Zu, X. L., and Besant, P. G. (2007) Focus on phosphohistidine, *Amino acids 32*, 145-156.

99.   Martić, S., Gabriel, M., Turowec, J. P., Litchfield, D. W., and Kraatz, H.-B. (2012) Versatile Strategy for Biochemical, Electrochemical and Immunoarray Detection of Protein Phosphorylations, *Journal of the American Chemical Society*.

100.   Patricelli, M. P., Szardenings, A. K., Liyanage, M., Nomanbhoy, T. K., Wu, M., Weissig, H., Aban, A., Chun, D., Tanner, S., and Kozarich, J. W. (2007) Functional interrogation of the kinome using nucleotide acyl phosphates, *Biochemistry 46*, 350-358.

101.   Patricelli, M. P., Nomanbhoy, T. K., Wu, J., Brown, H., Zhou, D., Zhang, J., Jagannathan, S., Aban, A., Okerberg, E., Herring, C., Nordin, B., Weissig, H., Yang, Q., Lee, J.

D., Gray, N. S., and Kozarich, J. W. (2011) In situ kinase profiling reveals functionally relevant properties of native kinases, *Chemistry & biology 18*, 699-710.

102.   Hanks, S. K., and Hunter, T. (1995) Protein kinases 6. The eukaryotic protein kinase superfamily: kinase (catalytic) domain structure and classification, *FASEB journal : official publication of the Federation of American Societies for Experimental Biology 9*, 576-596.

103.   Radhakrishnan, I., Perez-Alvarado, G. C., Parker, D., Dyson, H. J., Montminy, M. R., and Wright, P. E. (1997) Solution structure of the KIX domain of CBP bound to the transactivation domain of CREB: a model for activator:coactivator interactions, *Cell 91*, 741-752.

104.   Garcia, B. A., Shabanowitz, J., and Hunt, D. F. (2005) Analysis of protein phosphorylation by mass spectrometry, *Methods 35*, 256-264.

105.   Muszynska, G., Andersson, L., and Porath, J. (1986) Selective adsorption of phosphoproteins on gel-immobilized ferric chelate, *Biochemistry 25*, 6850-6853.

106.   Reinders, J., and Sickmann, A. (2005) State-of-the-art in phosphoproteomics, *Proteomics 5*, 4052-4061.

107.   Steinberg, T. H., Agnew, B. J., Gee, K. R., Leung, W.-Y., Goodman, T., Schulenberg, B., Hendrickson, J., Beechem, J. M., Haugland, R. P., and Patton, W. F. (2003) Global quantitative phosphoprotein analysis using multiplexed proteomics technology, *Proteomics 3*, 1128-1144.

108.   Mann, M., Ong, S. E., Gronborg, M., Steen, H., Jensen, O. N., and Pandey, A. (2002) Analysis of protein phosphorylation using mass spectrometry: deciphering the phosphoproteome, *Trends Biotechnol 20*, 261-268.

109.   Kawada, N. (2001) Characterization of a Stellate Cell Activation-associated Protein (STAP) with Peroxidase Activity Found in Rat Hepatic Stellate Cells, *J. Biol. Chem. 276*, 25318-25323.

110.   Marcus, K., Immler, D., Sternberger, J., and Meyer, H. E. (2000) Identification of platelet proteins separated by two-dimensional gel electrophoresis and analyzed by matrix assisted laser desorption/ionization-time of flight-mass spectrometry and detection of tyrosine-phosphorylated proteins, *Electrophoresis 21*, 2622-2636.

111.   Oh, J., Pyo, J. H., Jo, E. H., Hwang, S. I., Kang, S. C., Jung, J. H., Park, E. K., Kim, S. Y., Choi, J. Y., and Lim, J. (2004) Establishment of a near-standard two-dimensional human urine proteomic map, *Proteomics 4*, 3485-3497.

112.   Kim, Y. M., Song, E. J., Seo, J., Kim, H. J., and Lee, K. J. (2007) Proteomic analysis of tyrosine phosphorylations in vascular endothelial growth factor- and reactive oxygen species-mediated signaling pathway, *J Proteome Res 6*, 593-601.

113.   Ubersax, J. A., Woodbury, E. L., Quang, P. N., Paraz, M., Blethrow, J. D., Shah, K., Shokat, K. M., and Morgan, D. O. (2003) Targets of the cyclin-dependent kinase Cdk1, *Nature 425*, 859-864.

114.   Schulenberg, B., Goodman, T. N., Aggeler, R., Capaldi, R. A., and Patton, W. F. (2004) Characterization of dynamic and steady-state protein phosphorylation using a fluorescent phosphoprotein gel stain and mass spectrometry, *Electrophoresis 25*, 2526-2532.

115.   Sun, T., Campbell, M., Gordon, W., and Arlinghaus, R. B. (2001) Preparation and application of antibodies to phosphoamino acid sequences, *Biopolymers 60*, 61-75.

116. Larsen, M. R., Thingholm, T. E., Jensen, O. N., Roepstorff, P., and Jorgensen, T. J. D. (2005) Highly Selective Enrichment of Phosphorylated Peptides from Peptide Mixtures Using Titanium Dioxide Microcolumns, *Molecular & Cellular Proteomics 4*, 873-886.

117. Jensen, S. S., and Larsen, M. R. (2007) Evaluation of the impact of some experimental procedures on different phosphopeptide enrichment techniques, *Rapid Communications in Mass Spectrometry 21*, 3635-3645.

118. Yu, L.-R., Zhu, Z., Chan, K. C., Issaq, H. J., Dimitrov, D. S., and Veenstra, T. D. (2007) Improved Titanium Dioxide Enrichment of Phosphopeptides from HeLa Cells and High Confident Phosphopeptide Identification by Cross-Validation of MS/MS and MS/MS/MS Spectra, *J Proteome Res 6*, 4150-4162.

119. Schweppe, R. E., Haydon, C. E., Lewis, T. S., Resing, K. A., and Ahn, N. G. (2003) The characterization of protein post-translational modifications by mass spectrometry, *Accounts of Chemical Research 36*, 453-461.

120. Flora, J. W., and Muddiman, D. C. (2001) Selective, sensitive, and rapid phosphopeptide identification in enzymatic digests using ESI-FTICR-MS with infrared multiphoton dissociation, *Analytical chemistry 73*, 3305-3311.

121. Hogan, J. M., Pitteri, S. J., and McLuckey, S. A. (2003) Phosphorylation site identification via ion trap tandem mass spectrometry of whole protein and peptide ions: bovine alpha-crystallin A chain, *Analytical chemistry 75*, 6509-6516.

122. Janek, K., Wenschuh, H., Bienert, M., and Krause, E. (2001) Phosphopeptide analysis by positive and negative ion matrix-assisted laser desorption/ionization mass spectrometry, *Rapid Commun Mass Spectrom 15*, 1593-1599.

123.   Gao, X., Schutz-Geschwender, A., and Hardwidge, P. R. (2009) Near-infrared fluorescence detection of ATP-biotin-mediated phosphoprotein labeling, *Biotechnology letters 31*, 113-117.

124.   Parker, L. L., Schilling, A. B., Kron, S. J., and Kent, S. B. (2005) Optimizing thiophosphorylation in the presence of competing phosphorylation with MALDI-TOF-MS detection, *J Proteome Res 4*, 1863-1866.

125.   Adams, J. A., McGlone, M. L., Gibson, R., and Taylor, S. S. (1995) Phosphorylation modulates catalytic function and regulation in the cAMP-dependent protein kinase, *Biochemistry 34*, 2447-2454.

126.   Schagger, H. (2006) Tricine-SDS-PAGE, *Nature Protocols 1*, 16-22.

127.   Sambrook, J., and Russel, D. (2011) *Molecular Cloning: A Laboratory Manual*, Third edition ed., Cold Spring Harbor Press, New York.

128.   Tonks, N. K. (2006) Protein tyrosine phosphatases: from genes, to function, to disease, *Nature reviews. Molecular Cell Biology 7*, 833-846.

129.   Cohen, P. (1991) Classification of protein-serine/threonine phosphatases: identification and quantitation in cell extracts, *Methods Enzymol 201*, 389-398.

130.   Denu, J. M., and Dixon, J. E. (1998) Protein tyrosine phosphatases: mechanisms of catalysis and regulation, *Curr Opin Chem Biol 2*, 633-641.

131.   Villafranca, J. E., Kissinger, C. R., and Parge, H. E. (1996) Protein serine/threonine phosphatases, *Curr Opin Biotechnol 7*, 397-402.

132.   Barford, D. (1996) Molecular mechanisms of the protein serine/threonine phosphatases, *Trends in Biochemical Sciences 21*, 407-412.

133. Songyang, Z., Carraway, K. L., 3rd, Eck, M. J., Harrison, S. C., Feldman, R. A., Mohammadi, M., Schlessinger, J., Hubbard, S. R., Smith, D. P., Eng, C., and et al. (1995) Catalytic specificity of protein-tyrosine kinases is critical for selective signalling, *Nature 373*, 536-539.

134. Goldberg, J., Huang, H. B., Kwon, Y. G., Greengard, P., Nairn, A. C., and Kuriyan, J. (1995) Three-dimensional structure of the catalytic subunit of protein serine/threonine phosphatase-1, *Nature 376*, 745-753.

135. Egloff, M. P., Cohen, P. T., Reinemer, P., and Barford, D. (1995) Crystal structure of the catalytic subunit of human protein phosphatase 1 and its complex with tungstate, *Journal of molecular biology 254*, 942-959.

136. Griffith, J. P., Kim, J. L., Kim, E. E., Sintchak, M. D., Thomson, J. A., Fitzgibbon, M. J., Fleming, M. A., Caron, P. R., Hsiao, K., and Navia, M. A. (1995) X-ray structure of calcineurin inhibited by the immunophilin-immunosuppressant FKBP12-FK506 complex, *Cell 82*, 507-522.

137. Kissinger, C. R., Parge, H. E., Knighton, D. R., Lewis, C. T., Pelletier, L. A., Tempczyk, A., Kalish, V. J., Tucker, K. D., Showalter, R. E., Moomaw, E. W., and et al. (1995) Crystal structures of human calcineurin and the human FKBP12-FK506-calcineurin complex, *Nature 378*, 641-644.

138. Mueller, E. G., Crowder, M. W., Averill, B. A., and Knowles, J. R. (1993) Purple Acid-Phosphatase - a Diiron Enzyme That Catalyzes a Direct Phospho Group Transfer to Water, *J. Am. Chem. Soc. 115*, 2974-2975.

139. Jia, Z., Barford, D., Flint, A. J., and Tonks, N. K. (1995) Structural basis for phosphotyrosine peptide recognition by protein tyrosine phosphatase 1B, *Science 268*, 1754-1758.

140.   Zhang, Z. Y. (1995) Kinetic and mechanistic characterization of a mammalian protein-tyrosine phosphatase, PTP1, *The Journal of biological chemistry 270*, 11199-11204.

141.   Hiriyanna, K. T., Baedke, D., Baek, K. H., Forney, B. A., Kordiyak, G., and Ingebritsen, T. S. (1994) Thiophosphorylated substrate analogs are potent active site-directed inhibitors of protein-tyrosine phosphatases, *Anal Biochem 223*, 51-58.

142.   Jeong, S., and Nikiforov, T. T. (1999) Kinase assay based on thiophosphorylation and biotinylation, *BioTechniques 27*, 1232-1238.

143.   Oda, Y., Nagasu, T., and Chait, B. T. (2001) Enrichment analysis of phosphorylated proteins as a tool for probing the phosphoproteome, *Nat Biotechnol 19*, 379-382.

144.   Boeri Erba, E., Matthiesen, R., Bunkenborg, J., Schulze, W. X., Di Stefano, P., Cabodi, S., Tarone, G., Defilippi, P., and Jensen, O. N. (2007) Quantitation of multisite EGF receptor phosphorylation using mass spectrometry and a novel normalization approach, *J Proteome Res 6*, 2768-2785.

145.   Alberts, A. S., Montminy, M., Shenolikar, S., and Feramisco, J. R. (1994) Expression of a peptide inhibitor of protein phosphatase 1 increases phosphorylation and activity of CREB in NIH 3T3 fibroblasts, *Mol Cell Biol 14*, 4398-4407.

146.   Subramanian, G., and Sud, M. (2010) Computational Modeling of Kinase Inhibitor Selectivity, *ACS Medicinal Chemistry Letters 1*, 395-399.

147.   Jester, B. W., Gaj, A., Shomin, C. D., Cox, K. J., and Ghosh, I. (2012) Testing the promiscuity of commercial kinase inhibitors against the AGC kinase group using a split-luciferase screen, *Journal of medicinal chemistry 55*, 1526-1537.

148.   Comeau, A. B., Critton, D. A., Page, R., and Seto, C. T. (2010) A focused library of protein tyrosine phosphatase inhibitors, *Journal of medicinal chemistry 53*, 6768-6772.

149. McCluskey, A., Sim, A. T., and Sakoff, J. A. (2002) Serine-threonine protein phosphatase inhibitors: development of potential therapeutic strategies, *Journal of medicinal chemistry 45*, 1151-1175.

150. Tonks, N. K., and Neel, B. G. (2001) Combinatorial control of the specificity of protein tyrosine phosphatases, *Curr Opin Cell Biol 13*, 182-195.

151. Combs, A. P. (2010) Recent advances in the discovery of competitive protein tyrosine phosphatase 1B inhibitors for the treatment of diabetes, obesity, and cancer, *Journal of medicinal chemistry 53*, 2333-2344.

152. Murray, H. W., Berman, J. D., Davies, C. R., and Saravia, N. G. (2005) Advances in leishmaniasis, *Lancet 366*, 1561-1577.

153. Heneberg, P. (2009) Use of protein tyrosine phosphatase inhibitors as promising targeted therapeutic drugs, *Current medicinal chemistry 16*, 706-733.

154. Klammer, M., Kaminski, M., Zedler, A., Oppermann, F., Blencke, S., Marx, S., Muller, S., Tebbe, A., Godl, K., and Schaab, C. (2012) Phosphosignature predicts dasatinib response in non-small cell lung cancer, *Mol Cell Proteomics 11*, 651-668.

155. Yan, G. R., Xiao, C. L., He, G. W., Yin, X. F., Chen, N. P., Cao, Y., and He, Q. Y. (2010) Global phosphoproteomic effects of natural tyrosine kinase inhibitor, genistein, on signaling pathways, *PROTEOMICS 10*, 976-986.

156. Imami, K., Sugiyama, N., Imamura, H., Wakabayashi, M., Tomita, M., Taniguchi, M., Ueno, T., Toi, M., and Ishihama, Y. (2012) Temporal profiling of lapatinib-suppressed phosphorylation signals in EGFR/HER2 pathways, *Mol Cell Proteomics*.

157. Anderson, N. G., Matheson, A., and Anderson, N. L. (2001) Back to the future: the human protein index (HPI) and the agenda for post-proteomic biology, *Proteomics 1*, 3-12.

158.   Rabilloud, T. (2002) Two-dimensional gel electrophoresis in proteomics: old, old fashioned, but it still climbs up the mountains, *Proteomics 2*, 3-10.

159.   Lottspeich, F. (1999) Proteome Analysis: A Pathway to the Functional Analysis of Proteins, *Angewandte Chemie 38*, 2476-2492.

160.   Gygi, S. P., Corthals, G. L., Zhang, Y., Rochon, Y., and Aebersold, R. (2000) Evaluation of two-dimensional gel electrophoresis-based proteome analysis technology, *Proc Natl Acad Sci U S A 97*, 9390-9395.

161.   Khan, A., and Packer, N. H. (2006) Simple urinary sample preparation for proteomic analysis, *J Proteome Res 5*, 2824-2838.

162.   Kim, K. H., and Moon, M. H. (2009) High speed two-dimensional protein separation without gel by isoelectric focusing-asymmetrical flow field flow fractionation: application to urinary proteome, *J Proteome Res 8*, 4272-4278.

163.   Andersson, L., and Porath, J. (1986) Isolation of phosphoproteins by immobilized metal (Fe3+) affinity chromatography, *Anal. Biochem. 154*, 250-254.

164.   Li, S., and Dass, C. (1999) Iron(III)-immobilized metal ion affinity chromatography and mass spectrometry for the purification and characterization of synthetic phosphopeptides, *Analytical biochemistry 270*, 9-14.

165.   Posewitz, M. C., and Tempst, P. (1999) Immobilized gallium(III) affinity chromatography of phosphopeptides, *Analytical chemistry 71*, 2883-2892.

166.   Pinkse, M. W., Uitto, P. M., Hilhorst, M. J., Ooms, B., and Heck, A. J. (2004) Selective isolation at the femtomole level of phosphopeptides from proteolytic digests using 2D-NanoLC-ESI-MS/MS and titanium oxide precolumns, *Analytical chemistry 76*, 3935-3943.

167.   Wolschin, F., Wienkoop, S., and Weckwerth, W. (2005) Enrichment of phosphorylated proteins and peptides from complex mixtures using metal oxide/hydroxide affinity chromatography (MOAC), *Proteomics 5*, 4389-4397.

168.   Kweon, H. K., and Hakansson, K. (2006) Selective zirconium dioxide-based enrichment of phosphorylated peptides for mass spectrometric analysis, *Analytical chemistry 78*, 1743-1749.

169.   Bodenmiller, B., Mueller, L. N., Mueller, M., Domon, B., and Aebersold, R. (2007) Reproducible isolation of distinct, overlapping segments of the phosphoproteome, *Nat Meth 4*, 231-237.

170.   Meyer, H. E., Hoffmann-Posorske, E., Korte, H., and Heilmeyer, L. M., Jr. (1986) Sequence analysis of phosphoserine-containing peptides. Modification for picomolar sensitivity, *FEBS Lett 204*, 61-66.

171.   Oda, Y., Nagasu, T. T., and Chait, B. T. (2001) Enrichment analysis of phosphorylated proteins as a tool for probing the phosphoproteome., *Nat. Biotech. 19*, 379-382.

172.   Zhou, H., Watts, J., and Aebersold, R. (2001) A systematic approach to the analysis of protein phosphorylation, *Nat. Biotech. 19*, 375-378.

173.   Tao, W. A., Wollscheid, B., O'Brien, R., Eng, J. K., Li, X.-j., Bodenmiller, B., Watts, J. D., Hood, L., and Aebersold, R. (2005) Quantitative phosphoproteome analysis using a dendrimer conjugation chemistry and tandem mass spectrometry, *Nat. Methods 2*, 591-598.

174.   Warthaka, M., Karwowska-Desaulniers, P., and Pflum, M. K. H. (2006) Phosphopeptide Modification and Enrichment by Oxidation-Reduction Condensation, *ACS Chem. Biol. 1*, 697-701.

175.   Sugiyama, N., Masuda, T., Shinoda, K., Nakamura, A., Tomita, M., and Ishihama, Y. (2007) Phosphopeptide Enrichment by Aliphatic Hydroxy Acid-modified Metal Oxide

Chromatography for Nano-LC-MS/MS in Proteomics Applications, *Molecular & Cellular Proteomics 6*, 1103-1109.

176.   Leitner, A., Sturm, M., Hudecz, O., Mazanek, M., Smått, J.-H., Lindén, M., Lindner, W., and Mechtler, K. (2010) Probing the Phosphoproteome of HeLa Cells Using Nanocast Metal Oxide Microspheres for Phosphopeptide Enrichment, *Analytical chemistry 82*, 2726-2733.

177.   Nie, S., Dai, J., Ning, Z.-B., Cao, X.-J., Sheng, Q.-H., and Zeng, R. (2010) Comprehensive Profiling of Phosphopeptides Based on Anion Exchange Followed by Flow-Through Enrichment with Titanium Dioxide (AFET), *J Proteome Res 9*, 4585-4594.

178.   Holland, J. W., Deeth, H. C., and Alewood, P. F. (2006) Resolution and characterisation of multiple isoforms of bovine kappa-casein by 2-DE following a reversible cysteine-tagging enrichment strategy, *Proteomics 6*, 3087-3095.

179.   Shah, K., Liu, Y., Deirmengian, C., and Shokat, K. M. (1997) Engineering unnatural nucleotide specificity for Rous sarcoma virus tyrosine kinase to uniquely label its direct substrates, *Proc Natl Acad Sci U S A 94*, 3565-3570.

180.   Boyle, S. N., and Koleske, A. J. (2007) Use of a chemical genetic technique to identify myosin IIb as a substrate of the Abl-related gene (Arg) tyrosine kinase, *Biochemistry 46*, 11614-11620.

181.   Hengeveld, R. C., Hertz, N. T., Vromans, M. J., Zhang, C., Burlingame, A. L., Shokat, K. M., and Lens, S. M. (2012) Development of a chemical genetic approach for human aurora B kinase identifies novel substrates of the chromosomal passenger complex, *Mol Cell Proteomics 11*, 47-59.

182.   Ge, Y., Lawhorn, B. G., ElNaggar, M., Strauss, E., Park, J.-H., Begley, T. P., and McLafferty, F. W. (2002) Top Down Characterization of Larger Proteins (45 kDa) by Electron

Capture Dissociation Mass Spectrometry, *Journal of the American Chemical Society 124*, 672-678.

183.   Zhou, H., Ning, Z., E. Starr, A., Abu-Farha, M., and Figeys, D. (2011) Advancements in Top-Down Proteomics, *Analytical chemistry*.

184.   Llerena-Suster, C. R. F., Foresti, M. L., Briand, L. E., and Morcelle, S. R. (2009) Selective adsorption of plant cysteine peptidases onto TiO2, *Colloids and Surfaces B: Biointerfaces 72*, 16-24.

185.   Salisbury, C. M., and Cravatt, B. F. (2007) Activity-based probes for proteomic profiling of histone deacetylase complexes, *Proc Natl Acad Sci U S A 104*, 1171-1176.

186.   Kwon, S. J., Choi, E. Y., Seo, J. B., and Park, O. K. (2007) Isolation of the Arabidopsis phosphoproteome using a biotin-tagging approach, *Mol. Cells 24*, 268-275.

ABSTRACT

**DEVELOPMENT OF KINASE CATALYZED BIOTINYLATION TO STUDY
PHOSPHOPROTEOMICS**

by

KONA ARACHCHILAGE CHAMARA SENEVIRATHNE

AUGUST 2013

Advisor: Prof. Mary Kay Pflum

Major: Chemistry (Organic)

Degree: Doctor of Philosophy

Kinase-catalyzed protein phosphorylation is involved in a wide variety of cellular events. Development of methods to identify phosphoproteins in normal and diseased states is critical to fully characterize cell biology. Our lab recently discovered kinase-catalyzed biotinylation, where ATP-biotin is utilized by kinases to label phosphopeptides or phosphoproteins with a biotin tag. To explore kinase-catalyzed biotinylation, kinetic measurements were obtained with various kinases and the data indicated that kinase-catalyzed biotinylation occurs with catalytic efficiency appropriate for phosphoproteomics application. Next, the susceptibility of the biotin tag to phosphatases was characterized and found that the phosphorylbiotin group was relatively insensitive to protein phosphatases. Importantly, robust kinase-catalyzed biotinylation occurs without the need for phosphatase inhibitor treatment. The results suggest that kinase-catalyzed biotinylation is well suited for phosphoproteomics studies, with particular utility towards monitoring low abundance phosphoproteins. Finally, we report application of kinase-catalyzed biotinylation to the enrichment of the phosphopeptides in cell lysates for mass spectrometry-based phosphoproteomics analysis. Significantly, the biotinylation strategy was used to enrich full-length phosphoprotein, which is challenging using metal ion purification. With the utility of

ATP-biotin labeling for phosphoproteomics analysis established, kinase-catalyzed biotinylation can be applied to characterizing and understanding of the role of phosphorylation in various biological events.

AUTOBIOGRAPHICAL STATEMENT

KONA ARACHCHILAGE CHAMARA SENEVIRATHNE

Educational Background

Ph.D. (2008-2013)
Organic Division, Department of Chemistry, Wayne State University, Detroit, MI, 48202, USA

B.SC (2003-2007)
Department of Chemistry, Faculty of Science, University of Peradeniya, Peradeniya, Sri Lanka

Awards / Honors

2012-2013	Competitive Thomas C. Rumble Fellowship, Wayne State University
2011-2013	James C. French Graduate Award in Organic Chemistry, Wayne State University
2009-2010	Norman A. LeBel Endowed Graduate Award in Organic Chemistry, Wayne State University
2009-2010	Award for Excellence in Teaching, Wayne State University
2007-2008	Silver Medal in Inter University Chemistry Competition from Sri Lanka Association for the Advancement of Science (SLASS), Sri Lanka
2006-2007	Sulthanbawa Prize for the Best Performance in Organic Chemistry from University of Peradeniya
2006-2007	University Awards for the Academic Excellence from University of Peradeniya
2004-2005	Hayle's Prize for the Best Performance in Chemistry, University of Peradeniya
2003-2004	Hayle's Prize for the Best Performance in Chemistry, University of Peradeniya

Publications

Chamara Senevirathne, and Mary Kay Pflum, Biotinylated phosphoproteins from kinase-catalyzed biotinylation are stable to phosphatases: Implications for phosphoproteomics, *ChemBiochem,* **2012**, 14 (3) 381-387.

Sujith Suwal, **Chamara Senevirathne**, Satish Garre and Mary Kay Pflum, Structural Analysis of γ-phosphate modified ATP analogs Compatible with Kinase-Catalyzed Labeling, *BioConjugate chemistry,* **2012**, 23 (12) 2386-2391.

Chamara Senevirathne, Keith D. Green and Mary Kay Pflum, Kinase-Catalyzed Biotinylation of Peptides, Proteins, and Lysates, *Current Protocols in Chemical Biology*. **2012**, 4 (1) 83-100.

Chamara Senevirathne and Namal Priyantha, Correlation between firing temperature and defluoridation capacity of brick clay, *International Journal of Global Environmental Issues,* **2009**, 9 (3), 239-248.

Namal Priyantha, **Chamara Senevirathne**, Prasad Gunathilake and Rohan Weerasooriya, Adsorption behavior of fluoride at normal brick (NB)-water interface, *Journal of Environmental Protection Science,* **2009,** 3 140-146.